mfs 2025 CONFERENCE

Microscopy at the Frontiers of Science Conference 2025

VALÈNCIA, SPAIN · 23RD - 26TH SEPTEMBER

BOOK OF ABSTRACTS

scitoevents
SCIENCE & TECHNOLOGY ORGANIZERS



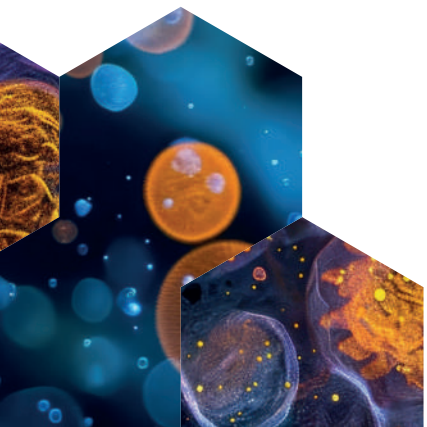

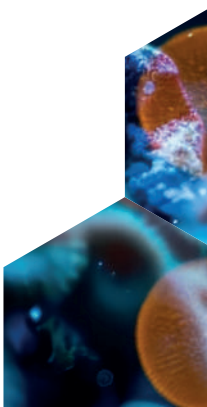

Microscopy at the Frontiers of Science Conference 2025

MFS25

MFS Conference Abstract Book

Table of contents

Welcome

Dear colleagues,

On behalf of the Organizing Committee and the directive boards of the Spanish and Portuguese Microscopy Societies, it is our pleasure to welcome you to *Microscopy at the Frontiers of Science 2025 (MFS2025)*, the Joint Meeting of the Spanish Microscopy Society (SME) and the Portuguese Society for Microscopy (SPMicros). The congress will take place from September 23rd to 26th, 2025, at the Centro de Investigaciones Príncipe Felipe (CIPF) in Valencia, Spain.

The program features keynote lectures by internationally recognized scientists, flash talks, poster sessions, symposia, a course in cryo-EM single-particle analysis and a broad commercial exhibition. We are delighted to host outstanding speakers such as Sjors Scheres, Giulia Zanetti, Manos Mavrakis, Wiebke Möbius, Amadeo López Vázquez de Parga, and José Sánchez Costa, who will share their latest advances in life sciences and in materials microscopy.

Topics will span (cryo)electron microscopy, advanced light microscopy, correlative and multimodal imaging, and innovations in instrumentation and sample preparation. In addition, networking activities and social events will provide opportunities to exchange ideas and strengthen collaborations.

Valencia, with its Mediterranean charm, rich cultural heritage, and renowned gastronomy, offers an inspiring setting for our meeting. We warmly encourage you to participate actively in all sessions, visit our sponsors' exhibition, and enjoy both the science and the city.

Welcome to MFS2025 — we look forward to seeing you in Valencia!

Jose Luis Llacer	Juan de Dios Alché	Paulo Ferreira
(President of the Organizing Committee)	(President of SME)	(President of SPMicros)

Abstracts of Plenary Speakers

Cryo-EM structures of amyloid filaments from human brain

Sjors Scheres [*a]

[a] MRC Laboratory of Molecular Biology (Cambridge, UK)

Abnormal assembly of the proteins tau, α-synuclein, TDP-43 and amyloid-β into amyloid filaments defines most human neurodegenerative diseases. Genetics provided a direct link between filament formation and the causes of disease. Developments in electron cryo-microscopy (cryo-EM) have recently made it possible to determine the atomic structures of amyloids from postmortem human brains. I will give an overview of the structures of brain-derived amyloid filaments that have been determined thus far and I will discuss their impact on research into neurodegeneration. Whereas a given protein can adopt many different filament structures, specific amyloid folds define distinct diseases. Amyloid structures thus provide a description of neuropathology at the molecular level and a handle on studying disease. Ongoing research focuses on model systems that replicate the structures observed in disease, to better understand the molecular mechanisms of disease, and to develop improved diagnostics and therapeutics.

Actin in action: novel tools for visualizing actin organization in living cells and tissues.

Manos Mavrakis [*a]

[a] Institut Fresnel (Marseille, France)

Essential physiological functions, including cell division, cell adhesion and motility, and tissue morphogenesis, rely on the capacity of animal cells to change and adapt their shape. To accomplish these force-dependent tasks, animal cells make use of actin cytoskeletal filaments. The precise way in which actin filaments organize, i.e. how actin filaments are physically oriented in space, and how filament organization is remodeled in time, is determinant for force generation. Being able to measure actin filament organization directly in living cells and tissues thus promises to advance our understanding of how proteins and signaling pathways individually and collectively control actin-driven cellular functions. I will present the development of novel genetically-encoded, green- and red-fluorescent-protein-based reporters that allow non-invasive, quantitative measurements of actin filament organization in living cells and tissues by using polarization-resolved fluorescence microscopy. I will show examples of actin organization measurements in living mammalian cells in culture, as well as in living fission yeast, Drosophila and C.elegans embryos.

Engineering Crystalline Switchable Dynamic Materials: From Selective Sensing to Energy-Efficient Applications

José Sánchez Costa*[a]

[a] IMDEA Nanociencia (Madrid)

Switchable compounds are an advanced class of materials that undergo reversible changes in their physical or chemical properties in response to external stimuli[1]. Among these, molecule-based spin crossover (SCO) complexes of specific transition metal ions stand out due to their ability to reversibly transition between low-spin (LS) and high-spin (HS) states. These transitions can be triggered by temperature, pressure, light, X-ray irradiation, or guest molecule inclusion, leading to significant variations in their magnetic, electronic, thermal, optical, and structural properties. The great potential of such materials lies in the possibility of obtaining functionality in a single molecule, thus achieving a very high level of miniaturization of technology.

This presentation will discuss our work with Spin Crossover (SCO) materials, focusing on addressing key challenges: 1) achieving high selectivity in SCO sensors through innovative receptor design; 2) overcoming the insulating and unstable nature of SCO-MOFs for spintronics by developing novel materials and integrating them with conductive matrices like carbon nanotubes; and 3) utilizing their thermal regulation properties for energy-efficient applications to reduce temperature fluctuations and could potentially be implemented for passive temperature control in buildings. (see figure). In addition, the SCO materials are remarkably stable upon cycling and highly versatile, allowing for the design of compounds adapting the intended properties (transition temperature and hysteresis) for the desired climatic conditions and comfort temperature.

References:

(1). Chemical Society Reviews, 2023, 452 doi.org/10.1039/D2CS00790H

(2) Chemical Science, 2019, doi.org/10.1039/C9SC02522G; Advanced Science, 2021, doi.org/10.1002/advs.202102619; Dalton Transactions, 2020, 10.1039/D0DT01533D; Inorg. Chem. Front., 2020, 10.1039/D1QI00059D

(3) Nature Communications 2021, 10.1038/s41467-021-21791-3; Chemistry of Materials, 2023, doi.org/10.1021/acs.chemmater.3c01049

(4) Adv. Science, 2022, 9, doi.org/10.1002/advs.202270150

Mechanisms of coated vesicle transport in the early secretory pathway

Giulia Zanetti[*a]

[a] Francis Crick Institute (London, UK)

Trafficking from the endoplasmic reticulum to the Golgi apparatus comprises the first steps toward the correct localization of 30% of eukaryotic proteins. Coat protein complexes COPII and COPI are involved in forward and retrograde transport of cargo and cargo receptors between the ER and the Golgi. Although COPII forms coated vesicles in vitro, the biogenesis, morphology and organization of transport carriers in mammalian cells is debated. We use in situ cryo-electron tomography and super resolution fluorescence microscopy to reveal the molecular architecture of ER exit sites in human cells. We visualise ribosome-exclusion zones enriched with COPII and COPI coated vesicles and thus resolve the debate regarding the existence of COPII coated vesicles. COPII vesicles derive from ER membranes, whereas COPI vesicles originate from the ER-Golgi intermediate compartment. We quantify coated vesicle morphology and positioning with respect to other ER exit site components, providing a molecular description of the mammalian early secretory pathway.

The contribution of volume EM to the understanding of myelin biology

Wiebke Möbius*[a]

[a] Max Plank Institute for Multidisciplinary Sciences

Investigation of the fine structure of myelin requires the resolution of transmission electron microscopy. With this technique, subtle changes in the characteristics of the myelin sheath in pathological states can be detected. To understand the myelin sheath in its entirety, volume electron microscopy (vEM) is an indispensable tool. By combining conditional knock-out mouse genetics and focused ion beam-scanning electron microscopy (FIB-SEM), fundamental myelin biology can be studied.

We were able to visualize the slow process of myelin turnover and maintenance in an inducible conditional knock-out of myelin basic protein (MBP). MBP is essential for myelin compaction in the central nervous system (CNS). Depletion of MBP by ablation of the *Mbp* gene in the adult mouse resulted in a slow demyelination. While compacted myelin served as marker for developmentally formed, resident myelin, newly generated myelin membranes remained non-compacted. This structural change revealed that newly formed membranes were added at the inner tongue of the myelin sheath in proximity to the paranode.

Myelinated axons exist in a close metabolic relationship with the myelinating oligodendrocyte. This is highlighted by the impact of genetic defects in oligodendrocytes on neuronal health. Deficiency of the major CNS myelin protein proteolipid protein (PLP) is the cause for spastic paraplegia type 2 (SPG2), an inherited X-linked leukodystrophy. The SPG2 mouse model, the $Plp^{-/Y}$ mouse, displayed disease hallmarks like axonal swellings and progressive length-dependent axonal degeneration. VEM revealed so far undescribed disease-related changes beyond axonal swellings. The myelin sheath was characterized by an increased occurrence of cytoplasmic openings, called myelinic channels, and excessive myelin outfoldings. Axonal mitochondria appeared fragmented and changed in shape. Axons underneath myelin outfoldings showed unusual sprouting and anastomosing features. Deficiency of another protein, myelin-associated glycoprotein (MAG), also induced the formation of similar outfoldings, although these proteins differ in their structure, function and localization. Such pathological changes in myelinated axons become visible only by vEM techniques.

Transition from a 2D Mott insulator to a Kondo lattice

Amadeo L. Vázquez de Parga*[a]

[a] Departamento Física de la Materia Condensada, Universidad Autónoma de Madrid, Condensend Matter Physics Center (IFIMAC) e IMDEA Nanociencia, Cantoblanco 28049, Madrid, Spain

When a magnetic impurity is placed in a metallic host, the screening of the magnetic moment by the conduction electrons is known as Kondo effect [1-2]. The presence of an ordered array of magnetic moments gives rise to the formation of a Kondo Lattice. Below a characteristic temperature, TKL, the Kondo clouds of the individual impurities are coherently superimposed and acquire the periodicity of the crystal. Bloch's theorem ensures the formation of a renormalized flat band of width of the order of TKL [3] and as consequence the conduction electrons increase their effective mass dramatically.

We study the physics of a two-dimensional Kondo lattice using a van der Waals heterostructure containing a two-dimensional Mott insulator (1T-TaS2) on a metallic substrate (2H-TaS2). By means of low temperature Scanning Tunneling Microscopy and Spectroscopy, we follow up the formation of the 2D Kondo lattice. When the sample temperature is lower than 27K, the magnetic moments present in the 2D Mott insulator experience the Kondo screening by the conduction electrons from the substrate, leading to the appearance of a Kondo resonance at the Fermi level. According to the quasi-interference maps (QPI) the 1T-TaS2 layer is still a Mott insulator. Below 11 K, a gap opens within the Kondo resonance, which is the signature of the formation of a coherent quantum state that extends all over the sample, i.e., a Kondo lattice [4]. The QPI maps show the appearance of a Fermi contour in the former Mott insulator probing unambiguously the formation of a Kondo lattice [5]. The observed modifications in the LDOS are well explained by state-of-the-art Density Functional Theory calculations.

References:

[1] Phys. Rev., **124**, 41 (1961).

[2] Prog. Theor. Phys., **32**, 37 (1964)

[3] Phys. Rev. Lett., **48**, 362 (1982).

[4] Small, **20**, 2303275 (2024).

[5] Nat. Commun. **15**, 10272 (2024)

PHD Awards

PhD Awards on Life Sciences Sponsored by Zeiss

Álvaro de la Gándara - “Structural and Molecular Mechanisms of ATP-dependent DNA transposition using IS21 as a model system”.

Mª Jesús Rodríguez Espinosa “Estructura y biomecánica de la cápsida del picobirnavirus humano: retención del cargo, desensamblaje y reensamblaje”.

PhD Awards on Material Science Sponsored by Thermofisher

Daniel del Pozo Bueno - “Advanced Machine Learning for EELS Spectroscopy: Magnetic Characterization, Classification and Data Generation”.

Marc Botifoll Moral - “End-to-End Automation in STEM Imaging and Spectroscopy: Revolutionising the Analysis of Quantum Materials and Beyond”.

PhD Awards on Technical Developments sponsored by Izasa

David Herreros Calero - “Deformation fields approximation by 3D Zernike polynomials for the analysis of continuous heterogeneity”.

PhD Awards on Technical Developments sponsored by Milexia

Rafael V. Ferreira - "Atomic-scale measurements of charge distribution-transport in 2D quantum structure".

Abstracts of oral talks - Topic: Materials

(order of presentation)

Combining UHR-HAADF, Image Simulation, Deep-Learning Methods and Density Functional Theory (DFT) Calculations to Understand the Ultimate Details of Metal-Support Interactions in High Surface Area Single-Atom Catalysts

Calvino, José Juan [*a], Aniceto-Ocaña, Paula [a], Marqueses-Rodríguez, José [a], Perez-Omil, José Antonio [a], Castillo, Carmen Esther [a], López-Haro, Miguel [*a]

[a]Departamento de Ciencias de los Materiales e Ingeniería Metalúrgica y Química Inorgánica, Facultad de Ciencias, Universidad de Cádiz, Campus Río San Pedro S/N, Puerto Real, 11510 Cádiz, Spain

High Resolution High Angle Annular Dark Field imaging has boosted the structural analysis of so-called Single Atom Catalysts. These are materials constituted by a metallic active phase in the form of ultra-highly dispersed species (either subnanometric sized clusters or even isolated atoms) [1]. The unique capabilities of directly imaging isolated metal species distributed on the surface or bulk of a second material which acts as a carrier is in fact at the roots of the development of this particular type of supported metal catalysts. In fact, STEM-HAADF images are routinely used to evidence the success of the synthetic routes used to prepare this type of materials, mainly by detecting contrasts in the images which can be specifically assigned to the ultradispersed metallic component. Figure 1 shows an example corresponding to a 0.1 wt% Pd/MgO catalyst. The dot-type bright contrasts in this image would correspond to location of isolated Pd atoms.

However, the analysis of the results obtained using this technique is still mainly based on a manual approach, which severely limits both its reliability and potential to reveal the ultimate structural analysis of this specific type of catalysts. In most papers some Single Atom (SA) contrasts are just encircled on the images, without any further analysis. Moreover, image simulation studies supporting contrasts interpretation is usually lacking. Clearly, such an approach is quite weak, prone to user bias, and very limited in terms of statistical significance. It also oversees other information underlying the local distribution of contrasts in the images, particularly that related to the actual nature of the sites in which the isolated atoms locate, a question particularly relevant to model and understand the actual nature of metal-support interactions.

In this scenario it becomes necessary to develop new tools which allow processing large sets of experimental STEM images to automatically detect SA species and determine their exact location on crystalline supports. Here, we present an approach to directly quantify the detailed structural nature of metal sites in single-

atom, high surface area, powder catalysts from the analysis of large sets of images. By combining advanced high-resolution High Angle Annular Dark Field scanning-transmission electron microscopy (HAADF-STEM) imaging, HAADF-STEM image simulation, deep learning and density functional theory calculations, we determine, with statistical significance, the exact location and coordination environment of Pd single-atoms supported on MgO nanoplates.

We will illustrate the analysis performed on experimental images and demonstrate how, not only the contrasts (brighter spots) associated, in agreement with simulated images, to the isolated Pd atoms are perfectly and automatically detected and segmented (separated from the irregular support background) but also how it is also possible to determine which of these atoms locate on sites corresponding to Mg in the oxide structure, i.e. as substitution of Mg^{2+} cations [2].

Importantly, a more in-depth analysis, with higher spatial resolution, of the local contrasts in the sites corresponding to the Pd atoms, involving also the use of neural networks, revealed a preferential interaction of Pd single-atoms with cationic vacancies (V-centers), followed by occupation of anionic defects on the {001} MgO surface. The former interaction results in stabilization of PdO species within V-centers, while partially embedded Pd states are found in F-defects. Therefore, this methodology opens a route to the ultimate structural analysis of metal-support interaction effects, key in the design of advanced nanocatalysts for sustainable and energy-efficient processes.

References:

[1] Ping Qi et al., RSC Adv., 2022, 12, 1216-1227

[2] Marqueses J. et al, Communications Materials, (2024)5:206

Acknowledgments:

This work has received support from Projects: PID2019-110018GA-I00 funded by MICIU/AEI/10.13030/501100011033, PID2020-113006-RB-I00 and PID2022-142312NB-I00 funded by MCIN/AEI/10.13039/501100011033 and by “ERDF A way of making Europe”. Project TED2021-130191B-C44 funded by MCIN/AEI/10.13039/501100011033 and European Union NextGenerationEU/PRTR) is also acknowledged. STEM experiments were recorded at the DME-UCA Node of the Spanish Singular Infrastructure for Electron Microscopy of Materials (ICTS ELECMI). P.A.O thanks FPI scholarship program from University of Cadiz.

Probing Nanoscale Strain and Electronic Structure in 1D CrX3 (X=I and Cl) Encapsulated in Carbon Nanotubes

Çaha, Ihsan [*a], Leonard Deepak, Francis [*a]

[a]International Iberian Nanotechnology Laboratory (INL), Avenida Mestre José Veiga, Braga, Portugal

One-dimensional (1D) van der Waals (vdW) magnets, such as halide-based CrX_3 (X = I, Cl), are emerging as promising candidates for nanoscale spintronic applications due to their intrinsic anisotropy, low damping, and confined magnetic textures. However, their extreme air sensitivity and low dimensionality present significant challenges for structural and functional characterization. In this work, we investigate the atomic and electronic structures of CrX_3 nanotubes and nanorods encapsulated within multi-walled carbon nanotubes (MWCNTs) using advanced electron microscopy techniques. Low-energy loss electron energy loss spectroscopy (EELS) is used to probe the dielectric environment and identify signatures of excitonic, interband, and collective electronic excitations. Simultaneously, 4D-STEM measurements allow for the mapping of local strain fields and charge redistribution at the CrX_3/MWCNT interface, providing insights into confinement-induced property modulation. This study builds upon our recent demonstration of monolayer CrI_3 encapsulation in carbon nanotubes, extending the methodology to other halide variants. The results aim to deepen the understanding of how curvature, interface coupling, and quantum confinement influence the physical properties of 1D vdW magnets.

References:

[1] B. Huang, G. Clark, E. Navarro-Moratalla, D.R. Klein, R. Cheng, K.L. Seyler, Di. Zhong, E. Schmidgall, M.A. McGuire, D.H. Cobden, W. Yao, D. Xiao, P. Jarillo-Herrero, X. Xu, Layer-dependent ferromagnetism in a van der Waals crystal down to the monolayer limit, Nature. 546 (2017) 270–273.

[2] T. Zhang, M. Grzeszczyk, J. Li, W. Yu, H. Xu, P. He, L. Yang, Z. Qiu, H. Lin, H. Yang, J. Zeng, T. Sun, Z. Li, J. Wu, M. Lin, K.P. Loh, C. Su, K.S. Novoselov, A. Carvalho, M. Koperski, J. Lu, Degradation Chemistry and Kinetic Stabilization of Magnetic CrI3, J. Am. Chem. Soc. 144 (2022) 5295–5303.

[3] D. Shcherbakov, P. Stepanov, D. Weber, Y. Wang, J. Hu, Y. Zhu, K. Watanabe, T. Taniguchi, Z. Mao, W. Windl, J. Goldberger, M. Bockrath, C.N. Lau, Raman Spectroscopy, Photocatalytic Degradation, and Stabilization of Atomically Thin Chromium Tri-iodide, Nano Lett. 18 (2018) 4214–4219.

[4] I. Çaha, A. Ahmad, L. Boddapatti, M. Bañobre-lópez, A.T. Costa, A.N. Enyashin, W. Li, P. Gargiani, M. Valvidares, J. Fernández-rossier, F.L. Deepak, One-dimensional

CrI3 encapsulated within multi-walled carbon nanotubes, Commun. Chem. 8 (2025) 155.

Acknowledgments:

We acknowledge financial support from the European Union (Grant FUNLAYERS - 101079184).

Structure and Property Analysis of $(Sm_{1-x}Y_x)S–TaS_2$ Nanotubes from Quaternary Misfit Layered Compounds.

Furqan, Mohammad [a, b], Hettler, Simon [a, b, c], Sreedhara, M. B. [d], Khadiev, Azat [e], Tenne, Reshef [f], Arenal, Raul [* a, b, g]

[a]Instituto de Nanociencia y Materiales de Aragon (INMA), CSIC-U. Zaragoza (Zaragoza), Spain, [b]Laboratorio de Microscopías Avanzadas (LMA), Edificio I+D, C/ Mariano Esquillor s/n, 50018 Zaragoza, Spain., [c]Laboratory for Electron Microscopy, Karlsruhe Institute for Technology, Karlsruhe, Germany, [d]Solid State and Structural Chemistry Unit, Indian Institute of Science, Bengaluru, 560012, India, [e]Deutsches Elektronen-Synchrotron DESY, Notkestr. 85, 22607 Hamburg, Germany, [f]Department of Molecular Chemistry and Materials Science, Weizmann Institute of Science, Rehovot 7610001, Israel, [g]ARAID Foundation Zaragoza 50018, Spain

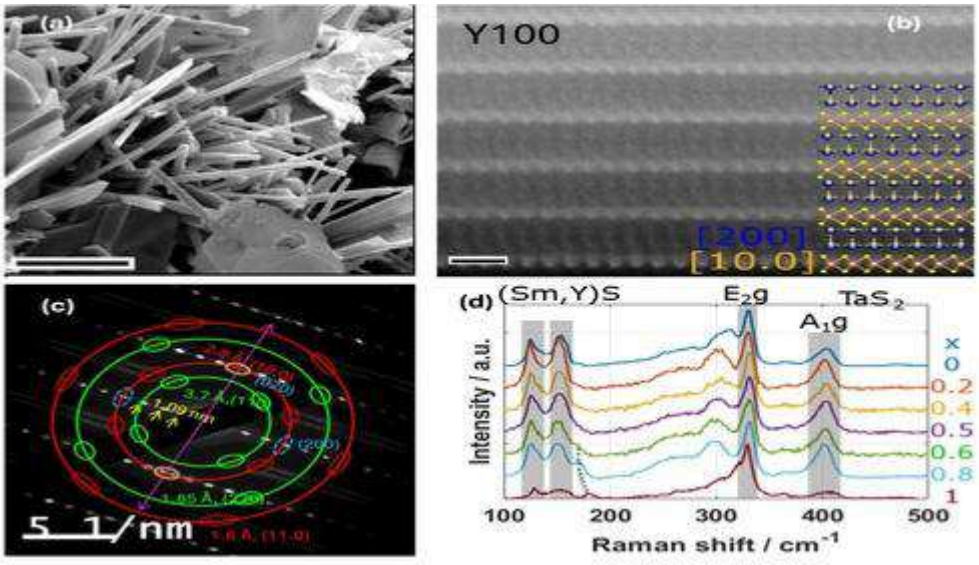

Misfit layered compounds (MLCs) have garnered considerable attention due to their fascinating chemistry and properties [1]. The structural foundation of MLCs is based on the alternating stacking of the two different layered components MX with a distorted rocksalt structure and TX_2 with a hexagonal structure, resulting in a composite or intergrowth structure [1,2]. The properties of MLCs are determined by the chemical and structural interplay between MX and TX_2.

MLC nanotubes (NTs) synthesized via the chemical vapor technique (CVT) offer potential applications in thermoelectrics [1,3]. Recently, a modified synthesis method of MLC-NTs has permitted the introduction of additional elements to form a quaternary compound starting from LaS-TaS_2 [3,4]. These quaternary MLCs are obtained by the partial substitution of one of the elements in the ternary MLC lattice,

enabling precise manipulation of charge carrier densities through substitutional doping and alloying. Our study presents a detailed electron microscopy analysis of one such quaternary $(Sm_xY_{1-x})S\text{-}TaS_2$ nanostructure family [5].

The $(Sm_xY_{1-x})S\text{-}TaS_2$ NTs were synthesized via CVT technique [1-3] by varying the precursor proportions of Sm_x vs Y_{1-x} between x=0 and x=1. The samples were designated by the Sm percentage such as Sm20 which corresponds to $(Sm_{0.2}Y_{0.8})S\text{-}TaS_2$ and so on. We used TEM techniques, including HR(S)TEM imaging, selected area electron diffraction (SAED), electron energy loss spectroscopy (EELS), energy-dispersive X-ray spectroscopy (EDS) and X-ray diffraction (XRD) to analyze these NTs. Raman spectroscopy was also utilized for further characterization.

The detailed analysis of the quaternary MLCs suggests that $(Sm_xY_{1-x})S\text{-}TaS_2$ NTs were successfully synthesized. The experimental results reveal that the Sm atoms in the SmS subsystem could be replaced by Y atoms for all studied values of x. SAED patterns reveal the c-axis periodicity of pure SmS-TaS2 to be 1.13nm while the c-axis periodicity of pure YS-TaS2 to be 1.10nm. Due to the very similar crystal structure of SmS and YS, the commensurate MLC lattice parameter 'b' is found to shrink by only 0.7% for x = 1 compared to x = 0, while the incommensurate (Sm,Y)S lattice parameter $a(Sm_{1-x}Y_xS)$ shows a linear decrease by 2.7%. The incommensurate TaS_2 lattice parameter $a(TaS_2)$ shows an increase by 0.5%, which is attributed to strain relaxation and which leaves the TaS_2 unit cell area in the a–b plane constant. The non-linear change of the MLC lattice parameters with x and a weak superstructure reflection possibly indicate an incommensurate–commensurate phase transition for the range of Y doping ratios x = 0.2–0.6. The $(Sm_xY_{1-x})S\text{-}TaS_2$ NT layers mostly adopted a superstructure, where adjacent stacks along the c-axis exhibited a fixed relative rotation by 30° with respect to each other. The EDS results show that the composition is homogenous within the cross section of the individual NTs, irrespective of the diameter (and the radius of curvature) of the wall. Spectroscopic analysis by EELS and Raman scattering indicate a complex interplay between the alloying degree on side and the charge transfer and thus the electronic structure as well as the phonon configuration on the other side, giving the possibility to fine tune the MLC properties by alloying the metal in the rock-salt unit of the MLC. Spectroscopic and structural analyses suggest that the characteristics of the quaternary compound is dominated by the heavy samarium atoms even for higher contents of yttrium in the MLC.

References:

[1] [1] M. Serra, R. Arenal, R. Tenne, (2019). Nanoscale 11, 8073-8090.

[2] [2] M.B Sreedhara et al. Chemistry of Materials 2022 34 (4), 1838-1853.

[3] [3] Radovsky et al. (2016). J Mater Chem C 4, 89–98.

[4] [4] S. Hettler et al. (2020), ACS Nano 14, 5, 5445–5458

[5] [5] S. Hettler*, M Furqan* et al. (2025), RSC Advances, 15, 9605-9617.

Acknowledgments:

Research supported by the Spanish MICIU (PID2023-151080NB-I00/AEI/10.13039/501100011033), the Aragon Government (DGA) through the project E13_23R and MICIU with funding from EU Next-Generation (PRTR-C17.I1) promoted by the DGA.

Analysis of Organic Thin-Film Transistors by Transmission Electron Microscopy

Hettler, Simon [*a], Peterlechner, Martin [a], Zschieschang, Ute [b], Klauk, Hagen [b], Eggeler, Yolita M. [a]

[a]Laboratory for Electron Microscopy, Karlsruhe Institute for Technology, Karlsruhe, Germany

[b]Max Planck Institute for Solid State Research, Stuttgart, Germany.

The active material of organic thin-film transistors (TFTs) is a thin, crystalline semiconductor layer of conjugated organic molecules. The TFT performance is predominantly determined by the mobility of carriers in the first few nanometers of the organic-semiconductor layer [1-2]. The orientation and crystallinity of the organic molecules critically influence this mobility, requiring a precise analysis of the structure of the employed organic molecule and the used synthesis conditions to improve the organic TFT performance. As the active channel of the organic semiconductor is confined to the first few nanometers above the dielectric, an analysis by microscopy with high spatial resolution is required to gain meaningful insights in the OTFT devices. In this work, transmission electron microscopy (TEM) and electron diffraction is applied to analyze organic crystals and organic TFTs prepared from state-of-the-art organic semiconductors [1-3], with the aim to resolve the relationship between the performance of the devices and the structure of the organic semiconductor.

Organic crystals were fabricated by thermal vacuum sublimation of the molecules, including pentacene and 2,9-diphenyl-dinaphtho[2,3-b:20,30-f]thieno[3,2-b]thiophene (DPh-DNTT).[3] The employed molecules possess a long axis that agrees with the [001] direction of the crystal. The crystals were deposited both on TEM grids with ultrathin amorphous carbon films and on the gate dielectric of TFT devices (Si substrate, Al gate electrode, AlO_x gate dielectric, organic semiconductor and Au source/drain contacts). A focused ion beam (FIB) was used to prepare cross-section lamellae for TEM analyses of the OTFT devices. TEM measurements and

selected-area electron diffraction (SAED) were performed in an image-corrected Titan microscope (Thermo Fisher Scientific) operated at 300 keV with typical electron doses of below 2 $e^{-}A^{-2}s^{-1}$.

SAED analyses performed on the different organic crystals allow to identify their crystal structure. SAED patterns acquired from pentacene thin films with a thickness of 50 nm reveal that the pentacene crystallized in the 'bulk' phase (COD #4109834). The molecules in the organic crystals are found to 'stand' on the substrate, meaning that the long axis of the molecules, i.e., the [001] direction of the corresponding crystal, agrees with the normal of the substrate. An exception is DPh-DNTT, where a significant amount of the thin film can be found with the long axis being parallel to the substrate surface, indicating that a different growth mechanism can be found.

A TEM analysis of a TEM lamella cross-section prepared from a DPh-DNTT device (see TOC graphic) reveals the expected layers with Si substrate, Al gate electrode, AlO_x gate dielectric, the active organic semiconductor and Au source/drain contacts. Fringes can be seen in the DPh-DNTT layer, whose periodicity is 2.4 nm, corresponding to the [001] interplanar distance of the crystal, thus confirming that the molecules are standing in the first layer of the organic semiconductor, which is the preferred orientation for lateral field-effect transistors.

The TEM analyses reveal considerable differences in the crystal structure of the organic crystals, which is crucial information to understand the carrier mobility in the organic-semiconductor layer and the organic TFT device performances. [4]

References:

[1] Hendrich et al, Adv Synth Catalysis, 363, 549-557, 2021.

[2] Hendrich et al, Adv Synth Catalysis, 363, 1401-1407, 2021.

[3] Kraft et al, Organic Electronics 35, 33-40, 2016.

Acknowledgments:

Funding by the German Research Foundation (DFG) through the collaborative research center CRC 1249 “N-Heteropolycycles as Functional Materials” (Project Number 281029004- SFB 1249, projects C01, C12) is gratefully acknowledged.

TEM-based failure analysis of GaAs/AlGaAs undoped-2DEG semiconductor devices

Maliakkal, Carina Babu [*a], Ahmed Ali, Athique [a], Meucci, Giulia [b], Rabelo Freitas, Helena [a], Genc, Aziz [a], J. Carrad, Damon [b], Reichl, Christian [c, d], Sand Jespersen, Thomas [b], Arbiol, Jordi [a, e]

[a]Catalan Institute of Nanoscience and Nanotechnology Nanotechnology - ICN2, (CSIC and BIST) (ES), [b]Technical University of Denmark (DTU), Denmark, [c]Laboratory for Solid State Physics, ETH Zürich, Zürich, Switzerland, [d]Quantum Center, ETH Zürich, Zürich, Switzerland, [e]ICREA, 08010 Barcelona, Barcelona, Spain.

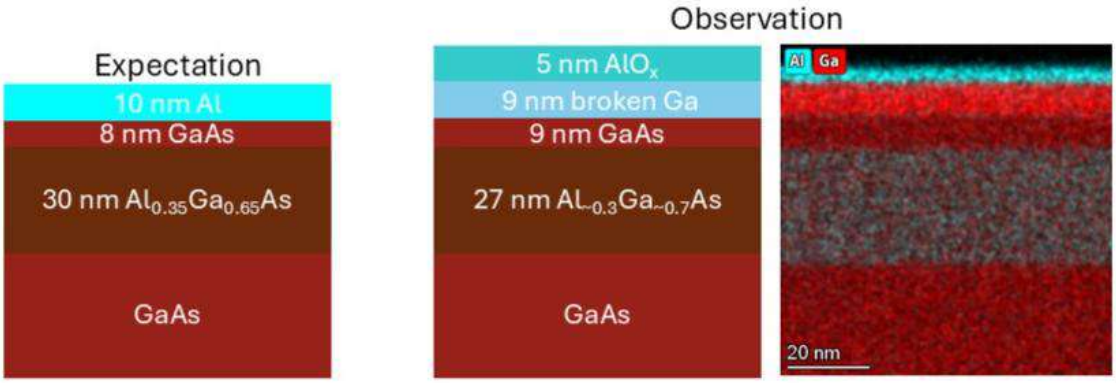

2-dimensional electron gas (2DEG) in GaAs/AlGaAs are one of the most studied systems in condensed matter physics. However, the dopants in such systems acts as scattering centers and impair the mobility.[1] Thus using undoped 2DEG improves the uniformity, in turn decreasing such impurity scattering events.[2] Undoped GaAs/Al0.35Ga0.65As/GaAs heterostructure were grown by Molecular Beam Epitaxy (MBE). An epitaxial layer of Al (with an intended thickness of 10nm) was grown in situ in the MBE chamber itself to act as the gate for inducing and controlling a 2DEG at the GaAs/AlGaAs interface. Clean oxygen was introduced into the MBE loadlock to oxidize the top layer of Aluminium. Parts of this Al layer were selectively etched, and Hall bar devices were fabricated with Ti/Au contacts to characterize the induced 2DEG. However, during electrical characterization, the Al gate was found to be leaky.

Failure analysis was done on the growth sample and device structures using scanning transmission electron microscopy (STEM) after preparing lamellae using a Ga focused ion beam (FIB). The STEM characterization involved various characterization techniques like high angle annular dark field (HAADF) imaging, bright field STEM imaging, energy dispersive X-ray (EDX) mapping, electron energy loss spectroscopy (EELS) mapping. In addition to the GaAs/Al0.35Ga0.65As/GaAs heterostructure, we found a broken layer of metallic Ga above the top GaAs layer,

up to 9 nm in thickness. This was observed not just in the device, but also on the growth sample implying the Ga sheet formation was not due to any high temperature processing during the device fabrication, but was an issue related to the heterostructure growth.

On the basis of EDX, high loss EELS and EELS plasmon peak we also found that the aluminium layer was completely oxidized, leaving no metallic Al to act as the top gate. The Aluminium oxide thickness was consistently less than 5 nm in thickness, implying that the MBE deposited Al thickness was much lesser than the expected 10 nm. This indicates that if a thicker Al layer is grown perhaps there would be some metallic Al remaining in the sample even after the controlled oxidation. The project is in the initial stage currently, but more details of how the growth and device fabrication was improved on the basis of STEM investigation will be presented.

References:

[1] Role of background impurities in the single-particle relaxation lifetime of a two-dimensional electron gas. MacLeod S. J.; Chan K.; Martin T. P.; Hamilton A. R.; See A.; Micolich A. P.; Aagesen M.; P. E. Lindelof. Phys. Rev. B 2009, 80, 035310

[2] Harrell, R. H.; Pyshkin, K. S.; Simmons, M. Y.; Ritchie, D. A.; Ford, C. J. B.; Jones, G. A. C.; & Pepper, M. Fabrication of high-quality one-and two-dimensional electron gases in undoped GaAs/AlGaAs heterostructures. Appl. Phys. Lett. 1999, 74, 2328-2330.

Acknowledgments:

The authors thank Dr. Kapil Gupta for technical support at TEM, and Noèlia Arias for project management.

In-Situ 3D SEM-EDX of Laser-Modified WC-Co Composite Material: Unveiling Oxidation and Surface Topography

Gallero, Enrique [*a, b], Ledesma, Javier [b], Outón, Javier [c, d], Salguero, Jorge [e], Gontard, Lionel C. [a, d]

[a]Department of Condensed Matter Physics, Faculty of Sciences, University of Cadiz. Puerto Real (Spain), [b]Zeppelin Metrology, S.L. Madrid (Spain), [c]Department of Applied Physics, Faculty of Marine and Environmental Sciences, University of Cadiz. Puerto Real (Spain), [d]IMEYMAT: Institute of Research on Electron Microscopy and Materials of the University of Cadiz. Puerto Real (Spain), [e]Department of Mechanical Engineering and Industrial Design, School of Engineering, University of Cadiz. Puerto Real (Spain)

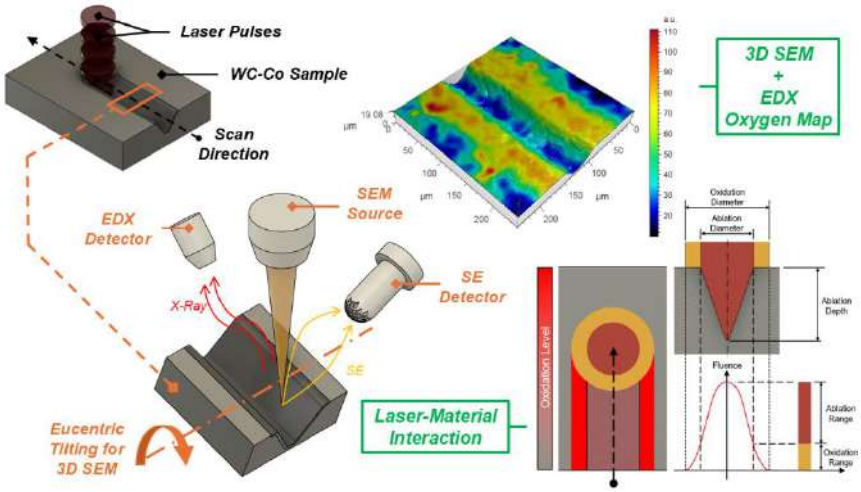

Laser treatments are extensively employed in various applications, including surface modification, material processing, and additive manufacturing. However, the oxidation generated during these processes, whether intentional or unintentional, necessitates careful control due to its potential impact on the material's properties. Beyond alterations in surface topography, laser irradiation can induce significant microstructural and chemical changes, particularly when performed in non-protective atmospheres. This study presents a comprehensive in-situ scanning electron microscopy (SEM) characterization of both the surface topography and the oxidation map resulting from laser single-line scans on a WC-10%Co alloy, a material widely used in cutting tools and tooling where enhanced tribological properties without compromising mechanical integrity are crucial.

Measurements were conducted within the SEM chamber, allowing for direct observation and analysis of the laser-treated surfaces. Surface topography was

quantitatively assessed through stereoscopic reconstructions derived from sequential SEM images acquired at different tilt angles [1]. Concurrently, in-situ energy-dispersive X-ray spectroscopy (EDX) analysis was performed to generate elemental maps, specifically focusing on oxygen distribution. Laser treatments consisted of single-line scans with systematically varied fluence parameter.

The integrated in-situ SEM and EDX approach enabled the simultaneous determination of the ablation diameter, a commonly studied parameter in laser processing [2], and the presence of laser-induced oxidation. An exploration of the relationship between the laser process and surface oxidation can be found in [3]. A novel methodology is proposed for estimating the oxidation diameter based on the spatial distribution of oxygen as revealed by the EDX maps.

The results demonstrate a clear correlation between the laser processing parameters and both the ablation and oxidation diameter. Notably, the spatial profile of the oxidation distribution, exhibited a Gaussian-like profile, mirroring the intensity distribution of the laser beam and the trend observed for the ablation diameter. This suggests that similar models used to predict ablation dimensions can potentially be adapted to estimate the extent of oxidation. The in-situ characterization provides valuable insights into the complex interplay between laser parameters, surface morphology evolution, and oxidation mechanisms in WC-Co alloys, contributing to a better understanding and control of laser surface treatments for this important class of materials.

References:

[1] Krishna, A.V.; Flys, O.; Reddy, V. V.; Rosén, B.G. Surface Topography Characterization Using 3D Stereoscopic Reconstruction of SEM Images. Surf. Topogr. 2018, 6, 2.

[2] Orlandini, A.; Baraldo, S.; Porta, M.; Valente A. Ablation Threshold Estimation for Femtosecond Pulsed Laser Machining of AISI 316L. Procedia CIRP 2022,107, 617-622.

[3] Wu, X.; Shen, J.; Jiang, F.; Wu, H.; Li, L. Study on the Oxidation of WC-Co Cemented Carbide Under Different Conditions. Int. J. Refract. Metals Hard Mater. 2021, 94, 105381.

Acknowledgments:

This work was supported by MCIN/AEI/10.13039/501100011033 and ERDF/EU [grants PID2022 138872OB-I00 EQC2019-005674-P]; the University of Cadiz [grant UCA/REC41VPCT/2022]; and the company Zeppelin Metrology S.L. (Spain).

InCAEM - STEM for In Situ and Correlative Characterization of Energy Materials

Bagués, Núria [*a], Arché-Núñez, Ana [a], Waqas Khaliq, Muhammad [a], Llorens, David [b], Garzón Manjón, Alba [b], Chen, Hui [b], Zhang, Yongchao [b], Garcia de Herreros, Antoni [a], Oró-Solé, Judith [c], Ballesteros, Belén [b], Ruiz-Gómez, Sandra [a], Arbiol, Jordi [b, d], Aballe, Lucía [a]

[a]ALBA Synchrotron Light Source Facility, Cerdanyola del Vallès, Spain, [b]Catalan Institute of Nanoscience and Nanotechnology (ICN2) CSIC and BIST, Barcelona, Spain, [c]Materials Science Institute of Barcelona (ICMAB-CSIC), Barcelona, Spain, [d]ICREA Institució Catalana de Recerca i Estudis Avançats, Barcelona, Spain

The In Situ Correlative Facility for Advanced Energy Materials (InCAEM) project aims to establish a cutting-edge open-access research infrastructure dedicated to advanced energy materials science. Launched in October 2022, InCAEM is a collaborative initiative led by four partner institutions — ALBA Synchrotron, ICN2, ICMAB, and PIC-IFAE — and is expected to be fully operational by the end of 2025. The facility will integrate state-of-the-art instrumentation, infrastructure, and expert personnel to support world-class research aligned with the European Green Deal.

InCAEM will enable true multi-modal and multi-length-scale characterization of functional materials by integrating operando sample environments with complementary characterization tools and advanced data analysis. While scanning transmission electron microscopy (STEM) and scanning probe microscopy (SPM) provide high spatial resolution and diverse contrast mechanisms, X-ray-based techniques offer efficient, highly specific chemical, structural, electronic, and magnetic insights, allowing the study of larger fields of view, thicker samples, and faster processes.

This presentation will introduce the InCAEM project and highlight the opportunities it offers to the scientific user community. We will focus on showcasing new STEM capabilities being installed at the Joint Electron Microscopy Center at ALBA (JEMCA), including a double-aberration-corrected STEM and in situ S/TEM holder systems. These systems enable biasing and temperature control from -160 °C to 800 °C, in situ gas-phase studies up to 2 bar for catalysis, and liquid environments for electrochemical measurements with simultaneous biasing. We will also present the adaptations being developed for various ALBA beamlines, enabling correlative workflows that integrate electron and X-ray microscopy and spectroscopy.

Acknowledgments:

InCAEM is part of the Advanced Materials programme within the Planes Complementarios, launched and funded by the Ministry of Science and Innovation (MCIN) with the support of NextGeneration EU funds (PRTR-C17.I1) and by the Generalitat de Catalunya

Degradation of LCO in aqueous electrolytes through in situ liquid-cell S/TEM

Serra Maia, Rui [*a], Karimi, Maryam [a], Konar, Rajashree [a], Costa, Pedro [a], Ferreira, Paulo [a, b]

[a]International Iberian Nanotechnology Laboratory - INL (PT)

[b]Instituto Superior Técnico

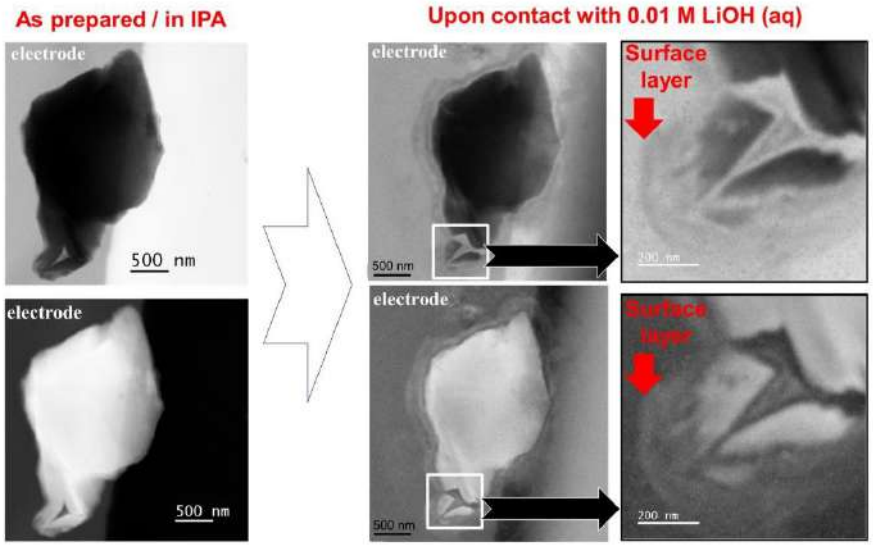

Lithium cobalt oxide (LCO) is a widely used cathode material in lithium-ion batteries [1, 2]. While aqueous electrolytes offer improved safety and lower cost compared to organic counterparts, LCO undergoes rapid degradation in aqueous environments, limiting its commercial viability. The mechanisms by which the LCO degrades remain poorly understood [3, 4].

We use *in situ* scanning/transmission electron microscopy (S/TEM) to directly observe the LCO failure mechanisms in aqueous conditions and their implication during charge-discharge cycling. This real-time approach reveals that degradation is spontaneous and primarily driven by surface dissolution, initiated at fracture sites and regions of increased surface roughness. A porous coating layer forms around LCO particles as they dissolve into the surrounding electrolyte. The rate of dissolution is faster on smaller LCO particles. The dissolution occurs even in the absence of externally applied electrochemical cycling, indicating a chemically driven process [5]. Replacing water by ethanol or IPA eliminated/drastically reduced spontaneous LCO dissolution.

LCO particles expand and contract upon lithiation and delithiation, respectively, which can also be accompanied by shape changes. Larger and thicker particles show milder susceptibility to cycling degradation. Using an aqueous electrolyte and a cathode material without significant air/moisture sensitivity simplified protocol

development while allowing us to obtain in-depth understanding of the challenges associated with *in situ* S/TEM battery studies. This study paves the way for advanced studies of other relevant battery systems in commercially relevant conditions, such organic electrolytes or sensitive air/moisture battery components.

References:

[1] Zhang, S.; Qi, M.; Guo, S.; Sun, Y.; Tan, X.; Ma, P.; Li, J.; Yuan, R.; Cao, A.; Wan, L. Advancing to 4.6 V Review and Prospect in Developing High-Energy-Density LiCoO2 Cathode for Lithium-Ion Batteries. Small Methods 2022, 6 (5), 2200148.

[2] Patnaik, S. Overview of Electrode Advances in Commercial Li-Ion Batteries. Ionics 2024, 30 (6), 3069–3090.

[3] Ramanujapuram, A.; Gordon, D.; Magasinski, A.; Ward, B.; Nitta, N.; Huang, C.; Yushin, G. Degradation and Stabilization of Lithium Cobalt Oxide in Aqueous Electrolytes. Energy Environ. Sci. 2016, 9 (5), 1841–1848.

[4] Pahari, D.; Puravankara, S. Greener, Safer, and Sustainable Batteries: An Insight into Aqueous Electrolytes for Sodium-Ion Batteries. ACS Sustainable Chem. Eng. 2020, acssuschemeng.0c02145.

[5] Serra-Maia, R.; Varley, J. B.; Weitzner, S. E.; Yu, H.; Shi, R.; Biener, J.; Akhade, S. A.; Stach, E. A. Decoupling CO2 Effects from Electrochemistry: A Mechanistic Study of Copper Catalyst Degradation. iScience 2025, 28 (3), 111851.

Acknowledgments:

The authors acknowledge the financial support of the project Moving2Neutrality (M2N), with the reference n.º C644927397-00000038, co-funded by Component C5 – Capitalisation and Business Innovation under the Portuguese Resilience and Recovery Plan, through the NextGenerationEU Fund.

Breaking Miscibility: Temperature-Triggered Phase Separation in Completely Miscible Au–Pd Alloys Uncovered by In-Situ TEM

Roy, Abhijit [*a, b], Hettler, Simon [a, b], Arenal, Raul [a, b, c]

[a]Advanced Microscopy Laboratory (LMA) and Institute of Nanoscience of Aragon (INA) (ES)

[b]Institute of Nanoscience and Materials of Aragon (INMA), CSIC-University of Zaragoza (ES)

[c]ARAID Foundation Zaragoza 50018, Spain

Research on plasmonic noble metal nanomaterials (NMNs) has surged in recent years due to their exceptional optical and electronic properties, which differ markedly from their bulk counterparts. These materials can generate energetic (hot) electrons and holes upon interaction with electromagnetic radiation, enabling them to drive surface chemical reactions under light or electron beam excitation—an ability that holds promise for replacing fossil-fuel-based catalytic processes. [1-3] Among NMNs, bimetallic systems have attracted considerable interest for their enhanced catalytic activity and stability, particularly in heterogeneous reactions.

Au@Pd core–shell nanoparticles and Au–Pd nanoalloys have demonstrated high efficiency in electrocatalytic applications such as ethanol oxidation and hydrogen peroxide (H_2O_2) production, outperforming monometallic Pd catalysts. Au is highly effective in converting alcohols to aldehydes, whereas Pd is superior in oxygen reduction reactions. Alloying Au and Pd can overcome the individual limitations of each metal. However, the resulting alloys often exhibit reduced electrochemical potentials compared to their monometallic counterparts, which can limit catalytic efficiency. [4]

To address this, a bimetallic nanostructure with intrinsic phase separation, wherein oxidation and reduction reactions are spatially segregated across distinct domains of a single nanoparticle. Such phase-separated systems preserve the intrinsic catalytic properties of each metal while enabling synergistic interactions at their interface. This architecture is known to enhance both activity and long-term stability. However, forming phase-separated Au–Pd nanoparticles is challenging due to their complete miscibility across all compositions and temperatures, as predicted by the bulk phase diagram. Phase separation in bimetallic systems typically requires a lattice mismatch >5%, which is absent in Au–Pd combinations. [5]

Although theoretical studies have suggested a potential miscibility gap in the nanoscale regime, direct experimental evidence for temperature-induced phase separation in Au–Pd nanostructures remains scarce. Prior studies, including those by Okamoto et al. and Wu et al., have reported alloy formation across a wide composition range, even under high-temperature annealing. [6-7] Other reports, such as that by Precot et al., suggest size-dependent segregation behavior driven by Ostwald ripening, yet clear in situ observations of phase separation within individual Au–Pd nanoparticles are lacking. [8]

In this work, we synthesize Au nanotriangles (AuNTs) via a seedless method and coat them with Pd layers of varying thickness by adjusting the concentration of H_2PdCl_4. In situ high-resolution transmission electron microscopy (HRTEM) and selected area diffraction (SAD) were performed using an image-corrected FEI TITAN at 300 kV, while elemental mapping and composition analysis were conducted using high-resolution STEM and EDS on a probe-corrected system. For in-situ heating, we used a DENS Solutions Wildfire MEMS-based double-tilt holder with Si_xN_Y membranes, capable of reaching 1300 °C.

A detailed investigation of AuNT and AuNT@Pd nanostructures revealed various interfacial defects—such as stacking faults and dislocations—within the Pd shell. Upon in situ annealing, distinct melting behavior was observed: the melting point increased with Pd content, confirming Pd's stabilizing effect. Most significantly, we observed temperature-induced phase separation within Au–Pd alloy nanotriangles, forming Au-rich and Pd-rich domains. This was verified by HRTEM and EDS mapping. At elevated temperatures, Pd atoms migrated outward due to their higher mobility, while Au atoms moved inward, leading to a stable, phase-separated configuration. [9]

This phase-separated state remained stable even after prolonged storage at room temperature, as confirmed by EDS spectra collected a year post-synthesis. These findings offer critical insight into the thermodynamic behavior of nominally miscible bimetallic systems at the nanoscale and pave the way for designing phase-

engineered nanocatalysts with enhanced bi-functional activity and long-term durability.

References:

[1] Eustis, S.; El-Sayed, M. A. Why gold nanoparticles are more precious than pretty gold: Noble metal surface plasmon resonance and its enhancement of the radiative and nonradiative properties of nanocrystals of different shapes. Chem. Soc. Rev., 2006,35, 209-217

[2] Roy, A.; Maiti, A.; Chini, T.K.; Satpati, B. Annealing Induced Morphology of Silver Nanoparticles on Pyramidal Silicon Surface and Their Application to Surface-Enhanced Raman Scattering. ACS Appl. Mater. Interfaces 2017, 9, 39, 34405–34415

[3] Jain, P.K. Taking the Heat Off of Plasmonic Chemistry. J. Phys. Chem. C 2019, 123, 40, 24347–2435

[4] Qiu, J.; Ngyuen, Q. N.; Lyu, Z. Bimetallic Janus Nanocrystals: Syntheses and Applications. Wang, Q.; Xia, Y.; Adv. Mater. 2022, 34, 2102591

[5] Lim, B.; Jiang, M.; Camargo, P. H. C.; Eun, C. C.; Tao, J.; Lu, X.; Zhu, Y.; Xia, Y. Pd-Pt Bimetallic Nanodendrites with High Activity for Oxygen Reduction. Science. 2009, 324, 1302-1305.

[6] Okomato, H.; Massalski, T. B. The Au–Pd (Gold-Palladium) system. Bull. Alloy Phase Diagrams. 1985, 6, 229-235.

[7] Wu, Z.; Tang, M.; Li, X.; Luo, S.; Yuan, W.; Zhu, B.; Zhang, H.; Yang, H.; Gao, Y.; Wang, Y. Surface faceting and compositional evolution of Pd@Au core–shell nanocrystals during in situ annealing. Phys. Chem. Chem. Phys., 2019,21, 3134-3139

[8] Prevot, G.; Ngyune, N. T.; Alloyeau, D.; Ricolleau, C.; Nelayah, J. Ostwald-Driven Phase Separation in Bimetallic Nanoparticle Assemblies. ACS Nano 2016, 10, 4, 4127–4133

[9] Roy, A.; Hettler, S.; Arenal. R. Direct Visualization of Temperature-Induced PhaseSeparation of Completely Miscible Au–Pd Alloy by In SituTEM. Small 2025, 21, 2408109

Acknowledgments:

This work was supported by funding from the EU Horizon 2020 programme (MSCA: GA No.101109165), the Spanish MICIU (PID2023-151080NB-I00/AEI/10.13039/501100011033, and CEX2023-001286-SMICIU/AEI/10.13039/501100011033), and by the DGA project E13-23R. The National Centre for Electron Microscopy (ELECMI, Spanish National Singular

Scientific and Technological Facility, MICIU) is also acknowledged for provision of access to corrected aberration microscopy facilities through ELECMI Competitive Open Access Protocol (Project No: Elecmi 463). The studies were conducted at the Laboratorio de Microscopias Avanzadas (LMA), U. Zaragoza, Spain.

Correlative In-Situ Liquid Cell Electron Microscopy of faceted HEA-Zr Nanoparticles used for electrocatalysis

Pal, Avnish Singh [*a], Guha, Puspendu [a], Deepak, Francis [a]

[a]International Iberian Nanotechnology Laboratory-INL Braga, Portugal

The demand for real-time, nanoscale materials characterization has long challenged the capabilities of **Transmission Electron Microscopy (TEM)**. Conventionally, TEM has been confined to the analysis of solid-state specimens, providing high-resolution imaging in dry, high-vacuum environments. This vacuum requirement precludes the direct investigation of liquid-phase systems, making it difficult to capture dynamic processes occurring in solution. Consequently, in-situ/operando observation of liquid-based phenomena has remained a persistent limitation in TEM applications. The advent of **liquid cell in-situ TEM holders** has transformed this landscape, enabling the direct visualization of samples in liquid environments [1, 2, 3]. These specialized holders sandwich a thin liquid layer between electron-transparent membranes (SiN), maintaining the liquid state even under vacuum. Recent innovations in liquid cell technology have greatly broadened the scope of TEM applications in areas, i.e., electrochemistry [1], photochemistry, corrosion, electroplating [3], electrocatalysis [2], battery and fuel cell materials [4], as well as biomedical applications. Furthermore, integrating analytical techniques like **Energy-Dispersive X-ray Spectroscopy (EDS)** [1] and **Electron Energy Loss Spectroscopy (EELS)** [4] within the liquid cell environment provides valuable insights into the elemental composition and electronic structure of materials, significantly enhancing the analytical capabilities of in-situ TEM. In this presentation, we employed both conventional and in-situ electrochemical testing on faceted high-entropy alloy (HEA) **CoFeNiRuZr-Pt nanoparticles decorated on graphene flakes**. These HEA nanoparticle-decorated graphene flakes were deposited onto a microfabricated chip designed specifically for in-situ liquid electron microscopy. **Cyclic voltammetry (CV)** was conducted both outside the microscope under ambient conditions and within the TEM itself. This approach enabled a direct correlation between the nanoparticles' electrochemical behaviour and their structural and compositional evolution at the nanoscale. In addition, morphological changes in the faceted HEA nanoparticles were also examined during the in-situ observations. The HEA nanoparticles were observed to undergo a phase transformation when an electric potential was applied. At the same time the particles are also been observed to undergo a morphological transition.

References:

[1] Nejc Hodnik, Gerhard Dehm, Karl J. J. Mayrhofer Importance and Challenges of Electrochemical in Situ Liquid Cell Electron Microscopy for Energy Conversion Research, Acc. Chem. Res. 2016, 49, 2015−2022.

[2] Franklin (Feng) Tao, Peter A. Crozier Atomic-Scale Observations of Catalyst Structures under Reaction Conditions and during Catalysis, Chemical Reviews 2016 116 (6), 3487-3539

[3] Rui Serra-Maia Rui Serra-Maia, Pawan Kumar, Andrew C. Meng, Alexandre C. Foucher, Yijin Kang, Khim Karki, Deep Jariwala, Eric A. Stach, Nanoscale Chemical and Structural Analysis during In Situ Scanning/Transmission Electron Microscopy in Liquids, ACS Nano 2021, 15(6), 10228–10240.

[4] Ziying Wang, Dhamodaran Santhanagopalan, Wei Zhang, Feng Wang, Huolin L. Xin, Kai He, Juchuan Li, Nancy Dudney, and Ying Shirley Meng, In Situ STEM-EELS Observation of Nanoscale Interfacial Phenomena in All-Solid-State Batteries, Nano Letters 2016 16 (6), 3760-3767

Acknowledgments:

We acknowledge the financial support of the Innovation Pact "Moving2Neutrality", with the reference n.º 644927397-00000038, co-funded by Component C5 – Capitalisation and Business Innovation under the Portuguese Resilience and Recovery Plan, through the NextGenerationEU Fund. The authors also acknowledge Rui Serra-Maia from INL-Braga, Portugal.

Atomic-Scale Dual-Atom Detection for Lithium–Sulfur Battery Catalysts via Advanced STEM Techniques

YU, JING [*a, b], Arbiol, Jordi [a], Cabot, Andreu [b]

[a]Catalan Institute of Nanoscience and Nanotechnology (ICN2), CSIC and BIST, Campus UAB, Barcelona, Spain

[b]IREC, Catalonia Institute for Energy Research, C/ Jardins de les Dones de Negre 1, Barcelona 08930, Spain

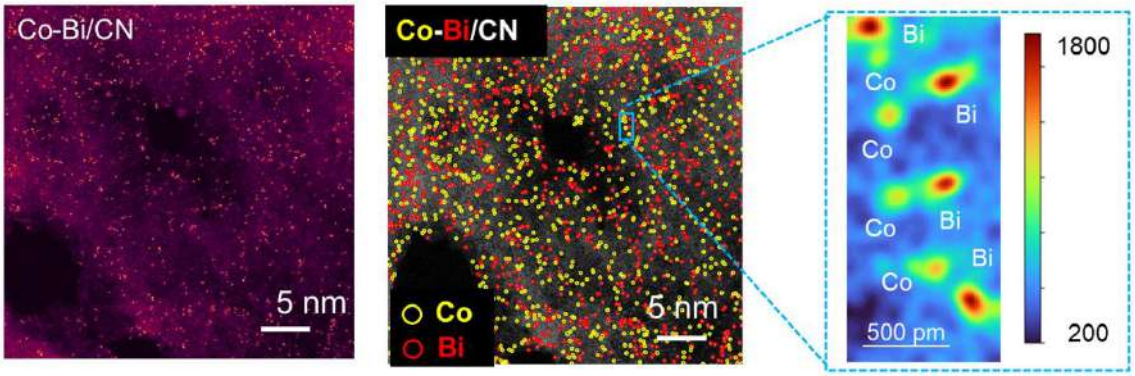

Understanding the precise atomic configuration of active sites is pivotal for unraveling catalytic mechanisms in lithium–sulfur (Li–S) batteries. Particularly, dual-atom catalysts (DACs) have emerged as promising candidates due to their synergistic electronic interactions and high catalytic activity.[1] However, direct observation and unambiguous identification of dual-atom configurations remain challenging due to their low loading and potential overlap with background signals. Here, we present an advanced atom detection strategy combining aberration-corrected scanning transmission electron microscopy (AC-STEM) with statistical atom counting and machine learning-assisted image analysis to reliably detect and distinguish dual metal sites within a sulfur-host framework. Utilizing high-angle annular dark-field (HAADF) imaging, we achieve sub-angstrom resolution that enables the visualization of isolated and paired atomic columns. The approach is validated on a Co–Bi dual-atom catalyst embedded in nitrogen-doped carbon, designed to regulate the polysulfide redox reaction in Li–S batteries. Our results reveal the spatial correlation and bonding environment of dual atoms, with electronic structure insights supported by electron energy loss spectroscopy (EELS) and density functional theory (DFT). This work offers a robust pathway for

detecting and characterizing dual-atom motifs, facilitating the rational design of next-generation sulfur cathode catalysts and advancing the atomic-level understanding of complex energy systems.

References:

[1] C. Li, J. Yu, D. Yang, H. Li, Y. Cheng, J. Wang, Y. Ren, X. Bi, J. Ma, R. Zhao, Y. Zhou, J. Wang, C. Huang, J. Li, I. Pinto-Huguet, J. Arbiol, H. Zhang, S. Xin, A. Cabo, Balancing Electronic Spin State via Atomically-Dispersed Heteronuclear Fe-Co Pairs for High-Performance Sodium-Sulfur Batteries, J. Am. Chem. Soc. 2025, 147, 10, 8250–8259.

Acknowledgments:

J.Y. thank the China Scholarship Council for the financial support. The authors acknowledge the use of instrumentation as well as the technical advice provided by the Joint Electron Microscopy Center at ALBA (JEMCA).

Atomic-Scale Insights into Ba-Doped $LiOCl_3$ Anti-Perovskite Electrolytes for Solid-State Batteries

Pradeepkumar, Maurya Sandeep [a], Mohan, Meera [a], Braga, M. Helena [b], Leonard Deepak, Francis [*a]

[1]International Iberian Nanotechnology Laboratory (INL), Braga-4715-330, Portugal

[2]Faculty of Engineering, University of Porto, 4200-465, Porto, Portugal

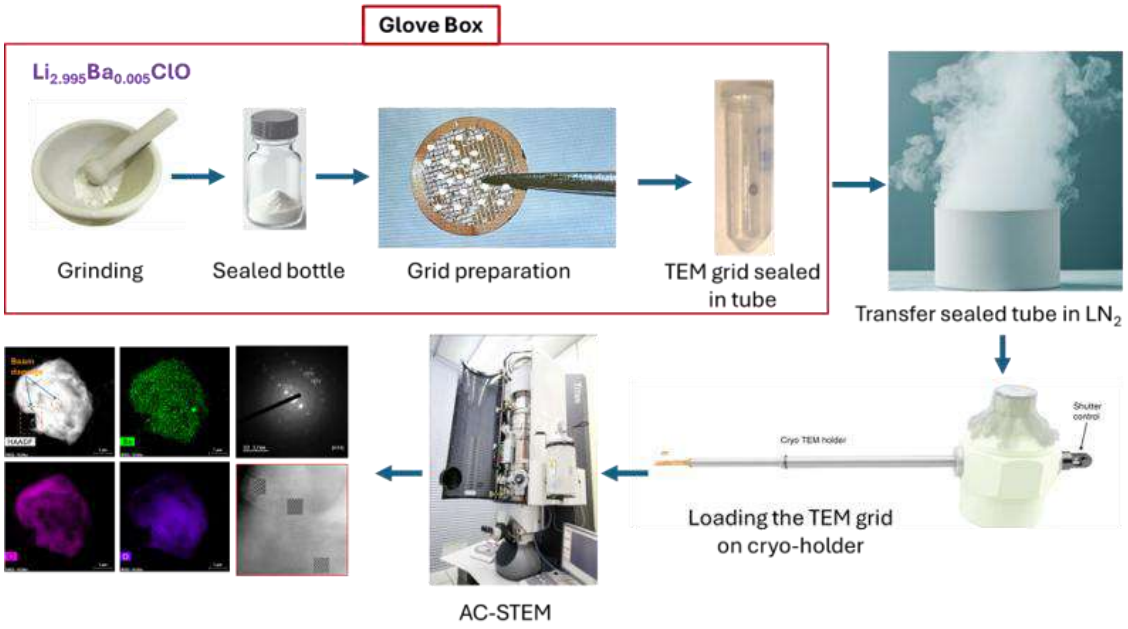

Solid-state batteries offer significant advantages, but their commercial adoption is limited by the poor ionic conductivity of solid electrolytes at practical temperatures and their inadequate stability with lithium metal. In the present work, Ba doped $Li_{2.99}Ba_{0.005}OCl$ a glassy electrolyte with anti-perovskite structure, exhibiting ultra-fast ionic conductivity, was synthesized and investigated [1]. To study the effect of Ba doping in Li_3OCl, aberration-corrected scanning/transmission electron microscopy (AC-S/TEM) was employed to observe lattice distortions caused by the larger ionic radius of Ba^{2+} compared to Li^+, which may induce phase instability, defect formation, or secondary phase precipitation if the doping limit is exceeded.

Initial TEM imaging was performed under low-dose conditions; however, radiation damage was still observed. To mitigate this, a cryo-holder was employed in combination with low-dose techniques, significantly reducing beam-induced damage. This enabled the successful acquisition of high-resolution TEM (HR-TEM) images, where lattice fringes were clearly resolved. High-resolution STEM (HRSTEM) images were obtained using an aberration-corrected STEM (AC-STEM) instrument, which has clear evidence of lattice distortion. Selected area electron diffraction

(SAED) confirmed that $Li_{2.99}Ba_{0.005}OCl$ adopts a cubic structure with space group Pm-3m, indicating that some clusters are single crystalline. However, SAED patterns revealed that most clusters are polycrystalline, with multiple grain orientations present within individual cluster. TEM images further confirmed that these clusters are approximately micron sized. STEM–EDX mapping revealed the successful incorporation of Ba into the Li_3OCl matrix. Additionally, electron energy loss spectroscopy (EELS) provided insights into the chemical environment and bonding characteristics of Ba within the Li_3OCl structure.

[1] M.H. Braga, J.A. Ferreira, V. Stockhausen, J.E. Oliveira, A. El-Azab, Novel Li 3 ClO based glasses with superionic properties for lithium batteries, J. Mater. Chem. A 2 (2014) 5470–5480. https://doi.org/10.1039/C3TA15087A.

References:

[1] [1] M.H. Braga, J.A. Ferreira, V. Stockhausen, J.E. Oliveira, A. El-Azab, Novel Li 3 ClO based glasses with superionic properties for lithium batteries, J. Mater. Chem. A 2 (2014) 5470–5480

Acknowledgments:

This work is a result of the Innovation Pact “NGS - New Generation Storage” (C644936001-00000045), by “NGS” Consortium, co-financed by NextGeneration EU, through the Incentive System “Agendas para a Inovação Empresarial” (“Agendas for Business Innovation”), within the Recovery and Resilience Plan (PRR)

Composition-Strain Correlation in 2D Metal-Halide Perovskite Lateral Heterostructures: A 4D-STEM Study

Khabbazabkenar, Sirous *[a], Schleusener, Alexander [b], Faraji, Mehrdad [b], Krahne, Roman [b], Divitini, Giorgio [a]

[a]Istituto Italiano di Tecnologia, Electron Spectroscopy and Nanoscopy, Genova 16163, Italy.

[b]Istituto Italiano di Tecnologia, Optoelectronics, Genova 16163, Italy.

Organic-metal halide perovskites, with a metal-halide octahedral framework separated by organic cations, offer tunable electronic properties, making them appealing for optoelectronic applications [1]. Their soft crystal lattice allows greater tolerance to lattice mismatch, making them promising for heterostructure formation [2]. Fabrication of in-plane heterostructures with varying halide composition in 2D lead-halide perovskites forms spatially separated halide phases with different band gaps, enabling additional control on charge carrier mobility [1].

Objectives

To understand how strain and composition in 2D-layered perovskite lateral heterostructures affect electronic structure and material stability, we combine compositional data from STEM-EDX, and strain maps from 4DSTEM diffraction patterns. We focus on how lattice parameters evolve across the heterostructure, as the composition transitions from chloride to bromide to iodide phases. Insight into the local crystallography will enable optimization of structural and electronic properties for optoelectronic applications.

Materials & Methods

Heterostructures were prepared via a solution-based process in microcrystalline phenethylammonium lead-halide 2DLPs, leading to PEA_2PbCl_4–PEA_2PbBr_4–PEA_2PbI_4 heterostructures. Four-dimensional scanning transmission electron microscopy (4D-STEM) datasets were acquired in microprobe mode on an aberration-corrected ThermoFisher Spectra 300 S/TEM, operated at 300 kV and a semi-convergence angle of 0.5 mrad. Strain mapping was performed using Digital Micrograph by analyzing the 4D-STEM dataset. Compositional information was extracted from Energy-Dispersive X-ray (EDX) signal collected on a Dual-X system.

Results

EDX revealed that the bromide phase exhibits an almost pure composition, with a Pb:Br ratio close to $PbBr_4$. However, compositional line profiles identified a degree of intermixing in the other two phases (chloride-rich core and iodide-rich shell); we also identified a gradual interface between the chloride core and bromide phase but a sharp interface between the bromide and iodide layers (Fig 1a-g).

Low dose (~e/A2) 4D-STEM measurements showed that the crystallinity was preserved across the entire heterostructure, with a change in diffraction patterns upon transition from the interfaces (Fig 1h-k). Furthermore, the strain mapping results revealed a distinct variation in lattice constants across the heterostructure, reflecting the composition-dependent lattice mismatch. Taking the bromide phase as the strain-free reference, the chloride phase exhibited a compressive lattice distortion relative to the bromide phase. Conversely, the iodide phase showed an expansion (Fig 2a-c). These findings were qualitatively consistent with the relative lattice constants expected for the three pure phases, where the chloride phase has a smaller d-spacing and the iodide phase has a larger d-spacing compared to the bromide phase (Fig 2d-f). However, the reduced difference in plane spacings compared to the relaxed phase-pure values suggests that local alloying occurs selectively and moderates lattice mismatch.

Conclusion

We mapped local d-spacing variations against a bromide-phase reference to visualize strain across the heterostructure. Combining 4D-STEM strain mapping with EDX spectroscopy revealed structural evolution and its link to composition. These insights clarify how heterostructures achieve tunable band gaps.

References:

[1] A. Schleusener et al., Heterostructures via a Solution-Based Anion Exchange in Microcrystalline 2D Layered Metal-Halide Perovskites. Advanced Materials, 2024. 36(31).

[2] E. Shi et al., Two-dimensional halide perovskite lateral epitaxial heterostructures. Nature, 2020. 580: p. 614-620.

Optimised earth abundant electrodes for energy storage applications

Spadaro, M. Chiara [*a, b, c], Russo, Daniela [b], Fischetti, Alessia [a, b], Mineo, Giacometta [a, b], Lentini-Campalleggio, Claudio [a, b], Bruno, Elena [a, b], Grimaldi, Maria Grazia [a, b], Salutari, Francesco [c], Arbiol, Jordi [c, d], Franzò, Giorgia [b], Mirabella, Salvo [a, b], Strano, Vincenzina [b]

[a]Physics and Astronomy Department, University of Catania, S. Sofia 64, Catania I-95123, Italy

[b]National Research Council, Institute of Microelectronics and Microsystems (CNR-IMM), Catania-University building, S. Sofia 64, I-95123 Catania, Italy

[c]Catalan Institute of Nanoscience and Nanotechnology (ICN2), CSIC and BIST, Campus UAB, Barcelona, Spain

[d]ICREA, Pg. Lluís Companys 23, 08010 Barcelona, Catalonia, Spain

There is an urgent need to implement the energy sector with earth abundant and sustainable strategies to minimize the environmental impact of current approaches. In this direction, electrochemical devices have a primary role for both producing and storing energy, such as supercapacitors that demonstrated to have high power density, although effort needs to be devoted to improve their energy density [1,2]. Here, nanostructured materials are promising candidate being able to increase the specific capacitance of the system by increasing the active surface area. Furthermore, the use of earth abundant elements is mandatory to ensure an all-in-one solution, avoiding side and undesired effects/products that could be harmful for the sustainability of our planet. Transition metal based devices demonstrated to be the optimal choice thanks to their optoelectronic properties and the possibility to easily prepare them in form of nanostructures with green chemistry approaches [3]. In this work, we will describe the preparation and in-depth investigation of Zn-based nanostructures, with particular attention to the correlation of the measured electrochemical performance with their structure, composition and optical properties. We will demonstrate that Zn-based electrodes are a promising material to face the energy transition in the near future.

References:

[1] He, G. et al, Joule, 5, 2, 2021, Pages 379-392

[2] Wu, Z., et al. (2016). Transition Metal Oxides as Supercapacitor Materials. Nanomaterials in Advanced Batteries and Supercapacitors. Nanostructure Science and Technology. Springer, Cham

[3] Strano, V. et al, J. Phys. Chem. C 2014, 118, 48, 28189−28195

Acknowledgments:

This work was funded by SAMOTHRACE ("Sicilian MicronanoTech Research And Innovation Center - SAMOTHRACE"), ECS_00000022, MUR. leader di Spoke 1.

Comparative Analysis of In-situ STEM Techniques in the Reduction Study of CeO_2-Based Catalysts

Piedra, Irene [a], Manzorro, Ramón [a], Nuez, Rafael [a], López-Haro, Miguel [a], Pérez-Omil, José Antonio [a], Calvino, José Juan [a], Hungría, Ana Belén [*a]

[a]Departamento de Ciencias de los Materiales e Ingeniería Metalúrgica y Química Inorgánica, Facultad de Ciencias, Universidad de Cádiz, Campus Río San Pedro S/N, Puerto Real, 11510 Cádiz, Spain

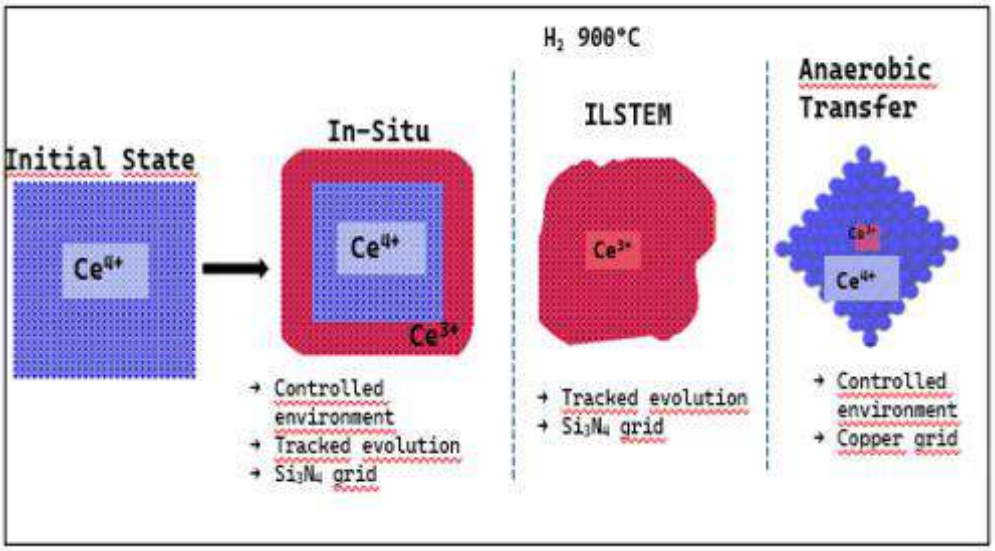

Cerium oxide has been widely studied, mainly because of its ability to rapidly and reversibly switch between Ce^{3+} and Ce^{4+} oxidation states within a cubic structure, facilitating reversible oxygen exchange with its surroundings[1]. Furthermore, the incorporation of noble metals, such as platinum, improves these redox properties by promoting the formation and mobility of oxygen vacancies[2].

In the study of the reduction of cerium oxide based catalyst, conventional transmission electron microscopy (TEM) procedures involve treating the sample in a quartz reactor outside the microscope, and then it is exposed to the air during transfer, grid assembling and inserting into the microscope using a standard sample holder. However, this approach has several limitations; i) potential changes in the oxidation state and ii) difficulties in tracking all the structural and chemical changes having place. To overcome this, performing in-situ experiments using specialized TEM holders[3] has emerged as a widely used, powerful and increasingly recognized technique. These experiments enable to track changes in real-time by recreating the reaction environment. This is achieved by using ultrathin silicon nitride windows to seal the sample in a tiny chamber where gases can flow while increasing the temperature, simulating real reaction conditions[4].

Alternatively, there are complementary techniques that partially address these limitations. On the one hand, ILSTEM involves analyzing the exact same spot on a catalyst before and after a reaction[5]. The catalyst is first loaded on a silicon nitride grid, examined under the microscope and then loaded into a quartz reactor. After the reaction, it is brought back to the microscope to study the same area again. On the other hand, another useful strategy is transferring the catalyst directly from a reactor to the microscope without exposure to air (anaerobic transfer)[6]. This is done by sealing the reactor after the reaction, moving it inside a glovebox with an inert atmosphere and loading it on a copper microscopy grid. From there, a special transfer holder keeps the sample isolated from the atmosphere until it's inside the microscope.

In our work, we propose to study the reduction of Pt/PrOx@CeO_2 nanocubes with the above mentioned techniques, to compare the results obtained of each approach. The oxidation state has been analyzed by means of EELS following the Ce-$M_{4,5}$ edge signal.

In the ILSTEM experiments initial surface reduction is observed at 500ºC and becomes more pronounced at 700ºC. By 900ºC, the nanocubes are fully reduced and have totally lost their original morphology. In anaerobic transfer experiments after reducing at 900ºC, most regions do not exhibit clear reduction, except for a few areas where some patches show signs of reduction and the morphology has transitioned to polyhedral particles close to octahedra. The in-situ experiments under a reducing atmosphere with H_2 reveal that surface reduction begins at 450ºC and progresses with temperature, becoming clearly visible by 850ºC. The reduction propagates from surface to bulk, creating a Ce^{3+} shell. Apart from this finding, no major morphological changes are observed except for a slight rounding of the edges.

The observed differences in reduction behavior and morphology among these approaches suggest that the interaction between the sample and the Si_3N_4 window may affect the catalyst reduction, potentially triggering a cerium diffusion or altering the local chemical environment. Overall, these results highlight how the intrinsic variables of each technique can influence the outcomes, stressing the importance of considering multiple perspectives in order to achieve accurate conclusions during in-situ experiments.

References:

[1] Trovarelli, A. Catalytic properties of ceria and CeO2-Containing materials. Catal Rev Sci Eng 38, (1996).

[2] Lee, J. et al. How Pt Influences H2 Reactions on High Surface-Area Pt/CeO2 Powder Catalyst Surfaces. JACS Au 3, (2023).

[3] Yaguchi, T., San Gabriel, M. L., Hashimoto, A. & Howe, J. Y. In-situ TEM study from the perspective of holders. Microscopy vol. 73 (2024)

[4] Qu, J., Sui, M. & Li, R. Recent advances in in-situ transmission electron microscopy techniques for heterogeneous catalysis. iScience vol. 26 (2023)

[5] Chinchilla, L. et al. Temperature-driven evolution of ceria-zirconia-supported AuPd and AuRu bimetallic catalysts under different atmospheres: insights from IL-STEM studies. Nanoscale 16, (2023)

[6] Kooyman, P. J., Hensen, E. J. M., De Jong, A. M., Niemantsverdriet, J. W. & Van Veen, J. A. R. The observation of nanometer-sized entities in sulphided Mo-based catalysts on various supports. Catal Letters 74, 49–53 (2001).

Acknowledgments:

Project PID2022-142312NB-I00 funded by Ministerio de Ciencia, Innovación y Universidades. Cofinanciado por la Unión Europea. Agencia Estatal de Investigación.

From Nano to Micro Scales: Probing Multi-Element Redox Dynamics in Sodium Manganese Oxide for Sodium-Ion Batteries Using SEM and TEM

Sun, Mingqing [*a], Arbiol, Jordi [*a]

[a]Catalan Institute of Nanoscience and Nanotechnology Nanotechnology (ICN2) (ES)

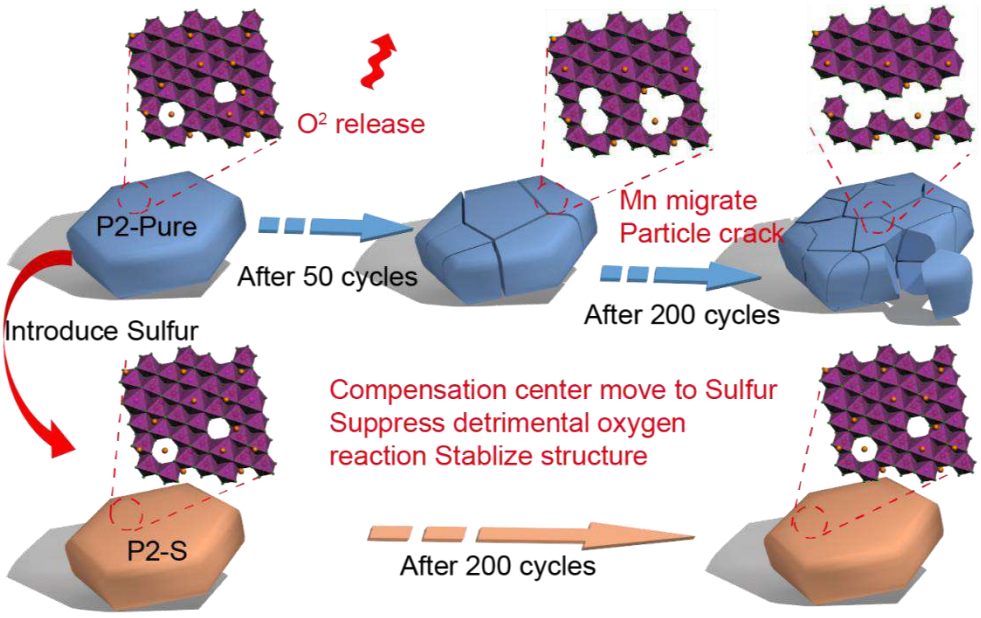

Text of the abstract:

Sodium-ion batteries (SIBs) are receiving increasing attention due to the abundance of sodium resources and their wide distribution compared to their lithium counterparts. Benefiting from the environment-friendly and cost-effective manganese resources, as well as a high theoretical specific capacity of 265 mAh g^{-1}, P2-type layered $Na_xMn_yO_2$ cathode exhibits great potential in SIBs community. However, given that the complexity of the battery system, the practical cathodic reaction mechanism is inherently complicated by several factors such as mass loading, particle size, interfacial deposition, charge transfer, electrolyte and diaphragm, which hinders the application of the P2 type layered $Na_xMn_yO_2$ in

sodium-ion batteries. Furthermore, these factors affect the cathodic reaction mechanism across multiple scales, from nano to micro scales, thereby completing the analysis. However, elucidation of the actual cathode reaction and degradation mechanisms is essential for optimizing cathode performance and developing sodium-ion batteries with high energy density and long cycle life.

In this study, we employ a comprehensive nano-to micro-to macro-length characterizations approach that combines Scanning Electron Microscopy (SEM), High Resolution-Transmission Electron Microscopy (TEM), *in-situ* X-ray diffraction (XRD), *in-situ* pair distribution function (PDF) analysis, *in-situ* Raman spectroscopy and *in-situ* differential electrochemical mass spectrometry (DEMS). This integrated characterization strategy provides a holistic understanding of the reaction mechanisms at the cathode of sodium-ion batteries. This work elucidates the degradation mechanism of the P2-type layered Na_xMn_yO2 cathode combining global structure and local-structure analysis that manganese atom migration induces severe phase transitions that lead to intense particle cracking after long-term cycling. To further analysis the origin of the manganese atom migration, HAADF, HR-TEM, *in-situ* Raman and *in-situ* DEMS techniques were employed to probe the anionic-redox reaction evolution from the local-scale to overall scale during battery cycling process. It was found that part oxygen released from $Na_xMn_yO_2$ at the sodium-deficient state, and these oxygen releases originate from an irreversible oxygen reaction, leading to a deterioration of its cyclic stability. Based on this finding, this work proposes a sulfuration approach to stabilize the $Na_xMn_yO_2$ structure, as sulfur anions are partially integrated into the oxygen sites within the lattice structure. Impressively, the oxygen redox reaction is significantly inhibited due to the higher gasification temperature of sulfur compared to oxygen. The sulfur anions within the internal lattice could reversibly participate in the muti-elements redox process and improve the integral coordination stability by mitigating undesired manganese migration. Moreover, after several cycles, there are no significant cracks in the material particles with sulfuration compared to the unmodified material. Consequently, the modified P2-$Na_xMnO_{2-y}S_y$ exhibits remarkably long-term cycling stability of >1000 cycles with 98% capacity retention at 0.5 A g^{-1} compared to the unmodified P2 sample which retains only 18% of its capacity after 1000 cycles. Our work not only reveals the degradation mechanism of the P2-type layered $Na_xMn_yO_2$ cathode but also presents a pathway for designing long-cycle-life SIB cathode materials.

References:

[1] Jin, T.; Wang, P.-F.; Wang, Q.-C.; Zhu, K.; Deng, T.; Zhang, J.; Zhang, W.; Yang, X.-Q.; Jiao, L.; Wang, C. Realizing Complete Solid-Solution Reaction in High Sodium

Content P2-Type Cathode for High-Performance Sodium-Ion Batteries. Angewandte Chemie International Edition 2020, 59 (34), 14511–14516.

[2] Chu, S.; Guo, S.; Zhou, H. Advanced Cobalt-Free Cathode Materials for Sodium-Ion Batteries. Chem. Soc. Rev. 2021, 50 (23), 13189–13235.

[3] Wang, C.; Liu, L.; Zhao, S.; Liu, Y.; Yang, Y.; Yu, H.; Lee, S.; Lee, G.-H.; Kang, Y.-M.; Liu, R.; Li, F.; Chen, J. Tuning Local Chemistry of P2 Layered-Oxide Cathode for High Energy and Long Cycles of Sodium-Ion Battery. Nat Commun 2021, 12 (1), 2256

[4] Zuo, W.; Qiu, J.; Liu, X.; Ren, F.; Liu, H.; He, H.; Luo, C.; Li, J.; Ortiz, G. F.; Duan, H.; Liu, J.; Wang, M.-S.; Li, Y.; Fu, R.; Yang, Y. The Stability of P2-Layered Sodium Transition Metal Oxides in Ambient Atmospheres. Nat Commun 2020, 11 (1), 3544

[5] Wang, C.; Liu, L.; Zhao, S.; Liu, Y.; Yang, Y.; Yu, H.; Lee, S.; Lee, G.-H.; Kang, Y.-M.; Liu, R.; Li, F.; Chen, J. Tuning Local Chemistry of P2 Layered-Oxide Cathode for High Energy and Long Cycles of Sodium-Ion Battery. Nat Commun 2021, 12 (1), 2256.

Acknowledgments:

This work was supported by the National Natural Science Foundation of China (Nos. 52272218 H.X.), the Jiangsu Province Carbon Peak and Neutrality Innovation Program (Industry tackling on prospect and key technology, No. BE2022002-4 H.X.). All authors thank the Nanjing University of Science and Technology for XRD and FESEM measurements, and the Shanghai Synchrotron Radiation Facility for PDF characterizations, the ALBA Synchrotron Facility for XAS characterization, the JEMCA for HAADF characterization.

Exploring the Electrocatalytic, Photoelectrocatalytic, and Structural Properties of Metal@MoS_2 Core-Shell Nanostructures

Lajaunie, Luc [*a], Medina Olivera, Antonio Jesus [a], Maynau, Céline [a], Valero Hernández, Conrado [a], Manzorro, Ramón [a], Hungría, Ana [a], Hernández Garrido, Juan Carlos [a]

[a]Departamento de Ciencia de los Materiales e IM y QI. F. Ciencias. IMEYMAT. Campus Río San Pedro. Universidad de Cádiz. 11510 Puerto Real (Cádiz). Spain.

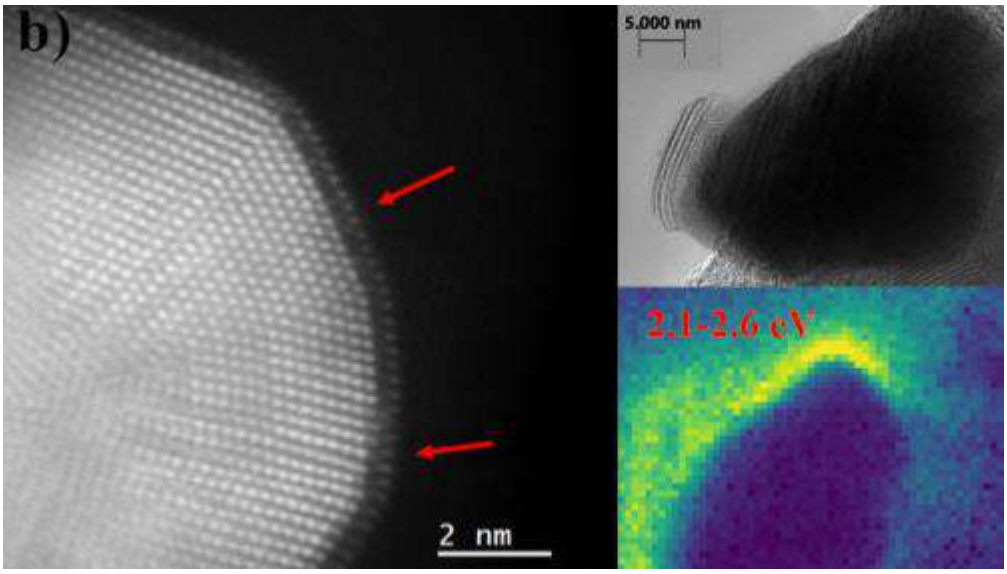

Transition metal dichalcogenides (TMDs), particularly molybdenum disulfide (MoS_2), have garnered significant attention as cost-effective alternatives to platinum-based catalysts for the hydrogen evolution reaction (HER). However, their catalytic performance is often limited by low electrical conductivity and a scarcity of active sites. Recent studies have demonstrated that integrating plasmonic metal cores such as gold (Au), silver (Ag), and copper (Cu) into MoS_2 shells can enhance photoelectrocatalytic activity through localized surface plasmon resonance effects.[1,2]

In this work, we present a comprehensive study on the synthesis, structural characterization, and electrochemical performance of various Metal@MoS_2 core-shell nanostructures (M=Au, Ag, Cu). By employing a multi-step synthesis approach, we successfully fabricated nanostructures with tunable morphologies and controlled defect densities in the MoS_2 shell. Defect engineering strategies included the introduction of sulfur vacancies, heteroatom doping with tungsten and vanadium, and thermal treatments under reducing atmospheres.

Advanced characterization techniques were employed to elucidate the structural and electronic properties of the synthesized nanostructures. Aberration-corrected scanning transmission electron microscopy (STEM) combined with electron energy loss spectroscopy (EELS) provided insights into shell crystallinity, interlayer spacing, and the nature of defects. In-situ transmission electron microscopy (TEM) studies under hydrogen atmospheres revealed dynamic structural changes during HER conditions. X-ray photoelectron spectroscopy (XPS) and Raman spectroscopy further confirmed the successful incorporation of dopants and the presence of vacancies.

Electrochemical analyses, including linear sweep voltammetry (LSV), cyclic voltammetry (CV), and electrochemical impedance spectroscopy (EIS), demonstrated that defect-engineered and heteroatom-doped Metal@MoS_2 nanostructures exhibited superior HER performance compared to pristine MoS_2. Specifically, Au@MoS_2 samples after reducing termal annealing achieved an overpotential of 203 mV at a current density of 10 $mA.cm^{-2}$, with a Tafel slope of 55.mV dec^{-1}, indicating enhanced catalytic kinetics.[1] These improvements are attributed to increased active site density and improved charge transfer.

Photoelectrochemical measurements under simulated LED illumination revealed that the incorporation of plasmonic metal cores significantly enhanced photocurrent densities. Light-assisted chronoamperometry showed a prompt, steady, and reversible response during repeated on/off cycles. In addition, the variations of the photoelectrochemical responses with the wavelength highlight the influence of a plasmon-based process. STEM-EELS plasmonic studies corroborated these findings by demonstrating strong localized surface plasmon resonances in the visible range, which are instrumental in promoting charge carrier generation and separation.

Our findings underscore the critical role of controlled defect introduction and plasmonic core integration in optimizing the electrocatalytic and photoelectrocatalytic properties of Metal@MoS_2 nanostructures. The tunability of these core-shell architectures offers a versatile platform for designing efficient and sustainable catalysts for hydrogen production. This work lays the groundwork for future studies aimed at the rational design of advanced nanostructured materials for clean energy applications.

References:

[1] Gonzalez, Juan Jose Quintana, et al. "Defects engineering of Au@ MoS2 nanostructures for conventional and plasmon-enhanced hydrogen evolution reaction." International Journal of Hydrogen Energy 51 (2024): 371-382.

[2] Bar-Ziv, Ronen, et al. "Au-MoS2 hybrids as hydrogen evolution electrocatalysts." ACS Applied Energy Materials 2.8 (2019): 6043-6050.

Acknowledgments:

We acknowledge funding from the Spanish Ministerio de Economía y Competitividad, the Ministerio de Ciencia e Innovación MCIN/AEI/10.13039/501100011033/FEDER UE, and the European Union "NextGenerationEU"/PRTR (PID2022-140370NB-I00, RYC2021-033764-I, CPP2021-008986 and CNS2024-154587). The (S)TEM measurements were performed at the National Facility ELECMI ICTS ("Division de Microscopia Electronica", Universidad de Cadiz, DME-UCA).

All Solid-State Batteries in the TEM: Novel Tools for Battery Degradation Assessment

Yedra, Lluís [*a], Nandi, Pranjal [a], Vargas, Beatriz [a], del-Pozo-Bueno, Daniel [a], Plana-Ruiz, Sergi [b], Castelló, Kevin [c], Monteiro Freitas, Fernanda [c], González-Rosillo, Juan Carlos [c], Morata, Alex [c], Estradé, Sònia [a], Peiró, Francesca [a]

[a]Laboratiry of Electron Nanoscopies - MIND - IN2UB - Dept. Enginyeria Electrònica i Biomèdica, Universitat de Barcelona

[b]Servei de Recursos Científics i Tècnics Universitat Rovira i Virgili (URV)

[c]Catalonia Institute for Energy Research (IREC) (ES)

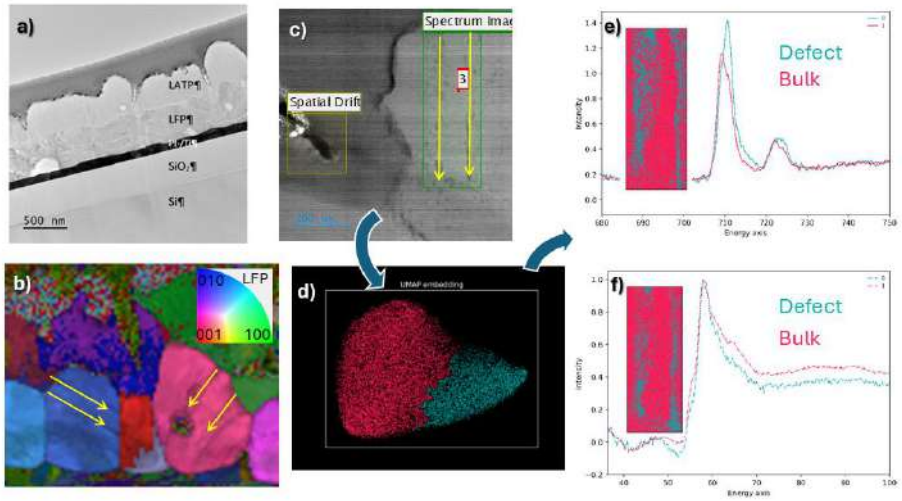

Cobalt-free, anode-less All Solid-State Batteries (ASSBs), identified as “Generation 4” in the EU Strategic Agenda on Batteries, represent a highly promising technology due to their safety, longevity, faster charging capabilities, environmental benefits, flexibility in application, and potential for high energy density. Nevertheless, their fabrication continues to face several challenges, such as interfacial contact resistance between the components and the stability of solid electrolytes in the presence of lithium metal. To evaluate this latter issue, the materials $Li_{1.3}Al_{0.3}Ti_{1.7}(PO_4)_3$ and $LiFePO_4$, serving as solid electrolyte and cathode respectively, have been examined through a series of Transmission Electron Microscopy (TEM)-based techniques, with a focus on structural defects originating

either from the fabrication process or from microstructural evolution during charge-discharge cycles.

The research has been organized into two principal areas: structural and analytical studies. From a structural perspective, High Resolution TEM has been employed to analyze the crystallinity in regions such as grain boundaries, interfaces, and cracks. Additionally, quasi-parallel precession-assisted 4D Scanning TEM[1] (4D-STEM), has been utilized to investigate the material's texture and its role in the development defective regions. From the analytical standpoint, Energy Dispersive X-ray Spectroscopy (EDS) has been used to monitor structural evolution in terms of elemental diffusion and degradation of layer composition, while Electron Energy-Loss Spectroscopy (EELS) has provided more detailed insights into the local chemical composition and bonding around defects. Furthermore, two innovative approaches have been implemented to capture the most subtle features present in the EELS spectrum. First, by applying dimensionality reduction and clustering algorithms[2], local variations in the oxidation states of transition metals have been successfully identified[3]. Second, *ab-initio* simulations using density functional theory, along with simulations of the free density of states, have been applied to investigate the lithium signature within the EELS spectrum.

The integration of these diverse characterization techniques has yielded a comprehensive and unprecedented understanding of the structural characteristics and their evolution during the charging process in ASSB electrodes. This lays the groundwork for future in-operando experiments, which will enable real-time observation of microstructural changes.

Figure: a) TEM overview of the layered structure, b) in-plane orientation from 4D-STEM, with arrows marking defects. c) HAADF-STEM image from the area analysed in EELS, with the UMAP data reduced map in d) and corresponding Fe $L_{2,3}$ and Fe $M_{2,3}$ - Li K edge regions in e) and f) respectively.

References:

[1] S. Plana-Ruiz et al. Quasi-parallel precession diffraction: Alignment method for scanning transmission electron microscopes, Ultramicroscopy 193 (2018) 39-51

[2] . Blanco-Portals, F. Peiró & S. Estradé, Strategies for EELS Data Analysis. Introducing UMAP and HDBSCAN for Dimensionality Reduction and Clustering, Microscopy and Microanalysis, 28, 1 (2022) 109–122

[3] D. del-Pozo-Bueno, F. Peiró & S. Estradé, Support vector machine for EELS oxidation state determination, Ultramicroscopy 221 (2021) 113190

In-depth TEM characterization of the earth-abundant photovoltaic absorber ZnSnP2 for sustainable energy production

Salutari, Francesco [*a], Spadaro, Maria Chiara [b], Steinvall, Simon Escobar [c], Urbonavicius, Aidas [c], Dick, Kimberly [c], Arbiol, Jordi [a, d]

[a]Catalan Institute of Nanoscience and Nanotechnology Nanotechnology - ICN2, (CSIC and BIST) (ES)

[b]Department of Physics and Astronomy "Ettore Majorana", University of Catania, Catania 95123, Italy

[c]Centre for Analysis and Synthesis and NanoLund, Lund University, Sweden

[d]ICREA, Pg. Lluís Companys 23, 08010 Barcelona, Catalonia, Spain

Recent interests in the PV industry have gravitated towards earth abundant materials suitable for large scale commercialization that can compete in terms of performance with their more expensive and scarce counterparts. Among various candidates, the ternary phosphide ZnSnP2 was reported to have optimal optoelectronic properties for a solar cell absorber [1]. $ZnSnP_2$ has a chalcopyrite structure and a tunable bandgap from 1.37-1.60 eV, depending on the order-disorder behavior of Zn and Sn atoms, which enables advanced solar cell technologies from a single material while maintaining recyclability [2]. So far, the main limitations have concerned the growth process mainly due to the poor control over the material composition and lack of a suitable substrate for epitaxial growth. Recently, ZnSnP2 was successfully grown via selective area epitaxy (SAE) on InP and Si in forms of nanopyramids. In this work, we successfully exploit annular dark field scanning TEM (HAADF-STEM) together with core-loss EELS analysis to prove the quality of the crystals in terms of defects formation, strain relaxation, and composition at the atomic level. We delve further into the composition analysis of ZnSnP2 nanostructures by focusing on the ELNES part of the EELS spectrum. The fine structure that extends approximately 50 eV after the ionization edge onset carries the information on the electronic structure in the material, which include the coordination of atoms and site symmetry in the local atomic environment. Based on the reshaping of the characteristic fine structure of both Zn and Sn from one sample to the other, we highlight the correlation between the order-disorder parameter and the growth conditions of the material. At last, we collect the low-loss interval of the EEL spectrum to retrieve the bandgap values of each sample with proper fit of the corresponding spectra [3]. The change in the bandgap values is then related to the atoms' coordination and site symmetry in the local atomic environment.

References:

[1] Scanlon, David O., and Aron Walsh. "Bandgap engineering of ZnSnP2 for high-efficiency solar cells." Applied Physics Letters 100.25 (2012).

[2] Nakatsuka, Shigeru, and Yoshitaro Nose. "Order–disorder phenomena and their effects on bandgap in ZnSnP2." The Journal of Physical Chemistry C 121.2 (2017): 1040-1046.

[3] Martí-Sánchez, S., Botifoll, M., Oksenberg, E. et al. Sub-nanometer mapping of strain-induced band structure variations in planar nanowire core-shell heterostructures. Nat Commun 13, 4089 (2022)

Charged domain walls revealed by electron ptychography

Ferreira, Rafael V. [b, c], Dearg, Malcolm [a], Beltrán, Juan I. [b, c], Bambrick-Sattar, Ellie-Mae [a], Tornos, Javier [b], Santamaria, Jacobo [b], Varela, Maria [b, c], Sánchez-Santolino, Gabriel [b, c], Clark, Laura [* a]

[a]School of Physics Engineering and Technology, University of York, York, UK

[b]GFMC, Departamento de Física de Materiales, Universidad Complutense de Madrid, Madrid 28040, Spain

[c]Instituto Pluridisciplinar, Universidad Complutense de Madrid, Madrid 28040, Spain

Text of the abstract:

The recent development of fast pixelated detectors has enabled routine collection of four-dimensional scanning transmission electron microscopy (4D-STEM) datasets, expanding our ability to investigate and understand material structures and even their functional properties at the atomic level [1]. In particular, 4D-STEM enables phase imaging methods such as differential phase contrast and ptychography, which are capable of probing electric and magnetic field structures in materials [2]. This capability is particularly interesting for the study of complex oxide heterostructures in which a wealth of exotic interfacial phenomena can arise due to the interplay between the physical and electronic structures of their constituent materials [3]. In this work, we present an analytical approach to the investigation of an artificial multiferroic tunnel junction system consisting of ferromagnetic $La_{0.7}Sr_{0.3}MnO_3$ (LSMO) electrodes separated by a thin ferroelectric $BaTiO_3$ (BTO) barrier, with interest for future applications such as non-volatile ferroelectric memories. In such heterostructures the domain organization resulting from the imposed electrostatic and mechanical boundary conditions [4] can lead to the formation of charged domain walls that modulate its functional properties [5]. Here, a combination of phase imaging techniques – namely, center-of-mass (CoM) and ptychographic reconstructions – are used to determine the configuration of our system, defining an approach that simultaneously reveals both its structural (local atomic arrangements) and functional (longer range field properties) aspects, culminating in the identification of a charged domain wall within the BTO layer. In addition, the conclusions of this investigation are supported by density functional theory calculations, which also help in further understanding the polar nature of the structure. In this way, we show how correlation between different methods allows for the exploration of charged atomic-scale features, enabling a direct connection between structural rearrangements and the resulting heterostructure functionality.

References:

[1] C. Ophus, Microscopy and Microanalysis, 25(3), 563–582 (2019)

[2] S. Toyama, et al., Nature Reviews Electrical Engineering, 2, 27–41 (2025)

[3] H. Y. Hwang, et al., Nature Materials, 11(2), 103–113 (2012)

[4] J. Junquera, et al., Rev. Mod. Phys., 95, 025001 (2023)

[5] G. Sanchéz-Santolino, et al., Nature Nanotechnology, 12, 655–662 (2017)

Acknowledgments:

This work was supported by funding from The Royal Society - University Research Fellowship (URF\R1\221270) & Enhanced Research Expenses (RF\ERE\221035); the Spanish MICINN, AEI, FEDER, UE under Grant Nos. PID2021-122980OB-C5I; and Comunidad de Madrid “Materiales avanzados” MAD2D-UCM3. G.S.-S. acknowledges financial support from Grants RYC2022-038027-I and CNS2024-154548 funded by MICIU/AEI/10.13039/50110001103. J.I.B. thanks very fruitful discussions with M.C. Muñoz. E.-M.B.-S. acknowledges EPSRC funding from grant reference number EP/W524657/1. Electron microscopy data acquisition was carried out at the ICTS Centro Nacional de Microscopia Electronica CNME-UCM.

Low-energy Core-loss EELS as a Dose-effective Approach for Oxidation State Mapping

Pelaez-Fernandez, Mario [*a,b,c], del-Pozo-Bueno, Daniel [d,e], Marinova, Maya [f], Teurtrie, Adrien [a], Estrader, Marta [e,g], Salazar-Alvarez, Germán [h], Arenal, Raul [b,c], Leroux, Hugues [f], Peiró, Francesca [d,e], Estradé, Sonia [d,e], de la Peña, Francisco [a]

[a]Unité Matériaux et Transformations (UMET UMR 8207), U. Lille (Villeneuve d'Ascq), France, [b]Instituto de Nanociencia y Materiales de Aragon (INMA), CSIC-U. Zaragoza (Zaragoza), Spain, [c]Laboratorio de Microscopias Avanzadas, Universidad de Zaragoza (Zaragoza), Spain, [d]LENS-MIND, Departament d'Enginyeria Electrònica i Biomèdica, U. Barcelona (Barcelona), Spain, [e]Institute of Nanoscience and Nanotechnology (IN2UB), U. Barcelona (Barcelona), Spain, [f]Institute of Nanoscience and Nanotechnology (IN2UB), U. Barcelona (Barcelona), Spain, [g]Univ. Lille, FR 2638-IMEC-Institut Michel-Eugène Chevreul, F-59000 (Lille), France, [h]Department of Inorganic and Organic Chemistry,U. Barcelona (Barcelona), Spain, [i]Department of Material Science and Engineering, Ångström Lab, U. Uppsala (Uppsala), Sweden

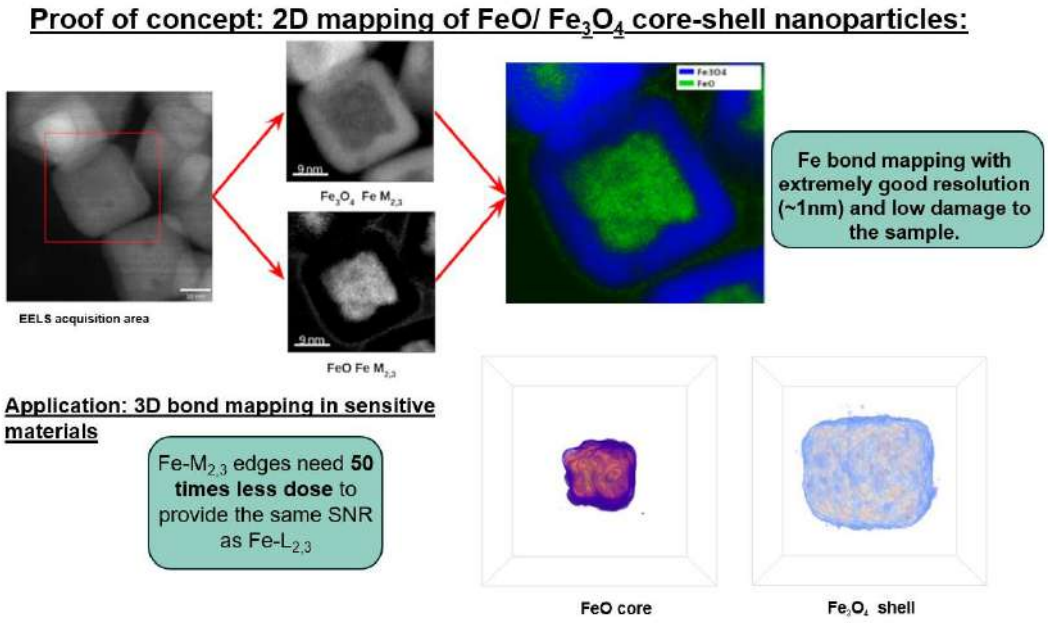

A current cornerstone of EELS research features the possibility to use STEM-EELS for oxidation state quantification by analyzing the fine structure of the elemental ionization edges [1,2]. Advances in the last decade include oxidation state mapping at the atomic level [3] as well as 3D tomography via EELS tilt-series reconstruction [4].

To date, most oxidation state analyses rely on ionization edges with onset energies >100 eV (e.g., Fe-$L_{2,3}$ ionization edges at ~708 eV). However, the small ionization cross-section of these edges challenges studies of beam-sensitive samples.

The advent of highly sensitive Direct Electron Detectors (DEDs) has expanded possibilities in EELS and microscopy. Their high dynamic range allows probing edges that could not be properly exploited before. While most research focuses on high-energy core-loss edges, this work explores a new avenue enabled by hybrid pixel DEDs: quantitative analysis using low-energy core-loss edges (LE-CLEELS) (50-100 eV).

We demonstrate this approach by performing EELS-bonding tomography on previously studied beam-sensitive FeO/Fe_3O_4 core-shell nanocubes[4]. These tomographic EELS studies have exploited the Fe-$M_{2,3}$ ionization edges, situated at an energy of 54 eV. The 2D and 3D acquisitions were analyzed using a combination of SVD decomposition, blind source separation, and curve fitting EELS quantification.

The results of this study, which can be seen in the TOC graphic, show a successful tomographic reconstruction enabled by the greatly enhanced signal-to-noise ratio (SNR) of the Fe-$M_{2,3}$ edges. After quantification, we have found out to need 50 times less electron dose when comparing to the widely used Fe-$L_{2,3}$ edges. Furthermore, this higher SNR has allowed us to perform this experiment with a much higher resolution with respect to previous studies on these materials, down to 1 nm.

This work challenges the conventional notion that EELS is mostly suited to the chemical analysis of light elements. This also highlights the potential of LE-CLEELS for low- dose analysis, opening new possibilities for advanced materials characterization on beam-sensitive materials.

References:

[1] Garvie, L. A. J., & Buseck, P. R. Ratios of ferrous to ferric iron from nanometre-sized areas in minerals. Nature 1998, 396(6712), 667–670.

[2] del-Pozo-Bueno, D., Peiró, F., & Estradé, S. Support vector machine for EELS oxidation state determination. Ultramicroscopy 2021, 221, 113190.

[3] Gloter, A., Badjeck, V., Bocher, L., Brun, N., March, K., Marinova, M., Tencé, M., Walls, M., Zobelli, A., Stéphan, O., & Colliex, C. Atomically resolved mapping of EELS fine structures. Materials Science in Semiconductor Processing 2017, 65, 2–17.

[4] Torruella, P., Arenal, R., de la Peña, F., Saghi, Z., Yedra, L., Eljarrat, A., López-Conesa, L., Estrader, M., López-Ortega, A., Salazar-Alvarez, G., Nogués, J., Ducati, C., Midgley, P. A., Peiró, F., & Estradé, S. 3D Visualization of the Iron Oxidation State in FeO/Fe 3 O 4 Core–Shell Nanocubes from Electron Energy Loss Tomography. Nano Letters 2016, 16(8), 5068–5073.

Acknowledgments:

MPF thanks the support of the Spanish Ministry for Science and Universities for its support via the “Ayudas para la recualificación del sistema universitario Margarita Salas”.

Advanced unsupervised clustering of Scanning Transmission X-Ray Microscopy spectral imaging using a UMAP and HDBSCAN framework

del Pozo Bueno, Daniel [*a], Sorrentino, Andrea [b], Tonti, Dino [b], Manas, Gabriel Jover [c], Estradé, Sònia [a], Peiró, Francesca [a]

[a]Departament d'Enginyeria Electrònica i Biomèdica & Institute of Nanoscience and Nanotechnology, Universitat de Barcelona, Martí i Franquès, 1, 08028 Barcelona.

[b]ALBA Synchrotron Light Facility, Carrer de la Llum 2-26, Cerdanyola del Vallès, 08290, Spain.

[c]Institut de Ciència de Materials de Barcelona (ICMAB), CSIC, Carrer dels Til·lers sn, Bellaterra, 08193, Spain

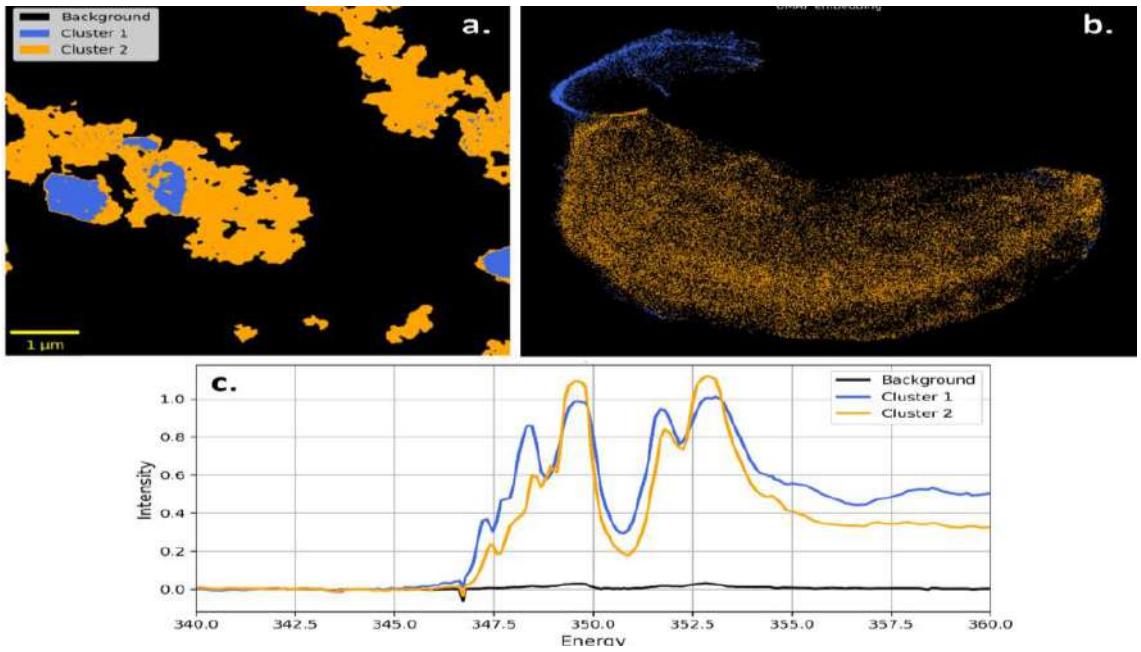

Full Field Transmission X-ray Microscopy (TXM) is a powerful synchrotron-based imaging technique that combines nanoscale spatial resolution (down to tens of nanometers) with spectroscopic sensitivity in the soft X-ray range (between 200–2000 eV). By acquiring energy-resolved transmission images across absorption edges, TXM allows high-fidelity mapping of elemental distributions, oxidation states, and chemical bonding environments. However, the high dimensionality and noise inherent to TXM spectral datasets present significant challenges for conventional analysis workflows, which often rely on manual analysis or linear classical decomposition methods, as multiple linear least squares fittings.

In 2021, Blanco-Portals et al. proposed an innovative analysis strategy for Electron Energy-Loss Spectroscopy (EELS) based on unsupervised learning techniques, combining UMAP (Uniform Manifold Approximation and Projection) for nonlinear

dimensionality reduction and HDBSCAN (Hierarchical Density-Based Spatial Clustering of Applications with Noise) for density-aware clustering. Their approach outperformed traditional methods, like Principal Component Analysis (PCA), Non-Matrix Factorization (NMF) or K-Means, in segmenting complex spectral data and identifying faint characteristics [1].

I In this work, we adapt the UMAP-HDBSCAN methodology for TXM spectral imaging demonstrating that this methodology preserves the physical information in spectral features while enhancing the accuracy and interpretability of spatial classification. Unlike linear techniques, UMAP effectively captures the nonlinear manifold structure of spectral variations, and HDBSCAN provides flexible, noise-robust clustering without requiring predefined component numbers, that is, number of clusters. This is illustrated in Figure 1, where UMAP–HDBSCAN is applied to a TXM spectromicroscopy measurement at the Ca L edge acquired at the Mistral beamline of the ALBA synchrotron [2], revealing distinct spatial regions with clear different Ca chemical state (Hydroxyapatite in orange, Calcite in blue). The results highlight the capacity of this methodology to identify complex spectral features and spatially map it. These results support the generalizability of this framework across other spectroscopic imaging techniques and support its expansion and implementation in X-ray Spectromicroscopy.

Figure 1. Application of the UMAP-HDBSCAN clustering strategy to STXM spectral data to study calcite (in orange) and hydroxyapatite (in blue) regions in a composite calcium-based material. (a) Spatial distribution of the two clusters identified by HDBSCAN on the UMAP-reduced dataset. (b) UMAP 2D embedding of the spectral dataset, showing the density-based clustering in the reduced manifold space. (c) Centroid spectra corresponding to each cluster.

References:

[1] J. Blanco-Portals; F. Peiró; S. Estradé. Strategies for EELS Data Analysis. Introducing UMAP and HDBSCAN for Dimensionality Reduction and Clustering. Microscopy and Microanalysis, 2022, 28, 1, 109–122.

[2] A. Sorrentino et al. MISTRAL: a transmission soft X-ray microscopy beamline for cryo nano tomography of biological samples and magnetic domains imaging. J Synchrotron Radiat, 2015, 22, 4, 1112–1117.

Acknowledgments:

The author acknowledges financial support from the Spanish project PID2022-138543NB-C21.

Quantitative Analysis of Metal-Metal Interactions in C-SACs from HAADF-STEM Images via Deep Learning, Mathematical Optimization, and DFT

Lopez-Haro, Miguel [*a] ,Aniceto-Ocaña, Paula [a], Marqueses-Rodriguez, José [a], Muñoz-Ocaña, Juan M. [b], Fernandez-Trujillo, María J. [a], G Algarra, Andrés [a], Rodriguez-Chia, Antonio M [b], Calvino, José J. [a], Castillo, Carmen E. [b]

[a]Departamento Ciencia de los Materiales, Ing. Metalúrgica y Química Inorgánica, Universidad de Cádiz, 11510 Puerto Real, Cádiz, Spain.

[b]Departamento de Estadística e Investigación Operativa. Universidad de Cádiz, 11510 Puerto Real, Cádiz, Spain.

The study of correlated single-atom catalysts (C-SACs) holds transformative promise for advancing electrocatalytic reactions, such as the oxygen evolution reaction and CO_2 electroreduction, by enabling precise control over active sites. A straightforward yet powerful strategy to synthesize C-SACs involves dispersing preformed homo- or heterodiatomic metal complexes onto high-surface-area supports via simple wet-chemistry routes. [1] In particular, macrocyclic ligands with intentionally arranged coordination pockets can host two metal centres in a well-defined configuration, providing a direct path to atomically dispersed, dual-metal sites. However, bridging the gap between synthesis and catalytic performance requires a detailed understanding of each metal's chemical environment and how the two centres interact under reaction conditions.

Characterizing such catalysts is challenging, because conventional methods, like NMR, XRD, IR, or mass spectrometry, are generally unsuited to resolve atomic-scale heterogeneity on a support. In contrast, aberration-corrected scanning transmission electron microscopy (HR HAADF-STEM) offers the spatial resolution needed to visualize individual atoms. Yet manual analysis of HR HAADF-STEM images remains subjective, unreliable, and insufficient for statistically robust conclusions.

To address these limitations, we have developed a methodology that combines; i) experimental HR HAADF-STEM imaging, ii) HAAD-STEM image simulation based on density functional theory (DFT)–optimized structures, iii) deep learning–driven segmentation, and iv) mathematical optimization for precise atom-pair identification. This workflow transforms HR HAADF-STEM data into quantitative, statistically robust characterizations of C-SACs. To illustrate our approach, we focus on a heterobinuclear Au(III)–Pd(II) complex featuring a hexaaza macrocyclic ligand supported on carbon.

A 3 μM aqueous solution of a heterobinuclear Au(III)–Pd(II) complex was prepared by reacting the hexaaza macrocycle (3,6,9,17,20,23-hexaazatricyclo[23.3.1.1]triaconta-1(29),11-(30),12,14,25(26),27-hexaene, L) with $Pd(NO_3)_2$ and $HAuCl_4$ in a 1:1:1 molar ratio. A 9 μL drop of the reddish complex solution was deposited onto a holey-carbon-coated gold grid, then freeze-dried under dark conditions for 24 h. HR HAADF-STEM images were recorded on an FEI Titan^3 Themis microscope operating at 200 kV.

HR HAADF-STEM image of the supported Au(III)–Pd(II) complex were acquired. To interpret observed contrasts, we simulated HAADF-STEM images based on the most stable DFT-optimized structure of the Au(III)–Pd(II) complex bound to the hexaaza ligand. These simulations confirm that Au–Pd pairs remain resolvable only when the supporting carbon film is thinner than approximately 10 nm. Beyond that limit, Au and Pd contrasts become indistinguishable from the amorphous carbon background. By matching experimental and simulated contrast profiles, we can establish confidence in our assignment of metal atoms versus substrate artefacts.

We evaluated supervised and unsupervised machine learning strategies to automate image analysis. Synthetic images, generated by scripts that mimic experimental contrast features, were used to train a residual U-Net architecture (AttenResUnet). Training was carried out in TensorFlow/Keras on an Intel Core i9-10900 workstation equipped with an NVIDIA GeForce RTX 3090 GPU. Among various supervised and unsupervised approaches, the AttenResUnet delivered the highest accuracy in distinguishing Au versus Pd atoms

With reliable segmentation in hand, we analysed time-series HR HAADF-STEM images to investigate the stability of Au–Pd pairs under the 200 kV electron beam. This analysis revals that most metal pairs remain intact over extended irradiation, and that the measured Au–Pd distances do not change significantly. These observations indicate a strong, ligand-mediated interaction that persists even after deposition on amorphous carbon, suggesting robustness under realistic imaging and reaction conditions. [2]

References:

[1] [1] Shan J.; Ye C.; Jiang Y.; Jaroniec M. ; Zheng Y.; Qiao S-Z. Metal-metal interactions in correlated single-atom catalysts.Sci. Adv. 2022, 8, abo0762

[2] [2] Aniceto-Ocaña P.; Marqueses-Rodriguez J.; Muñoz-Ocaña, Juan M et al. An AI-Powered Methodology for Atomic-Scale Analysis of Heterogenized Correlated Single-Atom Catalysts. Small Methods, 2025, 5:206

Acknowledgments:

This work has received support from Projects: PID2019-110018GA-I00 funded by MICIU/AEI/10.13030/501100011033, PID2020-113006-RB-I00 and PID2022-142312NB-I00 funded by MCIN/AEI/10.13039/501100011033 and by "ERDF A way of making Europe". Project TED2021-130191B-C44 funded by MCIN/AEI/ 10.13039/501100011033 and European Union NextGenerationEU/PRTR) is also acknowledged. STEM experiments were recorded at the DME-UCA Node of the Spanish Singular Infrastructure for Electron Microscopy of Materials (ICTS ELECMI). P.A.O thanks FPI scholarship program from University of Cadiz.

ePDF Mapping: Revealing Amorphous Structures at Nanometer Resolution in TEM

Das, Partha Pratim [*a], Gomez-Perez, Alejandro [a], Grivas, Evangelos [a], Nicolopoulos, Stavros [a], Billinge, Simon J. L. [b], Galanis, Athanassios S. [a], Rauch, Edgar F. [c], Portillo, Joaquim [a], Fransen, Martijn J. [a]

[a]NanoMEGAS SPRL, Rue Èmile Claus 49 bte 9, Brussels, 1050, Belgium

[b]Department of Applied Physics and Applied Mathematics, Columbia University, New York, NY 10027, USA

[c]SIMAP Laboratory, CNRS-Grenoble INP, BP 46 101 rue de la Physique, Saint Martin d'Hères 38402, France

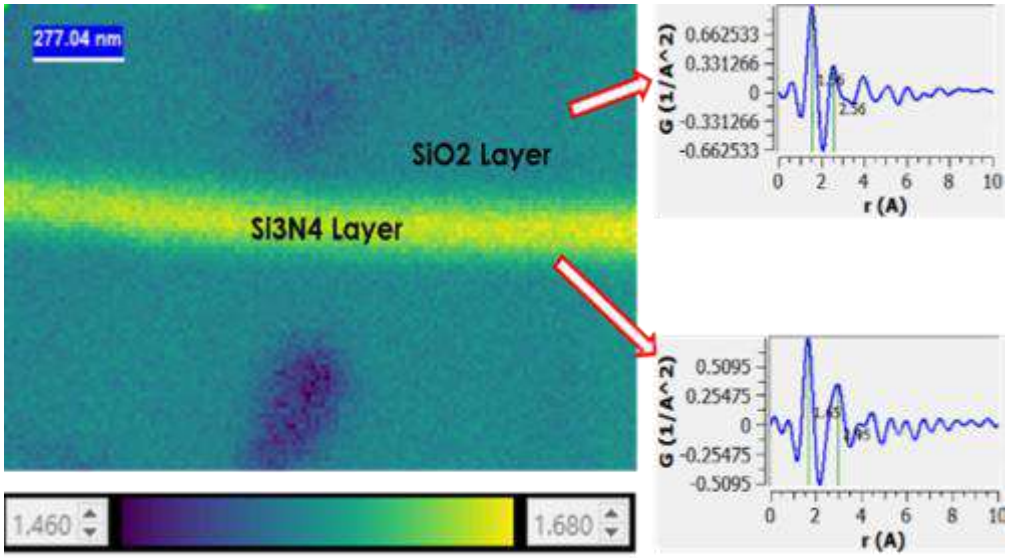

Understanding material properties requires access to their atomic structure. Traditional diffraction methods, which rely on sharp Bragg reflections, are often ineffective for nanocrystalline and amorphous materials due to the absence of long-range order. In such cases, Pair Distribution Function (PDF) analysis—using X-rays (xPDF), neutrons (nPDF), or electrons (ePDF)—provides critical insight into short- and medium-range atomic arrangements [1].

ePDF analysis in a Transmission Electron Microscope (TEM) offers several advantages over xPDF, including higher spatial resolution, faster data acquisition, and reduced sample requirements. While conventional ePDF approaches—such as Selected Area Electron Diffraction (SAED) or Nanobeam Diffraction (NBD)—require acquiring one pattern at a time, our method leverages automated workflows for more efficient data collection and analysis.

We introduce a user-friendly software solution capable of processing both single-pattern data and complete datasets acquired via Scanning Precession Electron Diffraction (SPED) or precession-enhanced 4D-STEM. These techniques employ a focused electron probe (1–10 nm) that scans the sample with fine step sizes (1–3 nm), enabling structural mapping at ~1 nm spatial resolution [2]. At each scan point, the software computes the ePDF and generates correlation maps, analyzing peak positions, widths, and integrated areas to reveal nanoscale structural variations [3].

This methodology is broadly applicable to a range of disordered materials, including semiconductors, glasses, catalysts, amorphous dispersions, and polymers. In one case study, ePDF mapping resolved two distinct amorphous layers in a semiconductor: a Si_3N_4 layer (first peak at 1.65 Å) and a SiO_2 layer (first peak at 1.56 Å, slightly shorter than expected), the latter likely affected by carbon incorporation during processing.

In summary, ePDF mapping provides a robust and versatile platform for high- spatial resolution local structural analysis of amorphous materials, uncovering variations beyond the reach of conventional diffraction techniques.

References:

[1] Abeykoon, M.; Malliakas, C. D.; Juhás, P.; Bozin, E. S.; Kanatzidis, M. G.; Billinge, S. J. L. Quantitative nanostructure characterization using atomic pair distribution functions obtained from laboratory electron microscopes. Z. Kristallogr. Cryst. 2012, 227(5), 248–256.

[2] Rauch, E. F.; Véron, M. Automated crystal orientation and phase mapping in TEM. Materials Characterization 2014, 98, 1-9

[3] Rakita, Y.; Hart, J. L.; Das, P. P.; Shahrezaei, S.; Foley, D. L.; Mathaudhu, S. N.; Nicolopoulos, S.; Taheri, M. L..; Billinge, S. J. L. Mapping structural heterogeneity at the nanoscale with scanning nano-structure electron microscopy (SNEM). Acta Mater., 2023, 242, 118426.

Acknowledgments:

Work in the S. J. L. B. Group was supported by U.S. Department of Energy, Office of Science, Office of Basic Energy Sciences (DOE-BES) under contract No. DE-SC0024141.

Advanced EELS Analysis of σ/π Bonding in Beam-Sensitive Materials

Luo, Shunrui [*a], Latifi, Fatemeh [a], Maia, Rui [a], Ferreira, Paulo [*a]

[a]INL International Iberian Nanotechnology Laboratory, Braga (PT)

Beam-sensitive materials with mixed carbon sp^2 and sp^3 hybridizations exhibit subtle variations in local bonding environments, which are critical to their electronic and structural properties. In this study, we develop an optimized methodology for analyzing the σ* and π* components in the C-K edge using electron energy loss spectroscopy (EELS). STEM with an energy filter and monochromator is employed to minimize beam damage and preserve sample integrity. Low-dose acquisition protocols are implemented, and the resulting spectra are processed using principal component analysis (PCA) and multiple linear least squares (MLLS) fitting to improve signal-to-noise ratios and isolate bonding-specific features.

Reference spectra from standard materials such as graphite and diamond-like carbon are used for calibration and validation. Additionally, initial machine learning-based approaches, such as unsupervised clustering and denoising algorithms, are explored to assist in identifying bonding-specific spectral features. These methods show potential for enhancing interpretation quality, especially in low-dose and low-SNR conditions.

This approach enables reliable σ/π bonding analysis in electron beam-sensitive systems and lays the groundwork for future studies on local bonding structures with high spatial resolution and chemical sensitivity.

Automating data processing in STEM: From micrographs to atomic models

Pinto-Huguet, Ivan [*a], Botifoll, Marc [*a], Arbiol, Jordi [*a]

[a]Catalan Institute of Nanoscience and Nanotechnology Nanotechnology - ICN2, (CSIC and BIST) (ES)

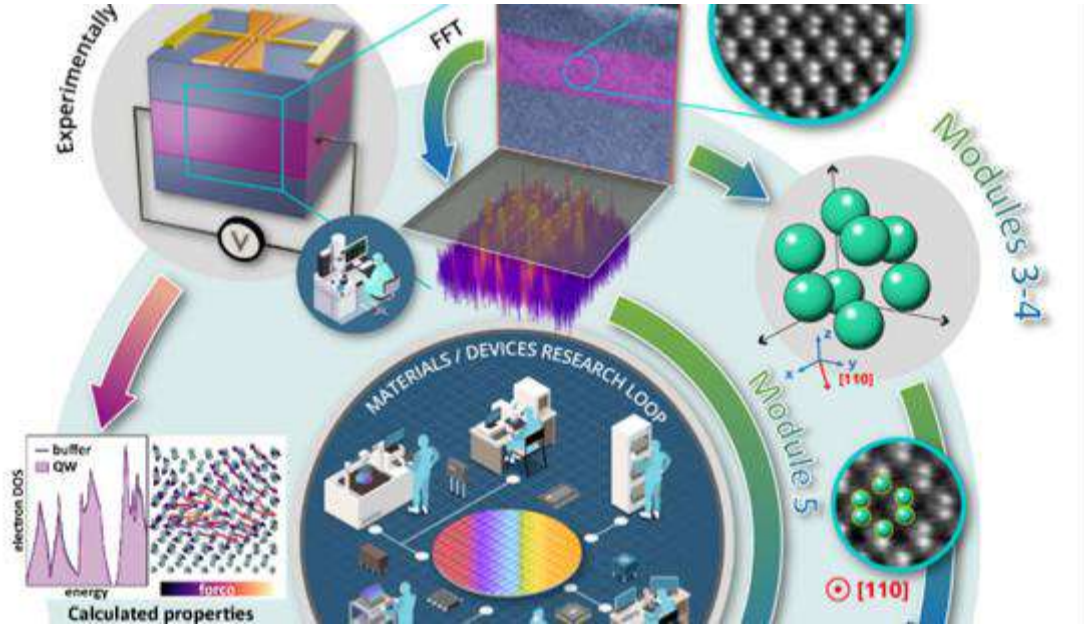

The process of discovering and refining new materials, as well as enhancing existing ones for a variety of uses, including quantum applications, is a complex and multifaceted endeavour. This involves identifying needs, reviewing existing literature, proposing materials, engineering devices, characterizing materials, and testing applications. However, the process can be hindered by its time-intensive and costly nature, especially when precision at the atomic level is necessary to comprehend the functionality of materials and heterostructured devices.

In this digital age and with quantum supremacy in the horizon, semiconductor heterostructures within a chip have become indispensable and ubiquitous, propelling significant industrial value chains. They facilitate progress in both emerging sectors like quantum applications and established ones. For that, the trend of miniaturization, which is now reaching nanoscale dimensions and nearing the atomic limit, is a key driver of progress which demands special characterisation needs. To answer to these needs, in this work, we present a revolutionary analytical

framework aimed at the comprehensive characterization of device heterostructures, with a particular focus on quantum devices and their materials.

The characterisation that must answer these demands is high-resolution Transmission Electron Microscopy (TEM), as the most optimal way to access structural information at the atomic level. We propose a workflow capable of processing both parallel illumination TEM and Scanning TEM (STEM) data, although it is specially designed for the latter. In addition, it can extract compositional information from Electron Energy Loss Spectroscopy (EELS), which is used to make the characterisation an exhaustive and complete process. Importantly, the workflow we suggest, combines traditional algorithmics, with unsupervised and supervised machine learning algorithms. This way, we ensure that model-based computing and artificial intelligence work hand by hand to provide the comprehensive and material-independent solution we seek for.

Our pioneering workflow autonomously determines material composition, crystallographic phase, and spatial orientation across various regions of analysed (S)TEM-based images or image datasets through detailed model comparison. It is completed with automated strain analysis, enabling a comprehensive characterization of the device's structural properties. Eventually, we incorporate the extracted knowledge to automate the creation of models that facilitate simulations and provide vital physical and chemical insights necessary for understanding the device's performance in practical applications.

Although the method is highly versatile, we focus on quantum computing devices to autonomously optimize their functional properties. In particular, we prove it with SiGe quantum well heterostructures that proved outstanding quantum performance for spin qubits generation. However, the main advantage placing our workflow beyond state of the art is its generalisation capabilities. It works for any material configuration and not only does it answer the pressing automation need, but unlocks getting physical models and simulations of complex devices with unprecedented accuracy.

References:

[1] Botifoll, M. et al, (2024) Submitted, https://doi.org/10.48550/arXiv.2411.01024

Automated Atomic Site Identification by 4D - Scanning Transmission Electron Microscopy

Fernandez-Canizares, Francisco [a, b], Rodriguez-Vazquez, Javier [a, b], Ferreira, Rafael V. [a, b], Tenreiro, Isabel [a], Rivera-Calzada, Alberto [a], Fernando-Saavedra, Amalia [c], Sanchez-Garcia, Miguel A. [d], Xie, Yong [e, f], Castellanos-Gomez, Andres [e], Varela, Maria [a, b], Sánchez-Santolino, Gabriel [* a, b]

[a]Departamento de Física de Materiales, Universidad Complutense de Madrid, Madrid 28040, Spain, [b]Instituto Pluridisciplinar, Universidad Complutense de Madrid, Madrid 28040, Spain, [c]3ISOM and Dept. Ingeniería Electrónica, ETSI Telecomunicación, Universidad Politécnica de Madrid, Av. Complutense 30, Ciudad Universitaria, 28040 Madrid, Spain, [d]ISOM and Dept. de Ingenería Eléctrica, Electrónica, Automática y Física Aplicada, ETSIDI-UPM, Ronda de Valencia 3, 28012 Madrid, Spain, [e]2D Foundry Research Group, Instituto de Ciencia de Materiales de Madrid (ICMM-CSIC), Madrid E-28049, Spain, [f]School of Advanced Materials and Nanotechnology, Xidian University, Xi'an 710071, People's Republic of China

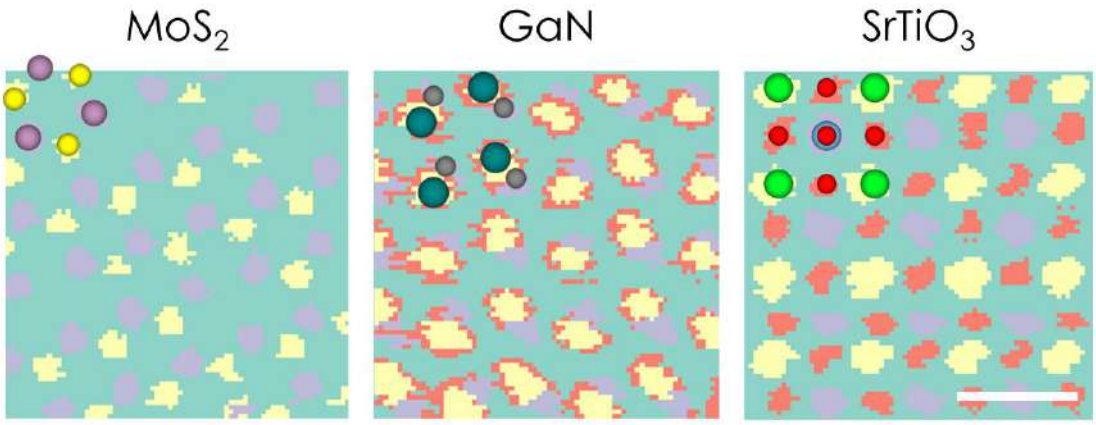

Figure 1: Atom site identification with cascaded agglomerative clustering algorithm. Spatial segmentation of the 4D-STEM datasets by the proposed algorithm provides classification maps with robust and accurate identification of all atomic species in the three tested materials: MoS_2, GaN, and $SrTiO_3$. Sketches showing the unit cells are overlaid, with Mo, S, Ga, N, Sr, Ti and O columns shown in purple, yellow, dark cyan, grey, green, blue and red, respectively. Scale bar corresponds to 0.5 nm.

Precise atomic arrangement and defects in materials critically influence their physical properties and emergent phenomena such as superconductivity, ferroelectricity or metal-insulator transitions [1]. Even small variations in local symmetry, chemical or electronical doping can lead to drastic changes in these physical properties, making it necessary to characterize materials at the nanoscale for understanding and engineering these functionalities.

Recent advances in four-dimensional scanning transmission electron microscopy (4D-STEM) have created new opportunities to tackle this challenge [2]. These rich datasets have been employed in numerous modalities including nano-diffraction,

ptychography, and differential phase contrast imaging. However, the large size and noise characteristics of 4D-STEM data present significant computational challenges. Moreover, data analysis workflows typically require customization for each material system or experimental condition.

To address these issues, machine learning and unsupervised clustering methods have increasingly been explored to extract meaningful structural and chemical information from 4D-STEM datasets [3]. For example, convolutional neural networks have been used to denoise data at low electron doses, and clustering algorithms have identified crystalline phases and grain orientations from nanobeam electron diffraction patterns [4]. However, automated identification of atomic column sites directly from atomic-resolution 4D-STEM data—particularly distinguishing subtle differences within unit cells—has remained unexplored.

In this work, we present a computational pipeline combining dimensionality reduction and hierarchical clustering to automatically detect and classify atomic columns within the unit cell from atomic-resolution 4D-STEM data. We apply this approach to three representative materials with distinct structural and compositional characteristics: monolayer MoS_2, the semiconductor GaN, and the complex oxide $SrTiO_3$. These materials span a broad range of atomic weights, symmetries, and column types, including heavy and light atoms, posing challenges for automated identification.

Our three-stage cascaded clustering strategy effectively distinguishes atomic columns from interatomic background regions across all tested materials, resolving even columns with closely related scattering profiles. This approach provides a new opportunity for information extraction, with potential live application at the microscope for data driven experiments, opening pathways for detailed defect analysis, phase identification, and strain mapping in future electron microscopy studies.

References:

[1] Hwang, H. Y.; Iwasa, Y.; Kawasaki, M.; Keimer, B.; Nagaosa, N.; Tokura, Y. Emergent Phenomena at Oxide Interfaces. Nat. Mater. 2012, 11, 103–113.

[2] Ophus, C. Four-Dimensional Scanning Transmission Electron Microscopy (4D-STEM): From Scanning Nanodiffraction to Ptychography and Beyond. Microsc. Microanal. 2019, 25, 563–582.

[3] Kalinin, S. V.; Ophus, C.; Voyles, P. M.; Erni, R.; Kepaptsoglou, D.; Grillo, V.; Lupini, A. R.; Oxley, M. P.; Schwenker, E.; Chan, M. K. Y.; Etheridge, J.; Li, X.; Han, G. G. D.; Ziatdinov, M.; Shibata, N.; Pennycook, S. J. Machine Learning in Scanning Transmission Electron Microscopy. Nat. Rev. Methods Primers 2022, 2, 11.

[4] Diebold, A. C.; Ophus, C.; Kordijazi, A.; Consiglio, S.; Lombardo, S.; Triyoso, D.; Tapily, K.; Mian, A.; Shankar, N. B. V. I.; Morávek, T.; Chandran, N.; Stroud, R.; Leusink, G. Template Matching Approach for Automated Determination of Crystal Phase and Orientation of Grains in 4D-STEM Precession Electron Diffraction Data for Hafnium Zirconium Oxide Ferroelectric Thin Films. Microsc. Microanal. 2025, 31, 1–13.

Acknowledgments:

This work was supported by the Spanish MICINN, AEI, FEDER, UE under Grant Nos. PID2021-122980OB-C51 and Comunidad de Madrid “Materiales avanzados” MAD2D-UCM3. G.S.-S. acknowledges financial support from Grants RYC2022-038027-I and CNS2024-154548 funded by MICIU/AEI/10.13039/50110001103. A.C-G. acknowledges funding by the Ministry of Science and Innovation (Spain) through the projects TED2021-132267B-I00, PID2020-115566RB-I00, PDC2023-145920-I00 and PID2023-151946OB-I00 and the European Research Council through the ERC-2024-PoC StEnSo (grant agreement 101185235) and the ERC-2024-SyG SKIN2DTRONICS (grant agreement 101167218). Y.X. acknowledges Open Fund of State Key Laboratory of Infrared Physics (Grant No. SITP-NLIST-ZD-2024-01). Electron microscopy data acquisition was carried out at the ICTS Centro Nacional de Microscopia Electronica CNM E-UCM. The authors acknowledge support from the Institute of Optoelectronic Systems and Microtechnology (ISOM) as a Singular Scientific and Technical Infrastructure (ICTS - Micronanofabs) in Spain.

STEM characterization of III-V nanowires using 4D-STEM and Differential Phase Contrast

Galiana, Beatriz [*a], García-Tabares, Elisa [a], Gonzalo, Alicia [a], Reynolds, Jose Miguel [a], Santiuste, Mario [a]

[a]Departamento de Física, Universidad Carlos III de Madrid (ES)

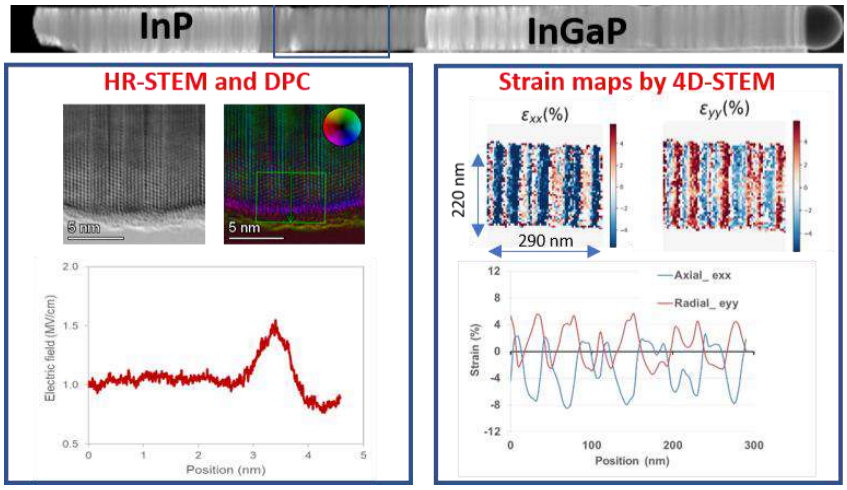

In recent decades, we have witnessed the development of new analytical tools in the frame of STEM/TEM characterization such as, Differential Phase Contrast (DPC) or 4D-STEM technique, which have changed the paradigm of its uses. The core idea behind DPC is to measure the differential phase shift between two orthogonally polarized beams of light transmitted through a sample. One of the most interested applications in semiconductors is the detection of local electric fields [1]. In 4D-STEM, a highly collimated electron beam scans over the sample, resulting in a diffraction pattern recorded for each scanning position. This creates a dataset that includes information about position (2D) and diffraction pattern (2D), resulting in a 4D dataset. It allows strain calculations or orientation mapping for nanoparticles, among other possibilities [2]. In this work, we present some preliminary results carried out on III-V nanowires as an example to show the potential of these novel techniques. We show HRSTEM and DPC data carried out at the surface of the nanowire revealing the existence of a local electric field which can be due to the formation of a core. Regarding 4D-STEM, by proper data analysis we present normal strain maps (e_{xx} and e_{yy}) carried out on the GaInP section of the nanowire using open scrips [3]. These first results reveal compression in growth direction (axial direction) and tension in y direction (radial direction). Preliminary EDS results reveal oscillations in Ga/In atomic composition. The data presented validate the 4D-STEM and DPC measurements and show the potential of these analytical tools.

References:

[1] Acc Chem Res;50(7): (2017)

[2] C. Ophus Microscopy and Microanalysis, 25 (3) 2019

[3] S Wang, et al. Ultramicroscopy 236 (2022) 113513

Acknowledgments:

The Ministry of Ministry of Economic Affairs and Digital Transformation supports this work through project TSI-064100-2023-31. This work has been partically support by COST ACTION CA20116 (Opera). B. Galiana is member of the Institute of Chemistry and Materials Technology “Álvaro Alonso Barba" of the UC3M.

Atomic-Scale Insights into CoWO4 for Water Splitting

Llorens Rauret, David [*a], Ram, Ranit [b], García de Arquer, F. Pelayo [b], Garzón Manjón, Alba [a], Arbiol, Jordi [b, c]

[a]ICN2 (CSIC and BIST), 08193 Campus UAB, Bellaterra, Barcelona, Spain, [b]ICFO and BIST, 08860 Castelldefels, Barcelona, Spain, [c]ICREA, 08010 Barcelona, Barcelona, Spain.

A key step in enabling hydrogen (H_2) as an efficient and scalable energy carrier is improving the oxygen evolution reaction (OER), crucial in water electrolysis for green H_2 production. However, the inherently sluggish four-electron transfer mechanism of the OER limits efficiency and typically requires noble metal-based catalysts such as IrO_2 and RuO_2 [1]. The scarcity and high cost of these materials remain major obstacles to widespread adoption of H_2 technologies.

First-row transition metal oxides offer a prospective alternative due to their high earth abundance and promising activity in acidic OER. Yet, their poor stability, especially under acidic conditions, remains a critical limitation [2]. One strategy to overcome this involves incorporating high-valence sacrificial elements such as W into a MWO_4-type crystal structure. Upon selective removal through a water/hydroxide - WO_4^{2-} anion exchange process, these structures can trap hydroxide and water species within a defective metal oxide framework [3]. However, this delamination–activation mechanism is not equally effective across all first-row transition metals. Among them, cobalt tungstate ($CoWO_4$) has shown exceptional OER performance [4]. Upon activation, $CoWO_4$ achieves activity comparable to IrO_2, along with significantly improved durability. When implemented in water electrolysis systems, $CoWO_4$-based anodes achieved a threefold improvement over Ir- and Ru-free alternatives, maintaining stability for over 600 hours at 1 A cm^{-2}.

To understand the role of the delamination process across different MWO_4 compounds, advanced characterization techniques with atomic-scale imaging resolution and spectroscopic information are essential [5]. In this work, scanning transmission electron microscopy (STEM) was employed to monitor structural and compositional transformations during activation. Integrated differential phase contrast (iDPC-STEM) enabled direct imaging of oxygen atoms within the MWO_4 lattices, facilitating assessment of potential Jahn–Teller distortions in the MO_6 octahedra. Electron energy loss spectroscopy (EELS) provided insights into the elemental evolution and oxidation states changes at various activation stages. High-angle annular dark field (HAADF-STEM) imaging confirmed the formation of surface vacancies in $CoWO_4$, features directly linked to its improved catalytic durability. Finally, post-OER STEM analysis revealed the remarkable structural stability of the activated material. These findings were supported by complementary

spectroscopic analyses, offering a comprehensive picture of the structure–property relationships that govern catalytic performance.

By revealing the mechanisms behind $CoWO_4$'s high activity and durability, this work contributes to the rational design of next-generation, earth-abundant OER catalysts. These insights pave the way for scalable, cost-effective solutions in hydrogen production and support the broader transition toward sustainable, zero-emission energy systems.

References:

[1] Suntivich, J., Hautier, G., Dabo, I. et al. Probing intermediate configurations of oxygen evolution catalysis across the light spectrum. Nat Energy 9, 1191–1198 (2024)

[2] Liu, L., Corma, A. Structural transformations of solid electrocatalysts and photocatalysts. Nat Rev Chem 5, 256–276 (2021)

[3] Lina Chong et al., La- and Mn-doped cobalt spinel oxygen evolution catalyst for proton exchange membrane electrolysis. Science 380, 609-616 (2023)

[4] Ranit Ram et al., Water-hydroxide trapping in cobalt tungstate for proton exchange membrane water electrolysis. Science 384, 1373-1380 (2024)

[5] Pastor, E., Lian, Z., Xia, L. et al. Complementary probes for the electrochemical interface. Nat Rev Chem 8, 159–178 (2024)

Acknowledgments:

ICN2 acknowledges funding from Generalitat de Catalunya 2021SGR00457. This study is part of the Advanced Materials program and was supported by MCIN with funding from the European Union NextGenerationEU (PRTR-C17. I1) and by Generalitat de Catalunya (In-CAEM Project). The authors acknowledge support from the project AMaDE (PID2023-149158OB-C43), funded by MCIN/AEI/10.13039/501100011033, and “ERDF A Way of Making Europe’’ via the European Union. ICN2 is supported by the Severo Ochoa program from Spanish MCIN/AEI (grant no. CEX2021-001214-S) and is funded by the CERCA Program/Generalitat de Catalunya. This study was supported by the EU HORIZON INFRA TECH 2022 project IMPRESS (ref. 101094299). Part of the present work has been performed in the framework of the Universitat Autònoma de Barcelona Materials Science PhD program. D.L.R. acknowledges Spanish MCIU grant PRE2022-102638. A.G.M. has received funding from grant RYC2021-033479-I funded by MCIN/AEI/10.13039/501100011033 and by European Union NextGenerationEU/PRTR.

Abstracts of oral talks - Topic: Life Science and CryoEm

Native Helical Assemblies of IBDV VP4 Protease

Martínez-Romero, Juan M. [a], Castrillo, Mariana [a], Fernandez-Palacios, José M. [a], Novoa, Guy [a], Martín-Forero, Esther [a], Rodríguez, Javier M. [a], Luque, Daniel [b], Castón, José R. [*a]

[a]Department of Macromolecular Structures, Centro Nacional de Biotecnología (CNB-CSIC), Madrid, Spain.

[b]School of Biomedical Sciences, Faculty of Medicine & Health, University of New South Wales, Sydney, Australia

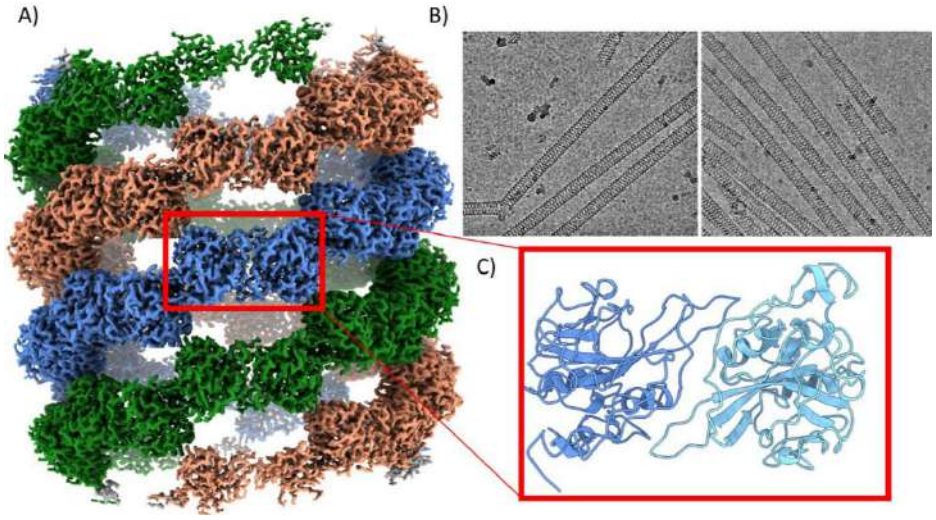

IBDV is an icosahedral virus from the *Birnaviridae* family, whose two dsRNA segments (A and B) are organized as ribonucleoprotein complexes. An ORF of segment A encodes a polyprotein, NH_2-pVP2-VP4-VP3-COOH, which is self-cleaved by the protease VP4 (243 residues) rendering pVP2 and VP3. Segment B encodes the RNA polymerase VP1. VP1-VP4 and the genomic dsRNA associate into three assemblies crucial during the viral life cycle: T=13 capsids, VP4 helical tubes, and the RNPs.

VP4 is naturally found as helical assemblies, ~25 nm in diameter, in IBDV-infected cells. VP4 atomic structures are conserved in birnaviruses, but no structural data are available for these in vivo assemblies. We determined the cryo-EM structure of VP4 helix at 2.4 Å resolution. The basic building blocks are VP4 dimers, arranged in a right-handed three-stranded helix, with an axial rise of 18.4 Å and an azimuth angle of 40.6º. The catalytic Ser/Lys dyad, located in a surface crevice, is blocked in cis by the VP4 C-terminal end, which is also involved in intra-dimeric interactions via the 227-243 C-terminal segment. Interdimeric interactions occur via segments 209-218

and 150-155 within the same helix, and via segment 89-112 between dimers of different helices. A collection of mutants has confirmed key residues for VP4 activity, self-assembly, and infection viability. Our study suggests that once VP4 has completed proteolysis, it is securely inactivated by assembly into helical structures to prevent lethal damage to the virus or to the host components needed for virus multiplication, and offers insights into new antiviral targets.

Like Two Peas in a Pod? A Combined Strategy To Obtain Two Distinct High-Resolution Structures of RNA Polymerase I from One Grid.

Santos-Aledo, Alicia [*a], Darriere, Tommy [a], Fernández-Tornero, Carlos [a]

[a]Centro de Investigaciones Biológicas Margarita Salas, CSIC (ES)

For many structural biology research groups, access to high voltage (300 kV) cryo-electron microscopes is a limiting step in their investigations. The experiment time is often limited to a few times every year, and much time is devoted to optimizing grid preparation. Some problems that may be encountered during this process, such as preferred orientation or inadequate complex ratios, are difficult to evaluate with lower voltage (120 kV) microscopes. Here, we report a procedure to obtain, from a single grid, two distinct and high-resolution structures (2 Å) of RNA Polymerase I (Pol I) bearing a functionally relevant point-mutation. To achieve this goal, a heterogeneous sample was prepared by incubating purified Pol I with sub-stoichiometric amounts of a DNA-RNA transcription scaffold. After standard procedures for vitrification on amorphous carbon-coated carbon grids and data collection, the dataset was processed with a combination of CryoSPARC and RELION-5, using the Scipion framework, for optimized particle classification and quick refinement. Two distinct particle sets were refined separately to obtain high-resolution electron maps, which will be used to elucidate precise mechanisms behind the behavior of the point mutation.

References: -

Acknowledgments:

We would like to thank David Gil-Cartón from the CIC bioGUNE Electron Microscopy facility for performing the data collection and to the CIB Cryo-EM facility for their help during sample preparation.

INTEGRATIVE STRUCTURAL BIOLOGY OF A T=219 MARINE GIANT VIRUS

San Martín, Carmen [*a], Otaegi-Ugartemendia, Sara [a], Marabini, Roberto [b], Herrera, Pablo [a], Condezo, Gabriela N. [a], Mühlberg, Lars [c], Wang, Haina [d], Ortiz, Lucía [a], Liu, Fan [c], Sandaa, Ruth-Anne [d],

[a]Centro Nacional de Biotecnología (CNB-CSIC) (ES), [b]Escuela Politécnica Superior, Universidad Autónoma de Madrid, [c]Leibniz-Forschungsinstitut für Molekulare Pharmakologie (FMP), [d]University of Bergen

Viruses with capsids larger than 150 nm are considered "giant viruses" *(1)*. *Prymnesium kappa* virus RF02 (PkV-RF02) has a 583 kbp linear dsDNA genome and 200 nm diameter capsid *(2)*. Using mass spectrometry, we have identified 140 different proteins in purified PkV-RF02, with nearly 70% of them having unknown function *(3)*. We used cryo-electron microscopy (cryo-EM) single particle analysis to obtain high-resolution maps of ordered components of the PkV-RF02 icosahedral capsid, and cross-linking (XL) followed by mass spectrometry (MS) to identify protein-protein interactions (PPIs) present in both the icosahedral shell and non-icosahedral core.

Our ~3 Å resolution structure shows that PkV-RF02 has a triangulation number *pseudo*T=219, previously observed only for *Phaeocystis pouchetii* virus (PpV01) *(4)*. The PkV-RF02 capsid is composed by more than 20 different proteins and nearly 12,000 protein copies. PkV-RF02 has novel characteristics among giant viruses: a protein channel within the virion, an unusual penton protein organization, and a multilayered stabilization network reinforced by disulfide bridges and O-linked glycosylations on the surface.

Using XL-MS, we detected 561 PPIs happening between 112 different viral proteins. These PPIs define symmetry-mismatched features escaping localization by cryo-EM, as well as numerous PPIs within the PkV-RF02 non-icosahedral core, showing highly complex functional enzymes packaged in the viral particle: bacteriorhodopsin-like protein, disulfide isomerase or RNA polymerase complex, among others. This work shows a complete structural characterization of the capsid and core components of a giant virus combining cryo-EM and XL-MS, and is the first high-resolution structure of a *p*T=219 virus.

References:

[1] R. N. Burton-Smith & K. Murata, Microscopy (Oxf) 70, 477 (2021)

[2] T. V. Johannessen et al., Virology 476, 180 (2015)

[3] H. Wang et al., Commun Biol 8(1):510 (2025) Research Square (2025)

[4] X. Yan et al., J Virol 79, 9236 (2005)

Acknowledgments:

Work supported by grants PID2019-104098GB-I00/AEI/10.13039/501100011033 and PID2022-136456NB-I00/AEI/10.13039/501100011033, co-funded by the Spanish State Research Agency and the European Regional Development Fund. The CNB-CSIC is further supported by AEI Severo Ochoa Excellence grant CEX2023-001386-S. S.O.U. held a Severo Ochoa and Maria de Maeztu fellowship (JAE-SOMdM20-20), a predoctoral contract from Ministry of Science, Innovation and Universities (FPU2020-05148) and an EMBO Scientific Exchange Grants (10981). We thank; Beatriz Martín, Javier Chichón and Noelia Zamarreño from Electron and Cryo-electron Microscopy facilities for the excellent technical support; as well as Gregory Effantin, Eaazhisai Kandiah, and Romain Linares, from European Synchrotron Radiation Facility (ESRF) for Titan Krios data collection under proposals MX-2443 and MX-2369: 10.15151/ESRF-ES-1061180097, 10.15151/ESRF-ES-925344867, 10.15151/ESRF-ES-781088676.

Three-dimensional imaging to study early bone mineralization

Macías-Sánchez, Elena [*a], Raguin, Emeline [b], Tarakina, Nadezda [b], Fratzl, Peter [b]

[a]Institute of Parasitology and Biomedicine López Neyra, CSIC (ES)

[b]Max Planck Institute of Colloids and Interfaces, Potsdam, Germany (DE)

Two-dimensional imaging represents a serious limitation when studying the structure of complex hierarchical materials such as bone. Three-dimensional visualization is essential for understanding the interactions that occur between the cellular network, collagen fibrils, and mineral precursors during the formation process. Over the last decade, FIB-SEM has revolutionized the study of mineralized tissues, providing not only three dimensional information in the nanometer range, but also the possibility to nanofabricate mineralized lamellae avoiding the mechanical stress caused by standard sectioning techniques.

These technical advances helped elucidate the mineral deposition in collagen-based materials, driven by a spherulitic-like crystal growth [1]. Initially, disordered mineral aggregates form in the interfibrillar spaces, and subsequently the mineral infiltrates adjacent collagen fibrils, which provide the structural framework for the formation of layered spherulites. These spherulites (also called mineral ellipsoids) imbricate forming a new hierarchical level of organization in bone termed tessellation [2]. Although the mechanism has been described in several systems [1, 2, 3], detailed data on the interaction of the organic and the mineral phases remain insufficient.

The present study combines electron tomography (FIB-SEM serial surface imaging) which provides 3D information, with the fabrication of lamellae for scanning/transmission electron microscopy (S/TEM), selected area electron diffraction (SAED) and energy dispersive spectroscopy (EDS) chemical mapping to elucidate crystal distribution and orientation throughout the collagen matrix.

The study reveals the internal structure of the forming fibrolamellar bone at nanometer resolution. A connective tissue with dispersed and non-preferentially oriented collagen fibrils seems to be deposited first, serving as a scaffold for the deposition of more aligned collagen. During embryonic development, these osteocytes initiate the mineralization process and become buried in the mineral matrix, which expands both vertically and laterally to form the nascent fibrolamellar units. At the collagen-mineral interface, a multitude of mineral spherulites proliferate and grow to confluence. Their profiles are still recognizable in the consolidated mineral layer.

Our study confirms that the formation of mineral spherulites also drives the mineral deposition in embryonic fibrolamellar bone. This fact demonstrates that this protein-mediated crystal growth mechanism occurs in different types of bone tissue and in different species, indicating that it is a common and homologous mineralization mechanism in type I collagen-based materials.

References:

[1] Macías-Sánchez, E.*; Tarakina N.; Ivanov, D.; Blouin, S.; Berlanovich, A.; Fratzl, P.* Spherulitic Crystal Growth Drives Mineral Deposition Patterns in Collagen-based Materials. Advanced Functional Materials, 2022, 32, 2200504

[2] Buss, D.; Reznikov, N.; McKee, M. Crossfibrillar mineral tessellation in normal and Hyp mouse bone as revealed by 3D FIB-SEM microscopy. Journal of Structural Biology 2020, 212, 107603

[3] Shah, F.; Ruscsák, K.; Palmquist, A. Transformation of bone mineral morphology: From discrete marquise-shaped motifs to a continuous interwoven mesh. Bone Reports 2020 13, 100283

Acknowledgments:

E.MS. is supported by the Ramón y Cajal Research Program (RYC2023-045512-I) funded by MCIN/AEI/10.13039/501100011033 and FSE+, and the project PID2022-141993NA-I00 funded by MICIU/AEI/10.13039/501100011033 and ERDF/UE.

Cryo-EM uncovers a sequential mechanism for RNA polymerase I pausing and stalling at abasic DNA lesions

Fernández-Tornero, Carlos [*a] ,Santos-Aledo, Alicia [a], Plaza-Pegueroles, Adrián [a], Sanz-Murillo, Marta [a], Ruiz, Federico M. [a], Hou, Peini [b], Xu, Jun [b], Gil-Carton, David [c], Wang, Dong [b]

[a]Centro de Investigaciones Biológicas Margarita Salas (CIB), CSIC, 28040 Madrid, Spain

[b]Skaggs School of Pharmacy and Pharmaceutical Sciences, UCSD, La Jolla, CA 92093, USA

[c]IKERBASQUE, Basque Foundation for Science, 48009, Bilbao, Spain

During synthesis of the ribosomal RNA precursor, RNA polymerase I (Pol I) monitors DNA integrity but its response to DNA damage remains poorly studied. Abasic sites are among the most prevalent DNA lesions in eukaryotic cells, and their detection is critical for cell survival. We report cryo-EM structures of Pol I in different stages of stalling at abasic sites, supported by in vitro transcription studies. Slow nucleotide addition opposite abasic sites occurs through base sandwiching between the RNA 3'-end and the Pol I bridge helix. Templating abasic sites can also induce Pol I cleft opening, which enables the A12 subunit to access the active center. Nucleotide addition opposite the lesion induces a translocation intermediate where DNA bases tilt to form hydrogen bonds with the new RNA base. These findings reveal unique mechanisms of Pol I stalling at abasic sites, differing from arrest by bulky lesions or from abasic site handling by RNA polymerase II.

Structural basis of high-affinity choline translocation across bacterial membranas

Jiang, Hanxing [b], Vílchez-García, Jesús [b],Martínez-Jiménez, Adrián [e], Ochoa, Lizarralde, Borja [b], López-Alonso, Jorge Pedro [b, c], Pérez-Lorente, Jerónimo [b], Bartoccioni, Paola [h], Estévez, Raúl [d, e], Guallar, Victor [f, g], Errasti-Murugarren,, Ekaitz [* d, e], Ubarretxena-Belandia, Iban [* a, b], Tascón, Igor [* a, b]

[a]Ikerbasque Foundation for Science, Bilbao, Spain, [b]Instituto Biofisika (UPV/EHU, CSIC), University of the Basque Country, Leioa, Spain., [c]Basque Resource for Electron Microscopy, Leioa, Spain., [d]The Spanish Center of Rare Diseases (CIBERER U-731), ISCIII, Madrid, Spain., [e]Physiological Sciences Department, Genes, Disease and Therapy Program, IDIBELL-Institute of Neurosciences, School of Medicine and Health Sciences, University of Barcelona, Bellvitge Campus. L'Hospitalet de Llobregat, Spain., [f]Electronic and atomic protein modelling group, Barcelona Supercomputing Center, Plaça d'Eusebi Güell, 1-3, E-08034 Barcelona, Spain., [g]Nostrum Biodiscovery, Av. de Josep Tarradellas, 8-10, E-08029 Barcelona, Spain., [h]Institute for Research in Biomedicine (IRB Barcelona), The Barcelona Institute of Science and Technology (BIST), Baldiri Reixac 10, E-08028, Barcelona, Spain.

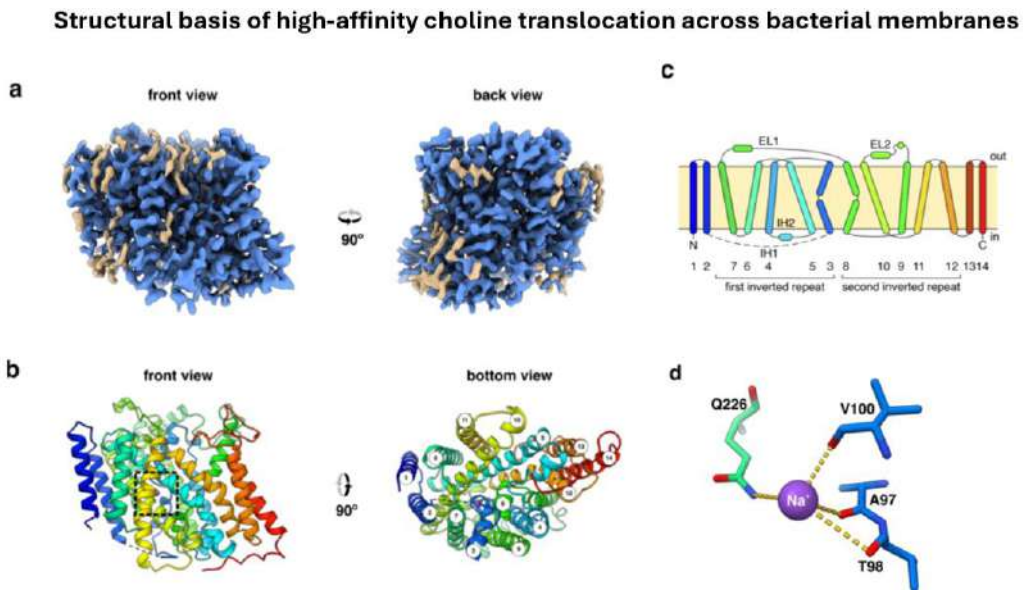

Choline is an essential nutrient across all domains of life. In prokaryotes, it acts as a precursor to osmoprotectants such as glycine betaine, which help maintain cellular turgor under osmotic stress, and it can also be metabolized as a source of carbon and nitrogen. In humans, choline plays critical roles in key physiological processes including cell membrane building, cholinergic neurotransmission, and methylation pathways.

In cholinergic signaling, choline serves as a precursor of the primary

neurotransmitter acetylcholine. After synaptic transmission, acetylcholine is hydrolyzed in the synaptic cleft, releasing choline, which must be reabsorbed by presynaptic neurons. This choline reuptake in cholinergic synapses is mediated by the human high-affinity choline transporter (hCHT) for the biosynthesis of acetylcholine to sustain neurotransmission. Mutations in hCHT are associated with several neurological disorders, highlighting its critical role in cholinergic functions. In this study, we identified a bacterial homolog of hCHT with high sequence identity from Salimicrobium flavidum, referred to as sfCHT, to investigate the high-affinity choline transport mechanism mediated by the CHT family. Cryo-EM structures of Na+- and Na+/choline-bound sfCHT, combined with computational structure prediction with Protein Energy Landscape Exploration (PELE) and mutational analysis, have revealed the choline translocation pathway from the substrate-binding site to the cytosol. The key residues involved in transport were found to be conserved in hCHT and essential for transport, supporting a conserved transport mechanism across the CHT lineage.

Structural Basis for the Compact Fold of Human RIPK1 Amyloid Fibrils

López-Alonso, Jorge Pedro [a, b], Polonio, Paula [c], Jian, Hanxing [a], Escobedo, Fátima [c], Titaux, Gustavo [c], Ubarretxena-Belandia, Iban [* a, d], Mompeán, Miguel [* c]

[a]Instituto Biofisika (UPV/EHU, CSIC), Leioa, Spain

[b]Basque Resource for Electron Microscopy, Leioa, Spain

[c]Instituto de Química Física Blas-Cabrera (IQF-CSIC), Madrid, Spain

[d]Ikerbasque Foundation for Science, Bilbao, Spain

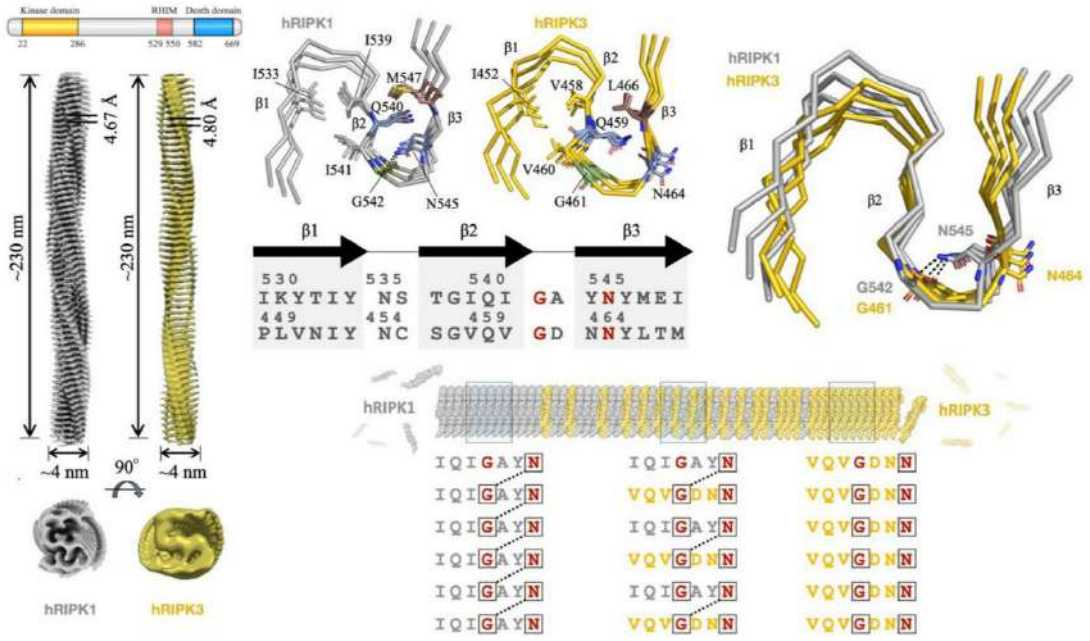

Amyloid fibrils, typically associated with neurodegenerative diseases, also play critical roles as functional assemblies in biological processes. The RIP homotypic interaction motifs (RHIMs) in receptor-interacting protein kinases 1 and 3 (RIPK1 and RIPK3) are essential for necroptosis, orchestrating the formation of amyloid-like fibrils that assemble into necrosomes. These supramolecular complexes propagate cell death signals and activate effectors like MLKL. While the structures of human RIPK3 (hRIPK3) homomeric fibrils and RIPK1-RIPK3 heteromeric fibrils have been resolved [1,2], the atomic structure of human RIPK1 (hRIPK1) homomeric fibrils has remained elusive.

Here, we present a high-resolution structure of hRIPK1 RHIM-mediated amyloid fibrils, determined using an integrative approach combining cryo-electron microscopy and cryoprobe-detected solid-state nuclear magnetic resonance

spectroscopy. The fibrils adopt an N-shaped amyloid fold consisting of three β-sheets stabilized by the conserved IQIG RHIM motif through hydrophobic interactions and hydrogen bonding. A key hydrogen bond between N545 and G542 closes the β2-β3 loop, resulting in denser side-chain packing compared to hRIPK3 homomeric fibrils. This structural feature likely contributes to the compact architecture of hRIPK1 fibrils, in contrast to the more relaxed S-shaped fold observed in hRIPK3.

These findings provide structural insights into how hRIPK1 homomeric fibrils nucleate hRIPK3 recruitment and fibrillization during necroptosis, offering broader perspectives on the molecular principles governing RHIM-mediated amyloid assembly and functional amyloids.

References:

[1] Wu, X., et al. The structure of a minimum amyloid fibril core formed by necroptosis-mediating RHIM of human RIPK3. Proc. Natl Acad. Sci. USA 118, e2022933118 (2021).

[2] Mompeán, M. et al. The Structure of the Necrosome RIPK1-RIPK3 Core, a Human Hetero-Amyloid Signaling Complex. Cell 173, 1244–1253.e10 (2018).

Acknowledgments:

Cryo-EM was performed at the Basque Resource for Electron Microscopy located at Instituto Biofisika (UPV/EHU, CSIC), supported by the Department of Science, Universities and Innovation and the Innovation Fund of the Basque Government, with additional support from MCIN (Recovery, Transformation and Resilience Plan) and the Basque Government “Biotechnology Complementary Plan Applied to Health” with funding from European Union NextGenerationEU (PRTR-C17.I1; PRTR-C17.I01.P01.S13) (AAAA_ACG_AY_2539/22_05). NMR experiments were performed in the “Manuel Rico” NMR Laboratory (LMR) of the Spanish National Research Council (CSIC), a node of the Spanish Large-Scale National Facility (ICTS R-LRB). G.T.A.-D. and P.P. acknowledge FJC2021-047976-I fellowships funded by MCIN/AEI/ 10.13039/501100011033 and European Union Next Generation EU/PRTR, and PIPF-2022/BIO-25611 funded by the Dept. of Education, Science and Universities from the Community of Madrid, respectively. This work has been supported by grant PID2022-143177NB-I00 to I. U.-B from the Spanish Ministry of Science, Innovation and Universities.We thank also Igor Tascón (Instituto Biofisika) for interesting discussions on this work.

ORF3a reshapes host cell architecture through vesicle remodeling and lipid mobilization

Oliva, Maria A. *[a], de Lucas, Ana [a], Perez-Berna, Ana J [b], Garcia-Garcia, Transito [c], Mendoza, Laura [a], Dies, Blanca [a], Gattini, Federico [a], Fernandez-Rodriguez, Raul [c], Zaldivar-Lopez, Sara [c], Rodriguez, Maria J. [d], Mandracchia, Biaggio [d], Megias, Diego [d], Luque, Daniel [d], Pereiro, Eva [b], Garrido, Juan [c], Montoya, Maria [a]

[a]Centro de Investigaciones Biológicas Margarita Salas (CIB), CSIC, Madrid 28040, Spain, [b]ALBA Synchrotron Light Facility, Spain, [c]Universidad Cordoba, [d]ISCIII

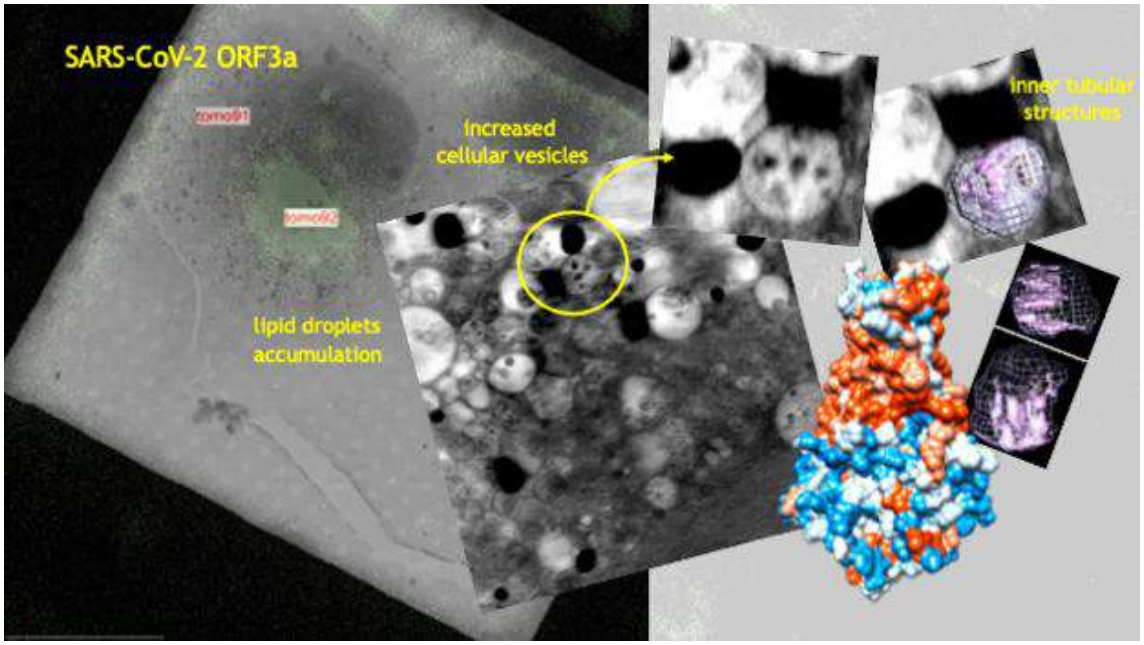

The SARS-CoV-2 genome encodes eleven accessory proteins, many of which remain poorly characterized but are increasingly implicated in viral pathogenesis. Among them, ORF3a, the largest, is a controversial viroporin known to impair immune responses and promote vesicle formation.

We have combined sections and soft-X-ray tomography studies to elucidate the molecular mechanism underlying ORF3a's impact on the host cell. In both A549 epithelial cells and differentiated THP1 dendritic cells, we observed a striking increase in intracellular vesicles, accompanied by fragmentation of the endoplasmic reticulum and Golgi apparatus. ORF3a localized to vesicles displaying distinctive inner tubular structures, whose origin appear variable based on co-immunostaining with fluorescent markers.

In addition, we detected an unusual accumulation of lipid droplets, which correlates with a shift in lipid metabolism as revealed by integrated transcriptomics, lipidomic and proteomic analyses. Further, our results explain previous reports showing lipids bound to ORF3a inner channels. Tomographic reconstructions also revealed altered mitochondria with abnormal cristae, consistent with recent

findings linking ORF3a to an increase in low-activity mitochondria exhibiting enhanced motility and reduced displacement.

Together, our findings demonstrate that ORF3a alone is sufficient to profoundly remodel cellular architecture, supporting its potential role in the formation of SARS-CoV-2 viral factories through lipid mobilization.

Fast and robust heterogeneity analysis in CryoEM though Orthogonal Group Synchronization

Lauzirika Zarrabeitia, Oier [*a], Vilas Prieto, José Luis [a], Carazo García, José María [a], Sorzano Sánchez, Carlos Oscar [a]

[a]Centro Nacional de Biotecnología (CNB-CSIC). Darwin, 3. 28049 Madrid, Spain

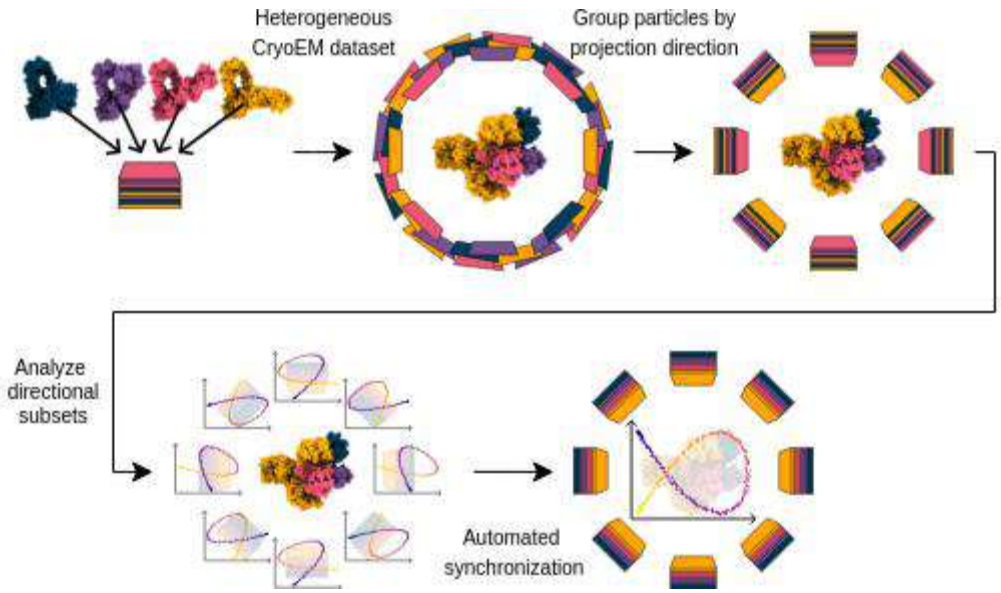

Structural heterogeneity presents a major challenge in Cryo-Electron Microscopy (Cryo-EM), where macromolecular complexes often exist in multiple compositional or conformational states. We propose a novel method that exploits the natural similarity of neighboring projections to perform localized dimensionality reduction on directionally clustered subsets of the data. This dimensionality reduction captures structural variability within narrow angular regions while mitigating the effects of the pose diversity. To integrate the resulting local analyses into a coherent global model, we employ Orthogonal Group Synchronization -an emergin technique from applied mathematics- that aligns local analises in a globally consistent manner. The method is designed to be user-friendly, requiring only a few parameters with clear physical and statistical interpretations, thus reducing manual tuning. Additionally, it is computationally efficient, significantly outperforming traditional heterogeneity analysis approaches in terms of runtime. We demonstrate the effectiveness of our approach on both synthetic and experimental datasets, recovering meaningful structural variations with high fidelity.

Facilitating CryoEM single-particle and tomography data analysis with EMhub

De la Rosa Trevin, Jose Miguel [*a]

[a]St.Jude Children's Research Hospital (US)

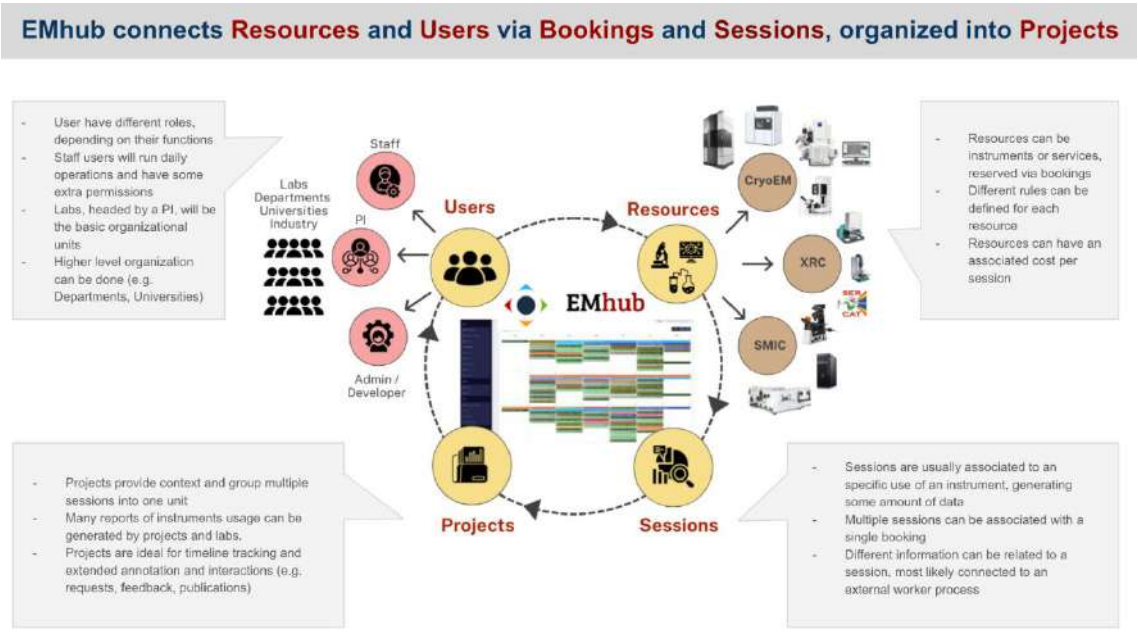

EMhub is a web framework designed to support the data management needs of scientific facilities (e.g., instrument bookings, user management, data transfer, and reporting). This application has been in use for several years at the Swedish National CryoEM Facility and, more recently, in some core centers within the Structural Biology department at St. Jude Children's Research Hospital. EMhub can be customized to meet different requirements and exposes a REST API that allows external processes to interact with the application. This feature has been leveraged to establish a fully automated CryoEM on-the-fly processing pipeline that can be monitored through the web interface. Here, we present the latest development of the framework, which enables the export of initial results from the pre-processing pipeline to facilitate continued data processing in other software packages, such as Relion or CryoSparc. Several new web tools have been integrated into the application to facilitate data curation and quality evaluation, providing a valuable complement to existing programs. These tools have already proven helpful at St. Jude during the initial tomography data processing efforts for instrument validation and software benchmarking, assessing the required computational resources.

References:

[1] de la Rosa-Trevin JM, Sharov G, Fleischmann S, Morado D, Bollinger JC, Miller DJ, Terry DS, Blanchard SC, Fernandez IS, Carroni M. EMhub: a web platform for data

management and on-the-fly processing in scientific facilities. Acta Crystallogr D Struct Biol. 2024 Nov

Acknowledgments:

The authors would like to thank all of the facility staff of the CryoEM facility at SciLifeLab in Stockholm and the CryoEM Center at St. Jude Children's Research Hospital for their valuable feedback and discussions. We thank the Biomolecular X-Ray Crystallography Center and the Single-Molecule Imaging Center at St. Jude for their engagement. We are also very grateful for the tremendous support from the HPC, Cloud and Networking teams of the Information Services Department at St. Jude Children's Research Hospital.

CryoEM structures of human P5CS reveal its oligomeric organization and provide insight into dominant and recessive pathogenic mechanisms

Marco-Marín, Clara [*a], Escamilla-Honrubia, Juan Manuel [b], López-Redondo, Maria Luisa [b], Pla Fanjul, Sara [a], Llácer, José Luis [a], Rubio, Vicente [a]

[a]Instituto de Biomedicina de Valencia of the CSIC and Centro para Investigación Biomédica en Red sobre Enfermedades Raras CIBERER-ISCIII, Valencia, Spain.

[b]Instituto de Biomedicina de Valencia of the CSIC, Valencia, Spain.

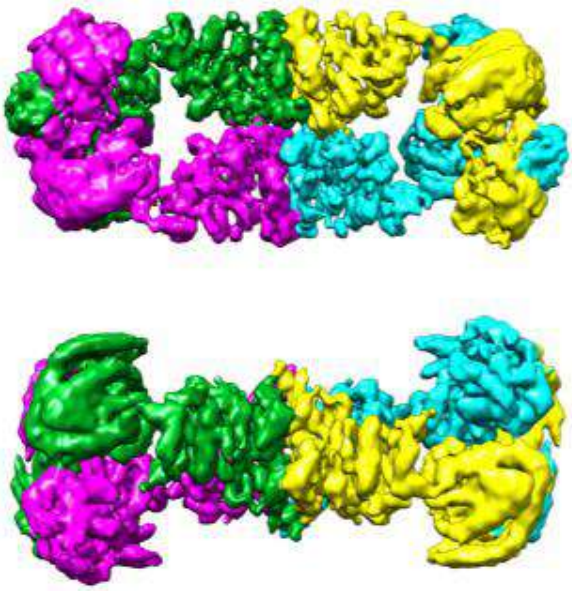

Pyrroline-5-carboxylate synthetase (P5CS) is a bifunctional single-polypeptide protein encoded by the *ALDH18A1* gene, comprising two enzymatic domains, glutamate 5-kinase (G5K) and glutamyl-5-phosphate reductase, which catalyze, respectively, the first and second steps of de novo synthesis of proline and ornithine/arginine. Two clinical syndromes, a neurocutaneous (NC) early-onset severe one and a later-onset complicated spastic paraplegia (SPG9), are associated with mutations in *ALDH18A1*, having recessive or dominant character, with mutation specificity for presentation and dominance or recessivity.

We concluded (Marco-Marin et al., J Inher Metab Dis 2012 and 2020) that all *ALDH18A1* pathogenic mutations cause loss of P5CS function, including dominant mutations, which would act by a negative dominance mechanism. To understand how is this possible, we determined the cryoEM structure of P5CS (3.4 Å), revealing a homotetrameric building block having point group 222 symmetry. The tetramer is formed by a central G5K planar tetramer, and by two peripheral globular blebs formed by pairs of G5PR domains. Anvil-like protrusions emerge

perpendicularly to the G5K plane at its center on both faces of the plane. Two tetramers stack via the anvil platforms to form octamers (3.8 Å) which could allow endless extension into approximately straight fibers defined by a torque rotation of the tetramer 60º around the fiber axis per step along the fiber, so that the same fiber orientation is seen every 180º. In fact, we have also observed two types of dodecamers (4.0 and 4.3 Å) of which one which could also be extended to the same linear fiber would represent three steps along the fiber, while the second would introduce bends in the fiber. Interactions between tetramers in the octamer and dodecamer are mediated by the central anvils and by contacts between G5PR domains of adjacent tetramers. Residues involved in these connections appear to be those causing dominance, giving the most severe presentation (NC) those affecting the anvil or residues at the interface between G5K domains within the tetramer. Thus, the ability to form fibers appears crucial for activity, and fiber distortion or abolition may decrease or abolish activity. As expected, mutations that cause misfolding and protein loss or kinetic aberrations that do not cause fiber distortion would be expected to be recessive. Experiments are under way to correllate structural derrangements with activity levels. The observed stacking in octamers and dodecamers is compatible with the filamentous assemblies reported for P5CS from *Drosophila melanogaster* or with optical microscopy observation in cells. It also resembles although with a different fiber torque the fiber of *Arabidopsis thaliana* P5CS, supporting the value of the plant enzyme as a potential model for human P5CS.

Acknowledgments:

Grants CIVP-20A6610 (Ramon Areces Foundation), BFU2017-84264-P and PID2020-116880GB-I00 (MICINN, Spanish Government).

Cryo-EM of influenza A polymerase in complex with small-molecule inhibitor

Modrego, Andrea [*a], Solanas, Lucía [a], Carlero, Diego [a], Bueno-Carrasco, María Teresa [b], Zamarreño, Noelia [a], Martín-Benito, Jaime [*a], Arranz, Rocío [*a]

[a]Centro Nacional de Biotecnología (CNB-CSIC) (ES)

[b]Instituto de Investigaciones Químicas (IIQ) - cicCartuja (ES)

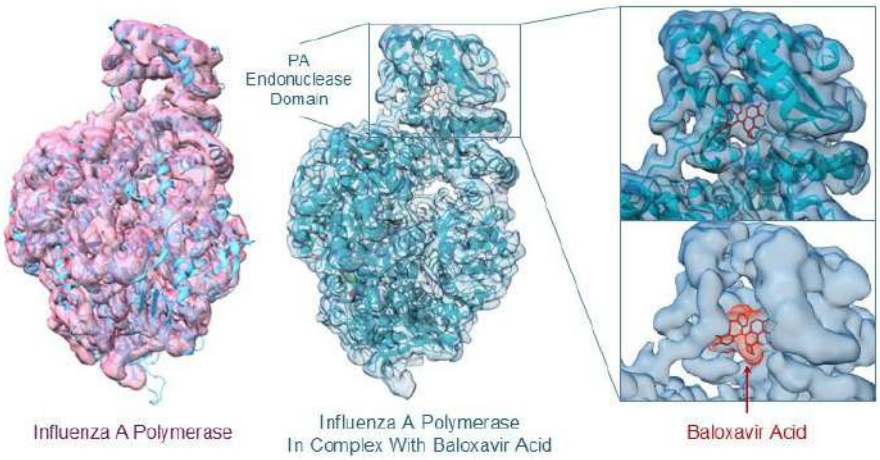

Influenza A virus replication relies on the activity of viral ribonucleoprotein complexes (vRNPs), which consist of a segmented RNA genome encapsidated by nucleoproteins (NP) and associated with a heterotrimeric RNA-dependent RNA polymerase (RdRp). This multifunctional polymerase, composed of the PB1, PB2, and PA subunits, meadiates both transcription and replication of the viral genome. PB1 serves as the catalytic core for RNA synthesis, PB2 binds host-derived capped primers, and PA harbors the endonuclease activity essential for the cap-snatching mechanism. Given its critical role in viral propagation, the polymerase is a prime target for antiviral development. Using cryo-electron microscopy (cryo-EM), we resolved the structure of the polymerase in complex with the endonuclease inhibitor baloxavir acid. The dataset revealed distinct conformational states, including classes where the PA endonuclease domain, harboring the drug-binding site, is well defined.

To complement the structural data, we assembled recombinant ribonucleoprotein complexes (RNPs) carrying a reporter RNA encoding nanoluciferase, enabling functional assessment of polymerase activity and inhibition.

These results highlight the utility of cryo-EM in capturing conformational dynamics relevant to drug binding and support structure-guided strategies for antiviral discovery against influenza A.

References:

[1] Omoto, S., Speranzini, V., Hashimoto, T. et al. Characterization of influenza virus variants induced by treatment with the endonuclease inhibitor baloxavir marboxil. Sci Rep 8, 9633 (2018).

[2] Todd, B., Tchesnokov, E. P., & Götte, M. The active form of the influenza cap-snatching endonuclease inhibitor baloxavir marboxil is a tight binding inhibitor. J Biol Chem 296, 100486 (2021).

Elucidating the Structure and Assembly Mechanism of Actinoporin Pores in Complex Membrane Environments

Martín-Benito, Jaime [*a], Arranz, Rocío [a], Santiago, César [a], Masiulis, Simonas [b], Rivera-de-Torre, Esperanza [c], Palacios-Ortega, Juan [c], Carlero, Diego [a], Heras-Márquez, Diego [c], Arias-Palomo, Ernesto [d], Martínez-del-Pozo, Álvaro [c], García-Linares, Sara [*c]

[a]Centro Nacional de Biotcnología, 28049, Madrid, Spain., [b]Materials and Structural Analysis Division, Thermo Fisher Scientific, Achtseweg Noord 5, 5651, Eindhoven, The Netherlands, [c]Departamento de Bioquímica y Biología Molecular, Universidad Complutense, Madrid, Spain, [d]Centro de Investigaciones Biológicas Margarita Salas, CSIC, 28040 Madrid, Spain.

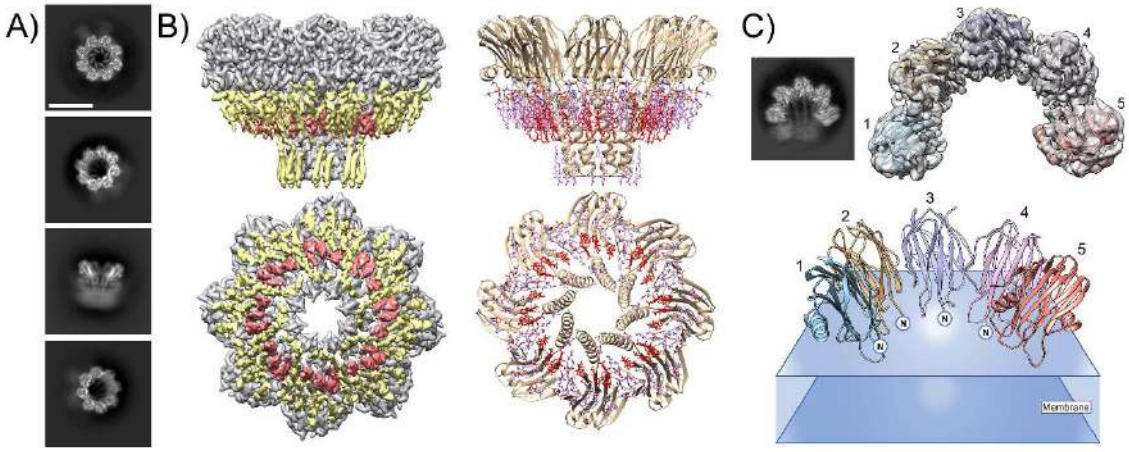

Figure 1. A) Two-dimensional class averages of sticholysin II pores reconstituted in lipid nanodiscs. Scale bar: 100 Å. B) Left: Side and bottom views of the cryo-EM map of fragaceatoxin C at 2 Å resolution, obtained from large unilamellar vesicles. Densities corresponding to protein, sphingomyelin (SM), and cholesterol are shown in grey, yellow, and red, respectively. Right: Side and bottom views of the atomic structure of the octamer, including eighty-eight lipid molecules and sixteen acyl chains. SM is shown in plink and cholesterol in red. C) Top: 2D class average of an intermediate pore composed of five monomers, along with the corresponding 3D reconstruction and atomic model of the sticholysin II pore intermediate. Bottom: Schematic representation of the atomic structure of the intermediate pore embedded in the membrane.

Pore-forming proteins exemplify the remarkable versatility of biological molecules. Initially produced as monomeric, water-soluble entities, they spontaneously assemble into multimeric integral membrane proteins upon encountering suitable target lipids [1]. Their functions span apoptosis, cell signaling, immunity, and inter-organismal attack and defense systems [2]. Among these are actinoporins, a family of pore-forming toxins from sea anemones that kill target cells by perforating their plasma membranes. Here, we present the structures of two such toxins, fragaceatoxin C and sticholysin II, in a complex membrane environment, determined using cryogenic electron microscopy. The structures reveal how dozens of lipid molecules interact in an orderly fashion, becoming integral components of the pore. We also isolated distinct pore-forming intermediates, in which only a subset of monomers is incorporated, forming non-closed, arc-shaped assemblies. Based on these structures, we propose a mechanism of action whereby sequential

monomer assembly onto the membrane, accompanied by conformational changes, drives pore formation and membrane perforation. Our findings provide new insights into the transformative capacity of these proteins, which are increasingly recognized for their diverse biotechnological applications [3,4].

References:

[1] Benton JT, Bayly-Jones C. Challenges and approaches to studying pore-forming proteins. Biochem Soc Trans. 2021 49(6):2749-2765.

[2] Dal Peraro M, van der Goot FG. Pore-forming toxins: ancient, but never really out of fashion. Nat Rev Microbiol. 2016. 14(2):77-92.

[3] Mutter NL, Huang G, van der Heide NJ, Lucas FLR, Galenkamp NS, Maglia G, Wloka C. Preparation of Fragaceatoxin C (FraC) Nanopores. Methods Mol Biol. 2021;2186:3-10.

[4] Robles-Martín, A., Amigot-Sánchez, R., Fernandez-Lopez, L. et al. Sub-micro- and nano-sized polyethylene terephthalate deconstruction with engineered protein nanopores. Nat Catal. 2023. 6, 1174–1185.

Insights into the dynamic architecture of GluA4-containing AMPA Receptors

Vega-Gutiérrez, Carlos [*a, b], Picañol-Parraga, Javier [c], Sánchez-Valls, Irene [a, b], Ribón-Fuster, Victoria [a, b], Soto, David [c], Herguedas, Beatriz [a, b]

[a]Institute for Biocomputation and Physics of Complex Systems, University of Zaragoza., [b]Advanced Microscopy Laboratory (LMA), University of Zaragoza., [c]Laboratory of Neurophysiology, Department of Biomedicine, Faculty of Medicine and Health Sciences, Institute of Neurosciences, University of Barcelona

AMPA receptors (AMPARs), part of the ionotropic glutamate receptor family, function as ligand-gated cation channels that mediate fast excitatory synaptic transmission and contribute to synaptic plasticity. These receptors form tetrameric assemblies composed of GluA1–GluA4 subunits. The presence or absence of the GluA2 subunit critically influences calcium permeability: GluA2-containing receptors are impermeable to Ca^{2+}, while those lacking GluA2 are permeable. AMPARs also interact with auxiliary proteins such as TARPs, CKAMPs, GSG1L, and CNIH, which modulate their functional properties, including gating dynamics and pharmacological profiles. Given their central role in synaptic function, AMPAR complexes represent important targets for the treatment of neurological diseases.

Here, we employed cryo-EM to analyse the structure of GluA4-containing AMPARs, both alone and in complex with the auxiliary subunit TARP-2, across three different conformational states. In the resting conformation, the GluA4 core exhibits a modular, Y-shaped structure and forms a dimer-of-dimers arrangement, consistent with previous observations in GluA2-based receptors. Notably, conformational changes associated with TARP-2 binding and channel gating reveal key structural deviations. In particular, we detected disruption of LBD dimer interfaces in a subset of the resting and desensitized particles, a feature reminiscent of GluA1-containing receptors. Additionally, our analysis uncovered a previously uncharacterized regulatory site implicated in TARP-2–mediated modulation.

Acknowledgments:

Project funded by Grant PID2019-106284GA-I00 and PID2022-140185NB-100 funded by MICIU/AEI /10.13039/501100011033. C.V.G. is funded by Grant PRE2020-092922 funded by MICIU/AEI /10.13039/501100011033

Precision Modulation of CXCR4 Function Through Allosteric Inhibition of Receptor Clustering

Santiago, César [*a], Garcia-Cuesta, Eva M. [a], Collado-Ávila, Javier [a], Rodríguez-Frade, José Miguel [a], Mellado, Mario [*a]

[a]Centro Nacional de Biotecnologia (CNB-CSIC) (ES)

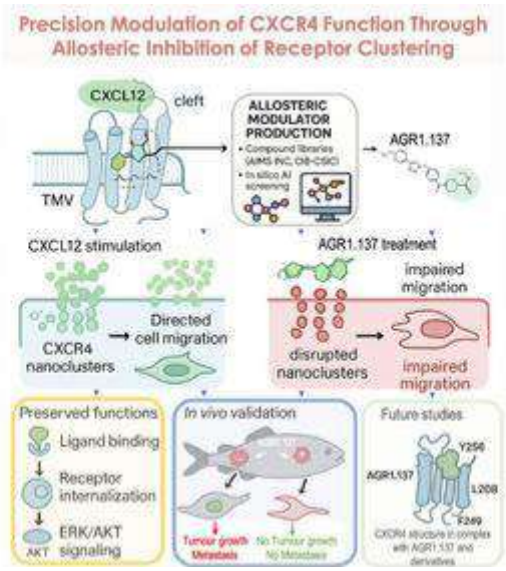

We have identified a novel allosteric region on the GPCR receptor CXCR4, defined by a cleft between transmembrane helices V and VI, as being essential for receptor nanoclustering and directional migration in response to CXCL12. Using in silico modelling and compound screening targeting this site, we have identified AGR1.137, a selective negative allosteric modulator. AGR1.137 disrupts CXCL12-driven nanoclustering and cell migration yet preserves ligand binding and canonical signalling. The functional importance of this allosteric region and the mechanism of action of AGR1.137 were validated using CXCR4 mutants that impair nanoclustering, as well as through in vivo experiments (including zebrafish tumour models), in which AGR1.137 reduced tumour progression and metastasis. These findings highlight the therapeutic potential of targeting CXCR4 allosteric sites to modulate cell migration with minimal side effects, offering an alternative to orthosteric antagonists such as plerixafor. To further advance our understanding, we are performing structural studies of CXCR4 and its complexes with AGR1.137 and related compounds using cryoelectron microscopy. This approach will provide high-resolution insights into the binding modes and conformational changes induced by allosteric modulators, informing the rational design of next-generation CXCR4-targeted therapies.

Acknowledgments:

Grants supporting this work: PID2020-114980RB-I00,P2022/BMD-7274,PID2022-140651NB-I00,SEV-2017-0712

Multimodal Correlative Imaging Using Cryo-SXT, Cryo-SIM, and Cryo-EM to Study Membranous Rearrangement Morphology in West Nile Virus-Infected Cells

Mamprin, Kevin [*a], Pérez Berná, Ana Joaquina [a]

[a]ALBA Synchrotron Light Source, Cerdanyola del Vallès (Barcelona), Spain

Positive-strand RNA viruses, such as hepatitis C virus (HCV), West Nile virus (WNV), and coronaviruses, hijack host cellular membranes to create specialized replication compartments [1]. Despite variations in membrane origin and structure, these compartments often share conserved features—most notably, the formation of double-membrane vesicles (DMVs) and invaginated vesicles (IVs) coronavirus [2]. In the case of WNV, a defining ultrastructural hallmark is the presence of convoluted membranes (CMs), which are intimately involved in the viral life cycle [3]. Traditional microscopy methods face significant limitations in visualizing such features within whole, unstained, and unperturbed cellular environments.

To overcome these challenges, we apply a correlative cryogenic imaging strategy—Cryo correlative Light and soft X-ray Tomography (CLXT)—that combines Structured Illumination Microscopy (SIM) with cryo soft X-ray tomography (cryo-SXT). This multimodal approach is designed to probe the 3D ultrastructure of infected cells at nanometric resolution while preserving native cellular architecture. Cryo-SXT operates in the water window energy range (520 eV), where carbon-rich structures absorb soft X-rays more strongly than their oxygen-rich, hydrated surroundings. This contrast mechanism allows label-free, quantitative imaging of whole vitrified cells with lateral resolutions of 50nm and depths up to 10 µm. Tilt series of X-ray projection images are reconstructed into 3D volumes that reveal the internal organization of infected cells with high structural fidelity.

Structured Illumination Microscopy (SIM), a super-resolution light microscopy technique, complements this by providing specific molecular context. SIM achieves resolutions below 100 nm using conventional fluorescent dyes and is compatible with cryo workflows. By projecting sinusoidal light patterns and reconstructing Moiré fringes, SIM reveals fine cellular details while preserving fluorescence signals. This makes it ideal for identifying and localizing fluorescently labeled structures in a cryogenic environment.

In this study, CLXT was employed to analyze the morphological alterations induced by WNV in whole cryo-preserved cells. We successfully identified convoluted membranes, characteristic of WNV replication, in the 3D reconstructed SXT volumes and verified their presence using SIM-based localization. This correlative

framework allowed us to spatially correlate ultrastructural features with fluorescent markers, significantly enhancing the interpretability and specificity of the dataset.

This work illustrates the power of correlative cryogenic multimodal imaging to investigate virus-induced cellular remodeling. The CLXT approach bridges the resolution gap between fluorescence and electron-based techniques while maintaining the contextual advantages of whole-cell imaging. By enabling the label-free, volumetric visualization of infection-related structures and correlating them with specific fluorescent markers, CLXT offers a robust and scalable platform for structural virology and cell biology research.

References:

[1] Paul, D.; Hoppe, S.; Saher, G.; Krijnse-Locker, J.; Bartenschlager, R. Morphological and Biochemical Characterization of the Membranous Hepatitis C Virus Replication Compartment. J Virol 2013, 87 (19), 10612–10627. https://doi.org/10.1128/JVI.01370-13.

[2] Castro, V.; Pérez-Berna, A. J.; Calvo, G.; Pereiro, E.; Gastaminza, P. Three-Dimensional Remodeling of SARS-CoV2-Infected Cells Revealed by Cryogenic Soft X-Ray Tomography. ACS Nano 2023, 17 (22), 22708–22721. https://doi.org/10.1021/acsnano.3c07265.

[3] Romero-Brey, I.; Merz, A.; Chiramel, A.; Lee, J.-Y.; Chlanda, P.; Haselman, U.; Santarella-Mellwig, R.; Habermann, A.; Hoppe, S.; Kallis, S.; Walther, P.; Antony, C.; Krijnse-Locker, J.; Bartenschlager, R. Three-Dimensional Architecture and Biogenesis of Membrane Structures Associated with Hepatitis C Virus Replication. PLoS Pathog 2012, 8 (12), e1003056. https://doi.org/10.1371/journal.ppat.1003056.

Acknowledgments:

This project has been founded by Marie-Slovodska Curie Training Network, CLEXM, under grant agreement No. 101120151 This study was funded by ALBA Synchrotron standard proposals 2024078517 and 2024098732

New opportunities for Electron Microscopy in Santander

Arechaga, Ignacio [*c], Rodriguez, Lidia [a], Fernandez, Luis [b]

[a]Servicio de Microscopía Electrónica de Transmisión (SERMET), Edif. Prof. Jose Luis García García de Ing. de Telecomunicación, Plaza de la Ciencia-4, 39005 Santander, [b]Dpto. Ciencias de la Tierra y Fisica de la Materia Condensada. Facultad de Ciencias. Avda. de los Castros 48, 39005 Santander, [c]Instituto de Biomedicina y Biotecnología de Cantabria (CSIC-UC). c/ Abert Einstein 22. PCTCAN. 39011 Santander

The SERMET (Transmission Electron Microscopy Service) at the University of Cantabria holds two electron microscopes to service both Material Sciences and Structure Biology needs. In addition, the service also holds a cryo-ultra-microtome to fulfill the requirements for both communities. The microscope for Material Science is a Jeol Jem 2100 (200 kV) equipped with a STEM unit, a XEDS microanalysis system and a CCD camera. On the Structural Biology side, the service hosts a Tundra Cryo-TEM (100kV), equipped with a high brightness XFEG gun, semi-automated sample loading, computerized stage with single-axis tilt holder, high resolution objective lens (SP-Twin) optimized for SPA (Single Particle Analysis) and a Thermo Scientific Ceta-F camera optimized for low dose imaging. This microscope has been designed following the ideas of Richard Henderson and Christopher Russo (1-2) on how a lower acceleration voltage could benefit the image contrast formation and reduce the dose electron damage in a cryo-electron microscope.

The Tundra Cryo-TEM setup at the SERMET also includes a cryo-loading workstation, a Vitrobot Mk IV for sample preparation, a PELCO glow discharge unit, and all the equipment necessary for sample preparation and preservation. Sample grids screened with the Tundra Cryo-TEM can be rescued for later use in top-end microscopes such as the Titan-Krios.

The microscope is setup with MiCo software and data acquisition is performed with EPU-2 software. It also includes Athena software to centralize and organize imaging data and experimental workflows.

The microscopes at the SERMET are open to be used for all the scientific community at reasonable competitive cost.

References:

[1] Peet MJ, Henderson R, Russo CJ. The energy dependence of contrast and damage in electron cryomicroscopy of biological molecular. Ultramicroscopy (2019) 203: 125-131

[2] McMullan et al. Structure determination by cryo-EM at 100 keV. Proc. Natl. Acad. Sci. USA (2023) 120 (49) e2312905120

Protofilament-specific nanopatterns of tubulin post-translational modifications regulate the mechanics of ciliary beating

Alvarez Viar, Gonzalo [a], pigino, gaia [*a], klena, nikolai [a], Martino, Fabrizio [a], nievergelt, adrian [b], bolognini, davide [a], capasso, paola [a]

[a]Human Technopole (IT)

[b]Max Planck Institut

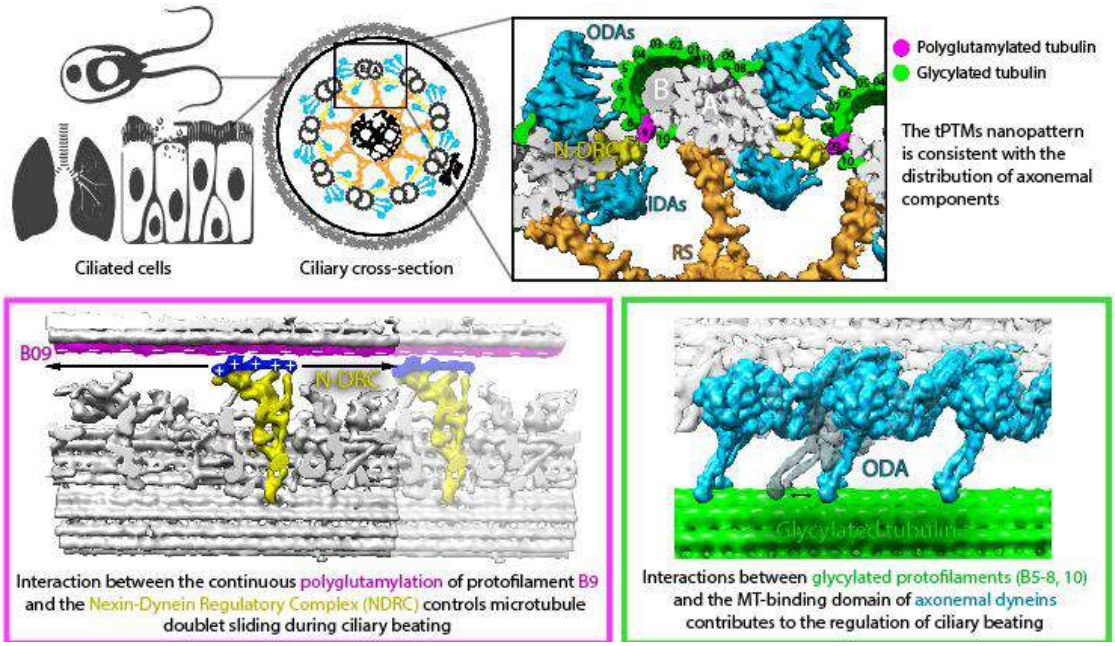

Controlling ciliary beating is essential for motility and signaling in eukaryotes. This process relies on the regulation of various axonemal proteins that assemble in stereotyped patterns onto individual microtubules of the ciliary structure. Additionally, each axonemal protein interacts exclusively with determined tubulin protofilaments of the neighboring microtubule to carry out its function. While it is known that tubulin post-translational modifications (PTMs) are important for proper ciliary motility, the mode and extent to which they contribute to these interactions remain poorly understood. Currently, the prevailing understanding is that PTMs can confer functional specialization at the level of individual microtubules. However, this paradigm falls short of explaining how the tubulin code can manage the complexity of the axonemal structure where functional interactions happen in defined patterns at the sub-microtubular scale. Here, we combine immuno-cryo-electron tomography (cryo-ET), expansion microscopy, and mutant analysis to show that, in motile cilia, tubulin glycylation and polyglutamylation form mutually exclusive protofilament-specific nanopatterns at a sub-microtubular scale. These nanopatterns are consistent with the distributions of axonemal dyneins and nexin-

dynein regulatory complexes, respectively, and are indispensable for their regulation during ciliary beating. Our findings offer a new paradigm for understanding how different tubulin PTMs, such as glycylation, glutamylation, acetylation, tyrosination, and detyrosination, can coexist within the ciliary structure and specialize individual protofilaments for the regulation of diverse protein complexes. The identification of a ciliary tubulin nanocode by cryo-ET suggests the need for high-resolution studies to better understand the molecular role of PTMs in other cellular compartments beyond the cilium.

Super-resolution microscopy reveals how viral infection reshapes host genome structure

Gonzalez-Almela, Esther [*a], Castells-Garcia, Alvaro [b], Le Dily, François [c], Merino, Manuel F. [c], Carnevali, Davide [c], Cusco, Pol [c], Di Croce, Luciano [c], Cosma, Pia [c]

[a]National Center for Biotechnology (CNB-CSIC) (ES)

[b]IMDEA-Nanociencia. C. Faraday, nº 9. 28049-Cantoblanco, Madrid, Spain (ES)

[c]Centre for Genomic Regulation (CRG)

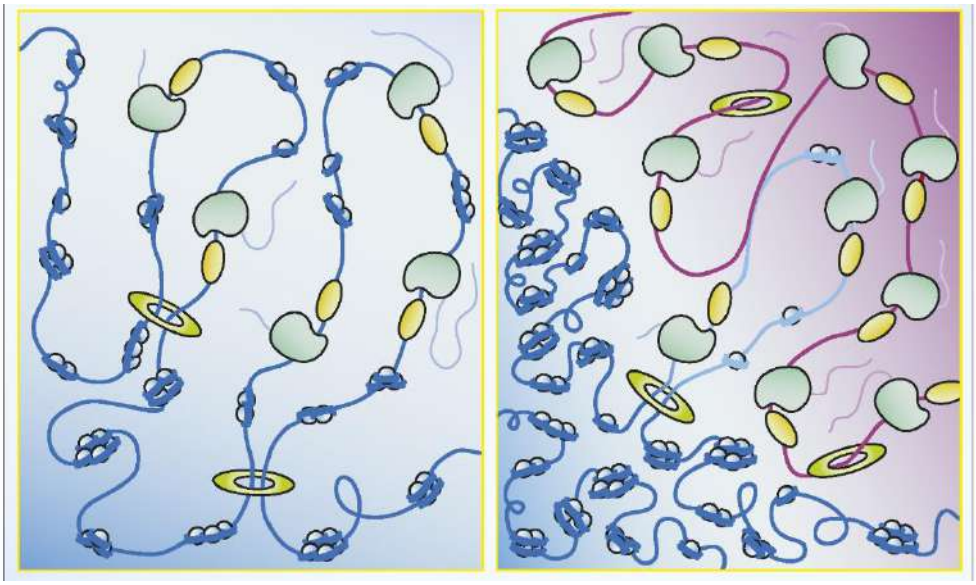

Herpes simplex virus type 1 (HSV-1) remodels the host chromatin structure and induces a host-to-virus transcriptional switch during lytic infection. We combined super-resolution imaging (STORM and PAINT) and chromosome-capture technologies to identify the mechanism of remodeling. We show that the host chromatin undergoes massive condensation caused not by epigenetic changes, but rather by the hijacking of RNA polymerase II (RNAP II) and topoisomerase I (TOP1). In addition, HSV-1 hijacking of cohesin results in the loss of topologically associating domains (TADs) and loops, although the A/B compartments are maintained in the host. The position of viral genomes and their association with RNAP II and cohesin was determined nanometrically. Strikingly, we reveal specific host–HSV-1 genome interactions and enrichment of upregulated human genes in the most contacting regions. This viral mechanism of host chromatin rewiring sheds light on the role of transcription in chromatin architecture and in viral infection.

Following the Interaction Between Microplastics, Biofilms and Antimicrobials Resistance

Jordao, Luisa [*c], Matias, Rui [a], Dias Nogueira, Isabel [b], [,] Rodrigues, Joao [a]

[a]Instituto Nacional de Saude Dr Ricardo Jorge (INSA), Departamento de Doenças Infeciosas (DDI), Lisboa, Portugal, [b]Instituto Superior Tecnico, Microlab, Lisboa, Portugal, [c]Instituto Nacional de Saude Dr Ricardo Jorge (INSA), Departamento de Saude Ambiental (DSA), Lisboa, Portugal

The intensive use of plastic, combined with its reduced and/ or extremely slow recyclability, leads to its accumulation in the environment, becoming a persistent pollutant. The plastic discarded in the environment originates by different mechanisms such as photo-degradation, high-temperature degradation, physical erosion and microbial degradation smaller particles known as microplastics (MPs ≤ 5mm) and nanoplastics (NPs≤ 1µm) that accumulate in the soil, water and organisms causing ecotoxicological issues. Microbial degradation of plastic is a sustainable remediation process for transforming and removing that is gaining growing attention. Biofilms can play an important role in this process but can also function as an environmental reservoir for potential human pathogens and antimicrobials resistance.

Here we studied the interaction between four MPs derived from some of most used plastic polymers, namely low-density polyethylene (LDPE), polypropylene (PP), polyethylene terephthalate (PET) and polystyrene (PET) and a consortium of four bacteria (*e.g. E. coli*, *Aeromonas sobria*, *Klebsiela pneumoniae* and *Enterobacter cloacae*) isolated from surface water over 46 days either in close or open systems. Biofilm assembly was assayed using crystal violet assay and colony forming units (CFU) enumeration. In addition, FISH and SEM were used to monitored biofilm assembly overtime. Bacteria were able to assemble biofilm on all plastics following a similar kinetic. SEM allowed the identification of heterogeneity in biofilm assembly on the MPs surface for the open system; as well as, differences between the two systems with enhanced biofilm formation in the open system.

Bacteria recovered from biofilm identification showed that *E. coli* was the less predominant bacteria. Bacterial susceptibility to antibiotics changed over the time course of the experiment. Since selection factors were not added to the media, we hypothesize that horizontal gene transfer between different isolates might be responsible for this result. Nevertheless, more studies must be performed to identify the genes responsible for the observed antibiotic susceptibility profiles.

Stranger Strands: Dissecting Transposition Through Cryo-EM and AI Prediction.

Arias-Palomo, Ernesto [*a] ,de la Gándara, Álvaro [a], Spínola-Amilibia, Mercedes [a], Araújo-Bazán, Lidia [a], Rizzuto, Irene [a], Núñez-Ramírez, Rafael [a], Berger, James M. [b]

[a]Centro de Investigaciones Biológicas Margarita Salas (CIB), CSIC (ES)

[b]Johns Hopkins University School of Medicine (US)

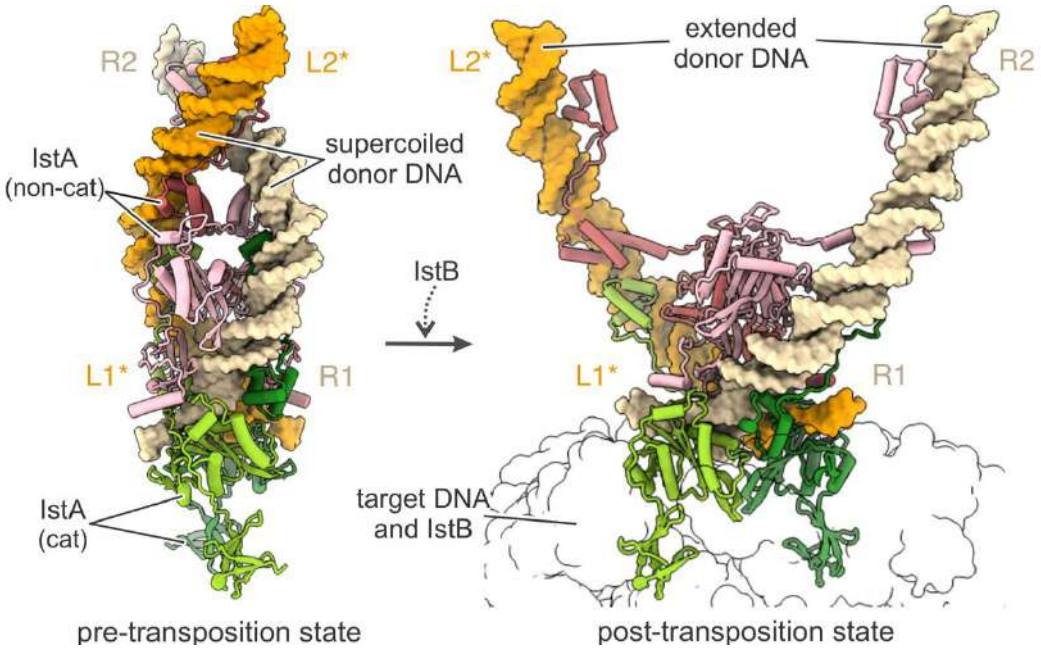

DNA transposition plays a central role in genome evolution and adaptation, contributing to the spread of antibiotic resistance and virulence factors. The IS21 family of bacterial transposons encodes a streamlined two-component system: IstA, the transposase, and IstB, a AAA+ ATPase that regulates transposition. Using cryogenic electron microscopy (cryo-EM), we captured key intermediates in the transposition process, providing insights into how IstA and IstB form autoinhibited DNA-bound assemblies and how ATP-driven remodeling of these complexes leads to catalytic activation and strand transfer.

Our structural analysis reveals how IstB oligomerization and nucleotide-dependent conformational changes drive site selection, transposase recruitment, and activation. These findings offer a molecular framework for understanding how AAA+ ATPases regulate transposition and related biological processes.

In parallel, we explored the potential of current structure prediction methods to model this dynamic system. This comparison highlights both the opportunities and

the limitations of computational tools when applied to large, multi-component protein–DNA assemblies. Together, our work provides a platform for dissecting the mechanisms of regulated transposition and evaluating integrative approaches in structural biology.

Acknowledgments:

Grant PID2023-152248NB-I00 funded by MICIU/AEI/10.13039/501100011033 and by ERDF, EU.

Structure and mechanism of human O-mannosyltransferase TMEM260 implicated in congenital heart disease

Ubarrechena, Ivan [*a], Halim, Adnan [*b], Cifuente, Javier O [a], Povolo, Lorenzo [b]

[a]Instituto Biofisika (UPV/EHU, CSIC), Leioa, Spain

[b]Copenhagen Center for Glycomics, University of Copenhagen, Copenhagen, Denmark.

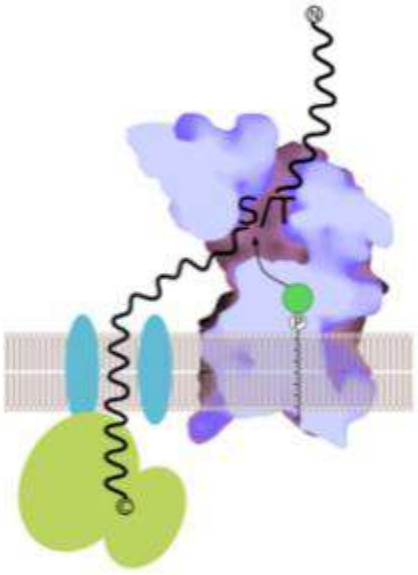

Congenital disorders of glycosylation (CDGs) are a growing group of genetic metabolic disorders caused by defects in protein glycosylation mediated by specific GlycosylTransferases (GTs). Among CDGs, structural heart defects and renal anomalies (SHDRA; OMIM 617478) syndrome is associated with early childhood mortality and features such as *corpus callosum* agenesis and persistent *truncus arteriosus* (PTA). Biallelic mutations in *TMEM260* (also known as *C14orf101*) have been identified in SHDRA syndrome cases. Notably, *TMEM260*-related congenital heart diseases may now be the leading cause of PTA in Japan, surpassing DiGeorge syndrome. We recently discovered human TMEM260 to be an endoplasmic reticulum (ER)-resident integral membrane O-mannosyltransferase. Three families of O-mannosyltransferases have been found in animal cells. They all localize to the ER and specialize in the transfer of α-mannose via O-linkage from the membrane embedded sugar donor dolichyl-phosphate-β-mannose (Dol-P-Man) to specific serine/threonine residues of their different protein substrate targets. TMEM260 is the founding member of the newly discovered third family and specializes in O-mannosylation (O-Man) of Immunoglobulin-like, Plexin, Transcription-factors (IPT) domains in cell-surface receptors, including plexins and receptor tyrosine kinases MET and RON. These receptors are implicated in intercellular communication and extracellular matrix signaling. SHDRA syndrome-linked *TMEM260* mutations disrupt

O-Man of the IPT domains of these receptors, leading to defects in their maturation and abnormal epithelial morphogenesis in 3D cell models. Despite its role in biology and disease the structure of TMEM260 is unknown. Here, we will present the cryo-electron microscopy (cryo-EM) structure of human TMEM260 in ternary complex (3.0-Å resolution) with the natural donor Dol-P-Man and an acceptor peptide derived from the IPT1-domain of the physiological substrate plexin-B2 semaphorin receptor. The structure reveals a new pGT architecture, the basis for IPT domain recognition and the mechanism of O-Man reaction. In addition, the structure serves as a framework to understand how disease-linked mutations impair TMEM260 function.

Fluorescence Localization and Quantitation of Nitric oxide-mediated PTMs in pollen grains

Alché, Juan de Dios [*a, b], Canón, José Luis [a], Pacheco, Rocío [a], Lima, Elena [a], Castro, Antonio Jesús [a]

[a]Estacion Experimental del Zaidin (EEZ-CSIC) (ES)

[b]University Institute of Research on Olive Grove and Olive Oils (INUO)

Pollen grains contain complex proteomes. A large proportion (between a quarter and a third) of these proteins have been predicted and even more, experimentally demonstrated to be modified through S- and Tyr- nitration. Both types of PTMs could represent key mechanisms in the regulation of the activity of enzymes involved in the primary metabolism of pollen, mainly through oxidation-reduction and transfer reactions, as well as in the modulation of the hydrolytic activity of cell wall enzymes of the pollen tube. Moreover, S-nitration could increase the allergenic potential of some proteins secreted by pollen grains.

In this context, the development of methods to visualize and quantify the extent of protein nitration is of paramount importance to stablish correlations between these parameters and microscopically-determined characteristics of pollen physiology like pollen germinability and the presence of phenotypic alterations affecting morphology and growth pattern of the pollen tube.

In this work, we have adapted fluorescence-based procedures to assess the level of nitration in pollen grains at the cellular level, by using confocal fluorescence microscopy.

As a first approach, germinated pollen grains were subjected to partial digestion of the cell wall by using cellulolytic and pectinolytic enzymes, in order to enhance the penetration of anti-Cys-NO and anti-Tyr-NO antibodies, which were then detected by immunofluorescence microscopy with Alexa488-labelled secondary antibodies.

In a different approach, we have adapted a protocol for the fluorescence-based localization and quantification of NO, released from protein Cys and Tyr nitrated residues after UV treatment of the samples [1], which has been adapted to the use of the DAF-2DA fluorophore, specific to identify NO molecules.

Both methods have been successfully assayed in pollen grains from olive tree (Olea europaea) and Eastern lily (Lilium longiflorum), cultured under standard conditions, as well as in the presence of NO donors such as SNP and GSNO, and NO scavengers like CPTIO.

References:

[1] Mioto, P. T.; Rodriguez-Ruiz, M.; Mot, A. C.; Zuccarelli, R.; Corpas, F. J.; Freschi, L.,; Mercier, H. Alternative fluorimetric-based method to detect and compare total S-nitrosothiols in plants. Nitric Oxide. 2017, 68, 7-13.

[2] Mioto, P. T.; Matiz, A.; Freschi, L.; Corpas, F. J. Fluorimetric-based method to detect and quantify total S-Nitrosothiols (SNOs) in plant samples. Nitrogen Metabolism in Plants: Methods and Protocols. 2020, 37-43.

Acknowledgments:

This work has been funded by Research Projects PID2020-113324GB-100 and TED2021-130015B-C22 (AEI, MCIN, Spain), partially co-funded by EU/ERDF and EU/PRTR

Validation of experimental CryoEM conformational landscapes with FlexConsensus

Herreros, David [*a], Sánchez Sorzano, Carlos Oscar [a], Carazo, José María [a]

[a]Spanish National Center for Biotechnology CNB-CSIC, Madrid, Spain

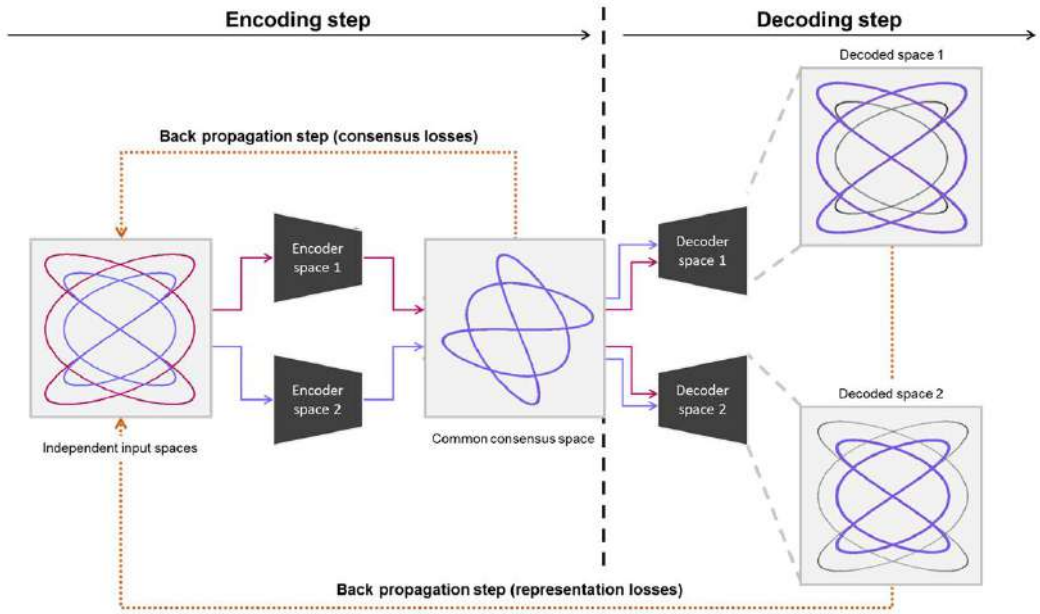

Biomolecules have varying degrees of conformational flexibility and compositional heterogeneity that complicates the image processing of large sets of cryo-electron microscopy images, especially when flexibility is continuous or there are many compositional options. New approaches like HetSIREN [1] and the Zernike3D family of algorithms [2] are capable of generating conformational landscapes representing complex heterogeneity cases while also producing higher resolution maps of the different states. However, the increasing pool of new algorithms approaching the conformational variability problem introduces a new challenge in comparing and assessing their estimations' reliability to extract more accurate landscapes and conformations.

In this work, we introduce FlexConsensus [3] as a new approach to comparing and validating conformational landscapes based on the estimations of different heterogeneity algorithms. This new method relies on a neural network designed and trained to learn how to merge different conformational landscapes into a common and meaningful consensus space. This consensus space leverages the preservation of the overall and local features of the input landscapes and their common characteristics.

Thanks to the properties of the consensus space, it is possible to measure each particle's stability. In this way, one can derive error histograms to easily identify particles estimated to have similar or different conformations and extract them to continue their analysis.

Additionally, FlexConsensus allows for the recovery of original spaces from the consensus space. Therefore, FlexConsensus also serves as a conversion tool, seamlessly moving from one landscape representation to another to recover and compare the structures determined by different methods.

To illustrate FlexConsensus capabilities, we tested the method's performance against a wide range of simulated and experimental datasets.

Among the simulated datasets, we analyzed a set of controlled but challenging datasets capturing a wide range of conformational variations integrated in CryoBench [4], such that a simulated disordered motion of an IgG antibody or a dataset obtained from a molecular dynamics simulation of the SARS-CoV-2 spike. In these tests, we proved a strong correlation between the location in the consensus space and the conformational states simulated in the images.

Moving to the experimental datasets, FlexConsensus was tested against the EMPIAR 10028 dataset, a realistic and well-studied set of images that illustrates the method's practical capabilities. Complementary to the EMPIAR 10028, we analyzed an experimental SARS-CoV-2 dataset capturing a wide range of the main spike motions to assess better how different methods' landscapes compare and to determine the stability of the distribution of states found by the algorithms.

FlexConsensus is publicly available through Scipion [5] and the Scipion Flexibility Hub [6].

References:

[1] Herreros, D.; Mata, C.P.; Noddings, C.; Irene, D.; Krieger, J.; Agard, D.A.; Tsai, M.D; Sorzano, C.O.S; Carazo, J.M. Real-space heterogeneous reconstruction, refinement, and disentanglement of CryoEM conformational states with HetSIREN. Nat Commun 2025, 16, 3751.

[2] Herreros, D.; Lederman, R.R.; Krieger, J.; Jimenez-Moreno, A.; Martinez, M.; Myska, D.; Strelak, D.; Filipovic, J.; Sorzano, C.O.S.; Carazo, J.M. Estimating conformational landscapes from Cryo-EM particles by 3D Zernike polynomials. Nat Commun 2023, 14, 154.

[3] Herreros, D.; Mata, C.P.; Sorzano, C.O.S; Carazo, J.M. Merging conformational landscapes in a single consensus space with FlexConsensus algorithm. BioRxiv 2025, 2025.01.07.631840.

[4] Jeon, M.; Raghu, R.; Astore, M.; Woollard, G.; Feathers, R.; Kaz, A.; Hanson, S.M.; Cossio, P.; Zhong, E.D. CryoBench: Diverse and challenging datasets for the heterogeneity problem in cryo-EM. 2024, arXiv:2408.05526.

[5] de la Rosa-Trevín, J.M. ; Quintana, A.; del Cano, L.; Zaldívar, A.; Foche, I.; Gutiérrez, J.; Gómez-Blanco, J.; Burguet-Castell, J.; Cuenca-Alba, J.; Abr-ishami, V,: Vargas, J.; Otón, J.; Sharov, G.; Vilas, J.L.; Navas, J.; Conesa, P.; Kazemi, M.; Marabini, R.; Sorzano, C.O.S.; Carazo. J.M.; Scipion: A software framework toward integration, reproducibility and validation in 3D electron microscopy. Journal of Structural Biology, 2016, 195, 93–99.

[6] Herreros, D.; Krieger, J.; Fonseca, Y.; Conesa, P.; Harastani, M.; Vuillemot, R.; Hamitouche, I.; Serrano Gutierrez, R.; Gragera, M.; Melero, M.; Jonic, S.; Carazo, J.M.; Sorzano, C.O.S. Scipion Flexibility Hub: an integrative framework for advanced analysis of conformational heterogeneity in cryoEM. Acta Crystallogr D Struct Biol, 2023, 79, 569-584

Cryo-EM studies on RNA polymerase III transcriptional pausing

Huecas, Sonia [*a], Plaza-Pegueroles, Adrian [a], Fernández-Tornero, Carlos [a]

[a]Centro de Investigaciones Biológicas Margarita Salas (CIB), CSIC (ES)

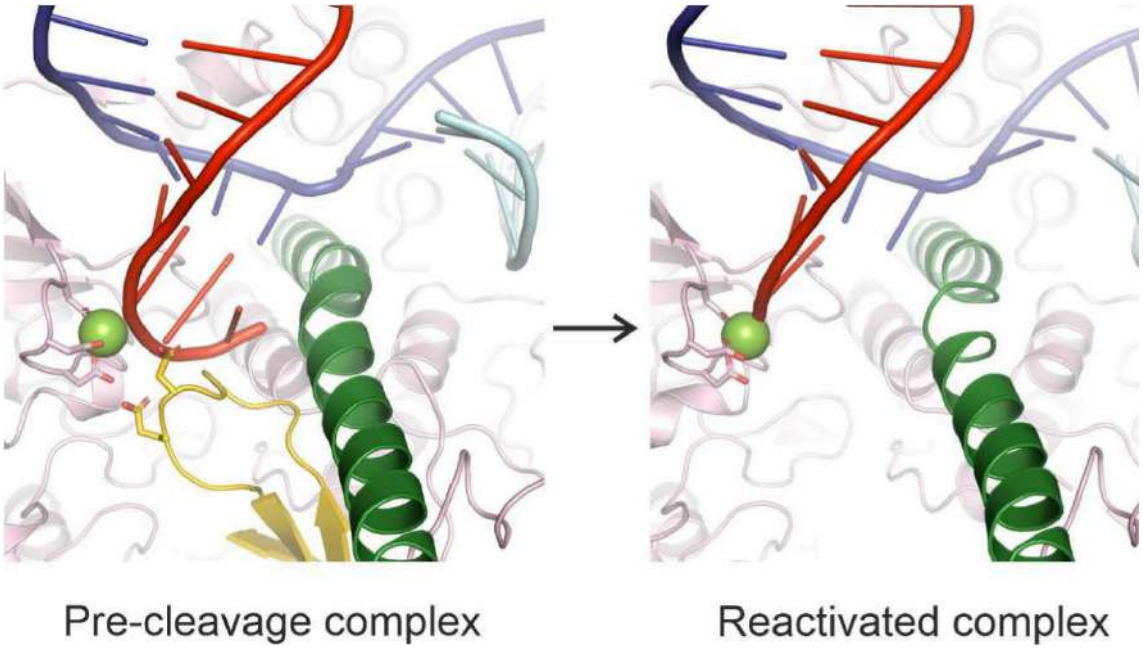

Eukaryotic cells employ RNA polymerase III (Pol III), an enzyme constituted by 17 subunits, to synthesize tRNAs and other short and abundant RNAs which are essential for cellular functions. Transcriptional barriers or nucleotide misincorporations during DNA transcription cause Pol III pausing. Reactivation of the enzyme requires RNA cleavage, which depends on subunit C11. We used cryo-EM combined with biochemical analysis to characterize different stages of Pol III transcriptional pausing. We report three structures representing the arrested complex, the pre-cleavage complex and the reactivated complex. Our results show that paused Pol III interacts more loosely with the hybrid formed by the template DNA strand and the newly-synthetized RNA. Moreover, the C-terminal domain of subunit C11 and the Pol III catalytic center coordinate to cleave backtracked RNA nucleotides. The high resolution of our structures allows to obtain mechanistic insights into Pol III pausing and opens the avenue to understand enzyme reactivation.

Multiscale Imaging Reveals the Role of APC-driven Actin Nucleation in Collective Cell Remodelling, Motility and Mechanotransduction in Cancer Cells

Baro, Lautaro [*a], Juanes Ortiz, Maria Angeles [*a]

[a]Cytoskeletal Dynamics in Cell Migration and Cancer Invasion Laboratory, Centro de Investigación Príncipe Felipe, 46012 Valencia, Spain.

Colorectal cancer (CRC) arises from perturbations in the colonic epithelium, including disruption of the epithelial cell polarity and motility. Gut epithelium maintenance relies on the fine-tuning function of the actin cytoskeleton. One of the proteins that governs actin cytoskeleton dynamics is the tumour suppressor Adenomatous Polyposis Coli (APC), well-known as the gatekeeper in colorectal cancer. *In vitro* work showed that APC interacts with cytoskeletal networks through its C-terminal basic domain, and this interaction has been shown to be critical for proper cell adhesion and directionality of individual cells. However, whether APC-driven actin activity contributes to any collective cell migration event in gut homeostasis and/or impacts on health is unknown.

Here, we began to decipher whether APC-driven actin nucleation plays a role in collective cell remodelling and, consequently, collective migration and invasion of colorectal cancer cells. We used cell monolayers and spheroids stably expressing either wild-type APC (APC-WT) or a separation-of-function mutant (APC-m4) incapable of nucleating actin filaments. We combined this genetic tool with different molecular and cellular biology assays and several bioimaging techniques – confocal microscopy (fixed & live imaging), scanning electron microscopy (SEM) and traction force microscopy (TFM) – a method to measure forces exerted by cells on their surrounding environment. Confocal imaging experiments using cell monolayers revealed that the lack of APC-driven actin nucleation activity perturbed the integrity of the cell-cell junctions and collective cell migration. Ultrastructural effects of APC-m4 mutation at the cell junctions were confirmed by SEM imaging. Moreover, confocal microscopy assays using APC-m4 collagen-embedded spheroids showed reduced and shorter cell finger-like protrusions emanating from spheroids compared to APC-WT spheroids. In addition, TFM experiments showed

that APC-m4 spheroids exhibited lower traction forces than APC-WT spheroids, which could explain the reduced abilities of the mutant spheroids to invade.

Together, microscopical approaches across scales have been instrumental in uncovering the importance of APC-driven actin nucleation activity, not only in maintaining the integrity of epithelial monolayers but also in facilitating the force of actin finger-like protrusions that penetrate the basement membrane and invade surrounding tissues. Further studies will be needed to validate APC's cytoskeletal functions in vivo and to exploit its potential as a therapeutic target for interventions aimed at preventing colorectal cancer progression.

Structural Characterization of the K50 Depolymerase

Francés-Castillo, Ignacio [*a, b], Hernandez Grimalt, Ana [c, d], Morais Ezquerro, Sergi [c], Domingo Calap, Pilar [d], López-Redondo, Marisa [f], Casino, Patricia [a, b, e]

[a]Instituto Universitario de Investigación en Biotecnología y Biomedicina (BIOTECMED), Burjassot 46100, Valencia, Spain, [b]Departamento de Bioquímica y Biología Molecular, Universidad de Valencia, Burjassot 46100, Valencia, Spain, [c]Instituto Interuniversitario de Investigación de Reconocimiento Molecular y Desarrollo Tecnológico (IDM), Universitat Politècnica de València-Universitat de València, Camino de Vera s/n, E46022 València, Spain., [d]Institute for Integrative Systems Biology, University of Valencia-CSIC, Paterna 46980, Valencia, Spain, [e]CIBER de Enfermedades Raras (CIBERER-ISCIII), Madrid, [f]Instituto de Biomedicina de Valencia (IBV), CSIC, Valencia 46010, Spain

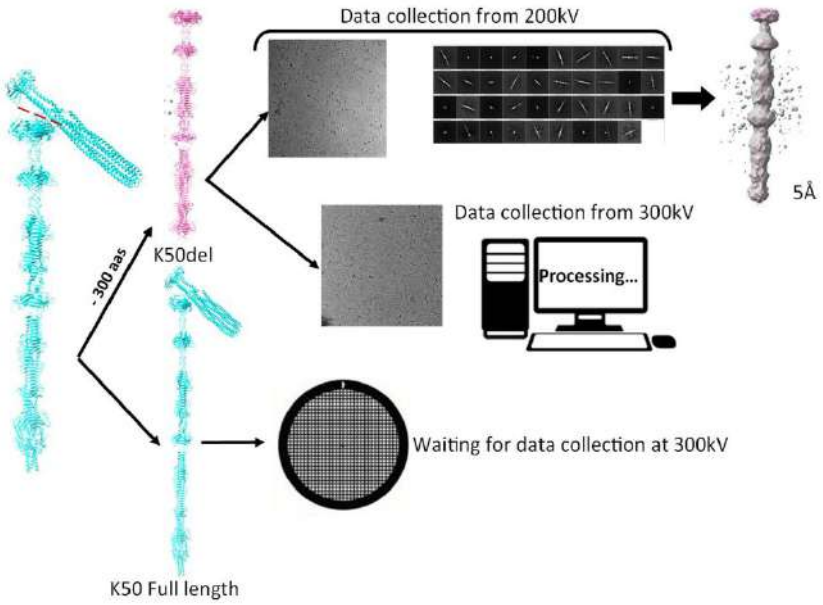

Receptor Binding Proteins (RBPs) are bacteriophage proteins found at the distal end of the phage tail that mediate recognition and binding to bacterial cell surfaces by specifically recognizing structural elements such as LPS, pili, porins, teichoic acids, etc. For encapsulated bacteria, the RBPs can also present a depolymerase domain capable of digesting oligosaccharide bonds to facilitate access to the cell surface.

Phage K50PH164C1 targeting *Klebsiella pneumoniae* presents a depolymerase at the end of its tail fiber of interest to develop phage-derived sensing proteins for diagnostic applications. For this, our group focused on solving its structure, an elongated fiber more than 40 nm long, which is of note since few structures alike have been solved.

Working with a deletion of the N-terminal, we obtained micrographs at the 200kV Glacios microscope at ALBA Synchrotron, and 2D classes which were used to model a preliminary 3D volume at 5Å. This model confirmed our predictions about the structure of the fiber protein, and we obtained data at the 300kV Titan Krios microscope at ESRF, which we hope will provide more information when processed.

Finally, grids were prepared and screened with the full-length protein. In this run we overcame the issues we found with the first run, obtaining better quality grids that will allow for improved data collection. We are currently waiting for time to perform a full data collection on the full-length protein to finally elucidate the structure of this interesting protein at high resolution.

Structural characterization and functional testing of surface-enhanced bacterial flagella

Estevan-Morió, Eva [*a], González-Pérez, Laia [a], Hedengrahn, Julia [a], Eckhard, Ulrich [*a]

[a]Molecular Biology Institute of Barcelona (IBMB-CSIC) (ES)

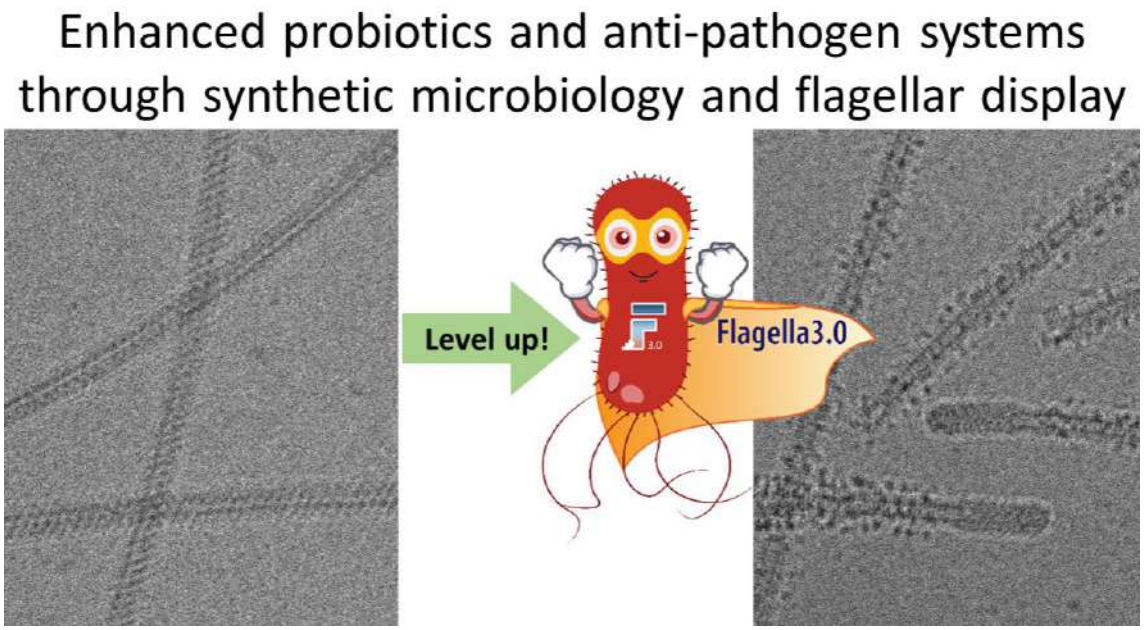

The bacterial flagellum is a highly sophisticated organelle primarily evolved for motility that exhibits a long whip-like filament consisting of up to 30,000 subunits of molecular building block, the protein flagellin. In 2017, our lab discovered and describe the very first enzymatically active bacterial flagella, displaying proteolytic domains on their filament surface (1). Based on this discovery, we now aim to re-engineer naturally occurring structural flagellins to encode for enzymatic activity, and to use these semi-synthetic functionalized nanomachines and bacteria for dedicated biotechnological applications.

To do so, we have first established a plasmid-based system for flagella and thus motility restoration in a flagellin-knockout *E. coli* strain. Next, we recreated proteolytically active flagella in *E. coli* – a first proof of concept of enzymatic flagellar display, and a key first step in the development of a robust flagellar surface display system for other functional domains. Over the last months, we have optimized sample preparation of intact flagellar filaments and collected several cryo-EM datasets of various semi-synthetic filaments displaying different functional domains.

We hope, this will allow us to understand how these displays affect at the molecular level the flagellum's overall architecture, the conformation of the displayed domain,

and its interaction with the filament, and enable us to develop a more rational approach for grafting functional domains onto the flagella surface.

References:

[1] Eckhard, U., Bandukwala, H., Mansfield, M.J. et al. Discovery of a proteolytic flagellin family in diverse bacterial phyla that assembles enzymatically active flagella. Nat Commun 8, 521 (2017)

In situ characterization of CCT during immune synapse

Muriel, Olivia [a], Sancho-González, Beatriz [a], Piccirillo, Jonathan Gabriel [a], Delgado-Gestoso, David [a], Cuervo, Ana [a], Cuéllar, Jorge [a], Martín-Cófreces, Noa Beatriz [b], Sánchez-Madrid, Francisco [b], Valpuesta, José María [*a]

[a]Department of Macromolecular Structures, Centro Nacional de Biotecnología (CNB-CSIC), Madrid, Spain.

[b]Immunology Service, Hospital Universitario de la Princesa, Universidad Autonoma Madrid (UAM), Instituto Investigacion Sanitaria-Instituto Princesa (IIS-IP), Madrid, Spain.

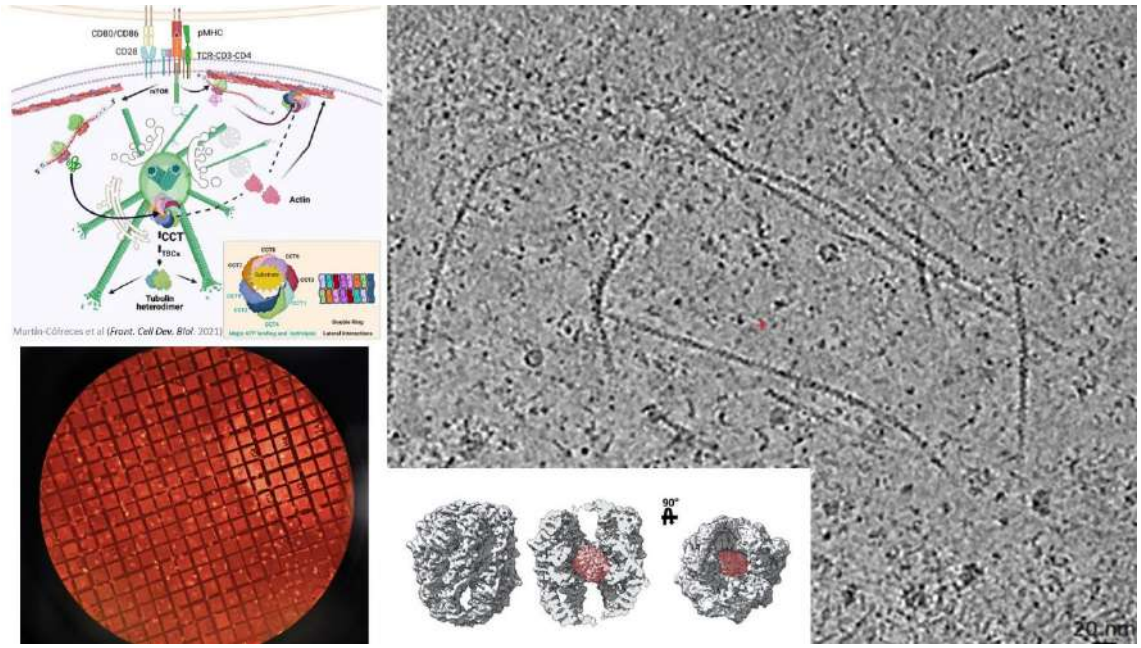

The immune synapse (IS) is a transient, dynamic cell-to-cell communication structure that forms at the interface of T cells and antigen-presenting cells (APCs)**.** During this interaction, the organelles and the cytoskeleton of the T-cell polarize to the IS.

Actin and tubulin cytoskeleton are major clients of the chaperonin-containing tailless complex polypeptide 1 (CCT). Therefore, we hypothesized that CCT must be highly concentrated in this process playing an important role.

Although the CCT structure has been largely characterized using single particle analysis, there is only a few works identifying CCT *in situ*, opening a new line of study for the characterisation of the CCT structure within the cell.

In this work we have performed cryoelectron tomography on thin T cell projections generated during IS. Our first batches of tomograms show an abundance of actin filaments surrounded by particles whose size and shape may match CCT. We are currently working on subtomogram averaging and map fitting of CCT.

Once CCT can be certainly identified, as well as its predominant conformation, we plan to explore further the biological functions of CCT during IS.

A New Era for the CryoEM Facility (CNB-CSIC)

Chichón, Francisco Javier [a], Zamarrreño, Noelia [a], Delgado, David [a], Muriel, Olivia [a], Santiago, Cesar [a], Picchirillo, Jonathan Gabriel [a], Bueno, Maria Teresa [b], Iceta, Mikel [a], Sánchez, Irene [a], Arranz, Rocio [*b]

[a]Spanish National Center for Biotechnology CNB-CSIC, Madrid, Spain

[b]Instituto de Investigaciones Químicas (IIQ) - cicCartuja (ES)

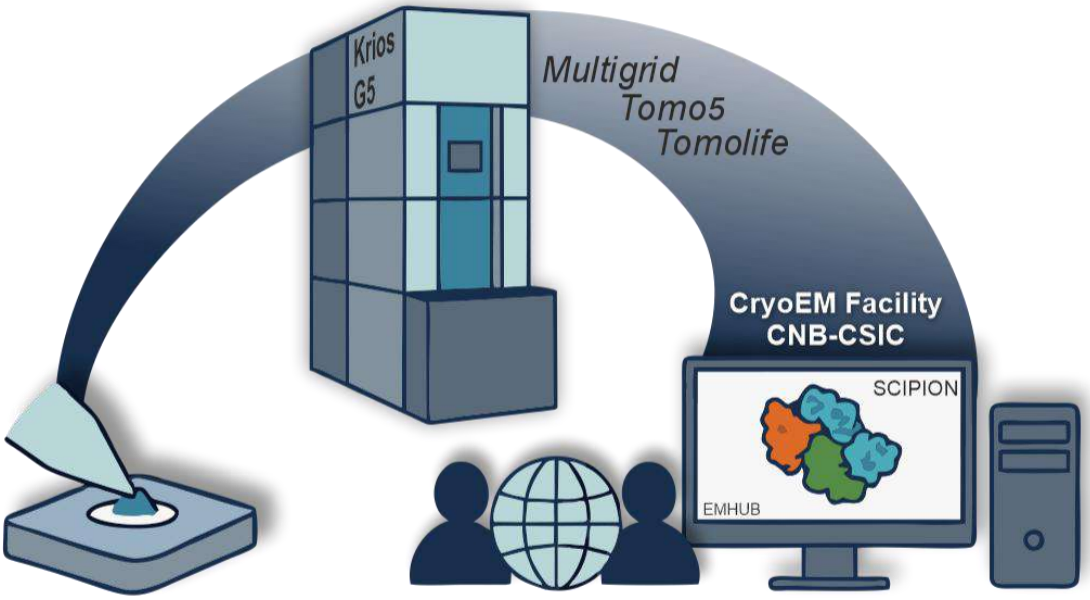

The CryoEM Facility at the National Centre for Biotechnology (CNB-CSIC), part of the Spanish node of INSTRUCT-ERIC, is entering a new phase. This year marks a significant renewal in infrastructure, services, and the way users interact with the facility and their data. The facility has undergone technical upgrades, and we are now better equipped to meet the growing demands of structural biology in cryo-electron microscopy.

At the core of this transformation is the installation of a new Titan Krios G5, a high-end instrument that complements our existing Talos Arctica. This setup increases our flexibility and throughput, allowing us to support a broader range of experimental needs. Both microscopes are equipped with the latest dedicated software for high-throughput and high-performance image acquisition.

In addition, we now offer dedicated instrumentation for cryo-lamella preparation (FIB-SEM), and enhanced capabilities for cryo-fluorescence imaging, enabling robust cryo-correlative workflows (CLEM). These upgrades allow us to cover the

entire pipeline, from sample preparation to data acquisition, across multiple cryoEM modalities.

Our current service offering includes:

- Preliminary screening and optimization of cryo-samples.
- High-throughput cryo-image acquisition for statistical analysis.
- High-resolution single particle analysis (SPA).
- Cryo-electron tomography (CryoET).
- Correlative light and electron microscopy (CLEM).
- Micro-electron diffraction (MicroED) for small crystals.
- Post-processing: Movie Alignment; Fully automated 2D/3D SPA workflows (Scipion [1]); Fully Automated tomographic reconstruction.

We remain committed to being a user-focused facility through EMHUB [2]. With this new phase, we are adopting more open access to data and post-processing resources. Users will benefit from clearer workflows, improved scheduling, and tailored support based on their level of experience, from direct access for expert users to fully supported projects for researchers new to the technique. We also aim to foster long-term scientific collaborations through training, consultation, and co-development of experimental strategies.

The CryoEM Facility (CNB-CSIC) continues to operate within the INSTRUCT-ERIC framework, providing access not only to national users but also to international researchers through transnational access programs. As part of a broader European infrastructure that promotes excellence in structural biology, we are committed to contributing high-quality data, reliable instrumentation, and expert support.

In summary, the CryoEM Facility at CNB-CSIC is entering a new chapter, one defined by advanced instrumentation, expanded capabilities, and a renewed approach to user interaction. We are prepared to enable the next generation of cryoEM research and to play an active role in driving forward structural biology

References:

[1] De la Rosa-Trevín, J. M.; Quintana, A.; Del Cano, L.; Zaldívar, A.; Foche, I.; Gutiérrez, J.; Gómez-Blanco, J.; Burguet-Castell, J.; Cuenca-Alba, J.; Abrishami, V.; Vargas, J.; Otón, J.; Sharov, G.; Vilas, J. L.; Navas, J.; Conesa, P.; Kazemi, M.; Marabini, R.; Sorzano, C. O. S.; Carazo, J. M. Scipion: A software framework toward integration, reproducibility and validation in 3D electron microscopy. J. Struct. Biol. 2016, 195, 93–99.

[2] De la Rosa-Trevín, J. M.; Sharov, G.; Fleischmann, S.; Morado, D.; Bollinger, J. C.; Miller, D. J.; Terry, D. S.; Blanchard, S. C.; Fernandez, I. S.; Carroni, M. EMhub: a web platform for data management and on-the-fly processing in scientific facilities. IUCrJ 2024, 11, 728–742

Acknowledgments:

We gratefully acknowledge José María Carazo and his group for their constant support. We also thank José Miguel de la Rosa Trevín for his assistance with the installation and operation of EMHUB. Financial support was provided by the CRIOMECORR project (ESFRI-2019-01-CSIC-16), Instruct-ERIC Projects, and the “Severo Ochoa” Programme for Centres of Excellence in R&D (CEX2023-001386-S).

Pestivirus assembly by cryo-ET and computational analysis

Martinez-Castillo, Ane [a], Charro, Diego [a], Koethe, Susanne [b], Maffeo, Chistopher [c], Santos-Perez, Isaac [a], Chaturvedi, Parth [c], Azkargorta, Mikel [d], Aebischer, Andrea [b], Vidaurrazaga, Ander [a], Castaño-Diez, Daniel [e], Dent, Kyle [f], Walsh, Martin M [f], Elortza, Felix [d], Aksimentiev, Aleksei [*c], Beer, Martin [*b], Abrescia, Nicola GA [*a]

[a]Structure and Cell Biology of Viruses Lab, Center for Cooperative Research in Biosciences (CIC bioGUNE) Basque Research and Technology Alliance (BRTA); Derio, Spain.

[b]Friedrich-Loeffler-Institut, Federal Research Institute for Animal Health; Greifswald - Insel Riems, Germany

[c]Department of Physics and Beckman Institute for Advanced Science and Technology, University of Illinois Urbana-Champaign, Urbana, IL, USA

[d]Proteomics Platform, CIC bioGUNE-BRTA, CIBERehd; Derio, Spain.

[e]Biofisika Institute (CSIC-UPV/EHU), Science Park of the UPV/EHU, Leioa, Spain

[f]Diamond Light Source; Didcot, United Kingdom

Pleomorphic Bovine Viral Diarrhea Virus (BVDV) is a positive-sense, single-stranded RNA virus belonging to the *Flaviviridae* family (genus *Pestivirus*). It infects cattle, alpacas, deer, sheep, and goats and is considered one of the most costly viral diseases affecting cattle, posing a significant burden on livestock welfare. Disease control relies on modified live and killed vaccines when prevention programs are in place. The viral envelope is composed of three BVDV glycoproteins - E^{rns}, E1, and E2 - which are responsible for viral entry and infection. Among these, E^{rns} and E2 are the primary targets of neutralizing antibodies. Although the crystal structures of the corresponding ectodomains have been determined [1-3], the overall 3D architecture and organization of the glycoproteins within the viral lipid bilayer, as well as the mechanisms of antibody recognition, remain poorly understood [4].

By integrating cryo-electron tomography (cryo-ET), proteomics, and molecular dynamics (MD) techniques, we provide new insights into the antibody recognition and assembly mechanisms of pestiviruses – essential prerequisites for the development of effective vaccines.

References:

[1] Krey, T.; Bontems, F.; Vonrhein, C.; Vaney, MC.; Bricogne, G.; Rümenapf, T.; Rey, FA. Crystal structure of the pestivirus envelope glycoprotein E(rns) and mechanistic analysis of its ribonuclease activity. Structure. 2012, 20(5):862-73.

[2] El Omari, K.; Iourin, O.; Harlos, K.; Grimes, JM.; Stuart, DI. Structure of a pestivirus envelope glycoprotein E2 clarifies its role in cell entry. Cell Rep. 2013, 3(1):30-5.

[3] Li, Y.; Wang, J.; Kanai, R.; Modis, Y. Crystal structure of glycoprotein E2 from bovine viral diarrhea virus. Proc. Natl. Acad. Sci. USA. 2013, 110(17):6805-10.

[4] Callens, N.; Brügger, B.; Bonnafous, P.; Drobecq, H.; Gerl, MJ.; Krey, T.; Roman-Sosa, G.; Rümenapf, T.; Lambert, O.; Dubuisson, J.; Rouillé, Y. Morphology and Molecular Composition of Purified Bovine Viral Diarrhea Virus Envelope. PloS Pathog. 2016, 12(3):e1005476.

Calcium and nitrogen biomineralization studies in frozen hydrated whole cells using transmission soft x-ray microscopy

Sorrentino, Andrea [*a], Rossi, Francesca [b], Noy, Yael [c], Barzilay, Yuval [c], Perez, Ana [a], Malucelli, Emil [b], Eyal, Zohar [c], Gur, Dvir [c], Iotti, Stefano [b]

[a]ALBA Synchrotron Light Source, Cerdanyola del Vallès, Barcelona, Spain

[b]) Department of Pharmacy and Biotechnology, University of Bologna, Bologna, Italy

[c]Department of Structural Biology, Weizmann Institute of Science, Rehovot, Israel

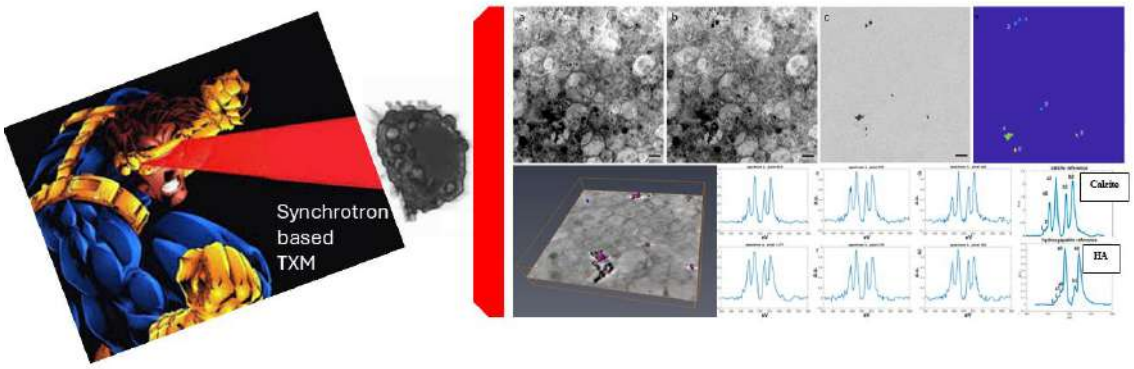

Biomineralization is the process by which living organisms form mineral crystals. It plays a crucial role in a wide range of biological functions, from skeletal formation to bio-mining. While the presence of mature crystals in various biomineralizing cells is well documented, the exact mechanisms underlying crystal formation often differ between organisms and remain not fully understood, especially during the early stages [1], [2].

Both the Calcium L-edge (~350 eV) and the Nitrogen K-edge (~400 eV) fall within the "water window" energy range. This spectral window enables the correlative use of cryo-tomography and cryo-spectromicroscopy to investigate early-stage Ca and N biomineralization processes in cryopreserved, frozen-hydrated whole cells.

These transmission X-ray microscopy (TXM) techniques are available at the Mistral beamline of the ALBA synchrotron with about 30 nm spatial resolution [3]. In this work examples of biomineralization studies performed at Mistral on both Ca and N in different biological cells will be presented [4], [5].

References:

[1]] Addadi L. and Weiner S., Control and Design Principles in Biological Mineralization, Angew. Chem. Int. Ed. Engl. 1999, 1, 123-456.

[2] Gur, D.; Politi, Y.; Sivan, B.; Fratzl, P.; Weiner, S.; Addadi L.; Guanine-based photonic crystals in fish scales form from an amorphous precursor. Angew. Chem. Int. Ed. Engl. 2013, 52, 388-391.

[3] Sorrentino, A.; Nicolás, J.; Valcárcel, R.; Chichón, F.J.; Rosanes, M.; Avila, J.; Tkachuk, A.; Irwin, J.; Ferrer, S.; Pereiro, E. MISTRAL: A Transmission Soft X-Ray Microscopy Beamline for Cryo Nano-Tomography of Biological Samples and Magnetic Domains Imaging. J. Synchrotron Rad. 2015, 22, 1112–1117.

[4] Sorrentino, A. ; Malucelli, E. ; Rossi, F. ; Cappadone, C. ; Farruggia, G. ; Moscheni, C. ; Perez-Berna, A.J. ; Conesa, J.J. ; Colletti, C. ; Roveri, N. ; Pereiro E. ; Iotti S. Calcite as a Precursor of Hydroxyapatite in the Early Biomineralization of Differentiating Human Bone-Marrow Mesenchymal Stem Cells. Int. J. Mol. Sci. 2021, 22, 4939 – 4955.

[5] Eyal, Z. ; Ggorelick-Ashkenazi. A. ; Deis, R. ; Barzilay, Y. ; Broder, Y. ; Kellum A. P. ; Varsano, N. ; Hartstein, M. ; Sorrentino, A. ; Kaplan-Ashiri, I. ; Rechav, K. ; Metzler, R. ; Houben, L. ; Kronik, L. ; Rez, P. ; Gur, D. Controlled pH Alteration Enables Guanine Accumulation and Drives Crystallization within Iridosomes. bioRxiv preprint

EM01-CRYO-TEM: a New Cryo Electron Microscopy Platform at ALBA

Guerra, Pablo [*a]

[a]Cryo Electron Microscopy Platform IBMB-CSIC

The recent development of transmission electron microscopy has opened the door to data acquisition at atomic resolution and, consequently, to a new dimension in the research of high resolution molecular structures, both from biological and materials samples. While other regions in Spain have made a strong commitment to equip themselves with state-of-the- art equipment, in Catalonia we are far behind with these kind of infrastructures. This situation has finally changed thanks to the installation of a Glacios 200kV TEM located in the JEMCA (Joint Electron Microscopy Center at Alba), in the ALBA synchrotron. This new infrastructure, devoted to high-end transmission electron microscopy analyses, emerged thanks to the collaboration between several local and national institutions.

The IBMB-CSIC Cryo-electron Microscope Platform possess a specialized cryo-electron microscope for structural biology applications. The platform will give access to state-of-the-art cryo-EM equipment for structure determination projects using the latest technology and methods. Glacios 200kV transmission electron microscope equipped with a cryogenic sample manipulator robot and with the last generation of direct electron detector, a Falcon 4 that can take up to 400 movies per hour. Its high level of automation and user guidance of experimental settings enable scientists to efficiently unravel protein structures in 3D, as well as understand their functional context in the biological cell.

In vivo Labelling of Specific mRNAs Using CRISPR-deadCas13 Strategies as a Tool for Cryo-correlative Light Electron Microscopy

Fernández-Fernández, María Rosario [*a, b, c]

Alcalá-Pérez, Saúl [a, b]

Fernández, José-Jesús [*a, b]

[a]Centro de Investigación en Nanomateriales y Nanotecnología-Consejo Superior de Investigaciones Científicas (CINN-CSIC). El Entrego, Asturias, Spain.

[b]Instituto de Investigación Sanitaria del Principado de Asturias (ISPA-FINBA). Oviedo, Spain.

[c]Instituto de Biomedicina y Biotecnología de Cantabria- Consejo Superior de Investigaciones Científicas (IBBTEC-CSIC) Santander, Spain.

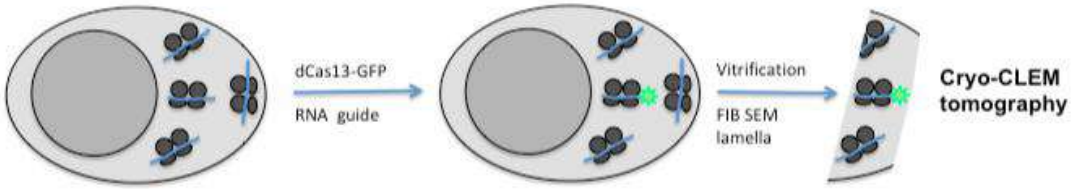

Beyond the gene editing applications of CRISPRCas, the development of nuclease-deadCas molecules offers an extension of the applications of the CRISPRCas technology without gene editing or RNAse processing. Despite Cas proteins being large and multi-domain proteins, early work showed silencing the two endonuclease domains in Cas9 via point mutations resulted in a nuclease-dead Cas9 that could still bind to DNA [1]. CRISPR-Cas13 is an RNA-guided and RNA-targeting RNAse protein. Cas13 functions similarly to Cas9, using a guide RNA (CRISPR RNA; crRNA) to encode target specificity. DeadCas13 mutants fused to EGFP have been recently successfully employed to visualize the location and dynamics of specific RNAs in live cells [2]. This is a very interesting and promising system to efficiently visualize specific mRNAs in live cells and learn how they relate to the translation machinery. This approach is currently of great interest as there is

growing evidence on the existence of specialized ribosomes that translate specific mRNAs that operate in certain physiological and pathological conditions. We have recently reported by using electron tomography that ribosomes in the neurons of a Huntington's disease (HD) knock-in mouse model show a remodelling towards a more compacted polysomal architecture, an aberrant polysomal architecture that is compatible with ribosome stalling [3]. Here we explore if deadCas13 strategies could allow the specific labelling of mRNAs coding for mutant huntingtin and image their relation to the ribosome stalling phenotype by cryo-correlative light and electron tomography. To start with we have set up the protocol for specific mRNA labelling in HEK293T cells by co-transfecting a plasmid overexpressing a deadCas13b protein fused to EGFP and a plasmid expressing specific guides for huntingtin mRNA. As a positive control we have used a guide directed against NEAT1 (a non-coding RNA present in nuclear paraspeckles) [2] and as a negative control a non-specific "non-target" guide that is not complementary to any known sequence. We will also present here the integration of the labelling protocol into the cryo-CLEM workflow.

References:

[1] Xu, X.; Qi, L.S. A CRISPR-dCas Toolbox for Genetic Engineering and Synthetic Biology. J. Mol. Biol. 2019, 431, 34-47.

[2] Yang, L-Z.; Wang, Y.; Li, S-Q.; Yao, R-W.; Luan, P-F.; Wu, H.; Carmichael, G.G.; Chen, L-L. Dynamic Imaging of RNA in Living Cells by CRISPR-Cas13 Systems. Mol. Cell. 2019, 76, 981-997.

[3] Martin-Solana E.; Diaz-Lopez I.; Mohamedi, Y.; Ventoso, I.; Fernandez, J-J.; Fernandez-Fernandez M.R. Progressive alterations in polysomal architecture and activation of ribosome stalling relief factors in a mouse model of Huntington's disease. Neurobiol. Dis. 2024; 195, 106488.

Acknowledgments:

We would like to thank Dr. Sandra Rodríguez Perales and Dr. Raúl Torres at CNIO, Madrid for their invaluable help with the CRISPRCas technology. This work was supported through grants PID2022-139071NB-I00 and PID2023-153013OB-I00, funded by MCIN/AEI/10.13039/501100011033, "ERDF A way of making Europe" and by the "European Union NextGenerationEU/PRTR.

Cryo-STEM and X-ray fluorescence imaging reveals Electron-Dense granules as dynamic metal reservoirs in response to stress

Romão, Célia [*a], Gouveia, André [a], Wolf, Sharon [b], Elbaum, Michael [c]

[a]ITQB NOVA - Universidade NOVA de Lisboa (PT), [b]Department of Chemical Research Support, Weizmann Institute of Science, 7610001 Rehovot, Israel., [c]Department of Chemical and Biological Physics, Weizmann Institute of Science, 7610001 Rehovot, Israel.

Electron-dense granules (EDGs) are known to exist within bacteria, and play a key role as intracellular metal and polyphosphate reservoirs. We have been investigating the function of electron dense granules in bacterium *Deinococcus radiodurans*, which is a model organism regarding its extreme resistance to radiation. Using X-ray fluorescence nano-imaging data (ID16A-NI and ID16-B beamlines at ESRF), we analyzed the metal content in these compartments. Our results show that EDGs are elemental-rich regions, particularly with phosphorous mostly in the form of poly-P, calcium and manganese under control conditions, and that these elements are mobilized in response to stress. To gain deeper molecular and structural insights, we performed Cryo-STEM coupled with Electron Dispersive X-ray Spectroscopy (EDS) on the *D. radiodurans* cells. The results reveal a heterogeneous metal composition across different cells, suggesting that EDGs contribute to a dynamic stress-responsive mechanism of metal regulation within the bacterial population.

Acknowledgments:

European Union's Horizon 2020 research and innovation programme under grant agreement No 857203- IMpaCT - Imaging life from Molecules to cells - building knowledge on Cryo-electron microscopy methodologies at ITQB NOVA – www.itqb.unl.pt/impact. Cryo-electron microscopy studies received partial support from the Weizmann Institute of Science (The Irving and Cherna Moskowitz Center for Nano and BioNano Imaging), and from the European Union (ERC-AdV grant, CryoSTEM, 101055413 to ME). This work benefited from access to the Weizmann Institute Electron Microscopy Unit, an Instruct-ERIC centre through the Access proposal PID: 19879. The image analysis of Cryo-EM images was made available thanks to the de Picciotto Cancer Cell Observatory in Memory of Wolfgang and Ruth Lesser of the MICC Life Sciences Core Facilities at the Weizmann Institute of Science. FCT Project: PTDC/BIA-BQM/31317/2017. We acknowledge the European Synchrotron Radiation Facility for the X-ray fluorescence imaging (XRF) at ID16B with the proposal LS-3037.

Structural Engineering of Poly-CCT5 Chaperonin: A Novel Platform for Nanoparticle Delivery

Gutiérrez Seijo, Jorge [*a], Pipaón, Sergio [a], Cuervo, Ana [a], G Ovejero, Jesús [b], Santiago, Cesar [a], Morales, María del Puerto [b], Valpuesta, José María [*a], Cuéllar, Jorge [*a]

[a]Centro Nacional de Biotecnología (CNB-CSIC) (ES)

[b]Instituto de Ciencia de Materiales de Madrid, ICMM-CSIC, C/Sor Juana Inés de la Cruz, 3, 28049 Madrid, Spain

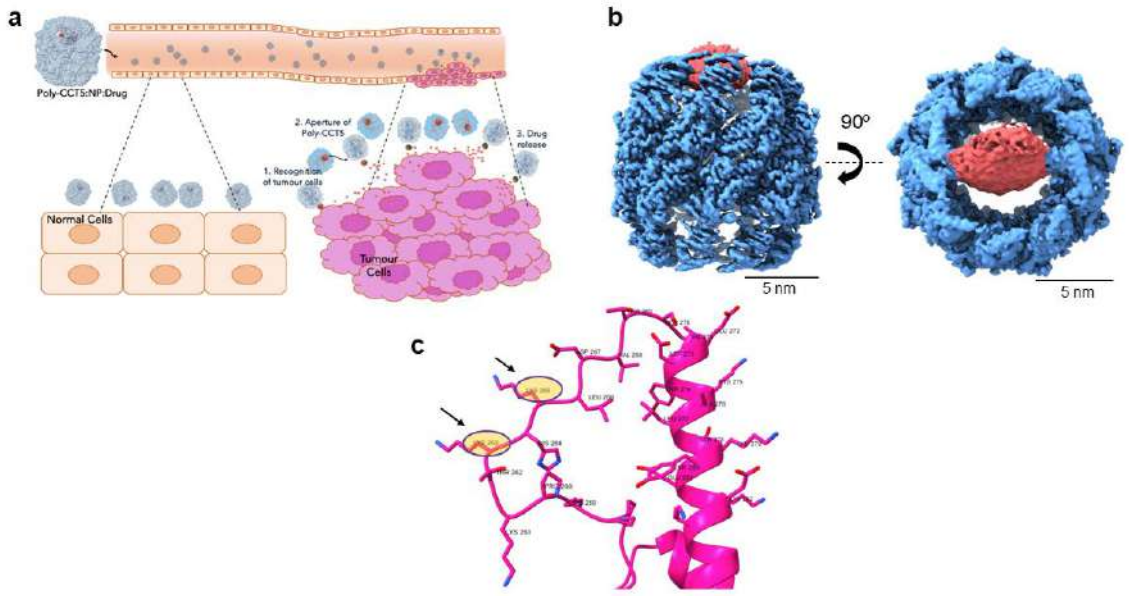

Chaperones assist in the de novo protein folding and prevent protein aggregation [1]. One of the most important chaperone families are the chaperonins (Hsp60s), which are organized as two oligomeric back-two-back rings generating a cavity in each ring where the substrate is placed for its folding [2]. The most complex and important of all chaperonins is the eukaryotic CCT (Chaperonin Containing TCP-1) whose structure and the folding mechanism are key for nanotechnological applications [3].

The main aim of this project is to build a stable synthetic cylindrical structure capable of encapsulating chemical reagents or small proteins. It has been shown that CCT5 is able to self-oligomerize. When compared to the eukaryotic CCT, poly-CCT5 is easier to purify, can be genetically modified in all subunits and has potential to be biocompatible [4]. These capabilities enable poly-CCT5 to act as a nanocontainer delivering molecules to specific targets (See Figure a).

Our group used negative staining EM to assess the encapsulation of various nanoparticles inside synthetic poly-CCT5. VENOFER, an iron-sucrose coating NP,

produced the best results overall and was chosen for Cryoelectron microscopy (CryoEM) analysis. We first generated a 3.2 Å 3D reconstruction of the NP-bound poly-CCT5, with the NP presumably held by CCT5 apical domains (See Figure b). Subsequently, our efforts shifted towards designing and structurally characterizing poly-CCT5 mutants, aimed at rearranging the charge distribution within the cavity to minimize undesired interactions (See Figure c). This approach led to the generation of an initial 5 Å 3D reconstruction of NP-bound poly-CCT5, demonstrating improved nanoparticle internalization. Currently, we are focusing on inducing the closure of the cavity to rearrange the N- and C-terminal, eliminating steric impediments and thereby achieving complete nanoparticle encapsulation.

Figure. Summary of the obtained results. a) Proof of concept illustrating the delivery of the Poly-CCT5:NP:Drug complex through the bloodstream, including tumor cell recognition, Poly-CCT5 aperture, and drug release mechanism.. b) 3D reconstruction of the poly-CCT5 complex (blue) with nanoparticle (red) at 3.16 Å resolution. c) Helical protrusion of the CCT5 subunit, with shaded areas and arrows highlighting the lysines selected for mutation.

References:

[1] Yébenes, H., Mesa, P., Muñoz, I. G., Montoya, G., & Valpuesta, J. M. (2011). Chaperonins: two rings for folding. Trends in biochemical sciences, 36(8), 424–432.

[2] Bueno-Carrasco MT, Cuéllar J. Mechanism and Function of the Eukaryotic Chaperonin CCT. eLS: John Wiley & Sons, Ltd; 2018. p. 1-9.

[3] Sergeeva OA, Chen B, Haase-Pettingell C, Ludtke SJ, Chiu W, King JA. Human CCT4 and CCT5 Chaperonin Subunits Expressed in Escherichia coli Form Biologically Active Homo-oligomers. J Biol Chem 2013 -6-14;288:17734-17744.

Structural characterization of a complex involved in chaperone-assisted UPS degradation

Muntaner, Jimena [*a], Maestro-López, Moises [a], Cheung Cheng, Tat [b], Cuéllar, Jorge [*a], Valpuesta, José María [*a], Sakata, Eri [*b]

[a]Centro Nacional de Biotecnología (CNB-CSIC) (ES)

[b]University of Goettingen (DE)

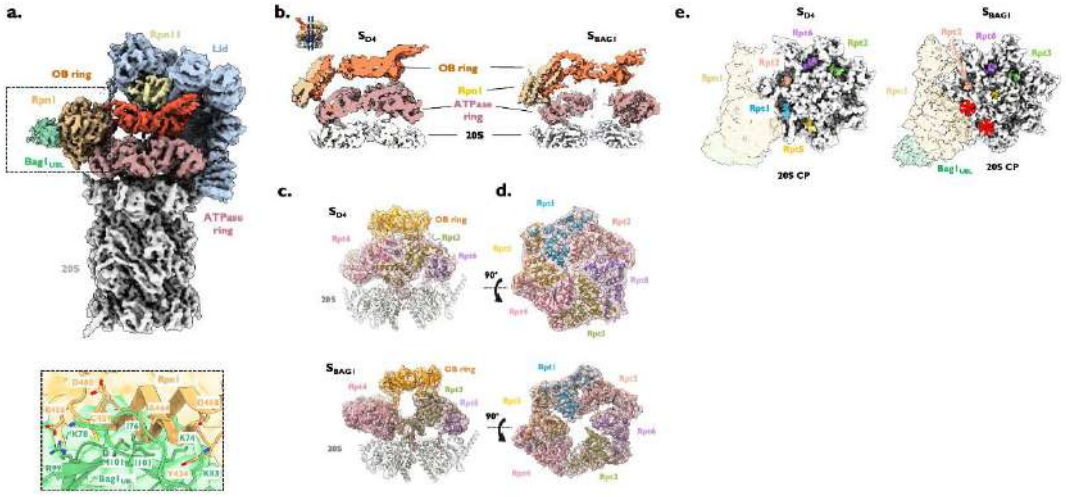

Protein homeostasis is sustained through a finely tuned balance of protein synthesis, folding, trafficking, assembly, and degradation, processes that are essential for proper cellular function[1]. Molecular chaperones act as key regulators within this proteostasis network, with their functional outcomes determined by specific co-chaperones. These co-chaperones modulate the Hsp70:substrate complex, directing it either towards folding or degradation via the ubiquitin-proteasome system (UPS) or autophagy[2]. Bag1 (Bcl-2-associated athanogene 1) is one such co-chaperone, serving as a nucleotide exchange factor (NEF) for Hsp70 and containing a ubiquitin-like (UBL) domain that mediates its interaction with the proteasome[3].

In this study, we demonstrate a strong interaction between Bag1 and the proteasomal subunit Rpn1. The ternary complex (Rpn1:Bag1:Hsp70) was successfully isolated and characterized through cryo-electron microscopy (cryo-EM) and cross-linking mass spectrometry, offering valuable mechanistic insights into the process of substrate transfer from Hsp70 to the proteasome.

A high-resolution cryo-EM map (3.6 Å) of the 26S proteasome in complex with Bag1 revealed binding of the UBL domain to the toroidal region of Rpn1 (Fig. 1a). This interaction induces significant structural rearrangements within the 19S AAA-ATPase, particularly at the Rpt4–Rpt5 interface, quite different from known structures (Fig. 1b-d). Such conformational changes may facilitate the positioning of Hsp70 near the proteasomal gate, promoting efficient substrate transfer. Furthermore, biochemical assays suggest that Bag1 binding induces an alternative open-gate conformation of the proteasome (Fig. 1e), enabling translocation and degradation of unfolded proteins in an ATP- and ubiquitin-independent manner.

Figure 1. Structural Reorganization of the 26S Proteasome Induced by Bag1 Binding. **(a)** Cryo-EM reconstruction of the 26S proteasome in the S_{BAG1} conformation (EMDB:52097) at 3.6 Å resolution, revealing only the UBL domain of Bag1 ($Bag1_{UBL}$). The inset highlights the interaction interface between Rpn1 and $Bag1_{UBL}$. **(b)** Cross-sectional view of the cryo-EM maps of S_{BAG1} and S_{D4} (EMDB: 32282; PDB: 7W3K) shows a distinct alignment of the OB, ATPase, and 20S rings in S_{BAG1}, indicating structural rearrangements upon Bag1 binding. **(c, d)** Segmentation of the OB-ATPase interface **(c)** and ATPase ring **(d)** reveals that Bag1 disrupts the ATPase ring symmetry, generating a large central cavity and inducing conformational shifts in Rpt3 (green) and Rpt4 (pink). These changes suggest an alternative substrate entry pathway (red arrow in **(c)**) into the 20S proteasome. **(e)** Differences in 20S gate opening between S_{D4} and S_{BAG1}. In S_{BAG1}, only Rpt2, Rpt3, and Rpt6 insert into the α-ring, yet the 20S gate remains open, suggesting a non-canonical activation mechanism. The S_{D4} conformation serves as a reference due to its structural similarity to S_{BAG1} in both 19S and 20S.

References:

[1] Hartl, F.U., Bracher, A., and Hayer-Hartl, M. (2011) Molecular chaperones in protein folding and proteostasis. Nature, 475, 324-332.

[2] Shiber, A. And Ravid, T. (2014) Chaperoning Proteins for Destruction: Diverse Roles of Hsp70 Chaperones and their Co-Chaperones in Targeting Misfolded Proteins to the Proteasome. Biomolecules, 4, 704-724.

[3] Lüders, J., Demand, J., & Höhfeld, J. (2000). The ubiquitin-related BAG-1 provides a link between the molecular chaperones Hsc70/Hsp70 and the proteasome. Journal of Biological Chemistry.

Insights into AAV stability and particle integrity during viral vector biopharmaceutical manufacturing

Abrescia, Nicola G. A [*a,d] ,Arriaga, Iker [a], Navarro, Aitor [b], Uribe-Echeverría, Esther [a], Isábal, Maria [b], Silva, Elisa [b], Guarinoni, Thomas [b], Lang, Valérie [b], Iribar, Haizea [b], Trigueros, César [b], Moullier, Philippe [b,c], François, Achille [b]

[a]Structure and Cell Biology of Viruses Lab, CIC bioGUNE, Basque Research and Technology Alliance (BRTA), Derio, Bizkaia, 48160, Spain.

[b]Viralgen Vector Core S.L., San Sebastian, Gipuzkoa, 20009, Spain.

[c]Asklepios BioPharmaceutical, Inc. (AskBio), 20 T.W. Alexander, Suite 110 RTP, Durham, NC 27709, USA

[d]Ikerbasque, Basque Foundation for Science, Bilbao, Bizkaia, 48015, Spain.

Many adeno-associate virus (AAV) serotypes are being investigated in preclinical and clinical trials. A few have been already approved by the US and European regulatory drug agencies. A major challenge in the AAV gene therapy applications is the large-scale production of a good-manufacturing-practice (GMP) AAV product that fulfils international regulations for clinical release.

Here, we investigated the capsid thermostability and transgene release of purified AAV vectors via differential scanning calorimetry, and by performing potency assays. We also determined by high-resolution cryogenic electron microscopy the 3D structure of AAV6 – a valuable tool for genome editing of hematopoietic cells– at different pHs.

We demonstrate that genome leakage occurs at temperatures below capsid unfolding temperatures and that acidic pH led to conformational changes detrimental to particle stability. These results agreed with the detected difference in cells transduction efficiency. These biophysical and structural analyses of AAV support the idea that sample handling might not only impact viral vector yields and purity but also modulate residues' interactions thus potentially impacting product potency.

Functional and Structural Insights into the Modulation of the Chaperonin CCT by Small Molecules

Pipaón Alcíbar, Sergio [*a], Cuervo, Ana [a], Moreno-Bautista, José [a], Pascual, Elena [b], García-Álvarez, Isabel [c], Martínez, Aurora [d], Valpuesta, José María [a], Cuéllar, Jorge [a]

[a]Centro Nacional de Biotecnología (CNB-CSIC). Darwin, 3. 28049 Madrid, Spain

[b]Faculty of Experimental Sciences, Francisco de Vitoria University (UFV). Carretera Pozuelo-Majadahonda KM 1800. 28223 Pozuelo de Alarcón, Madrid, Spain

[c]Instituto de Química Orgánica General (IQOG-CSIC). Juan de la Cierva, 3. 28006 Madrid, Spain

[d]Department of Biomedicine, University of Bergen. Jonas Lies vei 91. 5009 Bergen, Norway

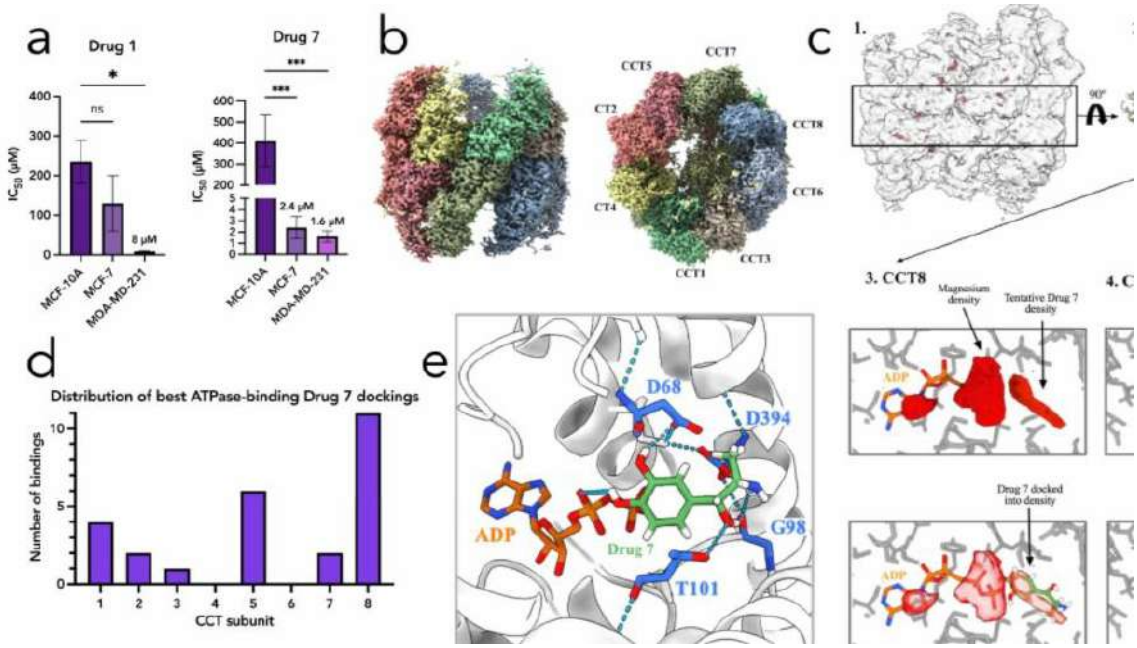

Molecular chaperones are key proteins in cellular homeostasis. One of the most important chaperones is CCT (chaperonin containing TCP-1), a large chaperonin composed of 16 subunits with ATP-dependent activity, which is responsible for the folding of ~10% of newly synthesized [1-4]. Multiple studies highlight the role of this macromolecular complex in cancer, where it is generally up-regulated, and in neurodegenerative diseases, where it is down-regulated [5-9]. For that reason, the aim of this project is to find potential therapeutic modulators of CCT.

A Differential Scanning Fluorimetry (DSF) Screening allowed us to identify a battery of small molecules that interact with CCT. Among these, two compounds -Drugs 1 and 7- stood out for their strong binding affinities and similar chemical structure.

Cell viability assays have shown that both of these compounds selectively inhibit the growth of cancer cells over healthy epithelial cells. Proteome Integral Solubility Alteration (PISA) assays and immunofluorescence imaging have been used to reinforce these results, proving that Drugs 1 and 7 target CCT in cells and compromise the integrity of the actin cytoskeleton.

Cryo-electron microscopy (CryoEM) was used to investigate the binding site of Drug 7 on the chaperonin CCT, since is is the small molecule that showed more selectivity towards cancer cells. Our CryoEM maps revealed additional densities in the ATP binding pocket of the CCT6 and CCT8 subunits. The extra density observed in CCT6 is likely attributable to the presence of ADP. In contrast, the density in the CCT8 subunit can be confidently modeled with Drug 7, along with a magnesium ion that appears to coordinate the phosphate groups of ADP. These observations are further supported by *in silico* docking analyses, which suggest that Drug 7 preferentially binds to the CCT8 subunit. Collectively, our data support the formation of a CCT–Drug 7–ADP ternary complex. However, limitations in the resolution of the apical domains currently prevent us from assessing potential Drug 7 binding at those sites. Further studies are necessary to elucidate the mechanism by which Drug 7 selectively inhibits the proliferation of cancer cells.

References:

[1] 1. Bueno-Carrasco, MT; Cuéllar, J. Mechanism and Function of the Eukaryotic Chaperonin CCT. eLS. 2018;1–9

[2] 2. Kalisman, N; Adams, CM; Levitt, M. Subunit order of eukaryotic TRiC/CCT chaperonin by cross-linking, mass spectrometry, and combinatorial homology modeling. Proc Natl Acad Sci U S A. 2012;109(8):2884–9

[3] 3. Leitner, A; Joachimiak, LA; Bracher, A; Mönkemeyer, L; Walzthoeni, T; Chen, B; et al. The molecular architecture of the eukaryotic chaperonin TRiC/CCT. Structure. 2012;20(5):814–25.

[4] 4. Yébenes, H; Mesa, P; Muñoz, IG; Montoya, G; Valpuesta, JM. Chaperonins: Two rings for folding. Trends Biochem Sci. 2011;36(8):424–32.

[5] 5. Carr, AC; Khaled, AS; Bassiouni, R; Flores, O; Nierenberg, D; Bhatti, H; et al. Targeting chaperonin containing TCP1 (CCT) as a molecular therapeutic for small cell lung cancer. Oncotarget. 2017;8(66):110273–88.

[6] 6. Guest, ST; Kratche, ZR; Bollig-Fischer, A; Haddad, R; Ethier, SP. Two members of the TRiC chaperonin complex, CCT2 and TCP1 are essential for survival of breast cancer cells and are linked to driving oncogenes. Exp Cell Res. 2015;332(2):223–35.

[7] 7. Showalter, AE; Martini, AC; Nierenberg, D; Hosang, K; Fahmi, NA; Gopalan, P; et al. Investigating Chaperonin-Containing TCP-1 subunit 2 as an essential component of the chaperonin complex for tumorigenesis. Sci Rep. 2020;10(1):1–14.

[8] 8. Shahmoradian, SH; Galaz-Montoya, JG; Schmid, MF; Cong, Y; Ma, B; Spiess, C; et al. TRiC's tricks inhibit huntingtin aggregation. Elife. 2013;2013(2):1–17.

[9] 9. Neef, DW; Turski, ML; Thiele, DJ. Modulation of heat shock transcription factor 1 as a therapeutic target for small molecule intervention in neurodegenerative disease. PLoS Biol. 2010;8(1).

Microscopy Across Scales: Visualizing Tunneling Nanotube-Mediated Mitochondrial Transfer in Glioblastoma

Sáenz de Santa María Fernández, Inés [*a], Brou, C [a], Tinevez, JY [b], Vitrenko, I [c], Cokelaer, T [d], Moyal-Jonathan- Cohen, E [e], Weigert, R [f], Zurzolo, C [a]

[a]Institut Pasteur, Université Paris Cité, CNRS UMR 3691, Membrane Traffic and Pathogenesis Unit, Paris, France, [b]Institut Pasteur, Université Paris Cité, Image Analysis Hub, 75015 Paris, France, [c]Institut Pasteur, Université Paris Cité, Plate-forme Technologique Biomics, F-75015 Paris, France, [d]Institut Pasteur, Université Paris Cité, Bioinformatics and Biostatistics Hub, F-75015 Paris, France, [e]Cancer Research Center of Toulouse (CRCT), Institut National de la Santé et de la Recherche Médicale (INSERM), Toulouse F-31000, France., [f]Laboratory of Cellular and Molecular Biology, Center for Cancer Research, National Cancer Institute, National Institutes of Health, Bethesda, MD, USA

Direct visualization of tumor–microenvironment interactions is essential for understanding cancer progression. Tunneling nanotubes (TNTs), dynamic membrane bridges that mediate intercellular organelle exchange, have recently emerged as important conduits of communication in cancer. Here, we applied a multi-scale live-imaging strategy integrating spinning disk, confocal, and intravital subcellular microscopy (ISMic) to investigate TNT- mediated mitochondrial transfer in glioblastoma (GBM).

In 2D cultures and 3D tumor organoids, we observed mitochondrial transfer via TNTs: damaged mitochondria from GBM cells were delivered to astrocytes, where they triggered mitophagy, while healthy astrocyte-derived mitochondria fused with the GBM mitochondrial network, thereby enhancing tumor metabolic activity. Strikingly, ISMic in live rodents provided the first direct evidence of TNT-mediated mitochondrial exchange in GBM in vivo, revealing structural and dynamic features consistent with our in vitro observations.

These findings establish TNTs as critical mediators of mitochondrial trafficking between GBM cells and astrocytes, underscoring their physiological relevance and potential role in tumor progression and therapy resistance

Resolving crystal structures through serial electron diffraction - Presenters: María J Rodríguez-Espinosa and César Santiago

Rodríguez-Espinosa, María J [a], Collado-Ávila, Javier [a], Santiago, César [a], P. Das, Partha [b] , Nicolopoulos, Stavros [*b], Martin-Benito, Jaime [*a]

[a]National Center for Biotechnology (CNB-CSIC) (ES)

[b]NanoMEGAS SPRL (BE)

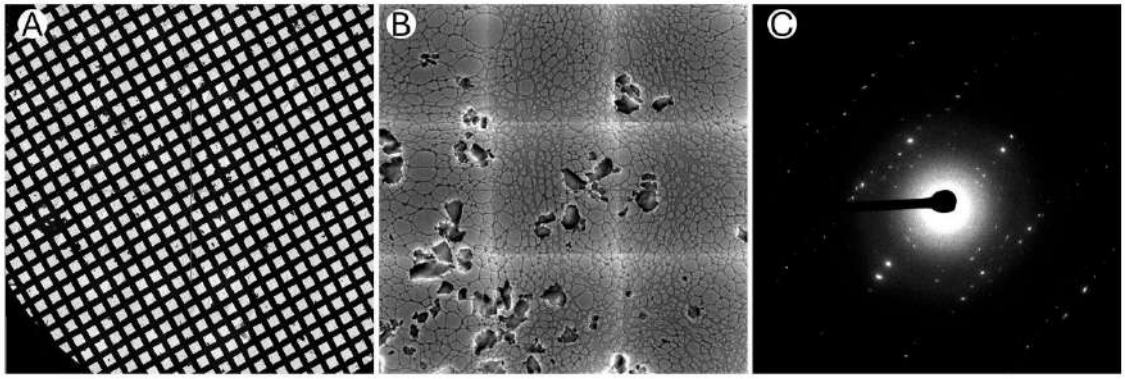

Serial electron diffraction is emerging as a powerful approach for structure determination from nanocrystals, combining the benefits of electron microscopy with the serial data acquisition strategy of X-ray free electron lasers. In this work, we present the successful implementation of a Serial electron diffraction pipeline for small organic molecules (e.g. carbamazepine), based on the collection of single-shot diffraction patterns from randomly oriented crystals dispersed on TEM grids. By collecting hundreds of patterns and merging them, we were able to reconstruct complete datasets and solve crystal structures at high resolution, with minimal radiation damage.

We have since successfully applied the method to data obtained from protein nanocrystals (e.g. lysozyme). In the future, we plan to combine it with beam precession to increase the number of spots in each diffraction pattern. This strategy could offer a low-dose, high-throughput alternative for protein structure determination using standard transmission electron microscopes. Our results support serial electron diffraction as a versatile technique, potentially bridging the gap between organic and biomolecular crystallography in electron microscopy.

Figure 1. Workflow of data collection using serial electron diffraction. (A) An overview image of the grid. (B) A close-up of a grid square containing crystals. (C) The diffraction pattern from one of these crystals.

References:

[1] Bücker, R., Hogan-Lamarre, P., & Miller, R. D. (2021). Serial Electron Diffraction Data Processing With diffractem and CrystFEL. Frontiers in Molecular Biosciences, 8, 624264.

[2] Bücker, R., Hogan-Lamarre, P., Mehrabi, P., Schulz, E. C., Bultema, L. A., Gevorkov, Y., ... & Dwayne Miller, R. J. (2020). Serial protein crystallography in an electron microscope. Nature communications, 11(1), 996.

[3] Hogan-Lamarre, P., Luo, Y., Bücker, R., Miller, R. D., & Zou, X. (2024). STEM SerialED: achieving high-resolution data for ab initio structure determination of beam-sensitive nanocrystalline materials. IUCrJ, 11(1), 62-72.

Acknowledgments:

Thank the members of the Cryo-Electron Microscopy facility at CNB (Spanish National Center for Biotechnology)

Correlative multimodal cryo-microscopy for the structural characterization of oxaliplatin-induced immunogenic cell death

Sancho-González, Beatriz [*a], Muriel-López, Olivia [a], Piccirillo, Jonathan Gabriel [a], Delgado-Gestoso, David [a], Conesa, José Javier [a], Martín-Cofreces, Noa Beatriz [b], Sanchez-Madrid, Francisco [b], Valpuesta, José María [*a]

[a]Centro Nacional de Biotecnología (CNB-CSIC) (ES)

[b]Immunology Service, Hospital Universitario de la Princesa, Universidad Autonoma Madrid (UAM), Instituto Investigacion Sanitaria-Instituto Princesa (IIS-IP), Madrid, Spain.

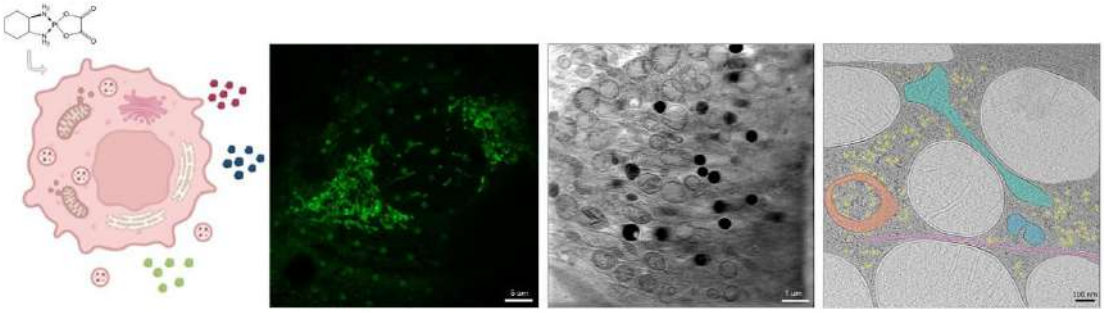

Immunogenic cell death (ICD) is a regulated form of cell death capable of activating an adaptive immune response. It is gaining relevance as a therapeutic mechanism in cancer, as cells undergoing ICD *in vitro* can function as vaccines promoting tumour clearance in vivo. ICD is characterized by a range of plasma membrane modifications and changes in the surrounding microenvironment. It is associated with endoplasmic reticulum stress and the release of damage-associated molecular patterns, including calreticulin, ATP, HMGB1, HSP70, and HSP90. In some instances, tumour cells undergoing ICD can release extracellular vesicles carrying bioactive molecules that modulate dendritic cell function[1]. However, there is still no definitive hallmark to unambiguously identify ICD.

Oxaliplatin is a third-generation platinum-based chemotherapeutic widely used in the treatment of colorectal cancer. Its primary mechanism of action involves the formation of DNA crosslinks that disrupt replication and transcription, ultimately leading to cell death. Unlike other platinum compounds such as cisplatin or carboplatin, it is also able to induce ICD[2]. Despite its clinical relevance, the cellular

and subcellular mechanisms underlying oxaliplatin-induced ICD remain incompletely understood.

In this study, we employed a correlative multimodal microscopy approach to investigate ICD induced by oxaliplatin in cancer cells. We combined fluorescence microscopy, cryo-electron tomography (cryo-ET), and cryo soft X-ray tomography (cryo-SXT) to visualize the morphological and molecular changes associated with ICD at high resolution and under near-native conditions. MC38 cells, either untreated or treated with oxaliplatin or cisplatin, were cultured in vitro and vitrified for imaging. Fluorescence microscopy was used to monitor dynamic changes in cellular compartments and ICD markers in real time. Cryo-ET provided nanometer-scale three-dimensional insights into intracellular organelle remodelling, while cryo-SXT enabled label-free, whole-cell imaging of structural transformations during ICD. This work highlights the power of integrated imaging platforms to dissect complex cell pathways.

References:

[1] Kroemer, G; Galluzzi, L; Kepp, O; Zitvogel, L. Immunogenic cell death in cancer therapy. Annu Rev Immunol. 2013;31:51-72.

[2] Alcindor, T; Beauger, N. Oxaliplatin: a review in the era of molecularly targeted therapy. Curr Oncol. 2011 Jan;18(1):18-25.

Acknowledgments:

Centro Nacional de Biotecnología (CNB)

Consejo Superior de Investigaciones Científicas (CSIC)

Insituto de Investigación Sanitaria - Instituto Princesa (IIS - IP)

Fundación La Caixa

Structural and Mechanistic Insights into Human Phenylalanine Hydroxylase

Fernandez-Leiro, Rafael [*a], Alcorlo-Pages, Martín [b], Miguez-Amil, Samuel [a], Støve, Svein I. [c], Innselset Flydal, Marte [c], Martinez, Aurora [*c], Hermoso, Juan A. [*b]

[a]Centro Nacional de Investigaciones Oncológicas (CNIO) (ES)

[b]Instituto de Química Física Blas-Cabrera (IQF-CSIC), Madrid, Spain

[c]University of Bergen

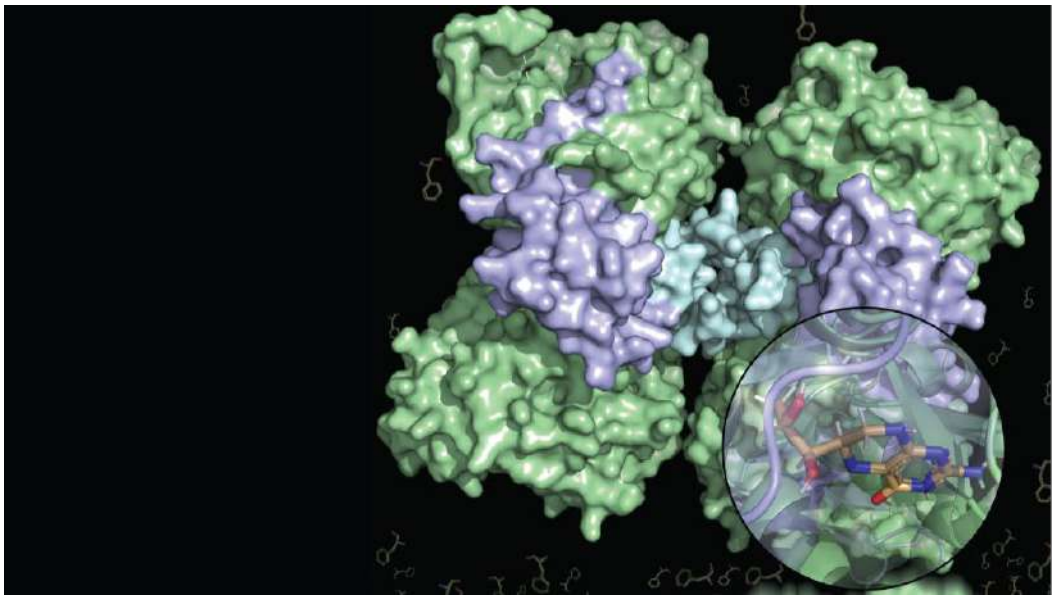

Phenylalanine hydroxylase (PAH) is the key metabolic enzyme responsible for the catabolism of phenylalanine. Mutations in the PAH gene cause phenylketonuria (PKU), a genetic disorder that, if left untreated, leads to brain damage and intellectual disability. While some patients benefit from supplementation with synthetic formulations of the natural cofactor tetrahydrobiopterin (BH4), which increases the activity of the PAH variants, more effective treatments are still needed. Our understanding of PAH activation and regulation remains incomplete, and advancing this knowledge is critical for the development of more effective therapeutic strategies.

Here, we will present and discuss four novel cryo-EM structures of full-length human PAH (hPAH) bound to phenylalanine at stimulatory concentrations, and in the presence of cofactors and inhibitors. These structures reveal how phenylalanine regulates PAH activity through conformational changes of its regulatory domain, providing essential insights into the enzyme's allosteric control and the molecular basis of disease associated mutations found in patients.

Abstracts of flash talks- Topic: Materials

Aberration Corrected STEM/TEM of LFP and TiO2 Electrode Materials for Solid State Thin Film Battery Applications

Gutu, Timothy [*a], Tiss, Belgacem [b], Miguel Silva Costa, Carlos [b], Leonard Deepak, Francis [*a]

[a]INL- International Iberian Nanotechnology Laboratory

[b]Center of Physics, University of Minho, Campus de Gualtar, 4710-057 Braga, Portugal

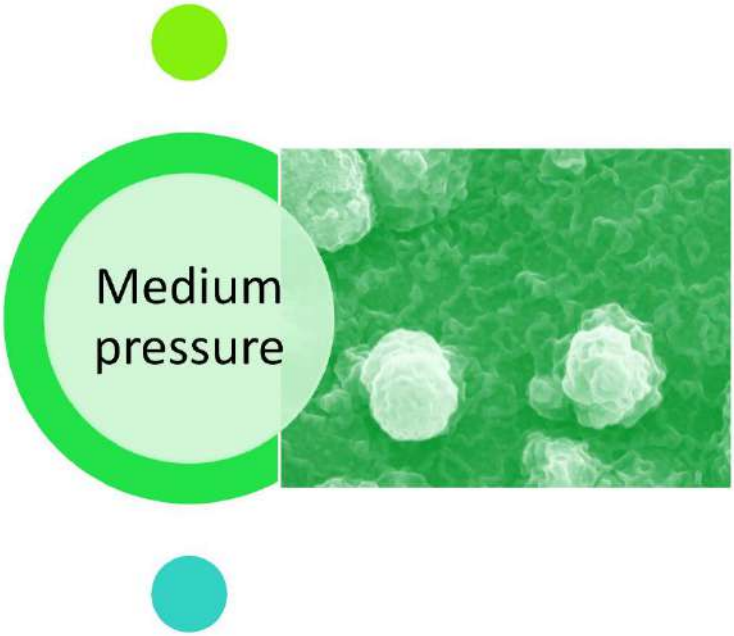

Technological innovation in battery electrodes is a rapidly evolving field, driven by the increasing demand for higher energy density, faster charging, longer lifespan, improved safety, and lower costs in applications like electric vehicles, portable electronics, and grid-scale energy storage. Solid-state thin-film batteries represent a significant advancement in battery technology, particularly for micro-scale and specialized applications. In this study we utilized aberration corrected STEM and associated electron microscopy techniques to investigate the effect of chamber pressure on structural properties of magnetron-sputtered $LiFePO_4$ (LFP) electrode materials for applications in solid state thin film batteries. We also investigated the effect of post-synthesis heat treatment on TiO_2 battery anode materials. The TiO_2 thin films were deposited on Si substrates and LFP films were deposited on Al substrates. FIB-STEM, TEM and HAADF-STEM imaging revealed that the chamber pressure strongly influenced the surface morphology, topography and thickness of the LFP cathode materials. The as-prepared TiO_2 films were amorphous. Annealing for 2 hours at 500°C resulted in transformation of the amorphous TiO_2 to the anatase phase which is good for battery anode material due to its open structure.

Acknowledgments:

The authors acknowledge the financial support of the project Moving2Neutrality (M2N), with the reference n.º C644927397-00000038, co-funded by Component C5 – Capitalisation and Business Innovation under the Portuguese Resilience and Recovery Plan, through the NextGenerationEU Fund.

The TiO_2 samples were obtained from Dr. Gustavo Santos, CeNTI-Center for Technology and Smart Materials, 4760-034 Vila Nova de Famalicao, Portugal.

This abstract will also be presented at the poster session on September 24th.

Phase Characterization of All-d-Metal Ni-(Co)-Mn-Ti Magnetic Shape Memory Alloys by Transmission Electron Microscopy

Santamarta, Rubén [*a], Vaquero-Crespí, Joan Miquel [a], Pons, Jaume [a], Salas, Daniel [a], Torrens-Serra, Joan [a], Cho, Woohyun [b], Torun, Serdar [b], Karaman, Ibrahim [b]

[a]Physics Department, University of the Balearic Islands, Palma, ES 07122, Spain

[b]Department of Materials Science and Engineering, Texas A&M University, College Station, TX 77843, USA

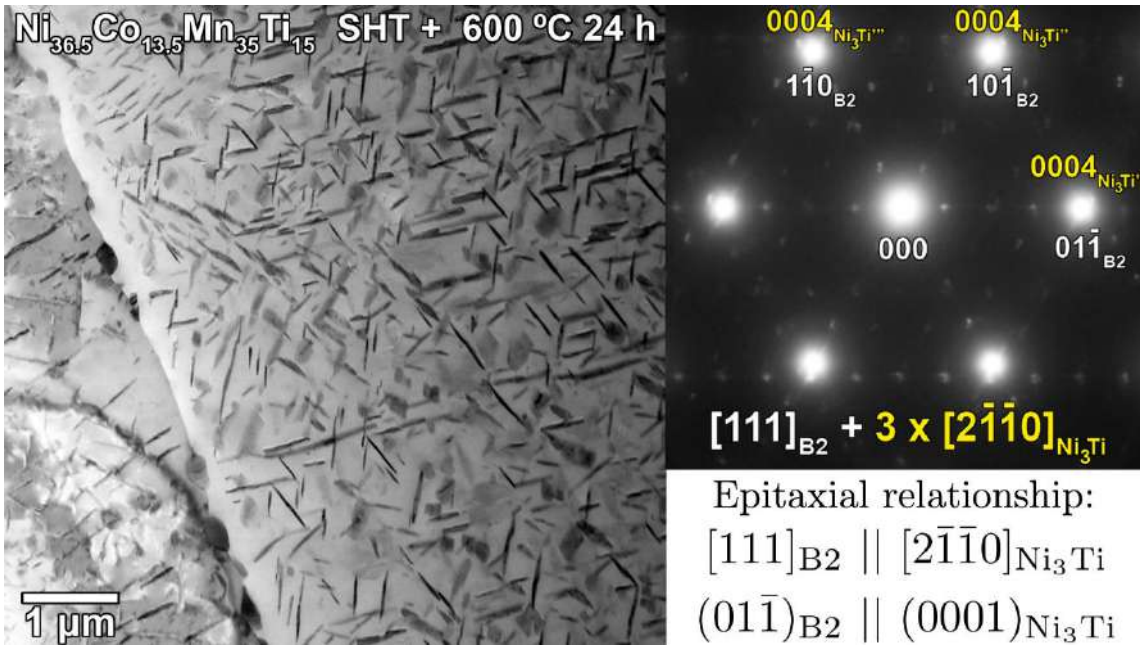

Shape memory alloys (SMAs) such as Ni-Ti, Ni-Mn-Ga, Cu-Zn-Al... can exhibit large recoverable strains when subjected to mechanical and/or thermal stimuli, giving rise to the well-known shape memory effect and superelasticity. These functional properties originate from a thermoelastic martensitic transformation between two different crystallographic phases, namely austenite and martensite. A subset of SMAs, known as magnetic shape memory alloys (MSMAs), can also show significant strains under external magnetic fields, and their strong magneto-structural coupling enables notable caloric effects. Among MSMAs, Ni-Mn-based systems can show excellent magnetocaloric properties, making them promising candidates for solid-state magnetic refrigeration [1]. However, the widely investigated Ni-(Co)-Mn-(In, Sb, Ga) alloys are intrinsically brittle, have poor mechanical performance, and degrade rapidly under cycling, which limit their use in refrigeration applications that require long-term cycling.

To address these drawbacks, two approaches have been widely studied. First, replacing In, Sb, or Ga by Ti to obtain Ni-(Co)-Mn-Ti alloys, composed exclusively of 3d transition metals. This system has been reported to exhibit enhanced mechanical properties compared to alloys containing *p*-orbital metals without sacrificing transformation characteristics or caloric efficiency [2]. Second, thermal treatments effectively tailor the martensitic transformation characteristics and improve their mechanical properties by promoting the formation of ductile second phases and coherent nanoprecipitates.

In this work, $Ni_{36.5}Co_{13.5}Mn_{35}Ti_{15}$ and $Ni_{50}Mn_{35}Ti_{15}$ alloys were solution heat treated (SHT) and then subjected to secondary thermal treatments at different temperatures (400-900 ºC) and durations (1-24 hours) to control their functional properties via precipitation. Transmission and scanning electron microscopy, combined with EDX analysis, were used to characterize the precipitate distributions induced by secondary thermal treatments and correlate them with the functional properties of the alloys. The precipitates were identified as Ni_3Ti-type particles with $D0_{24}$ hexagonal structure, previously reported in binary Ni-rich Ni-Ti alloys [3]. Notably, we report for the first time an epitaxial relationship between the B2 matrix and the Ni_3Ti-type precipitates.

As atomic ordering significantly affects the properties of some MSMAs, another key objective was to determine whether the austenite phase adopts a B2 (nearest-neighbor order) or $L2_1$ (next nearest-neighbor order) structure as a function of thermal treatments. Due to the similar atomic scattering factors of the constituent elements, X-ray diffraction can hardly distinguish between both structures. Therefore, in the present work electron diffraction patterns were used and unambiguously show that, in both alloys, the austenite present at room temperature after secondary heat treatments has B2 structure.

Additionally, multiple martensitic structures have been reported for the Ni-(Co)-Mn-Ti system. Most studies identify the martensite as either non-modulated (an $L1_0$ tetragonal crystal structure) or 10M (a five-layered modulated structure with a slightly monoclinic unit cell), both quite popular in MSMAs [4]. In the present work, electron diffraction revealed a non-modulated ($L1_0$ tetragonal) martensite in the $Ni_{36.5}Co_{13.5}Mn_{35}Ti_{15}$ alloy, and a novel 4O (four-layered orthorhombic) martensite in the $Ni_{50}Mn_{35}Ti_{15}$ alloy.

References:

[1] Moya, X.; Kar-Narayan, S.; Mathur, N. Caloric materials near ferroic phase transitions. Nature Materials 2014, 13, 439–450. (2014).

[2] Yan, H.L.; Wang, L.D.; Liu, H.X.; Huang, X.M.; Jia, N.; Li, Z.B.; Yang, B.; Zhang, Y.D.; Esling, C.; Zhao, X.; Zuo, L. Giant elastocaloric effect and exceptional mechanical

properties in an all-d-metal Ni-Mn-Ti alloy: Experimental and ab-initio studies. Materials & Design 2019, 184, 108180.

[3] Nishida, M.; Wayman, C.M.; Honma, T. Precipitation processes in near-equiatomic TiNi shape memory alloys. Metallurgical Transactions A 1986, 17, 1505-1515.

[4] Pons, J.; Chernenko, V.A.; Santamarta, R.; Cesari, E. Crystal structure of martensitic phases in Ni–Mn–Ga shape memory alloys. Acta Materialia 2000, 48, 3027–3038.

Acknowledgments:

The Spanish authors acknowledge the financial support from the Spanish agency MICIU/AEI/10.13039/501100011033, ERDF/EU "A way of making Europe" under the project PID2022-138108OB-C31, and an Instrumental agreement for the grant of a Transmission Electron Microscope financed by the Government of the Balearic Islands and ERDF/EU funds, "A way of making Europe". The American authors acknowledge the financial support provided by the U.S. Army Research Office through Grant No. W911NF-22-2-0117 and the U.S. Army Contract No. W911NF-25-1-0112.

This abstract will also be presented at the poster session on September 24th.

Morphological Analysis of NiFeP-Coated Nickel Felt via SEM and FIB-SEM: Structural Transformations Under OER Conditions

Muhmood, Tahir [*a], Amorim, Isilda

[a]INL- International Iberian Nanotechnology Laboratory

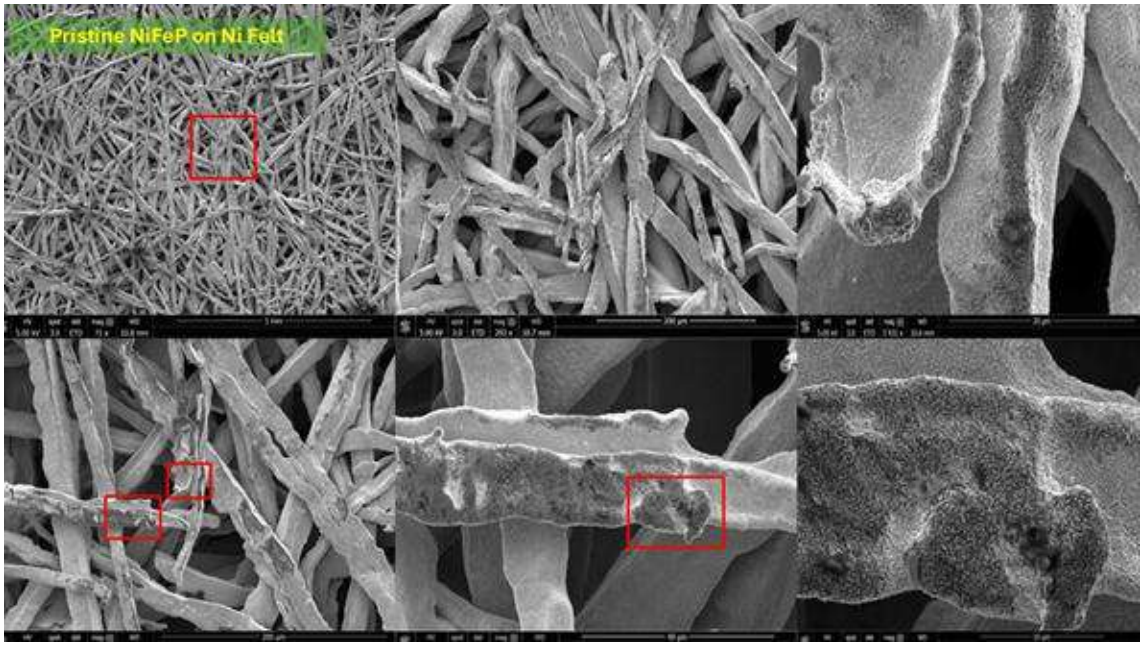

This study presents a detailed morphological analysis of nickel-iron-phosphide (NiFeP) coated nickel (Ni) felt before and after oxygen evolution reaction (OER) using scanning electron microscopy (SEM) and focused ion beam-scanning electron microscopy (FIB-SEM). The investigation focuses on the surface morphology, coating uniformity, elemental distribution, and structural changes induced by electrochemical cycling. SEM imaging of the pristine Ni felt reveals a three-dimensional network of nickel fibers with varying diameters. The structure is highly porous and interconnected, providing a large surface area for catalyst deposition and efficient electron transport pathways. The smooth surface morphology of the fibers ensures uniform coating adhesion, making it a suitable substrate for electrocatalytic applications. The SEM images of NiFeP-coated Ni felt confirm the successful deposition of a well-dispersed NiFeP nanosheet layer. The coating maintains the porous and interconnected nature of the Ni felt, which is essential for maximizing active surface area and catalytic performance. Elemental mapping via energy-dispersive X-ray spectroscopy (EDX) shows a homogeneous distribution of nickel (Ni), iron (Fe), and phosphorus (P), indicating uniform catalyst coverage. Cross-sectional FIB-SEM imaging further validates the strong adhesion of the NiFeP

layer to the Ni felt fibers. The coating is continuous and well-integrated with the substrate, ensuring structural stability under electrochemical conditions.

Acknowledgments:

Acknowledge the financial support of the project Moving2Neutrality (M2N), with the reference n.º C644927397-00000038, co-funded by Component C5 – Capitalisation and Business Innovation under the Portuguese Resilience and Recovery Plan, through the NextGenerationEU Fund.

Atomic-Level Insight into Multi-Carbon Product Formation via CO2RR on Chiral Catalysts

Domínguez-Ojeda, Eduardo [*a], Garcés-Pineda, Felipe A. [b], Golovanova, Viktoria [c], Garzón Manjón, Alba [a], Arbiol, Jordi [a]

[a]Institut Català de Nanociència i Nanotecnologia, Bellaterra, Spain

[b]Institut Català d'Investigació Química, Tarragona, Spain

[c]Institut de Ciències Fotòniques, Castelldefels, Spain

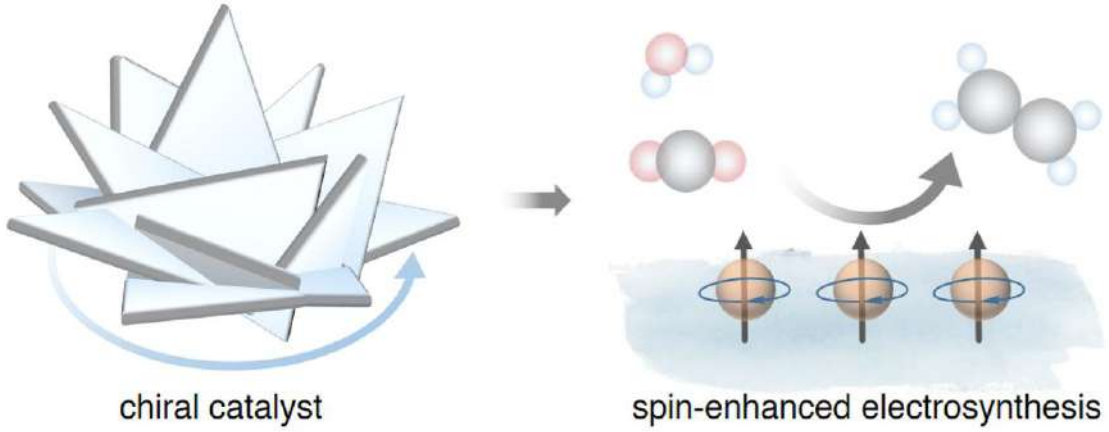

Figure 1. A sketch of a chiral catalyst that will be developed in this project and a scheme of a spin-enhanced electrosynthesis.

The global transition from fossil fuels to renewable energy is pivotal for combating climate change, with electrochemical CO_2 reduction (CO_2RR) emerging as a promising strategy for carbon mitigation. By coupling renewable electricity with efficient CO_2 utilization, CO_2RR enables the direct conversion of carbon dioxide into value-added chemicals and fuels. However, the selective generation of complex multi-carbon products remains a formidable challenge, rooted in the intricate interplay between catalyst structure, composition, and reactivity[1,2,3]. Recent breakthroughs—such as harnessing spin polarization effects via external magnetic fields or chiral molecular environments —have demonstrated remarkable enhancements in catalytic performance, particularly for copper-based systems[4,5,6].

In this research, we focus on the design and investigation of chiral CuOx nanostructures, which uniquely combine the catalytic versatility of copper with the tunable properties of oxide interfaces. Cu is nearly the only metallic catalyst capable of promoting C–C coupling through CO* dimerization, making it an ideal platform for exploring spin-dependent effects and selective CO_2RR.

Advanced electron microscopy techniques, especially (Scanning) Transmission Electron Microscopy ((S)TEM), are employed to unravel the atomic-scale features of these chiral CuOx catalysts. Correlative (S)TEM (performed before and after reaction), three-dimensional tomography, and (integrated) differential phase contrast ((i)DPC) imaging enable visualization of active sites and tracking of structural evolution. These insights are crucial for understanding degradation mechanisms, optimizing catalyst design, and ultimately improving selectivity and efficiency.

By integrating state-of-the-art electron microscopy with the synthesis of robust, intrinsically chiral CuOx electrodes, this research paves the way for the rational design of next-generation electrocatalysts.

References:

[1] Birdja, Y. Y. et al. Nature Energy. 2019. 4, 732–745.

[2] Gao, D. et al. Nature Catalysis. 2019. 2, 198–210.

[3] Wang, G. et al. Chemical Society Reviews. 2021. 50, 4993-5061.

[4] Garcés-Pineda, F. A. et al. Nat. Energy 2019. 4, 519–525.

[5] Sambalova, O. et al. Int. J. Hydrogen Energy. 2021. 46, 5, 3346–3353.

[6] Pan, H. et al. J. Phys. Chem. Lett. 2020. 11, 1, 48–53.

Acknowledgments:

The authors gratefully acknowledge financial support from the BIST Ignite Programme, 7th edition, for funding the BREATH-CO2 project. This support has been instrumental in advancing our research on CO2 electroreduction and catalyst development.

Design, construction and testing of a robust and safe gas line for in-situ gas TEM experiments

Costa, Pedro [*a], Maia, Rui [a], Santos, Margarida [a], Valente, Filipa [a], Cortez, Hugo [a], Alves, Cristiana [a], Carbo-Argibay, Enrique [a], Deepak, Leonard [a], Ferreira, Paulo [a, b]

[a]International Iberian Nanotechnology Laboratory (INL), Braga-4715-330, Portugal

[b]Instituto Superior Técnico

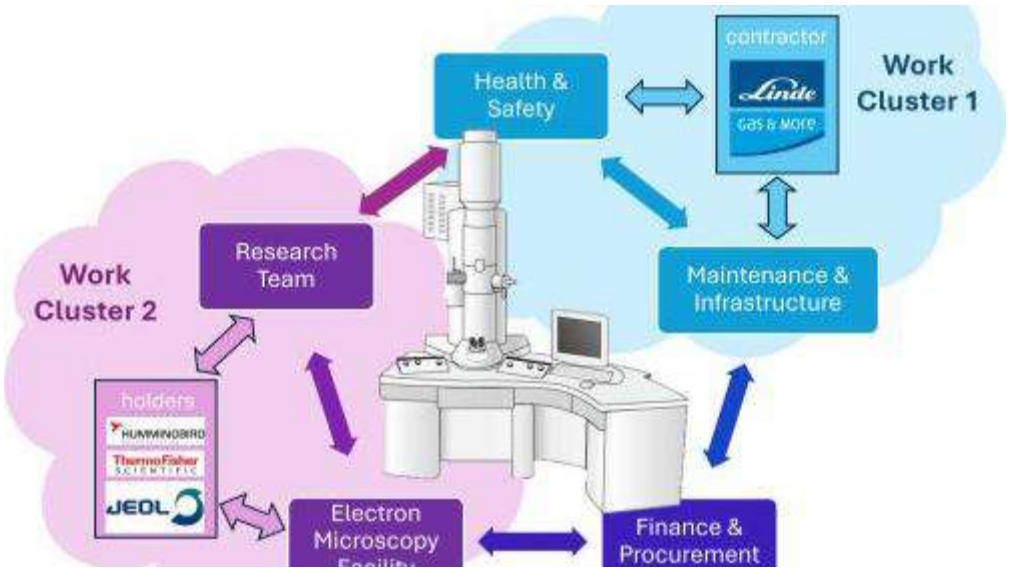

The design of rooms to host transmission electron microscopes (TEM) became a critical concern with the commercialization of the first aberration corrected instruments. [1] Suddenly, the limiting factor for performance was no longer the spatial resolution of the microscope but its sensitivity to the surrounding environment. Today, a top-performing instrument must be housed in specialized facilities, and any leading research work requires careful cradle-to-grave consideration of the equipment.

In parallel, the development of in-situ/operando TEM has been remarkable with a proliferation of methods and instrumentation, leading to a large variety of externally controlled stimuli now available, to cause a response from TEM specimens. Given the rapid advances in this field, it is prudent to start planning for the harmonization of protocols by addressing critical issues, such as safety.

One perfect example is the work of dynamical experiments performed in a gaseous environment, normally using a specialized TEM sample holder. Depending on the

brand, the entire setup may include a station to accommodate the gas cylinders that feed the holder. In the simpler configuration, it is up to the microscopist to arrange the feeding lines, gas cylinders and other diverse ancillary gears that provide a connection to the holder. In such a case, gas cylinders may be positioned just a few steps from the operator, while various gases, some potentially toxic and/or flammable, may pose a potential risk of leakage to the room.

At INL, we have conceived a permanent solution in order to integrate the design of gas lines, with the building and the microscope to carry in situ gas TEM experiments. For that, a multi-departmental team composed of microscopists, specialists in Health and Safety, lab maintenance/ installation and specialized gas engineers worked together to provide a design that allows for the safe operation of TEM gas holders, along with the remote storage of gas tanks, irrespective of their size, toxicity and/or flammability level. Progress towards this goal is communicated in this paper.

References:

[1] Muller, D. A., Kirkland, E. J., Thomas, M. G., Grazul, J. L., Fitting, L., Weyland, M., Ultramicroscopy 106 (2006), 1033-1040.

This abstract will also be presented at the poster session on September 24th.

Investigating the Degradation Mechanisms of IrO2 Catalysts for Proton Exchange Membrane Water Electrolysis Using In-Situ Scanning Transmission Electron Microscopy

Karimi, Maryam [a], Maia, Rui [a], Konar, Rajashree [a], Costa, Pedro [a], Ferreira, Paulo [*a]

[a]International Iberian Nanotechnology Laboratory - INL (PT)

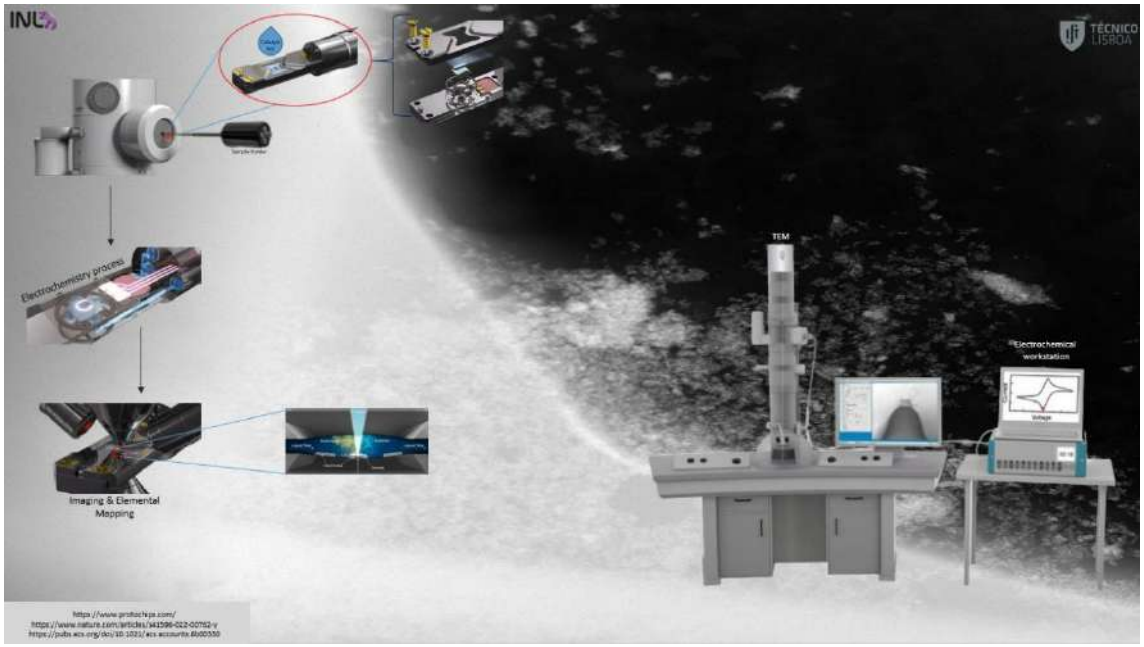

Hydrogen production through water electrolysis is a critical process for the renewable energy transition. The efficiency and durability of the electrocatalysts used in proton exchange membrane (PEM) water electrolysis, particularly for the oxygen evolution reaction (OER), are central to advancing this technology. Iridium oxide (IrO_2) is one of the most effective catalysts for OER, but its high cost and limited availability hinder large-scale applications. This study aims to investigate the degradation mechanisms of IrO_2 catalysts under real-world PEM electrolysis conditions using scanning transmission electron microscopy (STEM) techniques. Specifically, in-situ STEM will be employed to observe the structural and morphological changes of IrO_2 catalysts during electrochemical cycling. This technique will allow us to track particle migration, coalescence, Ostwald ripening, dissolution, and redeposition under working conditions. Key factors in this study will involve selecting high-quality liquid cell chips; for this observation, we used Indium Tin Oxide, and minimizing electron beam damage by employing low-dose imaging methods during in-situ characterization to prevent beam-induced damage and

ensure accurate imaging without interference. Ultimately, this study allows tuning the optimal operating conditions for further research into developing cost-effective and stable electrocatalysts for hydrogen production, particularly under realistic electrochemical conditions that closely simulate those in large-scale PEM water electrolysis systems.

This abstract will also be presented at the poster session on September 24th.

Atomic Force Microscopy and Electron Microscopy for the Autopsy of MD Desalination Membranes Containing 2D Nanoadsorbents

Navarro, Marta [*a,b], Moriones, Andoni [a,c], Luque, José Miguel [a,c], Téllez, Carlos [a,c], Gorgojo, Patricia [a,c]

[a]Instituto de Nanociencia y Materiales de Aragón (INMA) CSIC-Universidad de Zaragoza, Zaragoza 50018, Spain

[b]Laboratorio de Microscopías Avanzadas (LMA), Edificio I+D, C/ Mariano Esquillor s/n, 50018 Zaragoza, Spain.

[c]Departamento de Ingeniería Química y Tecnologías del Medio Ambiente, Universidad de Zaragoza, Zaragoza 50009, Spain

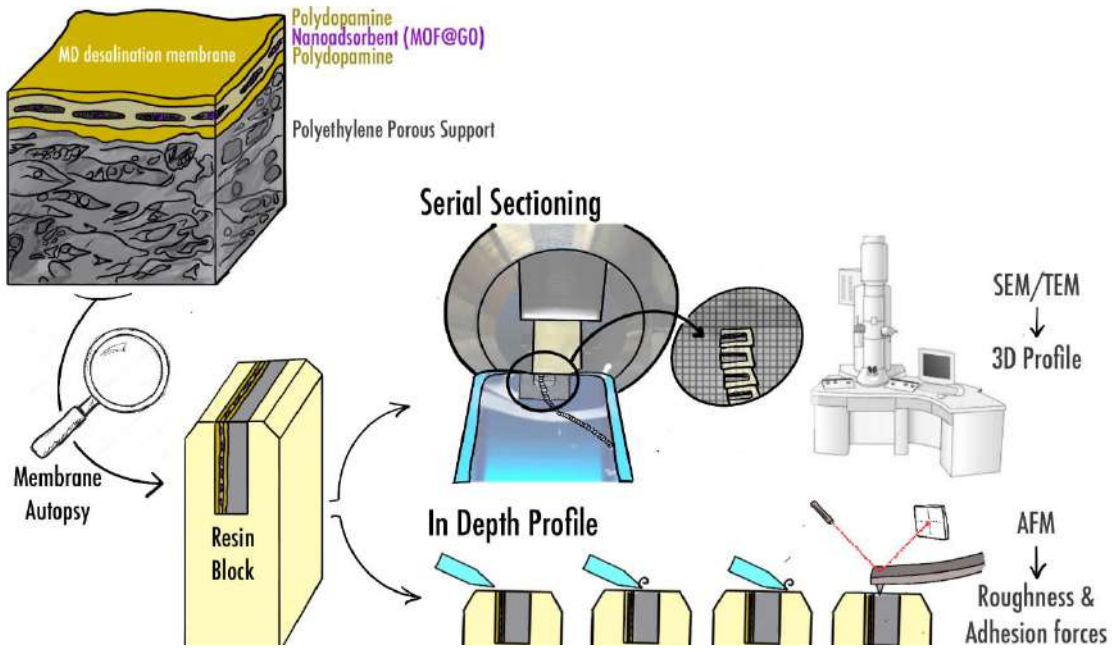

Membrane distillation (MD) is an emerging desalination technology that offers high salt rejection and the ability to treat hypersaline feedwaters, while operating at relatively low pressures and potentially utilizing low-grade or waste heat sources. However, despite these advantages, MD systems are hindered by limitations in permeate flux and overall energy efficiency. A critical challenge, particularly during extended operation, is membrane fouling and pore wetting, which adversely affect separation performance and reduce membrane lifespan [1].

The incorporation of nanomaterials represents a promising strategy to improve the anti-fouling performance of membrane systems [2]. In this study, composite membranes were fabricated using nanoadsorbents of metal-organic frameworks

(MOFs) grown on graphene oxide (GO), resulting in MOF@GO/polyethylene membranes [3]. This composite membrane design leverages the tuneable porosity, ease of functionalization, and thermal and chemical stability of MOFs, along with the high specific surface area and aspect ratio of GO nanosheets. Strong interfacial interactions between MOFs and GO promote uniform MOF growth on the basal planes of GO, improving dispersion and reinforcing the synergistic properties of both components, rendering the membranes highly effective for anti-fouling applications.

To investigate the mechanisms underlying membrane fouling and wetting, membrane autopsy analyses were performed using advanced microscopy techniques on both pristine and fouled membranes [4][5]. Membrane characteristics, such as surface roughness, adhesion, electrical and interaction tendencies, polymer elasticity, mechanical strength, hydrophilicity, and adsorption behaviour (including porous structure and distribution of hybrids) have been identified as key factors influencing filtration performance.

In this context, Atomic Force Microscopy (AFM) is a high-resolution technique well-suited for investigating the surface topography of various membrane materials. It enables the acquisition of three-dimensional surface images, valuable for gaining detailed insights into the ultrastructure of polymeric membranes. As a result, a more accurate and detailed representation of the membrane surface and profile can be achieved. To complement the topographical information provided by AFM, Scanning Electron Microscopy (SEM) will be employed to check the layout of the membrane and the possible presence and distribution of salts and other foulants, and Transmission Electron Microscopy (TEM) to assess the distribution and crystallinity of the MOF@GO hybrid nanostructures within the membrane matrix.

When in-depth profiling and three-dimensional structural analysis are required, meticulous sample preparation protocols may be necessary. These can include serial sectioning via ultramicrotomy and contrast enhancement through heavy metal staining.

References:

[1] Tai, Z.S.; Othman, M.H.D.; Koo, K.N.; Mustapa, W.; Kadirkhan, F. Membrane innovations to tackle challenges related to flux, energy efficiency and wetting in membrane distillation: a state-of-the-art review, Sustain. Mater. Technol. 2024, 39, e00780.

[2] Ray, S.S.; Bakshi, H.S.; R. Dangayach, Singh, R.; Deb, C.K.; Ganesapillai, M.; Chen, S.S.; Purkait, M.K. Recent developments in nanomaterials-modified membranes for improved membrane distillation performance, Membranes. 2020, 10 (7), 29.

[3] Moriones, A.; Cano-Herranz, L.; Luque-Alled, J. M.; Téllez, C.; Gorgojo, P. Metal-organic frameworks/graphene oxide nanohybrids to control pore wetting in membrane distillation. Desalination, 2025, 604, 118722.

[4]] Al-Abri, M.; Kyaw, H. H.; Al-Ghafri, B.; Myint, M. T. Z.; Dobretsov, S. Autopsy of used reverse osmosis membranes from the largest seawater desalination plant in Oman. Membranes. 2022, 12(7), 671.

[5] Kłosowski, M. M.; McGilvery, C. M.; Li, Y.; Abellan, P., Ramasse, Q.; Cabral, J. T.; Livingston, A. G.; Porter, A. E. Micro-to nano-scale characterisation of polyamide structures of the SW30HR RO membrane using advanced electron microscopy and stain tracers. Journal of Membrane Science. 2016, 520, 465-476.

Acknowledgments:

Financial support from the Project TED2021-130557A-I00 funded by MCIN/AEI/10.13039/ 501100011033 and the European Union NextGenerationEU/PRTR are gratefully acknowledged. The authors would like to thank the use of instrumentation as well as the technical advice provided by the National Facility ELECMI ICTS, node “Laboratorio de Microscopias Avanzadas”, at the “Universidad de Zaragoza”. The Government of Aragon is also gratefully acknowledged for financing the T68_23R group. Grant CEX2023-001286-S funded by MICIU/AEI/10.13039/501100011033 is also acknowledged

Atomic-Scale Characterization of Josephson Junctions for Superconducting Quantum Devices

Ali, Athique Ahmed [*a], Kallatt, Sangeeth [b], Maliakkal, Carina Babu [a], Genç, Aziz [a], Krogstrup, Peter [b], Arbiol, Jordi [a, c]

[a]Catalan Institute of Nanoscience and Nanotechnology (ICN2), CSIC and BIST, 08193 Barcelona, Catalonia, Spain

[b]NNF Quantum Computing Programme, Niels Bohr Institute, University of Copenhagen, Denmark

[c]ICREA, Pg. Lluís Companys 23, 08010 Barcelona, Catalonia, Spain

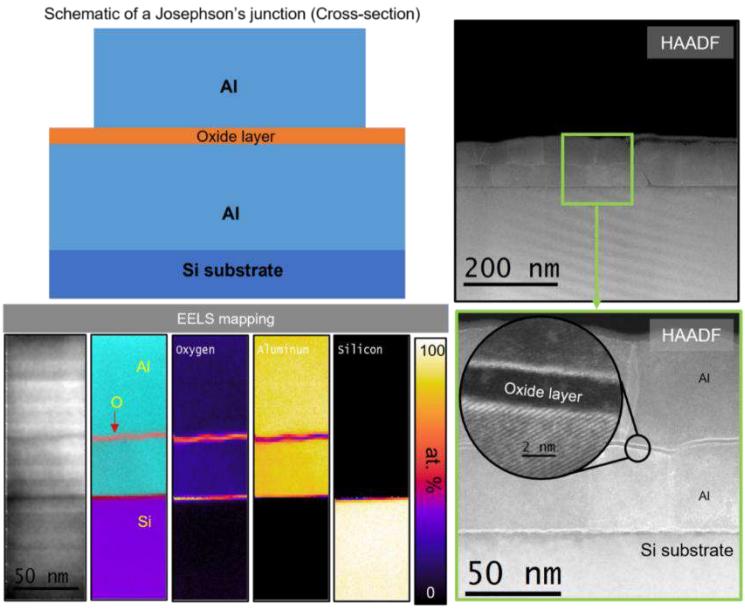

Josephson junctions (JJs) are foundational elements in superconducting quantum devices, where their operation is governed by complex interplays between superconductivity, quantum confinement, and Coulomb interactions. A precise understanding of these junctions at the nanoscale is essential for enhancing device coherence and reliability [1]. Advanced transmission electron microscopy techniques, including atomic resolution high angle annular dark field scanning transmission electron microscopy (HAADF STEM) imaging, energy-dispersive X-ray spectroscopy (EDS) and electron energy loss spectroscopy (EELS) analysis, were employed to investigate the structural and compositional properties of the JJs. Special attention was paid to the thin oxide barrier (AlOx) formed between the superconducting aluminum electrodes. We assessed the oxide thickness, uniformity, and growth conformity over the bottom Al layer, which are parameters

that critically influence tunneling properties, trap state formation, and overall junction performance [2]. This research employs aberration corrected atomic resolution HAADF STEM and EELS to elucidate the structural and electronic intricacies of Josephson junctions at the nanoscale [3]. We investigated the ways in which material interfaces, defects, and nonuniformities could possibly affect the properties of the junction. These observations provide valuable information on Josephson junctions and critical insights for the fabrication and optimization of superconducting quantum circuits.

References:

[1] Khan, S. A.; Lampadaris, C.; Cui, A.; Stampfer, L.; Liu, Y.; Pauka, S. J.; Cachaza, M. E.; Fiordaliso, E. M.; Kang, J. H.; Korneychuk, S.; et al. Highly Transparent Gatable Superconducting Shadow Junctions. ACS Nano, 2020, 14 (11), 14605–14615.

[2] Randeria, M. T.; Feldman, B. E.; Drozdov, I. K.; Yazdani, A. Scanning Josephson Spectroscopy on the Atomic Scale. Phys Rev B, 2016, 93 (16).

[3] Sahu, M. R.; Matute-Cañadas, F. J.; Benito, M.; Krogstrup, P.; Nygård, J.; Goffman, M. F.; Urbina, C.; Yeyati, A. L.; Pothier, H. Ground State Phase Diagram and "Parity Flipping''' Microwave Transitions in a Gate-Tunable Josephson Junction." 2023.

Acknowledgments:

The authors thank Dr. Sara Martí-Sánchez, Dr. Kapil Gupta and Dr. Bernat Mundet for technical support at TEM, Francisco Belarre for the technical support at FIB and Noèlia Arias for project management.

This abstract will also be presented at the poster session on September 24th.

Three-Dimensional Characterization of the Cathodoluminescence of as-Prepared Fluorite with 3DSEM-CL

Pérez García, Miguel Ángel [*a, b], Cervera Gontard, Lionel [a, b]

[a]IMEYMAT: Institute of Research on Electron Microscopy and Materials of the University of Cadiz. Puerto Real (Spain)

[b]Department of Condensed Matter Physics. Faculty of Science. University of Cádiz. Spain.

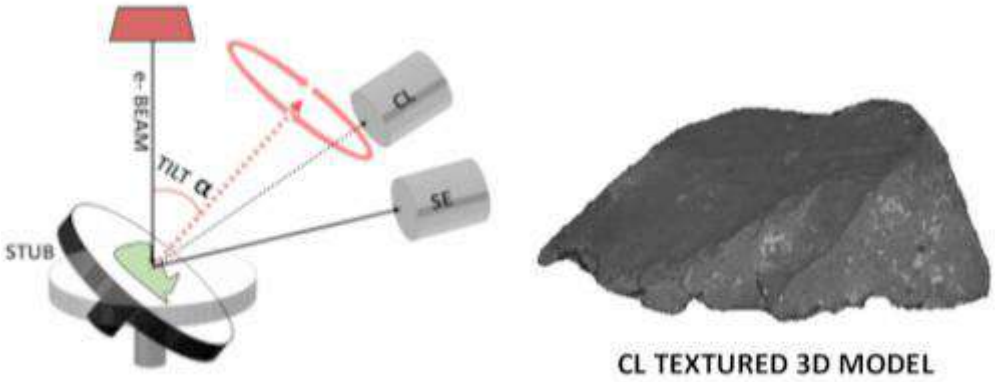

3DSEM is a technique that combines a series of secondary of backscattered electron (SE or BSE) microscopy images with photogrammetry methods to obtain a 3D surface model of a sample under investigation, which can be further analyzed digitally to extract quantitative features [1,2]. The technique can be used in any SEM microscope, is non-destructive, and can be applied with minimal preparation to many samples with the possible exception of those requiring conductive coating for reducing charging effects. Moreover, the reconstructed three-dimensional surface can be textured with physicochemical information obtained from different detectors available in a SEM. For example, 3DSEM combined with energy-dispersive X-ray spectometry (EDXS) has been applied to study adhesion wear in cutting tools, or carbon segregation in catalytic bodies [3,4].

In this work, we show to the best of our knowledge, the first application of 3DSEM combined with cathodoluminescence (CL), that is a technique extensively used in geology and ore mining as it allows researchers to distinguish different mineralogical phases inside a rock sample [5]. One difficulty found for the application of CL is sample preparation. CL in SEM often requires samples prepared with perfectly planar surfaces, as irregularities ocurring in fragments of a sample

(i.e. a rock) could hinder the differentiation of phases due to shadowing of the CL signal by the sample itself. Sample preparation is a lengthy procedure which, furthermore, can introduce artefacts that can be misinterpret as real features.

To overcome this drawbacks, we have measured simultaneously SE images and RGB and panchromatic-CL maps on a grain of fluorite, a material known for displaying strong CL and a lack of phosphorescence. No sample preparation beyond cutting the sample to fit inside the microscope and gold coating was performed in this study. The 3D surface was reconstructed and textured with the CL signal with a commercial photogrammetry software package.

Our results demonstrate the feasibility of 3DSEM-CL as a characterization tool to be added to gelogist's toolbox and, in general, for materials science valid for research as well as scientific dissemination.

References:

[1] M. Eulitz and G. Reiss, “3D reconstruction of SEM images by use of optical photogrammetry software,” J. Struct. Biol., vol. 191, no. 2, pp. 190–196, Aug. 2015

[2] L. C. Gontard, R. Schierholz, S. Yu, J. Cintas, and R. E. Dunin-Borkowski, “Photogrammetry of the three-dimensional shape and texture of a nanoscale particle using scanning electron microscopy and free software,” Ultramicroscopy, vol. 169, pp. 80–88, Oct. 2016

[3] L. C. Gontard, M. Batista, J. Salguero, and J. J. Calvino, “Three-dimensional chemical mapping using non-destructive SEM and photogrammetry,” Sci. Rep., vol. 8, no. 1, p. 11000, Dec. 2018

[4] L. C. Gontard, M. Á. Cauqui, M. P. Yeste, D. Ozkaya, and J. J. Calvino, “Accurate 3D Characterization of Catalytic Bodies Surface by Scanning Electron Microscopy,” ChemCatChem, vol. 11, no. 14, pp. 3171–3177, Jul. 2019

[5] J. Götze, “Application of cathodoluminescence microscopy and spectroscopy in geosciences,” Microsc. Microanal., vol. 18, no. 6, pp. 1270–1284, Dec. 2012

Acknowledgments:

This work is part of the eCOLOR project PID2022-143129OB-I00, funded by MCIN/AEI/10.13039/501100011033/FEDER, UE. Authors also want to acknowledge University of Cádiz for the concession of the FPI-UCA public predoctoral contract UCA/REC68VIT/2024.

Atomic-Scale Visualization of Moiré Patterns in Graphene Using TEM

Piedra Marin, Luis Eduardo [*a, b], Costa, Pedro [a], Ferreira, Paulo [a, b, c]

[a]International Iberian Nanotechnology Laboratory-INL Braga, Portugal

[b]Universidade de Lisboa, Campus Tecnológico e Nuclear, Instituto Superior Técnico, Portugal (PT)

[c]Materials Science and Engineering Program, Texas Materials Institute, The University of Texas at Austin, Austin, TX 78712-1591, USA

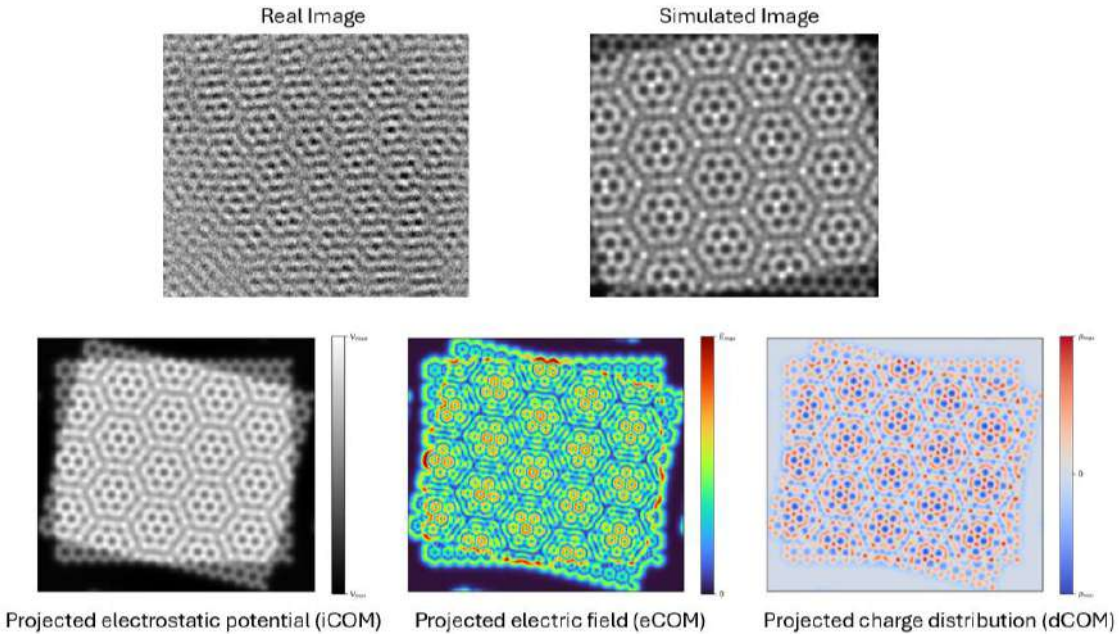

Twistronics is an emerging area of research focused on how rotating layers of 2D materials relative to each other affects their electronic behavior. By controlling the twist angle, researchers can engineer quantum materials with tailored properties. The formation of Moiré superlattices strongly influence the local electrostatic potential, charge distribution, and electric fields in 2D materials. Analyzing these Moiré patterns is essential for understanding their underlying properties. In this study, we used a JEOL JEM-2100 transmission electron microscope operating at 200 kV, to achieve atomic resolution of Moiré patterns in graphene. Twist angles were quantitatively extracted through fast Fourier transform (FFT) analysis of the TEM images, by identifying the relative orientation of diffraction spots corresponding to each atomic lattice. This method enables precise determination of interlayer rotation and provides critical insight into the resulting Moiré superlattice geometry. Multislice computer simulations were employed to complement the experimental observations by generating 4D-STEM images, enabling the calculation of the

projected electric field (eCOM), charge distribution (dCOM), and electrostatic potential (iCOM). The integration of TEM imaging and advanced computational modeling provides a detailed framework for investigating the electrostatic properties of twisted layers of 2D materials.

References:

[1] R. Ishikawa et al., "Interfacial atomic structure of twisted few-layer graphene," Sci Rep, vol. 6, pp. 1–9, 2016

[2] Y. Wen, M. J. Coupin, L. Hou, and J. H. Warner, "Moiré Superlattice Structure of Pleated Trilayer Graphene Imaged by 4D Scanning Transmission Electron Microscopy," ACS Nano, vol. 17, no. 20, pp. 19600–19612, 2023

Acknowledgments:

The authors would like to acknowledge the support from the AttoSwitch project N°101135571 funded by the European Commission (EC).

This abstract will also be presented at the poster session on September 24th.

Atomic-Scale Imaging of Beam-Sensitive Frameworks Using Electron Ptychography

Mayoral, Alvaro [*a] , Li, Daiyuan [a], Kayani, Sara [a], Zhang, Qing [b], Dong, Zhuoya [b], Pizarro, Daniel [*c]

[a]Instituto de Nanociencia y Materiales de Aragón (INMA), CSIC-Universidad de Zaragoza, 50009 Zaragoza, Spain

[b]Shanghai Key Laboratory of High-resolution Electron Microscopy, ShanghaiTech University

[c]Electronics Department, University of Alcala

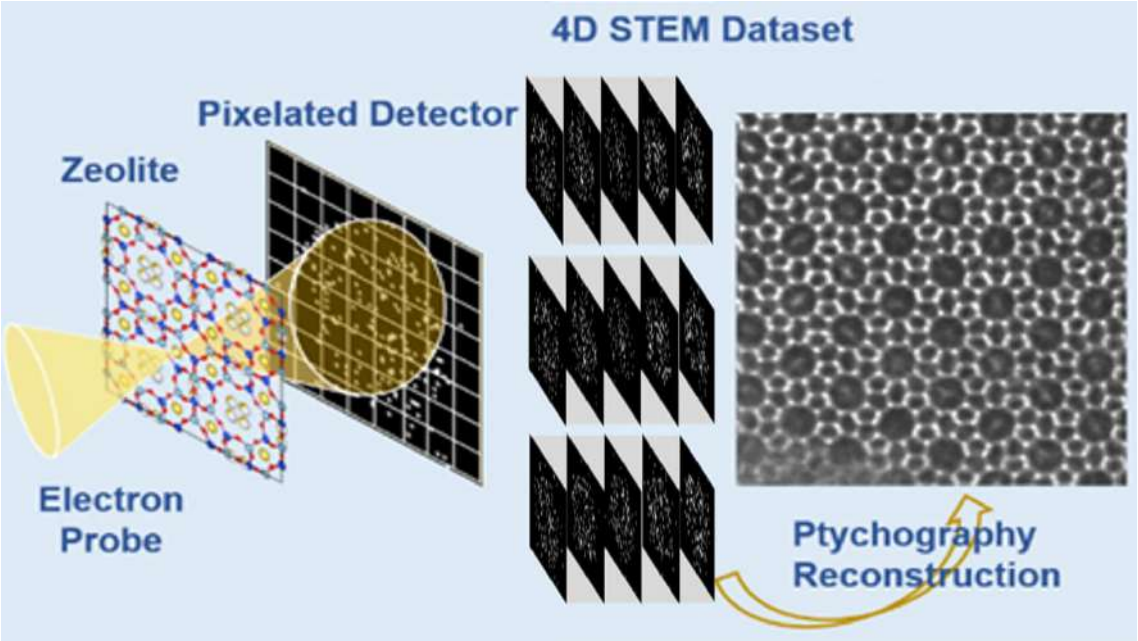

Zeolites are microporous materials with important industrial applications as desiccants and heterogeneous catalysts. Their structural features have traditionally been revealed through a combination of methods, with X-ray diffraction playing a central role by enabling the resolution of numerous new topologies. However, since the 1990s, transmission electron microscopy (TEM) has emerged as a powerful tool in zeolite science, as it enables the direct visualization of the framework—and more recently—even the various species incorporated into the porous network.

Unfortunately, despite their often high and tunable crystallinity, zeolites are highly sensitive to electron beam damage, which has limited the use of TEM for obtaining atomic-resolution information. This beam sensitivity results in a diminished image resolution due to a low signal-to-noise ratio (SNR), itself a consequence of both the

limited number of electrons used and the low detection efficiency of electron detectors.

Since 2010, with careful control of the electron dose, spherical aberration-corrected scanning transmission electron microscopy (STEM) has been successfully used to obtain atomic-resolution information on various zeolitic materials and even metal-organic frameworks (MOFs)[2]. Depending on the detector employed, complementary information can be extracted, and therefore, a complete dataset often requires the combination of multiple imaging techniques. Annular dark field (ADF) imaging is sensitive to atomic number and offers relatively straightforward interpretation, but it suffers from low SNR due to limited electron collection. Annular bright field (ABF) imaging provides enhanced spatial resolution and is better suited to light elements, though data collection and interpretation are more complex and also constrained by low detector efficiency. More recently, integrated differential phase contrast (iDPC) STEM has emerged as an effective low-dose imaging technique for visualizing both zeolite frameworks and guest species[3]. Four-dimensional (4D) STEM, which involves collecting 2D convergent beam electron diffraction (CBED) patterns at 2D scan positions, provides high-SNR data under low-dose conditions. It also enables extensive post-acquisition data analysis to retrieve various image contrasts. Among 4D-STEM techniques, **ptychography**—a phase contrast method based on a series of diffraction patterns—offers enhanced spatial resolution, high SNR, and dose efficiency. Although electron ptychography has been previously reported, its application to beam-sensitive materials remains underexplored.

We have developed a code that enables phase contrast imaging via ptychography with outstanding SNR under low-dose conditions (<500 $e^{-}/Å^{2}$). This method was applied to the titanosilicate ETS-10, which crystallizes as a mixture of two polymorphs and contains several structural defects. The experimental data were compared with simulations generated using the abTEM software, demonstrating the method's potential to enhance spatial resolution, improve SNR, and enable both average structure analysis and direct visualization of crystal surfaces without artefacts. The feasibility of this approach was validated using MFI zeolite (Figure 1)[4] and also applied to the structural elucidation of a highly complex zeolite NU-88, whose structure remained unknown since its discovery 20 years ago.

References:

[1] C. Li, Q. Zhang, A. Mayoral, Ten Years of Aberration Corrected Electron Microscopy for Ordered Nanoporous Materials, Chem. Cat. Chem., 12 (2020) 1248-1269.

[2] J. Li, A. Mayoral, Y. Kubota, S. Inagaki, J. Yu, O. Terasaki, Direct TEM Observation of Vacancy-Mediated Heteroatom Incorporation into a Zeolite Framework: Towards

Microscopic Design of Zeolite Catalysts, Angewandte Chemie International Edition, 61 (2022) e202211196.

[3] Z. Dong, E. Zhang, Y. Jiang, Q. Zhang, A. Mayoral, H. Jiang, Y. Ma, Atomic-Level Imaging of Zeolite Local Structures Using Electron Ptychography, Journal of the American Chemical Society, 145 (2023) 6628-6632.

Acknowledgments:

The Spanish Ministry of Science (RYC2018-024561-I; MICIU/AEI /10.13039/501100011033 and EU NextGenerationEU/PRTR: CNS2023-144346; PID2022-136535OB-I0, to the Grant CEX2023-001286-S funded by MICIU/AEI /10.13039/501100011033), the C$\hbar$EM, School of Physical Science and Technology, ShanghaiTech University (#EM02161943); Shanghai Science and Technology Plan (21DZ2260400), the regional govermetn of Aragon (E13_23R). This research work was also funded by the European Commission – NextGenerationEU, through Momentum CSIC Programme: Develop Your Digital Talent (MMT24-INMA-01).

Abstracts of flash talks - Topic: Life Science + CryoEm

Reconstitution of the complex of DNMT1 with hemimethylated DNA, doubly monoubiquitinated PAF15, and PCNA, for structural análisis

Ruiz-Albor, Antonio [a], Chaves-Arquero, Belén [b], Ferreras-Gutierrez, Mariola [b], Barbera, Miriam [b], Gonzalez-Magaña, Amaia [c], Núñez Ramírez, Rafael [b], De Biasio, Alfredo [d], J. Blanco, Francisco [*a, e]

[a]Instituto de Biomedicina de Valencia (IBV), CSIC, Valencia 46010, Spain

[b]Centro de Investigaciones Biológicas Margarita Salas (CIB), CSIC, Madrid 28040, Spain

[c]Instituto Biofisika, CSIC-UPV/EHU, 48940 Leioa, Spain.

[d]King Abdullah University of Science and Technology, Thuwal, Saudi Arabia.

[e]Centro de Investigación Príncipe Felipe (CIPF), Associated Unit to IBV, Valencia 46012, Spain

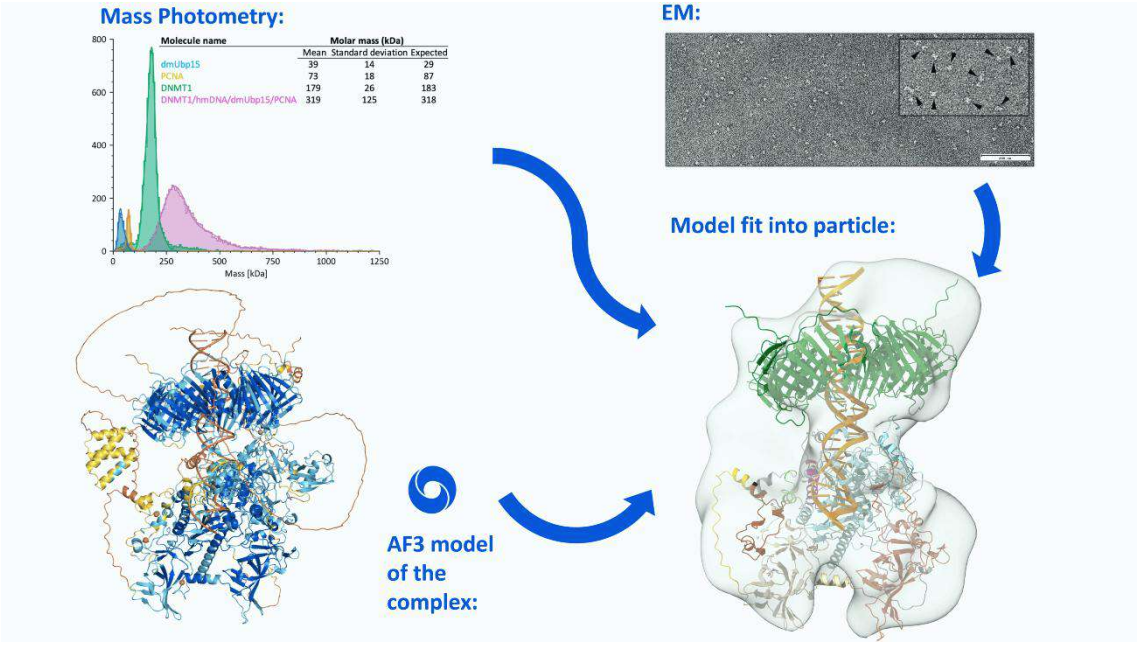

Eukaryotic cells use multiprotein complexes to make a copy of their chromosomes. Many of those complexes assemble on Proliferating Cell Nuclear Antigen (PCNA), a toroidal homotrimer that embraces the DNA duplex. The enzyme DNA Methyltransferase 1 (DNMT1) methylates cytosine bases in the daughter DNA strand, replicating the methylation pattern of the parental one. DNMT1 is recruited to the replication fork by the regulatory protein p15 when it is doubly monoubiquitinated in its N-terminal disordered tail, and the central region of p15 binds to the front face of the PCNA ring.

We have reconstituted the complex formed by DNMT1, a DNA duplex with a methylated cytosine, doubly monoubiquitinated p15, and PCNA from the isolated components. A complex with equimolar stoichiometry is detected in solution by mass photometry, and particles with the expected size are observed in negatively stained electron micrographs and with DNMT1 on the back side of the PCNA ring. A higher resolution structure was not attainable because the complex dissociates upon vitrification.

The structure of the complex predicted with AlphaFold is consistent with the available experimental information, providing a plausible model for DNMT1 action anchored to PCNA, and suggests that methylation of the newly synthesized DNA strand can occur in concert with lagging strand replication by DNA polymerase d.

References:

[1] Tomohiro Jimenji, Rumie Matsumura, Satomi Kori, Kyohei Arita, Structure of PCNA in complex with DNMT1 PIP box reveals the basis for the molecular mechanism of the interaction, Biochemical and Biophysical Research Communications, Volume 516, Issue 2, 2019, Pages 578-583, ISSN 0006-291X,

[2] Kikuchi, A., Onoda, H., Yamaguchi, K. et al. Structural basis for activation of DNMT1. Nat Commun 13, 7130 (2022). https://doi.org/10.1038/s41467-022-34779-4

[3] De I, Weidenhausen J, Concha N, Mu¨ller CW (2024) Structural insight into the DNMT1 reaction cycle by cryo-electron microscopy. PLoS ONE 19(9): e0307850.

This abstract will also be presented at the poster session on September 24th.

Advancing Cryo-EM Sample Preparation with Streptavidin Affinity Grids

Huerta, Marta [*a], Cookis, Trinity [b], Cuervo, Ana [a], Cuellar, Jorge [a], S Tai, Mary Dayne [c], Martínez, Aurora [c], Nogales, Eva [*b], Valpuesta, Jose María [*a]

[a]Centro Nacional de Biotecnología (CNB-CSIC) (ES)

[b]Department of Molecular and Cell Biology, University of California, Berkeley (US)

[c]Department of Biomedicine, University of Berge, Bergen, Norway

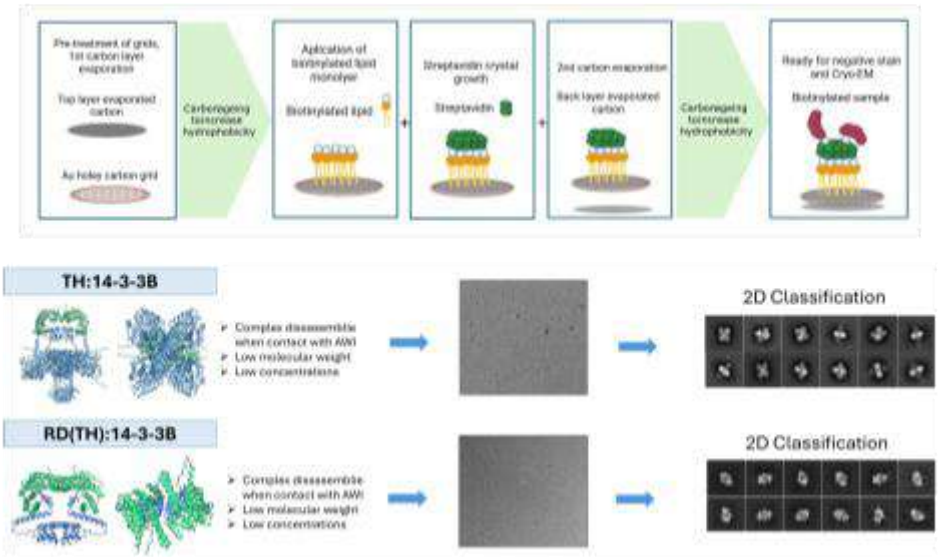

Cryo-electron microscopy (cryo-EM) has revolutionized the field of structural biology by allowing researchers to resolve macromolecular structures at near-atomic resolutions (better than 3 Å) without requiring crystallization. This technique is especially valuable for analyzing large, heterogeneous complexes in environments that closely simulate their native conditions. Despite these advantages, the process of sample preparation remains a significant challenge. Biological samples frequently encounter problems such as adopting preferred orientations or undergoing partial to complete denaturation during the vitrification process. These complications are largely due to interactions with the hydrophobic air–water interface (AWI), which particles can rapidly encounter. Such interactions may result in the disassembly of complexes, unfolding of proteins, or aggregation. Various approaches have been introduced to counter these issues, including chemical crosslinking, the addition of detergents or surfactants, and the use of grids functionalized with graphene oxide. However, these methods often present difficulties in optimization and reproducibility. An alternative approach involves the use of streptavidin affinity grids, a technology pioneered by Robert Glaeser at Berkeley and further refined by Eva Nogales' lab [1]. These specialized grids offer an

effective means to minimize sample denaturation and reduce the occurrence of preferred orientations caused by the AWI.

Streptavidin affinity grids exploit the strong binding between streptavidin and biotin (Kd ≈ 10^{-14} M) to selectively capture biotinylated molecules. The preparation of these grids involves growing two-dimensional streptavidin crystals on a biotinylated lipid monolayer, which is then applied to standard holey-carbon cryo-EM grids. This method not only enables the stable immobilization of biotinylated samples but also helps concentrate proteins present in low abundance and can even facilitate the on-grid purification of target protein complexes.

In this study, we have focused on optimizing streptavidin affinity grids to enhance the preparation and structural analysis of proteins such as 14-3-3 and tyrosine hydroxylase (TH). Our results demonstrate the potential of these grids to overcome challenges associated with imaging small and dynamic protein complexes.

References:

[1] [1] Cookis, T., Sauer, P., Poepsel, S., Han, B.-G., Herbst, D. A., Glaeser, R., & Nogales, E. (2023). Streptavidin-affinity grid fabrication for cryo-electron microscopy sample preparation. Journal of Visualized Experiments: JoVE, 202.

Acknowledgments:

Centro Nacional de Biotecnología – CSIC

This abstract will also be presented at the poster session on September 24th.

Mechanistic Insights on GTPase-Mediated Control of Endosomal Sorting Machinery

Blázquez-Ruano, David [a], Astorga-Simón, Elsa-N [a], Baños-Mateo, Soledad [b], Rojas-Cardona, Adriana [b], Hierro, Aitor [*a]

[a]Instituto Biofisika (UPV/EHU, CSIC), Leioa, Spain

[b]CIC bioGUNE, Basque Research and Technology Alliance (BRTA) (ES)

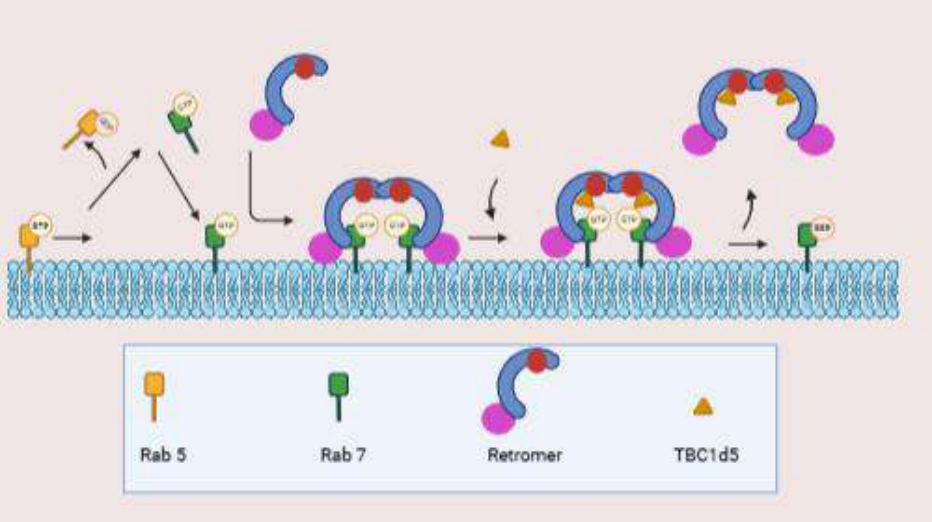

Rab7a is a key small GTPase associated with late endosomal membranes, where it regulates critical trafficking events such as endosome maturation, cargo sorting, and autophagy. Its functional cycle is tightly controlled by nucleotide binding, post-translational modifications, and interactions with effector proteins. Among these, the retromer complex, a heterotrimer composed of Vps26, Vps29, and Vps35, plays a central role in cargo recognition and endosomal recycling. The GTPase-activating protein (GAP) TBC1d5 has been shown to interface with both Rab7a and retromer, suggesting a coordinated mechanism for temporal regulation of membrane association and function. In this study, we explore the structural basis and regulatory dynamics of the Rab7–retromer–TBC1d5 axis. Using a combination of structural biology approaches and biochemical assays, we examine how TBC1d5 engages with retromer and how this interaction may influence retromer's function. Additionally, we investigate the impact of Rab7 on its capacity to associate with retromer and regulatory partners. Our findings provide new molecular insights into the interplay between Rab7 retromer and TBC1d5 for the spatiotemporal control of membrane transport pathways in the endosomal system.

NIPBL disruption in Cornelia de Lange Syndrome alters cohesin/NIPBL chromatin association

Vernia García, Isabel [*a], Picard Sánchez, Amparo [*a], Queralt, Ethel [*a], Reillo, Isabel [*a]

[a]Instituto de Biomedicina de Valencia-IBV-CSIC (ES)

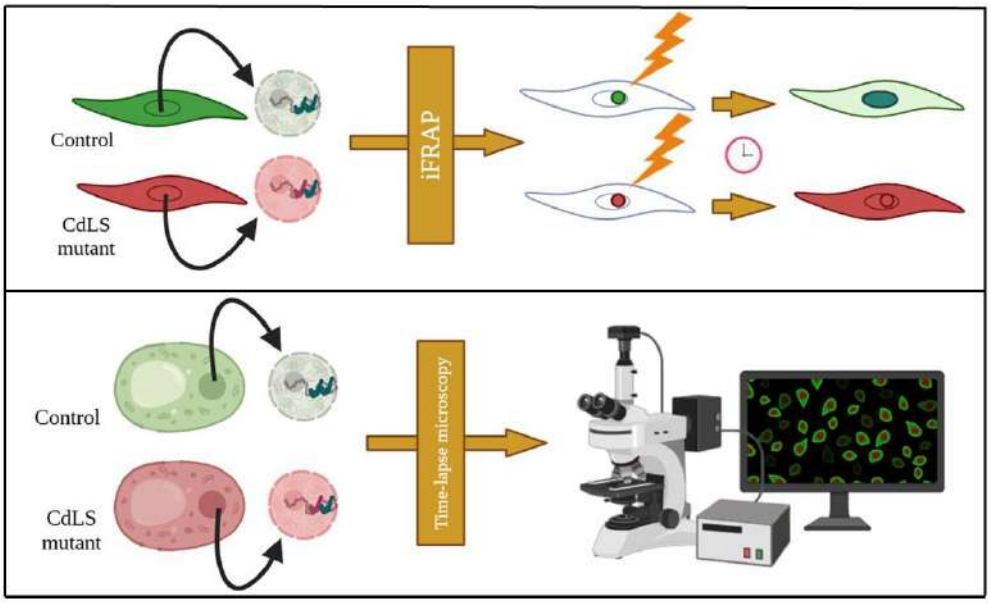

Cornelia de Lange syndrome (CdLS) is a developmental disorder most commonly caused by mutations in the cohesin loader NIPBL. Previous studies have shown that these mutations lead to reduced NIPBL occupancy at high GC content regions and altered cohesin distribution across the genome, potentially impairing chromatin organization and gene regulation. To explore whether NIPBL mutations affect its dynamic association with chromatin, we are employing inverse Fluorescence Recovery After Photobleaching (iFRAP) to monitor the mobility of NIPBL in living cells under physiological conditions. In addition, we study NIPBL/Scc2 localization using in vivo time-lapse microscopy combined with high-resolution imaging strategies. This approach will allow us to determine whether disease-associated mutations in NIPBL alter its chromatin binding kinetics, potentially leading to aberrant cohesin behavior and disrupted chromatin dynamics. Insights from this analysis may help elucidate how changes in NIPBL-chromatin interactions contribute to the disruption of genome organization and transcriptional regulation in CdLS.

Studying Retinal Repair Through 2D and 3D Calcium Imaging with Two-Photon Excitation Fluorescence Microscopy

Perez-Parets, Enric [*a], Denkova, Denitza [a], Castro, Gustavo [a], Cunquero, Marina [a], Isla-Magrané, Helena [b], Eriksen, Martin [c], Merino, Gonzalo [c], Duarri, Anna [b], Loza-Alvarez, Pablo [a]

[a]Instituto de Ciencias Fotónicas (ICFO) Mediterranean Technology Park, Avinguda Carl Friedrich Gauss, 3, 08860 Castelldefels, Barcelona

[b]Vall d'Hebron Institut de Recerca (VHIR), Edificio Mediterránea, Hospital Vall d'Hebron, Passeig de la Vall d'Hebron, 119-129, 08035, Barcelona, Spain

[c]Port d'Informació Científica (PIC), Campus Universitat Autònoma de Barcelona, Bellaterra, Spain

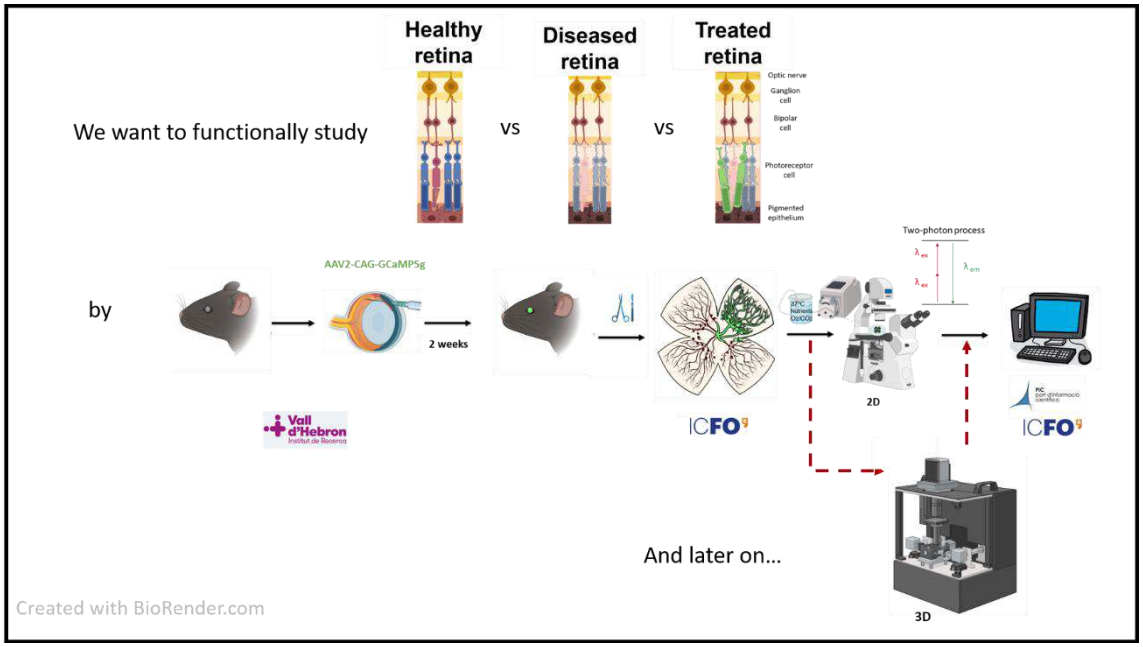

Retina degenerative diseases where photoreceptors are progressively lost, are currently the primary cause of untreatable low vision and blindness. A promising approach to finding a treatment is harvesting healthy photoreceptors from human-derived retinal organoids and transplanting them into the diseased retina. This has already been proven effective structurally, but its impact on retinal network signaling has not yet been fully understood.

To fill in this gap, we aim at developing a methodology to study neuronal networks in healthy, diseased and treated retinas. Currently, we are developing calcium imaging in 2D to study the retina's ganglion cell layer (GCL) under luminous

LED stimulation in the visible range. To be able to follow calcium dynamics, we first need to express the GCaMP calcium reporter in the retina. We achieve this by performing an intravitreal injection of the AAV2-CAG-GCaMP5 construct in Long Evans rats. Then, we dissect the retina using dim red-light illumination and oxygenated media to keep the tissue responsive to light and alive. To avoid bleaching the retina's light responsiveness, researchers use two-photon excitation fluorescence (2PEF) microscopy to image the calcium reporter, so we follow this same approach.

To this point, we have adapted and developed a methodology to image the healthy retinas using a custom-built 2PEF scanning microscope. Firstly, we checked the performance of our microscope by imaging single neurons with sufficient temporal resolution (5Hz) in cell culture and in the Rbfox1-GCaMP6s zebrafish larva's brain. Then, we validated our stimulation setup by recording light stimulated responses in the neurons of the optical tectum of these same zebrafish larvae. By doing so, we have been able to perform stable long-duration recordings from retinal organoids and retinal explants, where we observe robust calcium spikes. The following step will be to retrieve light-evoked responses from retinas using adequate light-stimulation schemes.

We have developed a steady methodology for 2D calcium imaging of retinal samples using a custom-built 2PEF microscope. In the future, we will evaluate the feasibility of using 2PEF light-sheet microscopy to perform fast volumetric imaging, capturing retinal dynamics in 3D. Connectivity maps will be constructed from the 2D and 3D datasets to analyze the functional responses of GCLs in the different retina cases and comparing the different imaging systems. This approach holds promise for advancing our understanding of retinal function and pathology.

Acknowledgments:

Results incorporated in this standard have received funding from PID2021-122807OB-C31 project funded by MCIN /AEI /10.13039/501100011033 / FEDER, UE and European Union's Horizon 2020 research and innovation programme under the Marie Sklodowska-Curie grant 101026297.

Structure of CONCR, a lncRNA that regulates DNA replication and chromatid cohesión

López-Perrote, Andrés [a], Martín-Cuevas, Eva María [b], Mérida-Cerro, José Antonio [c, d] Aicart-Ramos, Clara [b], González-Corpas, Ana [a], Le Coq, Johanne [a], Boskovic, Jasminka [a], Chillón, Isabel [e, f], Llorca, Oscar [* a], Moreno-Herrero, Fernando [* b], Huarte, Maite [* c, d]

[a]Spanish National Cancer Research Centre (CNIO), Structural Biology Programme, Melchor Fernández Almagro 3, 28029 Madrid, Spain

[b]Department of Macromolecular Structures, Centro Nacional de Biotecnología (CNB), CSIC, Madrid, Spain

[c]Center for Applied Medical Research, University of Navarra, Pamplona, Spain

[d]Institute of Health Research of Navarra (IdiSNA), Pamplona, Spain

[e]Institute of Molecular Genetics of Montpellier (IGMM), CNRS, 1919 route de Mende, 34293 Montpellier, France

[f]University of Montpellier, 163 rue Auguste Broussonnet, 34090 Montpellier, France

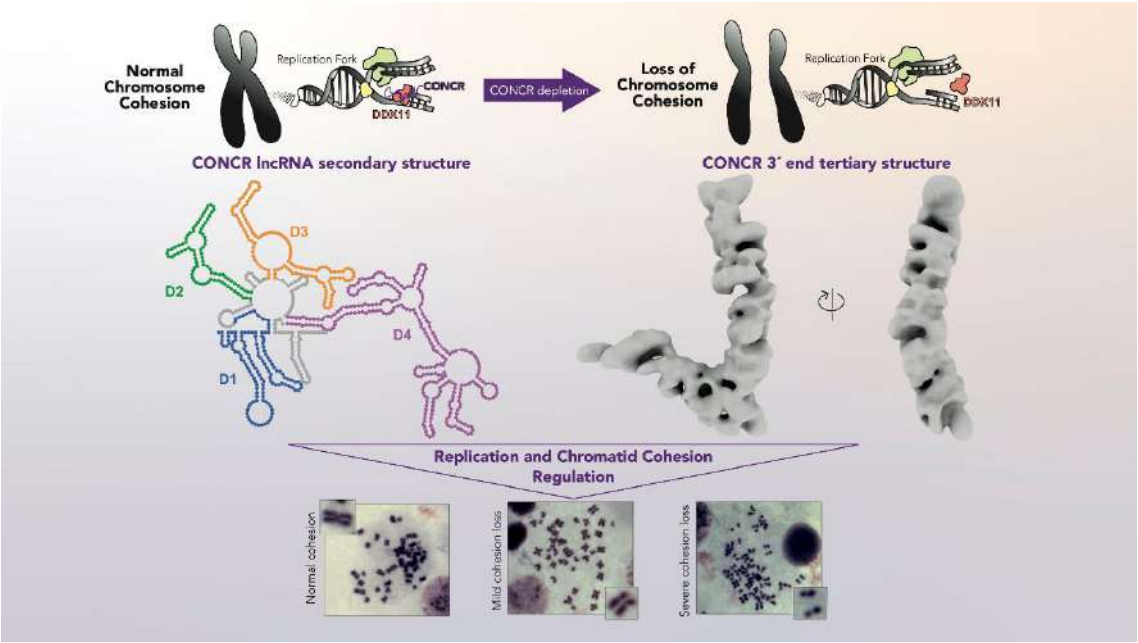

The long-noncoding RNA (lncRNA) CONCR (cohesion regulator noncoding RNA) plays a crucial role in regulating DNA replication and sister chromatid cohesion by modulating the activity of DDX11 helicase (1). Remarkably, its expression is significantly elevated in various cancer types (1,2). Recent studies highlighting the

structural-functional relationships of lncRNAs prompted us to investigate the structure of CONCR and its influence on functional mechanisms, an area that remains largely unexplored. We have combined biochemistry, SHAPE-MaP (Selective 2'-Hydroxyl Acylation analyzed by Primer Extension and Mutational Profiling), atomic force microscopy (AFM), and cryo-electron microscopy (cryo-EM) to elucidate the structure of CONCR. Our findings indicate that the lncRNA comprises multiple structural domains interconnected by flexible regions. Notably, the 3'-end of CONCR, specifically the segment encompassing nucleotides 419 through 718, forms a structural domain that efficiently interacts with DDX11 *in vitro*. The preliminary three-dimensional structure of the CONCR 3´-end domain, determined by cryo-EM, reveals a well-organized V-shaped architecture. Collectively, our results uncover a structurally defined domain within CONCR that is both necessary and sufficient for DDX11 binding. These findings support the idea that lncRNAs are organized into discrete structural domains with specific functional activities, interconnected within a larger flexible framework. Such organization may have important implications for understanding the regulatory roles of lncRNAs in cellular processes, particularly in cancer biology.

References:

[1] Marchese FP, Grossi E, Marín-Béjar O, Bharti SK, Raimondi I, González J, Martínez-Herrera DJ, Athie A, Amadoz A, Brosh RM Jr, Huarte M. 2016. A Long Noncoding RNA Regulates Sister Chromatid Cohesion. Mol Cell. 63(3):397-407.

[2] Calì F, Bharti SK, Di Perna R, Brosh RM Jr, Pisani FM. 2016. Tim/Timeless, a member of the replication fork protection complex, operates with the Warsaw breakage syndrome DNA helicase DDX11 in the same fork recovery pathway. Nucleic Acids Res. 44(2):705-17.

Introducing FlexibilityHub, a new service for the analysis of molecular motions in cryoEM data.

Melero, Roberto [a, b], Gragera, Marcos [* a, b], Herreros, David [a], Sorzano, Carlos Oscar Sanchez [a, b], Carazo, Jose Maria [a, b]

[a]Centro Nacional de Biotecnología (CNB), CSIC, 28049, Madrid, Spain

[b]Instruct Image Processing Center. Centro Nacional de Biotecnología (CNB), CSIC, 28049, Madrid, Spain.

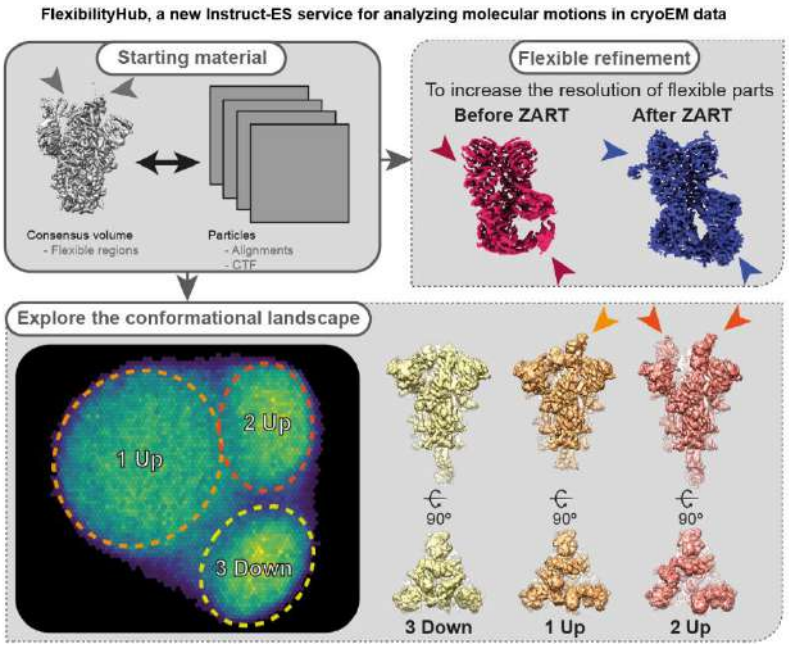

CryoEM has become a well-established technique for solving macromolecular complexes at high resolution [1]. By aligning and averaging thousands of individual projections of a biological specimen, single-particle analysis (SPA) allows for the generation of one or a few high-resolution structures from a single data collection. However, these static structures still represent discrete states within the complex motions that proteins typically undergo, despite the fact that the information on the dynamics of the sample is indeed contained in the data. Recently, the cryoEM community has begun to exploit this information, developing new image processing algorithms to gain insights into the conformational landscape of protein complexes and/or to correct for local motions, thereby increasing the resolution of moving subregions of a protein. Therefore, a growing demand is anticipated in the coming years from users seeking to unravel the molecular motions present in their samples of interest. We introduce FlexibilityHub [2], a new service/technology offered by the Instruct-ES centre, now available for users to utilize alongside our current SPA service. In this service, users are encouraged to provide a particle set that has undergone prior 2D and 3D classification but still exhibits a certain degree of

flexibility, whether compositional or conformational. Subsequently, we will conduct a comprehensive study of the dataset's flexibility using state-of-the-art software packages such as Zernikes3D, cryoDRGN, opusDSD, cryoSPARC 3DVA, and more, in combination with methods for flexible reconstruction to correct for motions such as Relion5 - DynaMight, cryoSPARC - 3D Flex, and Xmipp - ZART. This multi-algorithmic approach is facilitated by Scipion, a cryoEM image processing framework developed by our team, which integrates various tools into a single platform. To illustrate the potential of this service, we present several key use cases that highlight its capabilities and the benefits it offers to researchers.

References:

[1] Saibil H. R. (2022). Cryo-EM in molecular and cellular biology. Molecular cell, 82(2), 274–284. https://doi.org/10.1016/j.molcel.2021.12.016

[2] Herreros, D., Krieger, J. M., Fonseca, Y., Conesa, P., Harastani, M., Vuillemot, R., Hamitouche, I., Serrano Gutiérrez, R., Gragera, M., Melero, R., Jonic, S., Carazo, J. M., & Sorzano, C. O. S. (2023). Acta crystallographica. Section D, Structural biology, 79(Pt 7), 569–584.

This abstract will also be presented at the poster session on September 24th.

Exploring Different Conformations of Hepatic ABCB11 Transporter

Cuervo, Ana [*a], Liu, Hongtao [b], Kowal, Julia [b], Losana, Patricia [a], Herreros, David [a], Sorzano, Carlos Oscar [a], Locher, Kaspar P [b], Carazo, José María [a]

[a]Centro Nacional de Biotecnología, CSIC, Campus de Cantoblanco. Madrid. Spain

[b]Biochemistry department, ETH, Zurich, Switzerland.

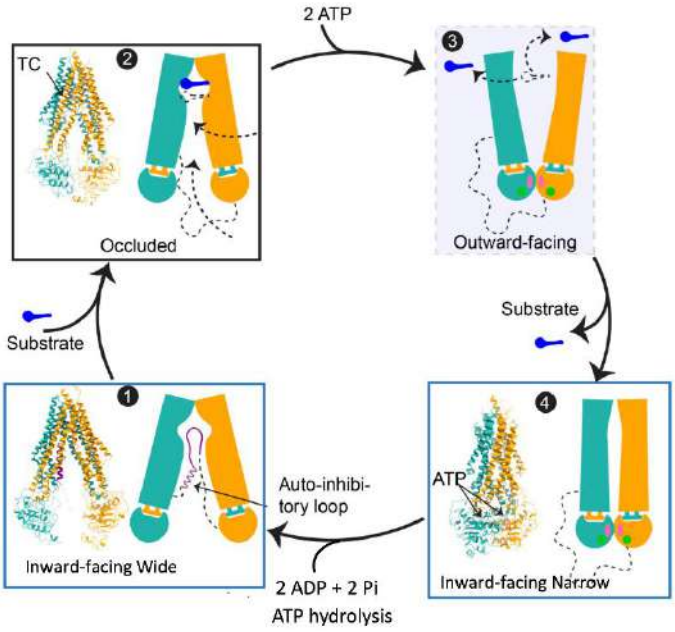

The Bile Salt Export Pump (BSEP), also known as ABCB11, is an ATP-binding cassette transporter expressed in hepatocytes, responsible for exporting bile salts into bile canaliculi. This process is powered by ATP hydrolysis, enabling the active transport of bile salts against their concentration gradient. Disruptions in BSEP function, due to genetic mutations or drug interactions, are commonly linked to severe liver disorders such as cholestasis. Structurally, ABCB11 comprises two transmembrane domains (TMDs), each formed by six helices, and two nucleotide-binding domains (NBDs). During its transport cycle, ABCB11 adopts multiple conformational states [1,2,3]: the inward-facing (IF) state, which permits bile salt binding from the cytoplasmic side; and the outward-facing (OF) state, triggered by the binding of two ATP molecules, which enables substrate release into the bile canaliculus. ATP hydrolysis and substrate release then reset the transporter to the IF state.

In this study, we employed cryo-electron microscopy (cryo-EM) and single-particle image analysis to investigate ABCB11 embedded in nanodiscs in the presence of ATP and chenodeoxycholic acid (CDCA), a major bile salt. Our analysis revealed two distinct inward-facing (IF) conformations: IFwide, characterized by an autoinhibitory loop that hinders substrate access; and IFnarrow, where the NBDs are closely

opposed with two ATP molecules bound, and no substrate present, suggesting a post-translocation state. These structural insights expand our understanding of ABCB11's dynamic mechanism and its critical role in bile salt transport.

References:

[1] Wang, L., et al. Cryo-EM structure of human bile salts exporter ABCB11. Cell Res. 2020, 30, 623–625.

[2] Wang, L., et al. Structures of human bile acid exporter ABCB11 reveal a transport mechanism facilitated by two tandem substrate-binding pockets. Cell Res. 2022, 32, 501–504 .

[3] Liu H, et al. Structural basis of bile salt extrusion and small-molecule inhibition in human BSEP. Nat Commun. 2023, 14:7296.

Acknowledgments:

This work was supported by Grant P2022/BMD-7232 TomoXliver2 to AC.

Implementing Cryo-CLEM Methodologies to Study Host–Pathogen Interactions in Influenza Infection

Delgado-Gestoso, David [a], Carlero, Diego [a], Modrego, Andrea [a], Cenisergue, Daniel [a], Zamarreño, Noelia [a], Martín-Benito, Jaime [a], Arranz, Rocío [*a]

[a]Centro Nacional de Biotecnología (CNB-CSIC) (ES)

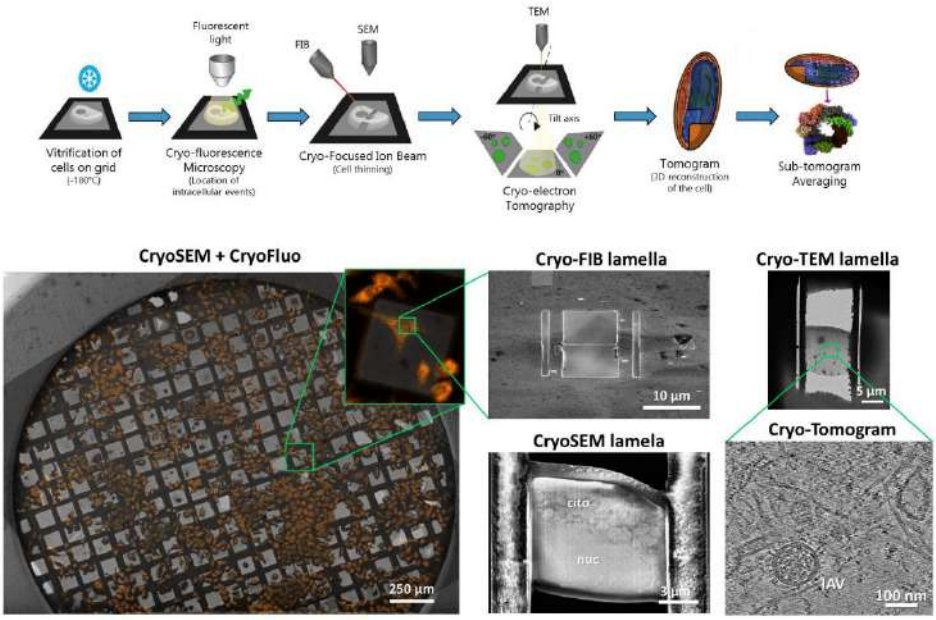

The influenza virus is a paradigm for understanding viral infections, providing critical insights into the complex host-pathogen interaction. As an opportunistic invader, influenza exploits the cellular endocytic machinery for infection, demonstrating a remarkable ability to hijack host processes. Our study focuses on a crucial stage of this viral journey: the release and transport of the virus from endosomes to the nucleus.

The objectives of this work start with the optimization of cryo-correlative light and electron microscopy (cryo-CLEM) techniques for the study of influenza virus structure and infection processes, with the aim of providing new insights into viral biology at the structural and cellular levels.

To solve this, we focused on critical aspects of the cryo-CLEM workflow, including:

- Virus purification to achieve higher viral titre and enable high Multiplicity of Infection (MOI).
- Infection process on Electron Microscopy (EM) grids.
- Vitrification by plunge freezing with cryoprotectants.
- Lamellae preparation by cryoFIB/SEM.
- Tomography by cryoTEM.

Additionally, we are developing fluorescent labeling techniques for the virus to enable precise correlation of the obtained tomograms.

Our optimizations resulted in improved sample preparation and imaging protocols for cryo-CLEM studies of influenza.

These advances in cryo-CLEM methodology for influenza research enable the collection of high-quality data on viral structure and host-cell interactions. This optimized approach has the potential to reveal new aspects of influenza virus biology and contribute to the development of improved prevention and treatment strategies against this significant global health problem.

Single particle analysis in a Talos L120C G2 cryo-electron microscope

Nuñez-Ramirez, Rafael [*a], Pou, Begoña [a], Arias-Palomo, Ernesto [a]

[a]Centro de Investigaciones Biológicas Margarita Salas (CIB), CSIC, Madrid 28040, Spain

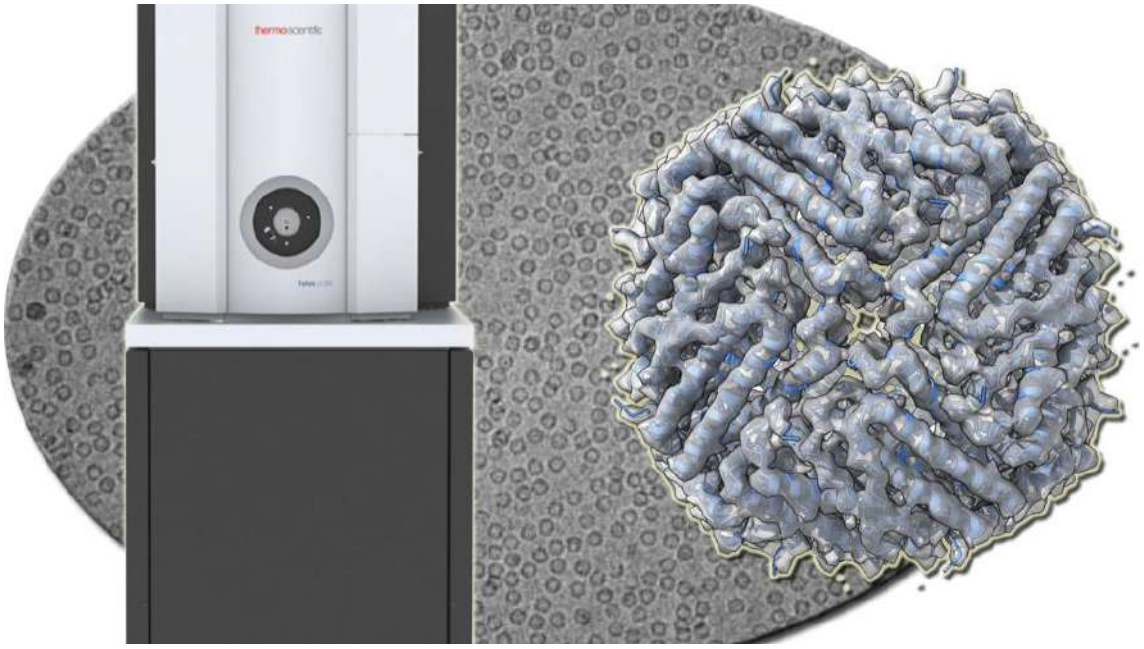

The study of high-resolution structures of biological macromolecular complexes by cryo-electron microscopy (cryo-EM) has undergone remarkable progress over the past decade. The improvement in resolution achieved by this technique has been driven by the development of new automated data acquisition methodologies, increased detector sensitivity, and the implementation of novel image processing algorithms.

Unfortunately, access to state-of-the-art electron microscopes remains limited and extremely costly, as only a few institutions in Spain have secured sufficient funding to acquire instruments equipped with the best source of illumination (FEGs) and direct electron detectors.

Given the limited access structural biologists have to these high-end instruments, it is crucial to optimize sample preparation and screening prior to high-resolution analysis. Low-voltage (120 kV) electron microscopes can be employed for this purpose through the use of both negative staining and cryo-EM techniques.

In this work, we present the results obtained using a Talos L120C G2 cryo-electron microscope, equipped with a 16-megapixel Ceta-F camera. This microscope is capable of autonomously acquiring data from macromolecular complexes and assessing whether the sample is suitable for analysis on high-voltage electron microscopes.

Among other parameters, it allows for the evaluation of ice quality, particle concentration and distribution, the number of suitable data collection areas on the grid, and angular distribution of views. Image processing of datasets collected with this type of microscope can provide insight, not only into the presence or absence of preferred orientation, but also offer preliminary information on the biochemical and structural homogeneity of the sample.

The study of standard samples, such as apoferritin, using low-voltage microscopes has shown that these instruments can reach resolutions below 3 Å when paired with direct electron detectors (1). In our work, we have explored the performance of the Ceta-F camera, a non-direct detector capable of frame acquisition, under different imaging conditions. Although this setup does not match the performance of direct detectors, it supports motion correction during acquisition and has enabled reconstructions reaching resolutions around 4.5 Å in favorable cases.

This level of resolution enables the identification of secondary structure elements, the assessment of proper protein folding, determination of the number of components in the complex, and much other critical information for evaluating the feasibility of structural biology projects and making informed decisions about accessing high-voltage electron microscopes.

References:

[1] Venugopal H., Mobbs J., Taveneau C., Fox D.R., ZVuckovic Z., Knott G., Grinter R.,Thal D,, Mick S,, Czarnik C., Ramm G. Sci Adv. 2025 Jan 3;11(1)

Spatial organization of the Retromer-SNX12 membrane coat

Pardo-Piñón, Marta [*a], Coray, Raffaele [a], Lucas, María [b], Romano-Moreno, Miguel [c], Rojas, Adriana L. [c], Castaño, Daniel [a], Hierro, Aitor [a]

[a]Instituto Biofisika (UPV/EHU, CSIC), Leioa, Spain

[b]Instituto de Biomedicina y Biotecnología de Cantabria (CSIC-UC). c/ Abert Einstein 22. PCTCAN. 39011 Santander

[c]CIC bioGUNE, Basque Research and Technology Alliance (BRTA), 48160 Derio, Spain.

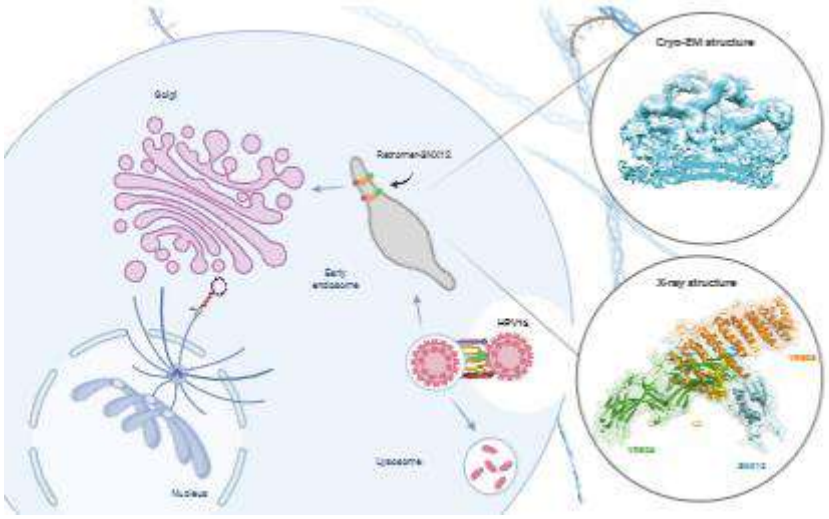

The endosomal system is responsible for receiving, classifying and redistributing hundreds of proteins in the cell. Proteins that enter in the endosomal pathway could follow two different destinations: be degraded in lysosomes or be recycled to continue developing their functions. A key component in the retrograde pathway is the retromer complex. Retromer is a highly conserved protein complex that mediates retrograde transport of hundreds of transmembrane proteins, known as cargos, from the endosomes to the *trans*-Golgi network and plasma membrane. To select cargo, retromer is recruited by members of the Sortin nexin (SNX) family to the endosomal membrane. Here, retromer promotes the emerging of tubulo-vesicular carriers that allow cargo to exit the endosome and avoid lysosomal degradation. Given its impact in the maintenance of cellular proteostasis, retromer machinery is hijacked of several intracellular pathogens to support their survival and replication. One of them is the Human Papillomavirus (HPV), that hijack retromer complex through the minor capsid protein L2 which in turn interacts with viral DNA. This interaction promotes the retrograde transport of the viral genome into the cell nucleus where its replicated.

This study combines biochemical and functional assays with X-ray crystallography and cryo-electron microscopy to establish the mechanism by which L2 subverts retromer function. Furthermore, the integration of Cryo-ET and STA has allowed to define for the first time the spatial organization of the retromer-SNX12 membrane coat around tubular vesicles.

References:

[1] Lucas, M.; Gershlick, D.C.; Vidaurrazaga, A.; Rojas, A.L., Bonifacino, J.S.; Hierro A. Structural mechanism for cargo recognition by the retromer complex. Cell 2016, 167, 1623-1635.

[2] Popa, A.; Zhang, W.; Harrison, M.S.; Goodner, K.; Kazakov, T.; Goodwin, E.C.; Lipovsky, A.; Burd, C.G.; DiMaio, D. Direct binding of retromer to Human Papillomavirus type 16 minor capsid protein L2 mediates endosome exit during viral infection. PLOS Pathogens 2015, 11: e1004699

[3] Zhang, P.; Monteiro da Silva, G.; Deatherage, C.; Burd, C.; DiMaio, D. Cell-penetrating peptide mediates intracellular membrane passage of Human Papillomavirus L2 protein to trigger retrograde trafficking. Cell 2018, 174, 1465-1476

Poster Session 24th September - Topic: Life Sciences and CryoEM

Cryo FIB-SEM Volume Imaging: issues and solutions

Piccirillo, Jonathan Gabriel [*a], Conesa, Jose Javier [a], Delgado-Gestoso, David [a], Chichon, Francisco Javier Chichon [a], Arranz, Rocio [*a], Valpuesta, Jose Maria [*a]

[a]Centro Nacional de Biotecnología (CNB-CSIC) (ES)

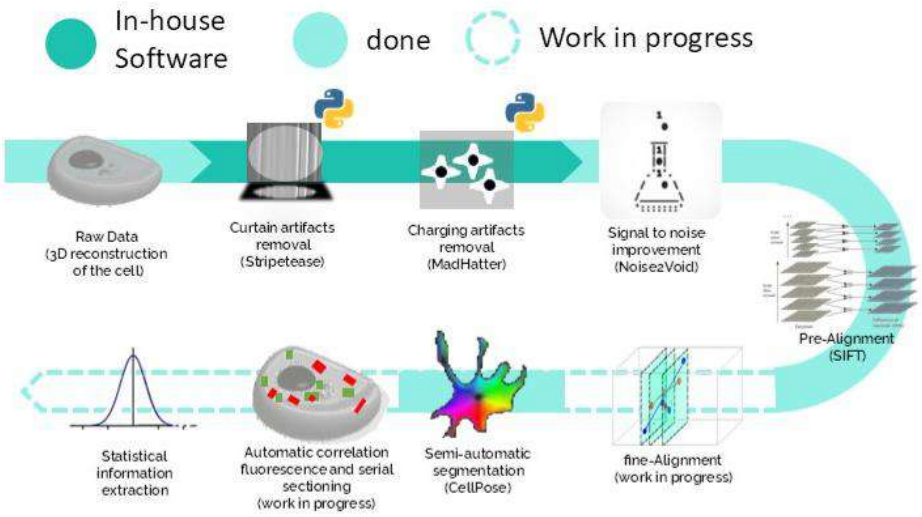

Preserving the native conditions and environment of our biological samples is essential to fully understand the complexity of living systems while maintaining accurate localization of target structures. Traditional high-resolution techniques for studying biological complexes often lack the ability to target structures without disrupting the cellular context. To address this limitation, it is crucial to integrate light microscopy with cryo-techniques, enabling the precise targeting of protein complexes and resolving their structure within their native environment.

The Valpuesta group, in collaboration with the Cryo-Electron Microscopy Facility at CNB-CSIC, is implementing cryo-correlative techniques that combine the strengths of visible light and electron microscopy (cryo-CLEM). Our equipment and expertise support two cryo-CLEM approaches. The first is a tomographic method involving lamella preparation, where thin sections (<300 nm) of the cell are created using FIB milling to achieve near-atomic resolution. The second is a serial sectioning approach, which reconstructs the entire cell volume at approximately 10 nm resolution. This method uses an iterative process of imaging with scanning electron microscopy (SEM) and surface milling with a focused ion beam (FIB), producing a stack of images that represent the cell volume (cryo-FIBSEM tomography).

However, serial sectioning introduces technique-specific artifacts that can compromise image quality. To mitigate these issues, we are developing an open-source, user-friendly software package for the processing of cryo-FIBSEM volumes to improve data accuracy. The first step in our pipeline is the removal of stripe artifacts caused by the "curtain effect," which results from the uneven shielding of material during milling. The second step addresses charging artifacts, which arise from electron accumulation in the sample, leading to uneven brightness in the images. Third, the software performs stack alignment—a challenging task due to local image distortions from non-uniform electron deflection. Finally, segmentation is carried out using deep learning tools from third-party software.

Virus-Free High-Throughput Screening of Influenza Antivirals Using Widefield Microscopy and a Fluorescent Mini-Replicon System

Coloma, Rocio [*a], Cancela, Irene [a], Carlero, Diego [a], Modrego, Andrea [a]

[a]Department of Macromolecular Structures, Centro Nacional de Biotecnología (CNB), CSIC, Madrid, Spain

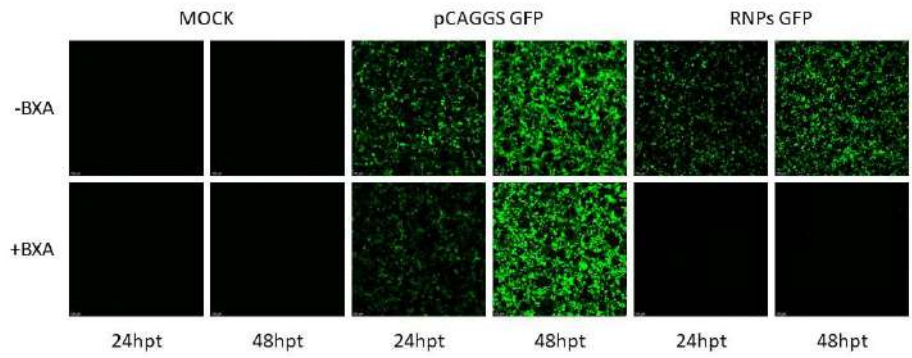

Influenza A viruses cause annual epidemics and occasional pandemics of respiratory disease, which have significant consequences for human health and the economy. Consequently, significant efforts have been devoted to developing new anti-influenza virus drugs targeting viral proteins, as well as identifying cellular targets for anti-influenza virus therapy. Current antiviral treatments, including M2 ion channel blockers and neuraminidase inhibitors, are increasingly compromised by the emergence of resistant strains. This highlights the urgent need for novel therapeutics with higher genetic barriers to resistance.

The influenza A virus genome consists of eight single-stranded, negative-polarity RNAs assembled into ribonucleoprotein (RNP) complexes that are incorporated into enveloped particles. After entering an infected cell, the RNPs are imported into the nucleus, where transcription and replication occur. The first step in viral gene expression is transcription from the parental RNPs. Translation of these early viral mRNA is essential for RNP replication. At least the viral nucleoprotein (NP) and polymerase proteins (PB1, PB2, and PA) are necessary to produce progeny RNPs. This process first involves the generation of complementary RNPs, which serve as efficient templates for producing large amounts of progeny RNPs. Progeny RNPs are then exported back to the cytoplasm and bud from the cell membrane.

In this study, we developed a virus-free, fluorescence-based mini-replicon system to safely evaluate influenza A virus (IAV) polymerase activity and streamline antiviral screening. We generated a negative-sense pseudoviral RNA that encodes enhanced green fluorescent protein (EGFP) and is flanked by the conserved 5' and 3' regions of the NS segment from the A/Victoria/3/75 (H3N2) strain. Recombinant ribonucleoproteins were reconstituted in HEK293T cells via co-transfection with plasmids expressing NS-EGFP RNA and PB1, PB2, PA, and NP proteins. After optimizing the transfection parameters and replication time, reproducible EGFP expression was observed in most cells. EGFP fluorescence, as measured by widefield microscopy, served as a direct readout of polymerase activity. Treatment with baloxavir acid, an endonuclease inhibitor that targets the PA subunit, completely suppressed EGFP expression. This validated the system's sensitivity and specificity.

In summary, this mini-replicon platform provides a robust, scalable, and biosafe approach for studying influenza A virus (IAV) polymerase functions and screening antiviral compounds in a high-throughput, virus-free format.

Identification of exosome modulators in 3d breast cancer models using exoscreen and cell painting technologies

Masia Sanchis, Esther [a, b], Đorđević, Snezana [d], Martinez, Esther [c], Vicent, Maria J. [* a, b]

[a]Laboratorio Polimeros terapeuticos y plataforma de cribado del CIPF

[b]Centro de Investigación Biomédica en Red Cáncer (CIBERONC)

[c]AREA DERMATOLOGIA Y REGENERACION TISULAR, HOSPITAL LA FE

[d]Separations Business Unit, TOSOH BIOSCIENCE

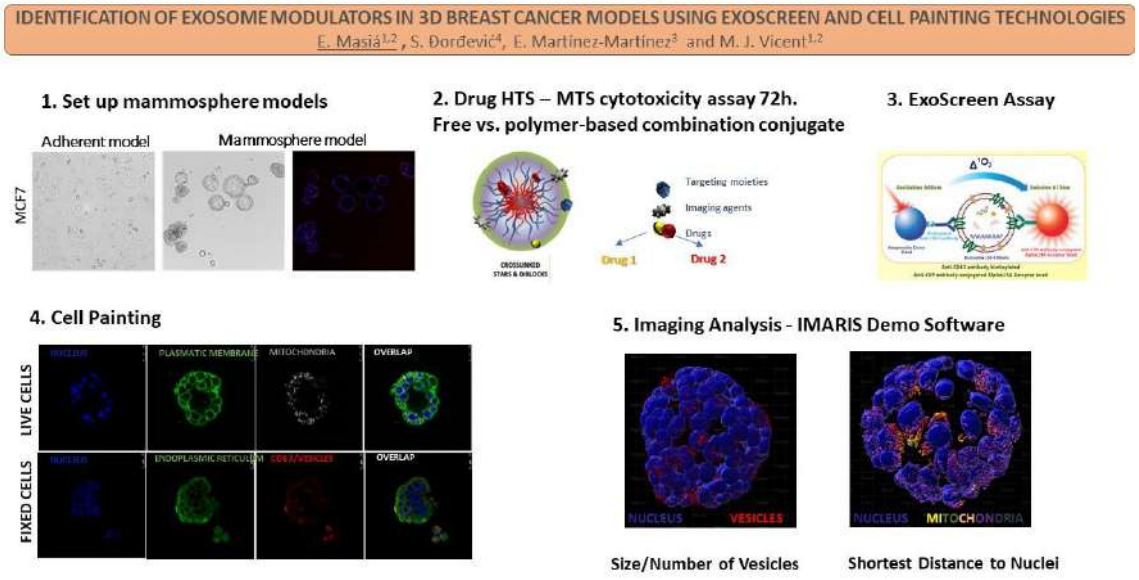

INTRODUCTION

3D spheroid cell cultures recapitulate the tumor micro-environment[1] better than their adherent 2D counterparts[2]. Spheroid models represent a valuable cancer research tool, allowing optimized drug selection and improved tumor distribution. 3D models of breast cancer will reduce the number of animals employed and drug screening costs[3-5]. Of note, the molecular complexity of breast cancer, especially when targeting metastasis, will require combinatorial drug treatments[6-7]. Exosomes - extracellular vesicles (EVs) that play essential roles in intercellular communicators[8] - help form the pre-metastatic niche[9] and support drug resistance[10]. EV markers include tetraspanins[11]; however, current methodologies to purify exosomes remain time-consuming and challenging to translate to clinical practice. We recently optimized a quick and reliable HTS methodology[12] to identify exosome modulators that combines external signals

measured by ExoScreen technology (a sensitive assay that measures protein-protein interactions) and internal exosomal markers in 2D models[13]. Our study employed MCF7 cells (Luminal A subtype).

OBJECTIVES

1. Study the effect of polymer-drug conjugates (single/combinations) on exosomes via the ExoScreen assay
2. Combine ExoScreen and Cell Painting[14] to discover exosome modulators (and other effects)

METHODOLOGY

Using low adherence plates, we cultured MCF7 mammospheres with EGF2/B27. We added free or polymer-conjugated drugs for 72 h and performed the ExoScreen assay using anti-CD9 acceptor beads and a biotinylated-anti-CD63 antibody. For Cell Painting, we employed markers of the mitochondria, endoplasmic reticulum, cell membrane, intraluminal/extracellular vesicles, and nucleus. Cell viability evaluations employed the MTS assay.

RESULTS

We identified “Drug 1” as an exosome biogenesis inhibitor (reducing ExoScreen and CD63 signals, extra- and intracellularly, respectively). “Drug 3” inhibited exosome release, manifested as a lower ExoScreen signal and accumulated intracellular CD63 signal, and modulated the endoplasmic reticulum. Both drugs mimic the behavior previously observed in a 2D model[13].

CONCLUSION

Employing this screening technique in 3D spheroids ensured the homogeneous distribution of labeling in a preclinically relevant model. We combined analysis of exosomal intracellular markers (CD63) with morphological features to create a multiplexed approach. We employed our approach to validate the antitumor/antimetastatic properties of a polypeptide-based-drug combination conjugates[7,15], with findings correlating with in vivo data. The following steps include applying suitable image analysis software and artificial intelligence tools to enhance intracellular signal quantification of different markers and establishing correlations with therapeutic outputs[7].

References:

[1] Moriah, E. et al., Frontiers in Bioengineering and Biotechnology 2016, 4:12

[2] Satchi-Fainaro R, et al. Adv. Drug Deliv. Rev. 2022, 183: 114140

[3] Boix-Montesinos et al Adv Drug Deliv Rev 2021, 173:306

[4] Juerguen, F.et al., Nature Protocols 2009, 4:3.

[5] Silvestri A.,et al Drug Discov. Today 2021, 26: 1369

[6] Greco, F. and Vicent, M.J. Adv Drug Deliv Rev, 2009, 61:1203

[7] Arroyo-Crespo J.J. et al Biomaterials 2018, 186:8

[8] Yanez-Mo, et al. J Extracell Vesicles 2015, 4:27066

[9] H. Peinado, Nat Med 2012, 18883

[10] Chou TC. Pharmacol Rev 2006, 58;621-681.

[11] Z. Andreu and Yanez-Mo. Frontiers in Immunology 2014, 5;442

[12] Yusuke Yosioka et al. Nature communication 2014, 5;3591.

[13] Z. Andreu et al. Nanotheranostics 2023

[14] Mark-Anthony Bray et al. Nat Protoc. 2016. September; 11(9): 1757–1774.

[15] Arroyo-Crespo JJ et al Adv Funct Mat 2018, 28: 1800931

Acknowledgments:

We thank Dr. Zoraida Andreu for 3D model optimization, David Charbonnier for ExoSreen assay development, Dr. Alicia García for cell painting, Alberto Hernández for confocal imaging, and Dr. Stuart P. Atkinson for English editing. This work is supported by the Tentacles excellence Network, RED2018-102411-T, and the Spanish Ministry of Science and Innovation PID2019-108806RB-I00. Equipment funded by the Generalitat Valenciana and co-financed with European Regional Development Fund (FEDER) funds (PO FEDER of Comunitat Valenciana 2014-2020).

Single-Molecule and Cryo-EM Approaches to Study the Folding Mechanism of Human CCT

Majano López de Madrid, Carmen [*a], Bocanegra, Rebeca [b], Ibarra, Borja [b], Rubio, Julia [a, b], Requejo, José [a, b], Rodriguez, Javier María [a], Cuellar, Jorge [a], Valpuesta, José María [a]

[a]CENTRO NACIONAL DE BIOTECNOLOGIA (CNB-CSIC) (ES)

[b]Madrid Institute for Advanced Studies, IMDEA Nanoscience (ES)

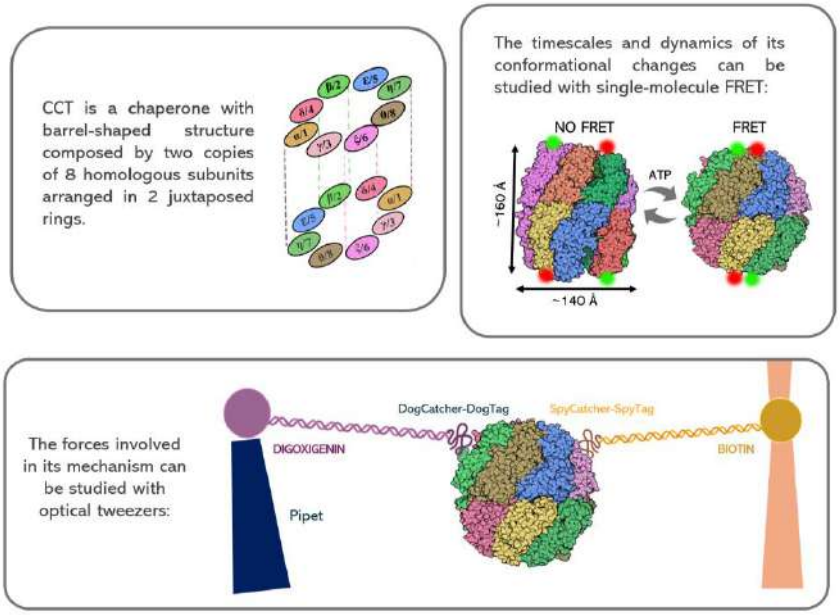

The eukaryotic chaperonin CCT (chaperonin-containing TCP-1) is a key player in cellular homeostasis since it assists the folding of 10% of cytosolic proteins and its malfunction is linked to cancer and neurodegenerative diseases. CCT is the most complex of all chaperonins with each of the two rings composed of eight paralogous subunits.

To understand how this chaperonin can interact with and fold such variety of substrates and cofactors, we can combine single molecule techniques, such as optical tweezers and single-molecule FRET with cryo-microscopy. This will undoubtedly contribute to understand how CCT works and how to deal with malfunctions that can lead to cell dysregulation.

With this aim, we have optimized the heterologous production and purification of human CCT, introducing specific recombinant tags to allow its study with single-

molecule techniques, as well as for structural studies. This step of the project has been a considerable technical challenge due to its intricate multimeric nature. The eight different CCT subunits have been cloned and expressed using the Multibac modification of the Bac-to-Bac baculoviral expression system, in which insect cells are infected with recombinant baculoviruses expressing all the subunits simultaneously.

Different baculoviruses have been constructed with the subunits containg purification tags (His tag in subunit 1, CBP-Strep-his tag in subunit 3) as well as other tags for single molecule experiments in the equatorial regions of subunits 1 and 7. These tags are Ppant sequences for AcpS and Sfp enzimes3 ,and DogTag and SpyTag for their corresponding catchers.

Using this system, we have succeeded at purifying the human CCT. Using mass spectrocopy we identified all subunits with a good q-value (<0,01). Currently we are working towards improving sample concentration and homogeneity in order to be able to vitrify the sample, perform a large acquisition and obtain a high-resolution 3D reconstruction.

Cryo-EM reveals conformational changes in the RUVBL1-RUVBL2 ATPase induced by ATP binding

García, Carmen [*a], López-Perrote, Andrés [a], Boskovic, Jasminka [a], Llorca, Óscar [*a]

[a]Spanish National Cancer Research Centre (CNIO), Structural Biology Programme, Melchor Fernández Almagro 3, 28029 Madrid, Spain

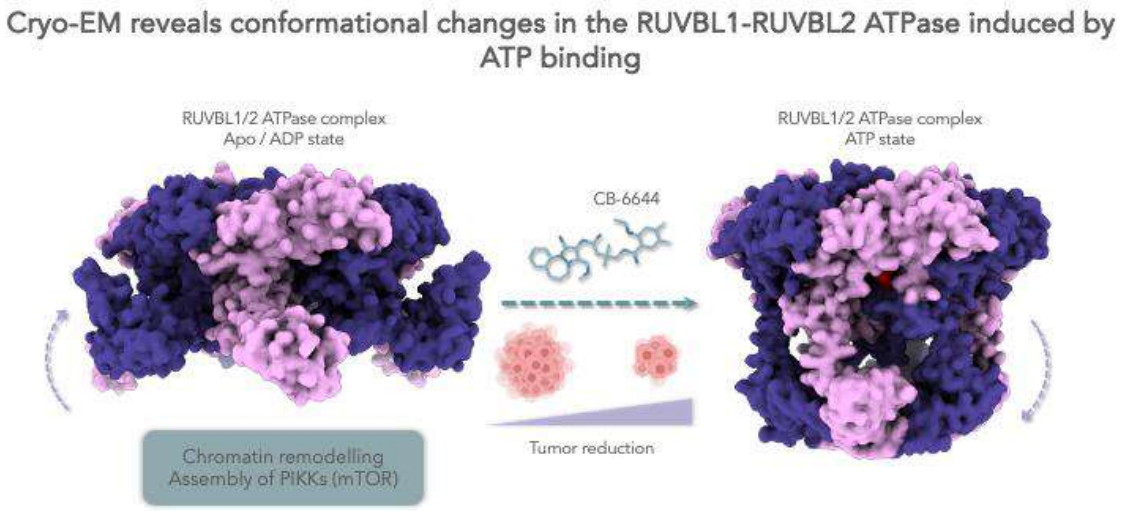

RUVBL1-RUVBL2 is a hetero-hexameric ATPase involved in essential cellular processes such as chromatin remodeling and the assembly of mTORC1 and mTORC2 complexes (1, 2). To investigate how ATP binding affects the conformation of this ATPase, we determined the structures of RUVBL1-RUVBL2 incubated with ATP and with ATP and CB-6644, an aminopyrazolone-based small molecule with demonstrated antitumor activity in animal models (3). CB-6644 allosterically inhibits RUVBL1-RUVBL2, but its binding mode and mechanism of action remain unclear.

Using cryo-electron microscopy, we determined the structure of the RUVBL1-RUVBL2 complex bound to ATP and bound to ATP and CB-6644. Combined with biochemical analyses, these data reveal that ATP binding induces substantial conformational rearrangements in RUVBL1-RUVBL2, creating an interface that allows for the binding of CB-6644. This CB-6644 stabilizes this ATP-bound state by binding between two subunits, effectively locking the complex in a pre-hydrolysis conformation and preventing ATP hydrolysis.

Interestingly, our findings suggest a mechanism whereby CB-6644 disrupts the coupling between nucleotide state, the positioning of the DII domains, and

interactions with partner proteins. This work elucidates how ATP binding alters the conformation of RUVBL1-RUVBL2 and how CB-6644 inhibits this ATPase by interfering with the ATPase hydrolysis cycle.

References:

[1] Lynham, J. and W. A. Houry. The Role of Hsp90-R2TP in Macromolecular Complex Assembly and Stabilization. Biomolecules 2022, 12(8).

[2] Dauden M.I., Lopez-Perrote, A. Llorca, O. RUVBL1–RUVBL2 AAA-ATPase: a versatile scaffold for multiple complexes and functions. Current Opinion in Structural Biology 2021, 67:78–85.

[3] V. A. Assimon, Y. Tang, et al. CB-6644 is a selective inhibitor of the RUVBL1/2 complex with anticancer activity. ACS Chemical Biology 2019, 14 (2), 236-244.

Characterization of the yeast Cdc13 dimeric protein

Coloma, Javier [*a], Gonzalez-Rodriguez, Nayim [a], Alegrio Louro, Jaime [a], F. Lue, Neal [b]

Llorca, Oscar [*a]

[a]Structural Biology Programme, Spanish National Cancer Research Centre (CNIO), Madrid, Spain.

[b]Department of Microbiology and Immunology, W. R. Hearst Microbiology Research Center, Weill Cornell Medicine, New York, United States.

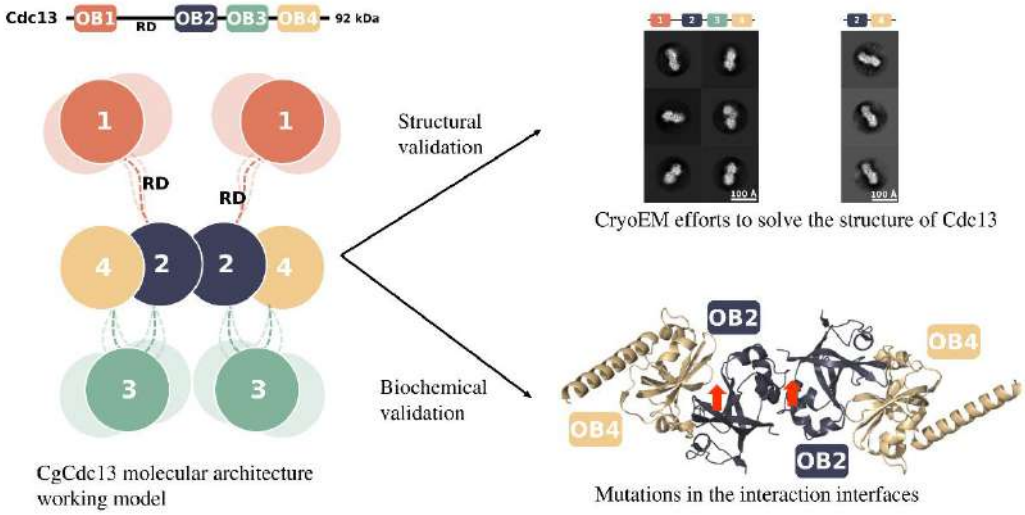

CgCdc13 molecular architecture working model

CryoEM efforts to solve the structure of Cdc13

Mutations in the interaction interfaces

The CST complex is involved in telomere replication, DNA repair, and chromosome cohesion. Its best-characterized functions are telomere capping and the regulation of telomere replication. The complex specifically binds to telomeric single-stranded DNA (ssDNA) regions in a sequence-specific manner. Additionally, it directly interacts with both telomerase and DNA polymerase alpha (Polα). These direct interactions—telomerase, which elongates the G-strand of telomeres, and Polα, which is responsible for the fill-in of the C-strand—place CST components at the center of telomere replication regulation. The complex consists of a large subunit, CTC1 in humans or Cdc13 in yeast, and two smaller subunits, STN1 and TEN1, which are well conserved across species.

Several structural studies of the human CST complex have revealed a decameric configuration when bound to DNA, and a heterotrimeric CTC1-STN1-TEN1 structure containing one CTC1 subunit when bound to Polα. However, Cdc13 does not

resemble its mammalian counterpart CTC1, neither in sequence nor in domain organization. All yeast species analyzed to date show that Cdc13 dimerizes, but whether the dimerization mechanism is conserved across different yeast species remains unclear.

Our work with the CST complex from Candida glabrata has provided new insights into Cdc13 dimerization upon interaction with telomeric DNA [1]. Our proposed model identifies the OB2 domain of CgCdc13 as the primary driver of protein dimerization. This contrasts with the model proposed for ScCdc13, where the OB1 domain is essential for dimerization. Our current efforts to validate this model are focused on the structural analysis of the Cdc13 dimerization core using both cryo-electron microscopy (cryo-EM) and structure prediction algorithms. To verify the structural information, point mutations in the predicted interaction interfaces are being analyzed using biophysical techniques.

References:

[1] Coloma J, Gonzalez-Rodriguez N, Balaguer FA, Gmurczyk K, Aicart-Ramos C, Nuero ÓM, Luque-Ortega JR, Calugaru K, Lue NF, Moreno-Herrero F, Llorca O. Molecular architecture and oligomerization of Candida glabrata Cdc13 underpin its telomeric DNA-binding and unfolding activity. Nucleic Acids Res. 2023 Jan 25;51(2):668-686.

Poster Session 24th September - Topic: Materials

Twist-induced Polar Structures in Free-standing Oxide Membranes

Hu, Xinxin [*a,b], Lun, Yingzhuo [a], Saeed, Umair [a,b], Pinto-Huguet, Iván [a,b], Gupta, Kapil [a], Mundet, Bernat [a], Santiso, José [a], Pesquera, David [a], Catalan, Gustau [a,c], Arbiol, Jordi [a,c]

[a]Catalan Institute of Nanoscience and Nanotechnology (ICN2), CSIC and BIST, 08193 Barcelona, Catalonia, Spain

[b]Autonomous University of Barcelona, 08193 Barcelona, Catalonia, Spain

[c]ICREA, Pg. Lluís Companys 23, 08010 Barcelona, Catalonia, Spain

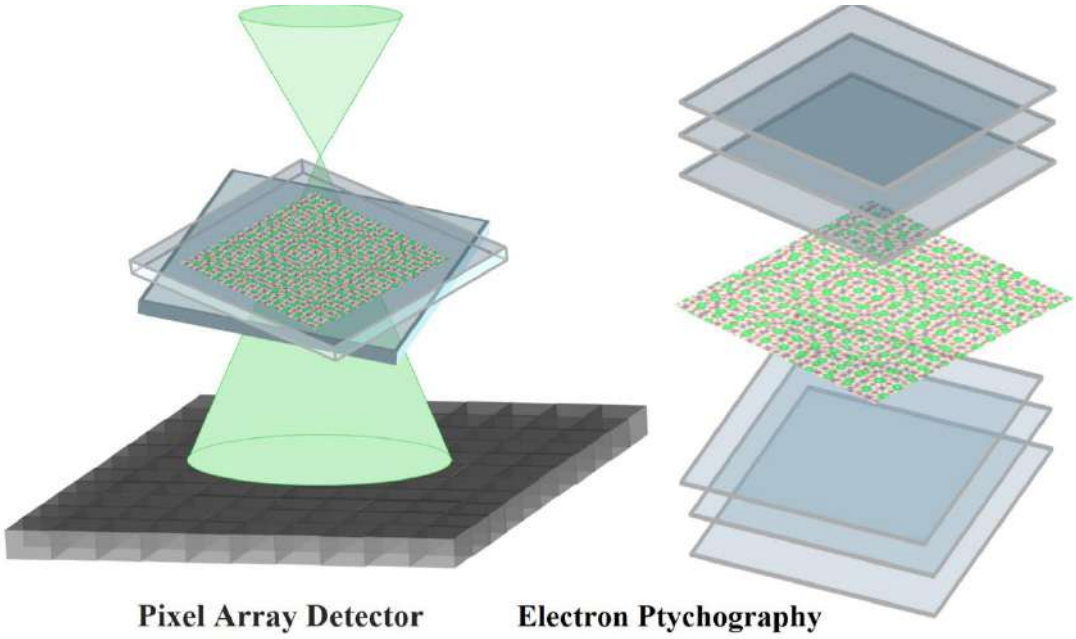

In recent years, ferroelectric polarization-induced topological structures—such as polar skyrmions, vortices, flux-closure domains, and related configurations—have garnered considerable attention due to their novel physical properties and potential applications in next-generation electronic devices. However, these complex topological patterns have predominantly been observed in superlattice systems grown on substrates, where limited tunability and fabrication challenges restrict their broader application. In contrast, twisted free-standing thin films have emerged as a promising platform owing to their structural flexibility and tunable polar properties. The formation of polar patterns in these systems is strongly influenced by strain gradients and lattice rotations under controlled twist angles. Nonetheless, exploring the interfaces and individual layers within such systems remains a significant challenge, as a comprehensive understanding of their underlying mechanisms requires atomic-level resolution.

In this study, we fabricated a series of twisted free-standing oxide ferroelectric membranes. Using aberration-corrected scanning transmission electron microscopy (STEM), we directly observed the emergence of diverse polar topological structures and elucidated their underlying mechanisms. Our findings provide new insights into the formation and evolution of complex polar textures in twisted free-standing membranes and offer a foundation for future explorations and potential device applications.

References:

[1] Sánchez-Santolino, G.; Rouco, V.; Puebla, S.; Aramberri, H.; Zamora, V.; Cabero, M.; Cuellar, F. A.; Munuera, C.; Mompean, F.; Garcia-Hernandez, M.; Castellanos-Gomez, A.; Íñiguez, J.; Leon, C. & Santamaria, J. A 2D Ferroelectric Vortex Pattern in Twisted BaTiO3 Freestanding Layers. Nature 2024, 626, 529–534.

[2] Chen, Z.; Jiang, Y.; Shao, YT.; Holtz, ME.; Odstrčil, M.; Guizar-Sicairos, M.; Hanke, I.; Ganschow, S.; Schlom, DG.; Muller, DA.; Electron Ptychography Achieves Atomic-Resolution Limits Set By Lattice Vibrations. Science 2021, 372,826-831.

[3] Sha, H.; Zhang, Y.; Ma, Y.; Li, W.; Yang, W.; Cui, J.; Li, Q.; Huang, H.; Yu, R.; Polar Vortex Hidden in Twisted Bilayers of Paraelectric SrTiO3. Nat Commun. 2024, 15, 10915. Twisted Bilayers of Paraelectric SrTiO3. Nat Commun. 2024, 15, 10915.

Acknowledgments:

The authors acknowledge ICN2 and ALBA (JEMCA) for providing key facilities and technical guidance. ICN2 is supported by the Severo Ochoa program from Spanish MCIN / AEI (Grant No. CEX2021-001214-S), the European Regional Development Fund from European Union (Grant No. IU16-014206 (METCAM-FIB)), and the CERCA Programme, Generalitat de Catalunya. ICN2 is a founding member of e-DREAM. J.A. and X.H. acknowledge funding from Generalitat de Catalunya (Grant No. 2021SGR00457). This study is part of the Advanced Materials programme and was supported by MCIN with funding from European Union NextGenerationEU (PRTR-C17.I1) and by Generalitat de Catalunya (In-CAEM Project). We acknowledge support from CSIC Interdisciplinary Thematic Platform (PTI+) on Quantum Technologies (PTI-QTEP+). This work has been funded by the European Commission – NextGenerationEU (Regulation EU 2020/2094), through CSIC's Quantum Technologies Platform (QTEP). Y.L. acknowledges support from the Severo Ochoa Seed Funding program (Grant CEX2021-001214-S/MICIU/AEI/10.13039/501100011033). X.H. acknowledges PhD scholarship support from the China Scholarship Council (CSC) (Grant No. 202304910019). The authors acknowledge the use of the Spectra 300 microscope, provided under ALBA Synchrotron proposal (Grant No. 20240320035).

FFneT Project: Automated Approach to FFT Peak Detection

Cruañes, Josep [*a], Pinto, Ivan [*a], Arbiol, Jordi [*a, b],

[a]ICN2 (CSIC and BIST), 08193 Campus UAB, Bellaterra, Barcelona, Spain

[b]ICREA, 08010 Barcelona, Barcelona, Spain.

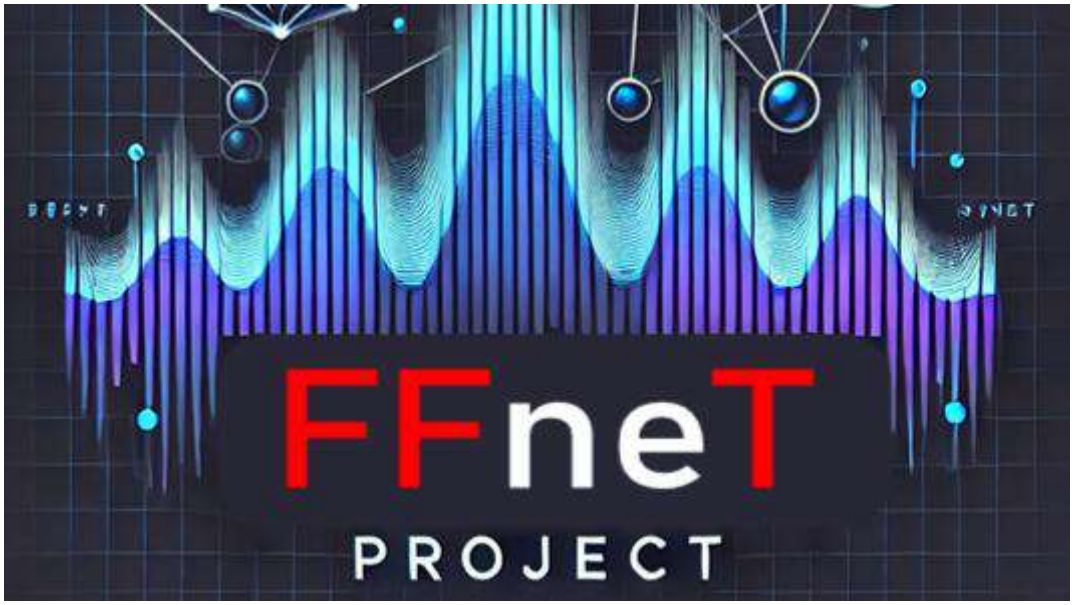

Fast Fourier Transforms (FFTs) are fundamental tools in the analysis of crystalline structures through electron microscopy, providing key insights into lattice periodicities, orientations, and defects. Despite their widespread use, the process of identifying and indexing diffraction peaks within FFTs remains a manual and expertise-dependent task, prone to variability and time constraints. In this work, we introduce FFneT, a comprehensive framework designed to automate FFT peak detection and streamline the indexing process using deep learning.

FFneT integrates three core components: (i) the construction of a curated and expandable database of FFTs indexed by crystal orientation and structure type; (ii) the development of a graphical user interface (GUI) to facilitate efficient FFT visualization, annotation, and validation; and (iii) the implementation of a convolutional neural network based on the U-Net architecture, trained to robustly detect diffraction peaks across a wide range of conditions, including varying noise levels and symmetries.

Our preliminary results show that the trained model achieves high accuracy in detecting relevant features in both simulated and experimental FFT data. This framework offers a scalable solution for high-throughput analysis and lays the

groundwork for future developments in automated crystallographic characterization. FFneT aims to democratize advanced electron microscopy analysis, enabling both expert and non-expert users to access fast, reliable, and reproducible structural information.

Chemical evolution of polymer materials for additive manufacturing during STEM-EELS electron beam irradiation

Valencia Liñán, Luisa María [*a], Herrera Collado, Miriam [b], Molina Rubio, Sergio Ignacio [b]

[a]Instituto de Ciencia de Materiales de Sevilla, Universidad de Sevilla, CSIC, Av Americo Vespucio, Seville, Spain

[b]Departamento de Ciencia de los Materiales e IM y QI. F. Ciencias. IMEYMAT. Campus Río San Pedro. Universidad de Cádiz. 11510 Puerto Real (Cádiz). Spain.

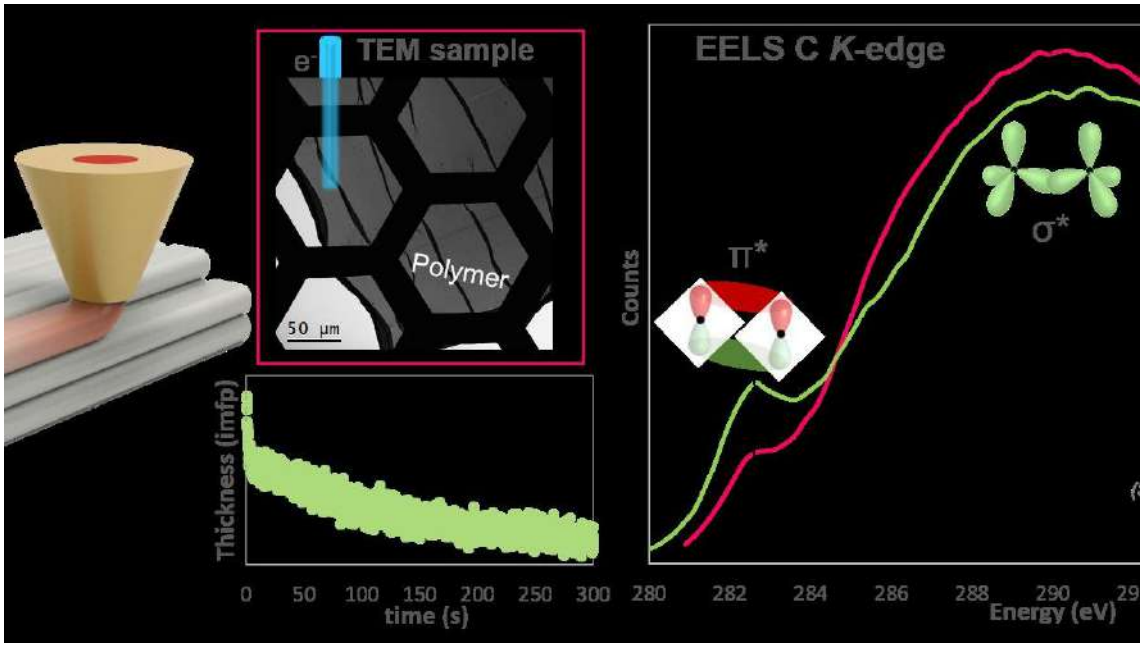

Additive manufacturing (AM) techniques impose an advantageous methodology for the fabrication of devices, providing the ability to reproduce complex geometries, unattainable by traditional manufacturing technologies. The continuous growth of these techniques promotes the development of new materials meeting the requirements of the fabrication methods while providing enhanced properties [1]. Transmission electron microscopy (TEM) is one of the main tools to study materials from subnanometer to micrometer length scales, while its performance strongly depends on the material under study [2]. The interaction of electrons with soft systems, such as polymers, causes different types of radiation damage, e.g., electrostatic charging, radiolysis and knock-on damage [3], limiting the resolution that can be achieved. Therefore, it is important to understand the beam damage and the underlying mechanisms inducing the polymer degradation

upon electron exposure to pave the way towards an accurate analysis by means of TEM techniques.

The chemical changes on a specimen during TEM analyses can be monitored under a variety of techniques, including Electron Energy Loss Spectroscopy (EELS). EELS studies allow addressing thickness variations of the specimen due to degradation during irradiation, as well as chemical or bonding changes due to alterations of the chemical structure [4].

In this work, we examine the effect of electron beam damage in different polymers for AM by studying the variations on the low- and core-loss EELS signals when increasing the exposure time (Figure 1). Based on the evolution of the C, N and O signal during the beam irradiation, including the inspection of the spectral shape, as well as the thickness reduction, we propose likely underlying mechanisms explaining the polymers degradation. The results obtained allow the optimization of the working conditions for structural characterization experiments, which are extremely important in the development of novel materials.

Presenting author details

Full name: Luisa María Valencia Liñán
Contact e-mail: luisa.valencia@icmse.csic.es
Category: (Oral presentation/ Poster presentation)

References:

[1] Gibson, I.; Rosen, D.; Stucker, B., Additive Manufacturing Technologies, 2019, ISBN 9781493921126

[2] Williams, D.B.; Carter, C.B., Transmission Electron Microscopy. A textbook for Materials Science, 2009, ISBN 9780387765006

[3] Egerton, R.F. Radiation damage to organic and inorganic specimens in the TEM. Micron 2019, 119, 72–87

[4] Singh, P.K.; Venugopal, B.R.; Nandini, D.R. Effect of electron beam irradiation on polymers. J. Mod. Mater. 2018, 5, 24–33

WhatEELS 2.0: open source software based in Python for EELS análisis

Costa-Ledesma, Vanessa [*a], del Pozo-Bueno, Daniel [a], Peiró, Francesca [a], Estradé, Sònia [a]

[a]Laboratiry of Electron Nanoscopies - MIND - IN2UB - Dept. Enginyeria Electrònica i Biomèdica, Universitat de Barcelona

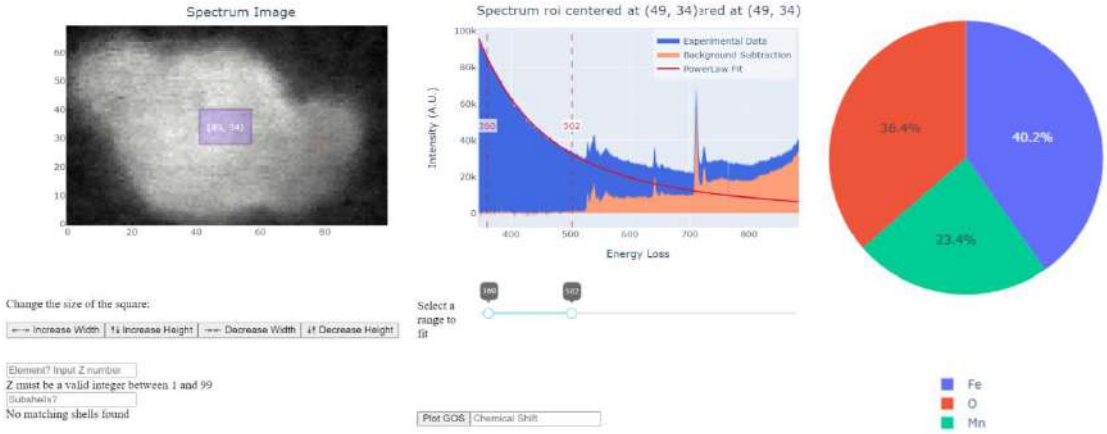

Electron Energy Loss Spectroscopy (EELS) using a Scanning Transmission Electron Microscope (STEM) enables precise elemental characterization with exceptional spatial resolution. Among the various approaches for spectral unmixing, Non-Linear Least Squares (NLLS) fitting stands out for its ability to provide detailed information on each component in the fitted model without requiring calibrated reference spectra. This makes it a preferable alternative in certain analytical scenarios, particularly when spectral references are unavailable or insufficient.

To facilitate the analysis of complex datasets, combining clustering-based segmentation with NLLS fitting enhances parameter control and proves especially effective for samples with mixed compositions.

To support this analytical framework, a modular Python-based software package called WhatEELS was developed by J. Blanco-Portals and made publicly available in 2022 [1].

In the present work, we introduce an update to WhatEELS that incorporates elemental quantification tools based on fully relativistic cross-sections.

WhatEELS features an interactive shell developed in Python, using libraries such as Panel and Holoviews, with Bokeh serving as the graphical backend. Internally, NLLS

fitting and background removal rely on the lmfit library, which extends SciPy's fitting functionalities. The software also includes machine learning methods such as Hierarchical Density-Based Spatial Clustering of Applications with Noise (HDBSCAN), Uniform Manifold Approximation and Projection (UMAP), and Support Vector Machines (SVM)—with HDBSCAN and SVM implemented via the Scikit-learn library. Relativistic cross-sections are calculated using quantum mechanical formulations following the methodology of Salvat.

We have successfully implemented relativistic elemental quantification in WhatEELS. The updated software was tested on iron oxide core–shell nanocubes and iron–manganese oxide core–shell nanoparticles, yielding quantification results in agreement with expected values.

WhatEELS is a versatile and user-friendly tool designed for the analysis of multi-pixel EELS datasets. By integrating clustering algorithms for image segmentation with NLLS fitting routines, it streamlines workflows and improves analytical precision. Its open-source nature and low programming requirements make it particularly suitable for researchers and students beginning their work in EELS data analysis within materials science.

References:

[1] J. Blanco-Portals, P. Torruella, F. Baiutti, S. Anelli, M. Torrell, A. Tarancón, F. Peiró, S. Estradé,

Acknowledgments:

The authors would like to acknowledge the financiation from PID2022-138543NB-C21, 2021SGR00242

Transmission electron microscopy studies on the changes in the cathode structure of high-load electrodes with spatial arrangements

Liu, Jinhai [*a], YU, Jing [a], Cabot, Andreu [b], Arbiol, Jordi [a]

[a]ICN2 (CSIC and BIST), 08193 Campus UAB, Bellaterra, Barcelona, Spain

[b]IREC, Catalonia Institute for Energy Research, C/ Jardins de les Dones de Negre 1, Barcelona 08930, Spain

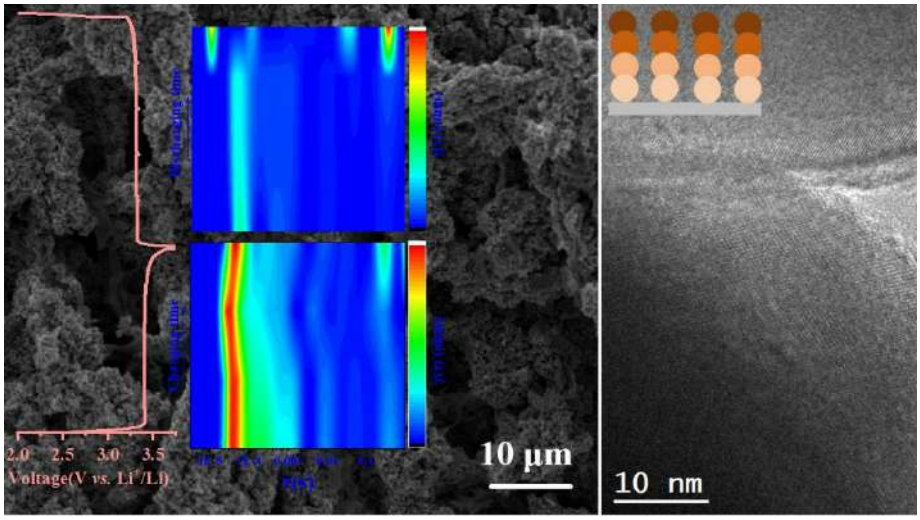

In the process of preparing high-energy-density batteries, designing high-load electrodes can reduce the mass redundancy of current collectors and other materials during the packing process and improve the energy density of the battery cell. However, in recent years' research, the same phenomenon has been shown: The capacity of high-load electrodes is significantly lower than that of low-load electrodes at the same rate. And the explaination about "Active materials cannot be fully utilized" is generally accepted. It is specifically attributed to the fact that the ion transmission distance in the electrolyte increases due to the increase in high-loading electrode thickness, and its diffusion is limited, resulting in severe concentration polarization on the electrode surface. These lead to the inability to fully utilize the active materials. However, the differences in the solid-phase diffusion coefficients of active materials under different spatial arrangements of the electrode are ignored in this process. Therefore, this paper uses the ice template method to construct a 3D porous electrode to reduce the influence of concentration polarization, and uses transmission electron microscope to explore the performance differences caused by the differences in the solid-phase diffusion of ions in high-load electrodes under different spatial arrangements.

Poster Session 25th September - Topic: Life Sciences and CryoEM

Reconstitution of the Mycobacterium tuberculosis translation system to understand translation initiation control

Villamayor-Belinchón, Laura [a], Bresó, Rosendo [a], Llácer, José Luis [a], Cortés, Teresa *

[a]Instituto de Biomedicina de Valencia (IBV-CSIC) (ES)

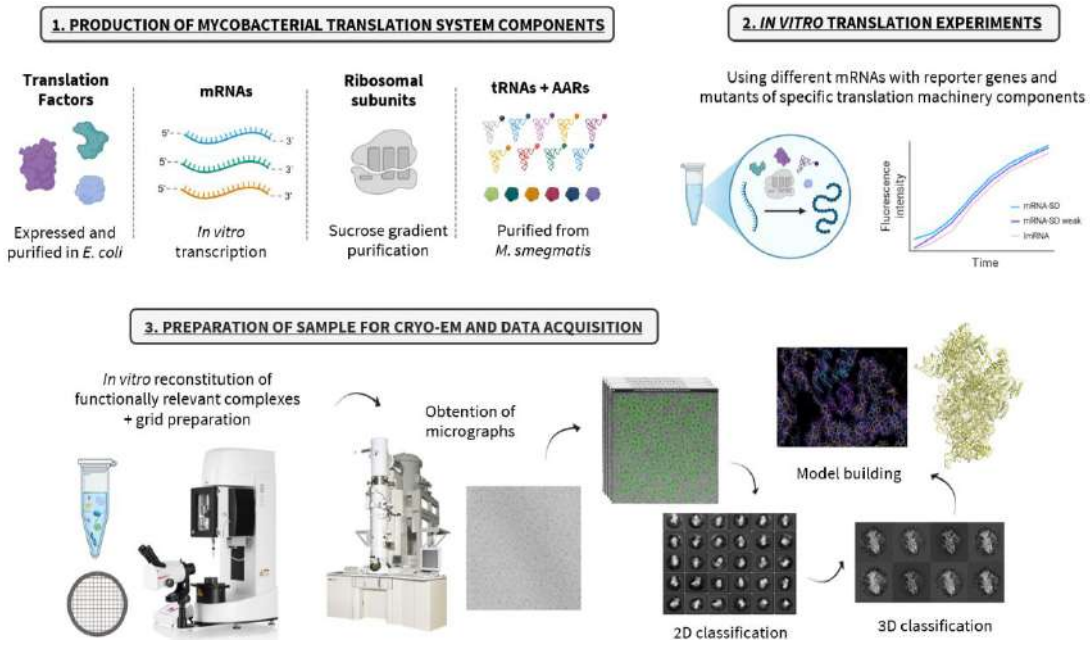

Mycobacterium tuberculosis, the causative agent of tuberculosis, is one of the deadliest human pathogens. During infection, this pathogen usually persists for prolonged periods in a non-replicating state and must adapt to a variety of harsh environments. Recent studies have revealed unique features of translational control in *M. tuberculosis*, which may contribute to its adaptability during infection.

We have found that over 50% of its genes lack canonical translation initiation signals, yet they are efficiently translated during exponential growth and under conditions that mimic persistence inside the host. This suggests the existence of alternative mechanisms for translation initiation in this organism. However, the molecular basis and the biological relevance of these non-canonical translation mechanisms remain poorly understood.

To investigate this, we aim to reconstitute a mycobacterial *in vitro* translation system and use it to study how *M. tuberculosis* regulates translation. To this end, we have acquired *M. tuberculosis* genes encoding translation factors for recombinant expression and purification in *Escherichia coli*. We have successfully purified all the translation factors, including two different versions of IF2, one lacking the N-terminal unstructured, species-specific extension of the factor. We have also

optimized protocols for isolating ribosomal subunits from *M. smegmatis* and obtaining fMet-tRNA^{fMet} from *E. coli*. Moreover, we have produced the enzymes required for tRNA aminoacylation. Currently, we are producing canonical and non-canonical mRNA templates encoding reporter genes and optimizing the purification of all the tRNAs and aminoacyl-tRNA synthetases (AARs) directly from *M. smegmatis*. Our next objective is to establish an *in vitro* translation system to analyse variations in initiation mechanisms using these mRNAs and mutants of specific components of the translation machinery.

Additionally, while several structures of mycobacterial ribosomes have been reported, none correspond to a functional translation initiation complex. To complement the molecular characterization, we aim to obtain high-resolution structures of canonical and non-canonical initiation complexes using cryo-electron microscopy. We expect that these structures, together with our *in vitro* translation experiments, will help us identify crucial elements involved in translational control in *M. tuberculosis*.

COPII (Coat Protein II) vesicles and response to stress in plants

Pérez-Rueda, Javier [a, b], Marcote, María Jesús [a, b], Aniento, Fernando [* a, b]

[a]Departamento de Bioquímica y Biología Molecular, Universidad de Valencia, Burjassot 46100, Valencia, Spain

[b]Instituto Universitario de Investigación en Biotecnología y Biomedicina (BIOTECMED), Burjassot 46100, Valencia, Spain

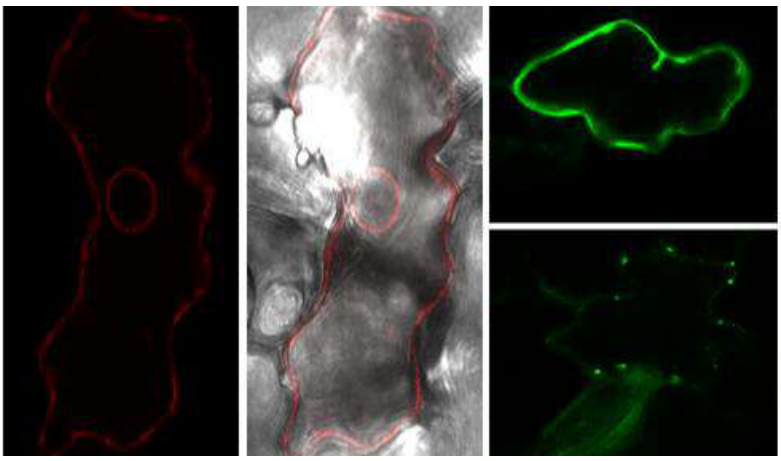

Proteins are essential for virtually all cellular functions, and their accurate localization is crucial for proper activity. In eukaryotic cells, proteins synthesized at the endoplasmic reticulum (ER) are directed to other cellular compartments through vesicular trafficking, primarily via COPII-coated vesicles. The COPII complex, consisting of the subunits SAR1, SEC23, SEC24, SEC13, and SEC31, is responsible for the selective packaging of cargo proteins and the budding of vesicles from the ER.

Arabidopsis thaliana is a small plant from the mustard family (Brassicaceae) that is a model organism to study genetic, cellular, and molecular biology of flowering plants. In Arabidopsis there is a notable expansion in COPII component isoforms, including different isoforms of the SEC24 subunit (the one involved in cargo selection during ER export), that points to potential functional specialization or redundancy among paralogs. Recent studies have identified Arabidopsis specific COPII vesicles induced by the main phytohormone involved in abiotic stress responses, abscisic acid (ABA). The formation of these vesicles is regulated by the isoform SAR1A but not by SAR1C. The aim of this work is to uncover the role of specific SEC24 isoforms in modulating ABA responses by influencing protein trafficking dynamics. To this end, we decided to analyze by confocal microscopy the localization of transiently expressed XFP-tagged COPII specific cargos with a putative involvement in plant responses to abiotic stress, with special emphasis in components of the ABA synthesis / transport / signaling pathway.

Structural studies for the development of allosteric drugs against CXCR4

Collado-Ávila, Javier [a], García-Cuesta, Eva [a], Arranz, Rocío [a], Rodríguez, Jose Miguel [a], Mellado, Mario [a], Santiago, César [*a]

[a]CENTRO NACIONAL DE BIOTECNOLOGIA (CNB-CSIC) (ES)

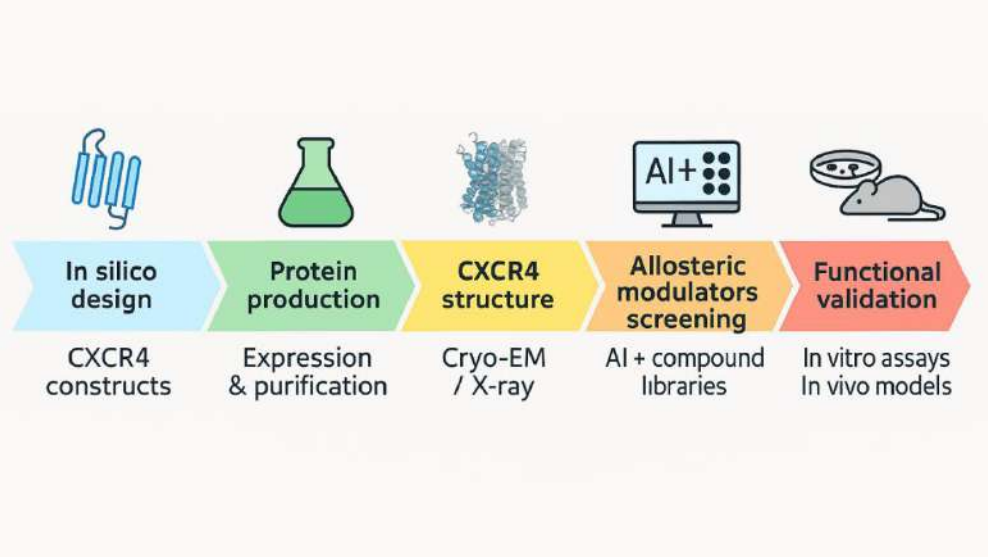

CXCR4 is a member of the G protein-coupled receptor (GPCR) family, playing a critical role in physiological processes such as cell migration, hematopoiesis, and immune response. It is also involved in multiple pathologies, including HIV infection, cancer, and inflammatory diseases. Understanding its interaction with endogenous and pharmacological ligands at the structural level is essential for the development of new therapeutic strategies. However, due to its membrane-bound nature and conformational flexibility, structural characterization of CXCR4 remains technically challenging.

In this work, we present our current progress in the expression, purification, and structural analysis of CXCR4 using cryo-electron microscopy (cryo-EM). The receptor was purified in micellar form, yielding a homogeneous and stable preparation suitable for cryo-EM analysis. Preliminary data collections were performed on a 200 keV microscope, resulting in 2D class averages that suggest the formation of tetrameric assemblies. However, the particle quality is currently limited, prompting future optimization of sample conditions, including reconstitution into nanodiscs. This study represents an initial step towards resolving the structure of CXCR4 in a near-native membrane environment.

Atypical G Protein Coupling and Activation Mechanism of GPR15 Revealed by Cryo-EM

Carrión-Antolí, Ángela [*a], Maciej Stepniewski, Tomasz [b, c], Gonzalez Ramirez, Andrés [a], Arroyo-Urea, Sandra [a], Selent, Jana [b, d], García-Nafría, Javier [a]

[a]Institute for Biocomputation and Physics of Complex Systems (BIFI) and Laboratory of Advanced Microscopy (LMA), University of Zaragoza, Zaragoza, Spain

[b]Research Programme on Biomedical Informatics (GRIB), Hospital del Mar Medical Research Institute (IMIM), Barcelona, Spain

[c]InterAx Biotech AG, Villigen, Switzerland

[d]Department of Medicine and Life Sciences, Pompeu Fabra University (UPF), Barcelona, Spain

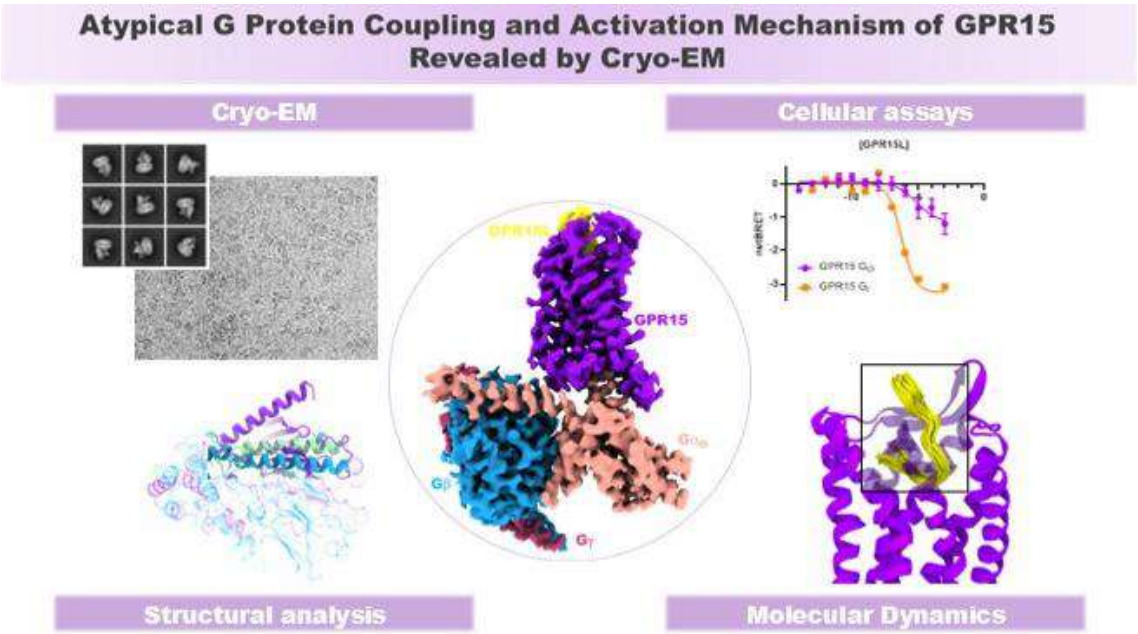

GPR15 is a G protein-coupled receptor (GPCR) involved in immune system regulation, including lymphocyte homing to epithelial barriers and modulation of inflammatory responses. Despite its physiological significance, the structural basis of GPR15 signaling remains poorly understood.

Using cryo-electron microscopy, we determined the structure of GPR15 in complex with a heterotrimeric $G\alpha_o$ protein, revealing unique features that distinguish it from other GPCRs. Notably, the G protein engages the receptor at an atypical angle, differing from canonical coupling modes. Meanwhile, the peptide ligand binds in a distinctive "hook-like" configuration.

In the absence of ligand, the orthosteric pocket, especially in the extracellular regions of TM1 and TM7, exhibits increased flexibility, as shown by poor cryo-EM density and elevated root mean square fluctuations (RMSF) from molecular dynamics simulations. Ligand binding stabilizes this region, suggesting that ligand–receptor interactions play a key role in shaping the orthosteric site.

These findings provide new insights into the structural and functional biology of GPR15, offering a framework for therapeutic development.

Structural and Dynamic insights into the IS21 Transpososome

Rizzuto, Irene [*a], Spìnola Amilibia, Mercedes [a], Arias Palomo, Ernesto [a]

Centro Investigaciones Biológicas Margarita Salas (ES)

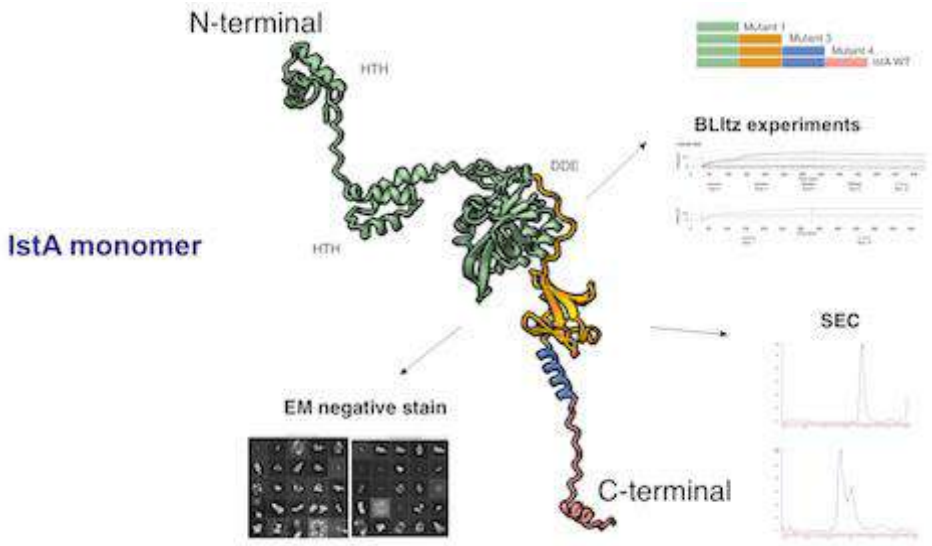

The transposition of mobile DNA elements - nucleic acid sequences that can move from one locus to another in the genome - is a fundamental driver of genome evolution, enabling the movement of discrete DNA segments (transposons) within genomes. This process can modulate gene expression and contributes to the spread of antibiotic resistance and virulence factors. We recently determined the cryo-electron microscopy (cryo-EM) structures of the IS21 transposon, a widespread mobile genetic element that encodes IstA, a transposase, and IstB, a AAA+ ATPase essential for DNA transposition. The reconstructions of these factors in the pre- and post-transposition states revealed key insights into the architecture and conformational dynamics of the transpososome. However, critical aspects of the mechanism, such as how IstB selects the insertion site, recruits IstA, and how ATP hydrolysis drives the process, remain unclear. Here, we present new structural and biochemical data that provide insight into these open questions, advancing our understanding of the molecular choreography underlying nucleotide dependent DNA transposition.

References:

[1] Spínola-Amilibia M, Araújo-Bazán L, de la Gándara Á, Berger JM, Arias-Palomo E. IS21 family transposase cleaved donor complex traps two right-handed

superhelical crossings. Nat Commun. 2023 Apr 22;14(1):2335. doi: 10.1038/s41467-023-38071-x. PMID: 37087515; PMCID: PMC10122671.

[2] de la Gándara Á, Spínola-Amilibia M, Araújo-Bazán L, Núñez-Ramírez R, Berger JM, Arias-Palomo E. Molecular basis for transposase activation by a dedicated AAA+ ATPase. Nature. 2024 Jun;630(8018):1003-1011. doi: 10.1038/s41586-024-07550-6. Epub 2024 Jun 26. PMID: 38926614; PMCID: PMC11208146.

Role of the SARS-CoV-2 Membrane protein hinge region and C-terminus tail on protein trafficking and virus assembly

Ortiz Mateu, Juan [*a], Pearson, Guy [b], Carlton, Jeremy [b], Skehel, Mark [c], Sánchez del Pino, Manuel Mateo [a], García Murria, Maria Jesús [a], Martinez Gil, Luis [a], Mingarro, Ismael [a], [a]University of Valencia (Spain). Biotecmed Institute, Faculty of Biochemistry and Molecular Biology., [b]King's College London (UK). The Francis Crick Institute, London (UK)., [c]The Francis Crick Institute, London (UK).

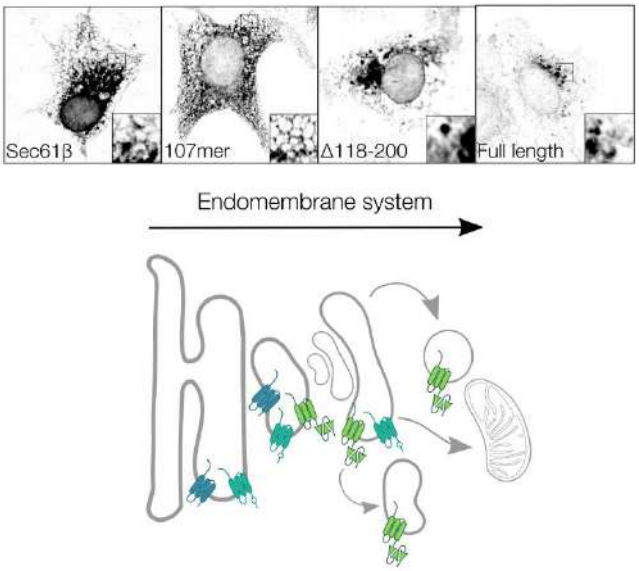

The Severe Acute Respiratory Syndrome Coronavirus 2 (SARS-CoV-2) Membrane (M) organizes the assembly and structure of new virions and is essential for virus formation. [1][2] It interacts with Envelope (E) protein [3] to induce curvature in the membrane,[4] thus allowing the assembly of viral particles and promoting maturation of Spike (S). [5] It also interacts with Nucleocapsid (N) protein to allow genomic RNA stabilization. [6] Cryo-EM structure of M protein confirms the presence of three transmembrane domains (TMDs) and a homo-dimeric conformation that might allow/promote viral assembly. [7][8] In this work, we use super-resolution confocal microscopy to show that while full-length M is located in the ERGIC-Golgi, a truncated version of the protein that includes only the TMDs does not co-localize in the ERGIC when other SARS-CoV-2 structural proteins are co-expressed and remains in the ER. Surprisingly, a deletion of the whole ß-sheet region in the cytosolic domain (residues 118-200) recovers the ERGIC-Golgi localization on its own and when the other proteins are present. This indicates that the cytosolic hinge region (108-118) and the C-terminal tail (201-222) are key for M trafficking. We then used proximity labeling coupled to mass-

spectrometry [9] revealing promising host cell M traffic co-factors that specifically interact with these two non-ß-sheet regions. Finally, we focused on the hinge region and performed a four-residue Alanine scan, showing that every tested mutation on this region is key for virus-like particle (VLP) formation. Overall, we characterize two short regions that are essential for M protein ER export and its potential interaction with other SARS-CoV-2 structural proteins. We provide a promising set of host cell trafficking co-factors that might interact with these regions to allow M ERGIC localization and demonstrate that the whole hinge region is essential for virus assembly and egress.

References:

[1] Pezeshkian, W., Grünewald, F., Narykov, O., Lu, S., Arkhipova, V., Solodovnikov, A., Wassenaar, T.A., Marrink, S.J., and Korkin, D. (2023). Molecular architecture and dynamics of SARS-CoV-2 envelope by integrative modeling. Structure 31, 492-503.e7.

[2] Finkel, Y., Gluck, A., Nachshon, A., Winkler, R., Fisher, T., Rozman, B., Mizrahi, O., Lubelsky, Y., Zuckerman, B., Slobodin, B., et al. (2021). SARS-CoV-2 uses a multipronged strategy to impede host protein synthesis. Nature 594, 240–245.

[3] Plescia, C.B., David, E.A., Patra, D., Sengupta, R., Amiar, S., Su, Y., and Stahelin, R.V. (2021). SARS-CoV-2 viral budding and entry can be modeled using BSL-2 level virus-like particles. J. Biol. Chem. 296.

[4] Neuman, B.W., Kiss, G., Kunding, A.H., Bhella, D., Baksh, M.F., Connelly, S., Droese, B., Klaus, J.P., Makino, S., Sawicki, S.G., et al. (2011). A structural analysis of M protein in coronavirus assembly and morphology. J. Struct. Biol. 174, 11–22.

[5] Boson, B., Legros, V., Zhou, B., Siret, E., Mathieu, C., Cosset, F.-L., Lavillette, D., and Denolly, S. (2021). The SARS-CoV-2 envelope and membrane proteins modulate maturation and retention of the spike protein, allowing assembly of virus-like particles. J. Biol. Chem. 296, 100111.

[6] Kuo, L., Hurst-Hess, K.R., Koetzner, C.A., and Masters, P.S. (2016). Analyses of Coronavirus Assembly Interactions with Interspecies Membrane and Nucleocapsid Protein Chimeras. J. Virol. 90, 4357–4368.

[7] Zhang, Z., Nomura, N., Muramoto, Y., Ekimoto, T., Uemura, T., Liu, K., Yui, M., Kono, N., Aoki, J., Ikeguchi, M., et al. (2022). Structure of SARS-CoV-2 membrane protein essential for virus assembly. Nat. Commun. 13, 4399.

[8] Dolan, K.A., Dutta, M., Kern, D.M., Kotecha, A., Voth, G.A., and Brohawn, S.G. (2022). Structure of SARS-CoV-2 M protein in lipid nanodiscs. eLife 11, e81702.

[9] Branon, T.C., Bosch, J.A., Sanchez, A.D., Udeshi, N.D., Svinkina, T., Carr, S.A., Feldman, J.L., Perrimon, N., and Ting, A.Y. (2018). Efficient proximity labeling in living cells and organisms with TurboID. Nat. Biotechnol. 36, 880–887.

Acknowledgments:

UV-INV_PREDOC-1911519 "Atracció de Talent" 2021 Programme

PID2023-152568NB-I00

CIPROM/2022/062

CryoSIM at ALBA: a new facility for high-resolution correlative cryo fluorescence and soft X-ray tomography

Otón, Joaquín [*a], Mamprin, Kevin [a], Gómez-Blanco, Josué [a], Groen, Johannes [a, b], Pérez-Berná, Ana Joaquina [a], Pereiro, Eva [a, c]

[a]ALBA Synchrotron - CELLS (ES), [b]Institute Pasteur, [c]Synchrotron SOLEIL, L'Orme des Merisiers Saint-Aubin, BP 48, 91192 Gif-sur-Yvette, France

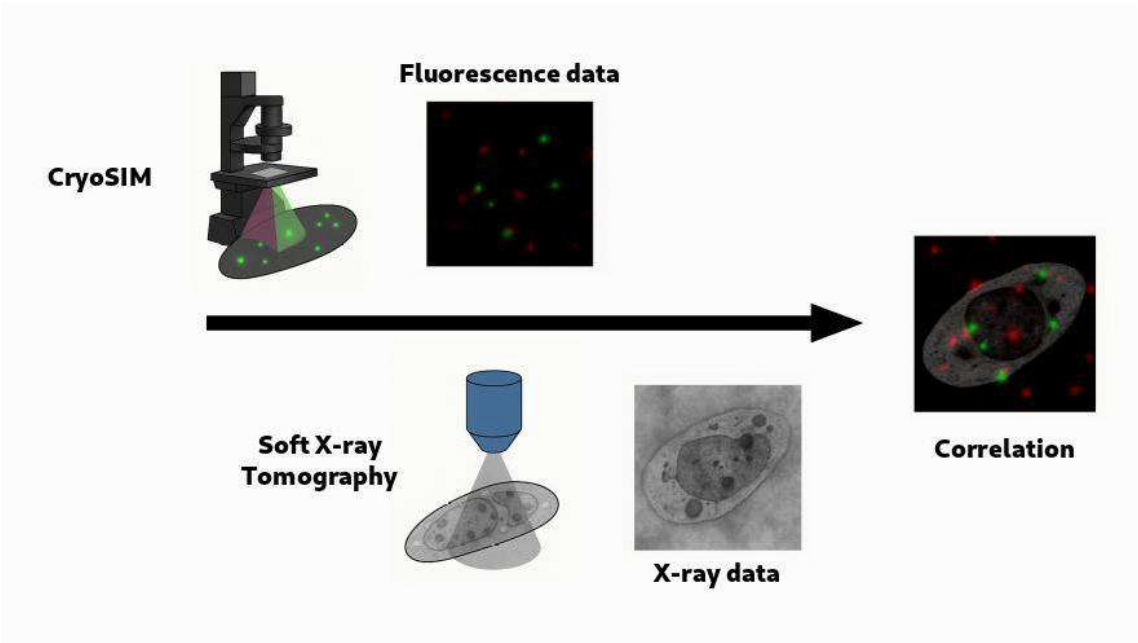

The study of biological systems at high spatial resolution requires complementary imaging modalities capable of capturing both molecular specificity and ultrastructural context under close-to-native conditions. To address this need, ALBA Synchrotron has established a new facility for cryogenic structured illumination microscopy (cryoSIM), expanding the correlative imaging capabilities available to the life science community.

CryoSIM enables the acquisition of three-dimensional fluorescence maps of vitrified biological samples with resolution beyond the diffraction limit. Using structured illumination with dual laser excitation and emission filtering, it supports dual fluorescent labeling, providing precise localization of tagged molecules or organelles in intact cells without the need for chemical fixation or staining. However, while fluorescence microscopy offers high specificity, its structural resolution remains limited.

To complement this, samples are subsequently imaged at the ALBA MISTRAL beamline using soft X-ray tomography (SXT) in the "water window" energy range. SXT provides quantitative 3D reconstructions of entire cells at nanometric resolution,

revealing organelles and cellular compartments in their native environment. Combined, cryoSIM and MISTRAL offer a unique correlative workflow in which molecular signals identified by fluorescence are precisely positioned within the cellular architecture observed by X-rays.

A key challenge in this correlative light and X-ray tomography approach lies in the accurate alignment of datasets from two distinct modalities. At ALBA, dedicated computational pipelines have been developed to reconstruct cryoSIM volumes and perform automated correlation with MISTRAL data. These custom algorithms reduce user intervention, enhance reproducibility, and achieve correlation accuracies down to tens of nanometers, enabling high-throughput studies of complex biological processes.

With the installation of cryoSIM, ALBA now offers users a complete pipeline for correlative imaging, from fluorescence acquisition to ultrastructural mapping and automated data integration. The integrated cryoSIM–MISTRAL workflow enables simultaneous visualization of fluorescently tagged biomolecules and their structural environment, facilitating studies in cell biology, infection research, and nanomedicine. For instance, this workflow has been applied to determine the intracellular localization of therapeutic nanomaterials [1], where cryoSIM pinpointed molecular signals and SXT revealed their compartmentalization within multivesicular bodies. Such results underscore the potential of correlative cryo-imaging to unravel cellular responses and molecular mechanisms with unprecedented detail.

References:

[1] Groen, J., Palanca, A., Aires, A., Conesa, J. J., Maestro, D., Rehbein, S., Harkiolaki, M., Villar, A. v., Cortajarena, A. L., & Pereiro, E. (2021). Correlative 3D cryo X-ray imaging reveals intracellular location and effect of designed antifibrotic protein-nanomaterial hybrids. Chemical Science, 12(45), 15090–15103.

Acknowledgments:

This project has received funding from the European Union's Horizon 2020 research and innovation programme under grant agreement No. 871037 (iNEXT-Discovery). It has also received funding from the European Union's Horizon Europe research and innovation programme under grant agreement No. 101120151 (CLEXM), a Marie Skłodowska-Curie Doctoral Networks Action (MSCA-DN).

Structural Insights into the Regulation of BOK Pore Formation by MCL1: First Findings

Buffa, Milagros [a], Leiva, Diego [a], García-Jareño, Alicia [a], Garcia-Sáez, Ana [b], Shalaby, Raed [b], Sancho, Mónica [a], Orzáez, Mar [*a]

[a]Targeted Therapies on Cancer and Inflammation, Príncipe Felipe Research Center (CIPF), Av. Eduardo Primo Yúfera 3, 46012 Valencia, Spain

[b]Max Planck Institute of Biophysics, Max-von-Laue-Strasse 3, 60439 Frankfurt am Main, Germany

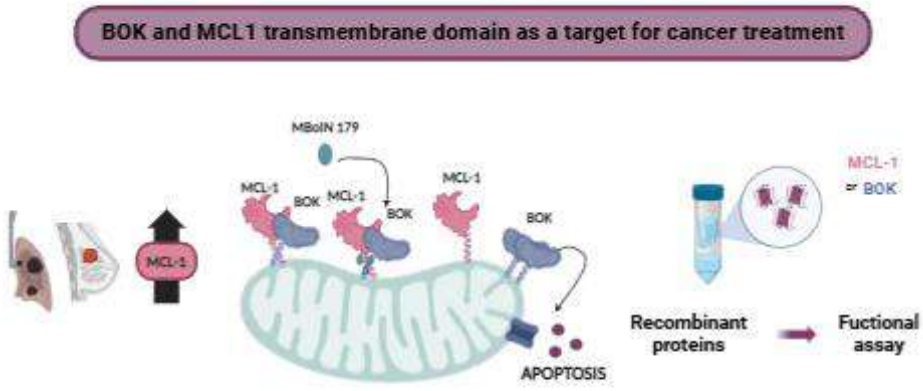

MCL1 is an anti-apoptotic BCL2 family protein frequently overexpressed in tumors, where it drives poor prognosis and therapy resistance. Current clinical trials with BH3-mimetics targeting MCL1 have shown limited success, as dose-limiting cardiotoxicity halted their clinical development, underscoring the need for alternative strategies. Recent studies, including our own, have revealed that MCL1 interacts with the pro-apoptotic protein BOK through their transmembrane domains, thereby restraining its pro-death activity.

We identified MBoIN179, a first-in-class small molecule capable of disrupting this interaction and selectively releasing BOK to trigger cell death. Initial studies confirmed its ability to induce BOK-dependent apoptosis, while avoiding the cardiotoxic limitations associated with conventional MCL1 inhibitors. To further explore its mechanism, we initiated a structural study of the MCL1–BOK transmembrane interaction. After extensive efforts, we successfully expressed and purified both proteins in E. coli, enabling detailed mechanistic investigations.

Recombinant proteins were used in calcein-release assays to assess membrane permeabilization, and co-precipitation experiments were performed to analyze protein–protein interactions and the effect of the compound on MCL1–BOK binding.

Calcein-release assays revealed that MBoIN179 enhances BOK-induced membrane permeabilization and counteracts the inhibitory effect of MCL1 in vitro, confirming its mechanistic action on the mitochondrial membrane. Importantly, these tools will allow us to further pursue structural studies aimed at deepening our understanding of this interaction.

Our findings reveal a novel strategy to overcome resistance in MCL1-overexpressing tumors by targeting its transmembrane interaction with BOK. MBoIN179 selectively activates BOK-mediated apoptosis and is effective in breast and lung cancer models without inducing cardiotoxicity. This unique mechanism offers a promising and safer alternative to conventional MCL1 inhibitors and supports the therapeutic potential of BOK modulation in resistant tumors.

References:

[1] Lucendo, E.; Sancho, M.; Lolicato, F.; Javanainen, M.; Kulig, W.; Leiva, D.; Duart, G.; Andreu-Fernández, V.; Mingarro, I.; Orzáez, M. Mcl-1 and Bok Transmembrane Domains: Unexpected Players in the Modulation of Apoptosis. Proc. Natl. Acad. Sci. U.S.A. 2020, 117 (45), 27980–27988

[2] Shalaby, R.; Diwan, A.; Flores-Romero, H.; Hertlein, V.; García-Saéz, A. J. Visualization of BOK Pores Independent of BAX and BAK Reveals a Similar Mechanism with Differing Regulation. Cell Death Differ. 2023, 30 (3), 731–741.

Acknowledgments:

We thank financial support from projects PID2023-149242OB-I00 funded by MICIU/AEI/10.13039/501100011033 and by ERDF/EU and Generalitat Valenciana (PROMETEO 2019/065). MB is supported by Santiago Grisolia pre-doctoral grant (GRISOLIAP/2021/132) and DL was supported by AECC pre-doctoral grant.

Accelerating Drug Discovery with CryoEM: An Expanding Strategic Infrastructure

Bueno-Carrasco, M.Teresa [*b], Chichón, Francisco Javier [a], Zamarreño, Noelia [a], Delgado, David [a], Piccirillo, Jonathan [a], Muriel, Olivia [a], Modrego, Andrea [a], Santiago, César [a], Valpuesta, José María [a], Arranz, Rocío [*a]

[a]CENTRO NACIONAL DE BIOTECNOLOGIA (CNB-CSIC) (ES)

[b]Instituto de Investigaciones Químicas (IIQ) - cicCartuja (ES)

Cryo-electron microscopy (CryoEM) is revolutionizing structural biology and rational drug design by enabling the visualization of biomolecular complexes at atomic resolution under near-native conditions. The CryoEM facility at CNB-CSIC, located at the National Center for Biotechnology, provides a comprehensive service encompassing sample vitrification, high-quality data acquisition, and a close and efficient collaboration with the Instruct Image Processing Centre (I2PC) for advanced 3D reconstruction. As part of the Spanish node of Instruct-ERIC, it offers researchers across Europe access to state-of-the-art technologies.

The facility hosts a unique infrastructure in Spain, soon to be strengthened by the upcoming incorporation of the Thermo Scientific Krios 5 Cryo-TEM, a 300 kV microscope representing the global gold standard in cryo-electron microscopy. This system delivers atomic resolution with high data fidelity, enhanced automation, and energy efficiency, while greatly expanding structural analysis capabilities, including single-particle analysis, cryo-electron tomography (cryoET), and microcrystal

electron diffraction (MicroED). The installation also houses a 200 kV FEI Talos Arctica and Spain's first cryoCLEM (correlative cryo-microscopy) platform, positioning it as a national technological reference in structural biology.

Our infrastructure has been pivotal in high-impact studies in virology and structural biology, and is increasingly supporting research involving chemistry and materials science samples. Within the framework of MFS2025, we aim to establish new synergies that will strengthen Spain's large-scale science ecosystem and consolidate our facility as a strategic hub for biomedical innovation in Europe.

Acknowledgments:

Acknowledgments

We acknowledge CNB-CSIC facility in the context of the CSIC Intramural Project ID 280306. Financial support also provided by Instruct-ERIC Projects.

Structural characterization of macromolecular complexes involved in PCNA unloading and deubiquitination (K164).

Aguilella Porcar, Jose Manuel [a], Muñoz Guijarro, Eduardo [a], Ortega Portero, Esther [*a]

[a]CENTRO NACIONAL DE BIOTECNOLOGIA (CNB-CSIC) (ES)

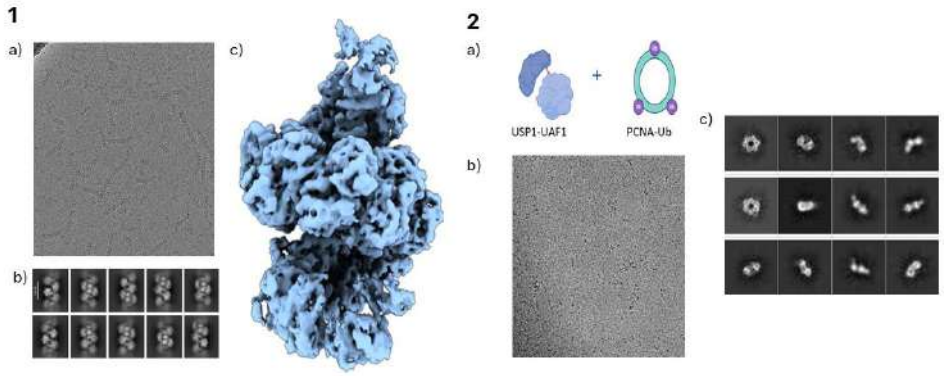

PCNA is a DNA clamp that plays a crucial role in eukaryotic DNA replication by interacting with DNA polymerases ε and δ increasing their processivity. PCNA adopts a closed ring-shaped conformation that encircles the DNA and slides along its strands during replication. The structure of this protein is highly conserved and exhibits a homotrimeric conformation. The loading of PCNA onto chromatin is mainly carried out by the pentameric RFC complex (Replication Factor C).

Once DNA synthesis is completed, PCNA must be unloaded from the newly synthesized DNA. Although this release can occur spontaneously, an active PCNA unloading machinery is required to ensure proper replication balance. The protein complex responsible for this unloading task is an RFC homolog called ATAD5-RLC which is specialized in PCNA unloading. ATAD5-RLC is composed of the ATAD5 and RFC2–5 subunits.

One of the most important post-translational modifications of PCNA is its monoubiquitination at lysine 164 which is key for specific DNA repair pathways during replication. This modification is primarily carried out by the E2/E3 enzymes (Rad6/Rad18) in eukaryotes. When DNA damage occurs, this post-translational modification reduces the binding affinity between PCNA and replicative DNA polymerases and serves as a signal for the recruitment of TLS polymerases, which are capable of repairing DNA damage. Once DNA damage has been repaired, PCNA must be deubiquitinated to restore the replication process. This deubiquitination is

carried out by the USP1–UAF1 complex. It has been reported in the literature that the N-terminal domain of ATAD5 (residues 1–500) plays an important role in the deubiquitination of PCNA.

We are focused on the structural characterization of molecular complexes involved in PCNA unloading and its K164 deubiquitination, using cryo-electron microscopy (Cryo-EM).

Poster Session 25th September - Topic: Materials

Detailed STEM-EELS Investigations of Iron-Oxide Nanoparticles with Co/Ni-Ferrite Shells

Hettler, Simon [*a, b, c], Arenal, Raul [b, c, d]

[a]Laboratory for Electron Microscopy, Karlsruhe Institute for Technology, Karlsruhe, Germany

[b]Laboratorio de Microscopías Avanzadas (LMA), Edificio I+D, C/ Mariano Esquillor s/n, 50018 Zaragoza, Spain.

[c]Instituto de Nanociencia y Materiales de Aragón (INMA) CSIC-Universidad de Zaragoza, Zaragoza 50018, Spain

[d]Fundación Agencia Aragonesa para la Investigación y el Desarrollo (ARAID), Av. de Ranillas 1-D, 50018 Zaragoza, Spain

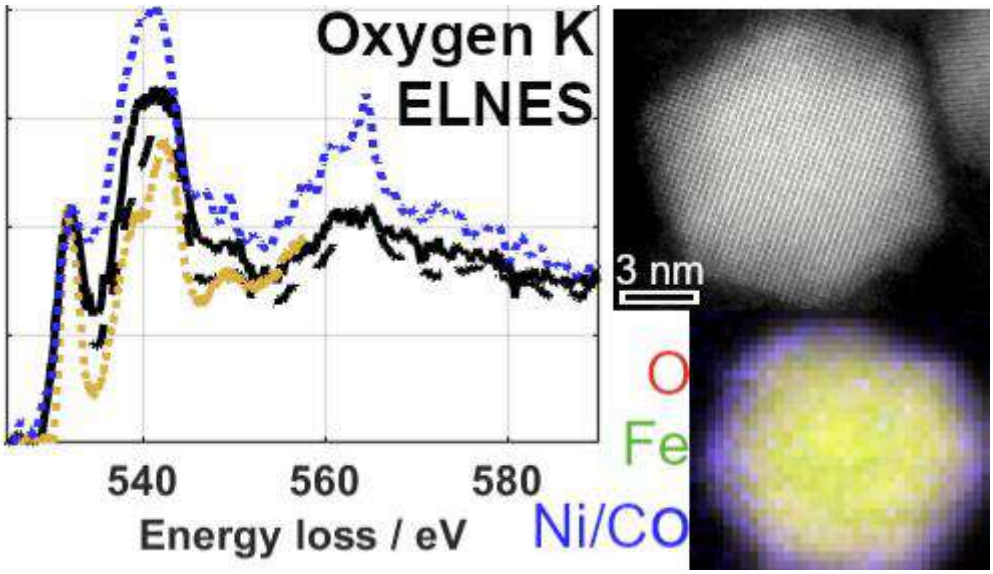

Iron-oxide nanoparticles are of interest for a large number of applications [1]. A controlled adjustment of their macroscopic properties aiming for specific applications can be achieved by synthesizing nanoparticles with varying diameter and with shells with defined thickness and composition. Specifically, shells based on cobalt ferrite have shown to be promising for both magnetic and catalytic applications [2,3]. A detailed knowledge of composition and structure down to the atomic scale is required to fully explain the properties observed on a macroscopic scale. Scanning transmission electron microscopy (STEM) in combination with electron energy-loss spectroscopy (EELS) is frequently used to obtain this knowledge. Here, we present detailed investigations on EELS and energy-loss near-

edge structure (ELNES) of iron-oxide nanoparticles with thin cobalt and/or nickel ferrite shells, focusing mainly on the oxygen K edge [4].

The specimens were prepared by drop-casting of the dispersed nanoparticles on holey carbon TEM grids, followed by a cleaning step using activated carbon and ethanol. STEM-EELS data was acquired using a probe-corrected Titan microscope (TFS) and a Gatan Imaging Filter (GIF) Tridiem 865 EEL spectrometer. The electron energy was 300 keV for imaging and 80 keV for EELS. The acquired data was treated by a custom Matlab-based software.

The EELS data obtained from a pure magnetite iron-oxide nanoparticle shows a good agreement with corresponding bulk references. The oxygen K edge of magnetite exhibits a sharp pre-peak followed by a valley. The analysis of the pure nanoparticles revealed that, without the mentioned specimen cleaning step, a beam-induced surface reduction can be observed. The reduction is revealed by a change in the ELNES signal of the oxygen K edge and the intensity ratio between pre-peak and valley, called O-K ratio in the following, is decreased. For nickel-containing nanoparticles, the overlap between Fe-L1 and Ni-L2,3 edges was corrected by establishing an intensity ratio between Fe-L2,3 and Fe-L1 edges. The presence of both nickel and cobalt-ferrite in the shell of the nanoparticles leads to a reduction of the O-K ratio. A detailed quantitative analysis of the relationship between nickel/cobalt content and the O-K ratio shows that the O-K ratio depends not only on the local but as well on the global nickel/cobalt content in the investigated nanoparticles with sizes below 20 nm.

In conclusion, the experimental results demonstrate that STEM imaging and STEM-EELS analyses are a powerful tool to not only investigate the composition and structure, but also detect minor chemical modifications on the very local scale below 1 nm spatial resolution.

References:

[1] Tartaj et al, Adv Mater 23 (44), 5243-5249 2011.

[2] Sartori et al, ACS Appl Mater Interfaces 13, 16784-16800, 2021.

[3] Royer et al, Sustain. Energy Fuels 7, 3239-3243, 2023.

[4] Hettler, Arenal, Micron 196-197, 103858, 2025.

Acknowledgments:

The microscopy works have been conducted in the Laboratorio de Microscopias Avanzadas (LMA) at Universidad de Zaragoza. Sample courtesy from B. Pichon, I. Makarchuk, L. Royer and K. Sartori (Université de Strasbourg). We acknowledge the support from the Spanish MICIU with funding from European Union Next Generation

EU (PRTR-C17.I1) promoted by the Government of Aragon as well as from the Spanish MICIU (PID2023-151080NB-I00/AEI/10.13039/501100011033 and CEX2023-001286-S MICIU/AEI /10.13039/501100011033) and the Government of Aragon (DGA) through the project E13 23R.

Electron Microscopy Study of the Interzeolite Transformation from Natural Mordenite to ZSM-5

Li, Daiyuan [a], Arnaiz, Itziar [b], Awoke, Yaregal [c], Kayani, Sara [a], Zhang, Qing [d], Diaz, Isabel [b], Pizarro, Daniel [e], Alvaro, Mayoral [*a]

[a]Instituto de Nanociencia y Materiales de Aragón (INMA), CSIC-Universidad de Zaragoza 50009, Spain

[b]Instituto de Catálisis y Petroleoquímica, ICP-CSIC. C/Marie Curie 2, 28049 Madrid

[c]Chemistry Department Addis Ababa University, Addis Ababa Ethiopia

[d]School of Physical Science and Technology, ShanghaiTech University, Shanghai 201210, P. R. China

[e]Electronics Department, University of Alcala, 28801 Alcalá de Henares, Madrid, Spain.

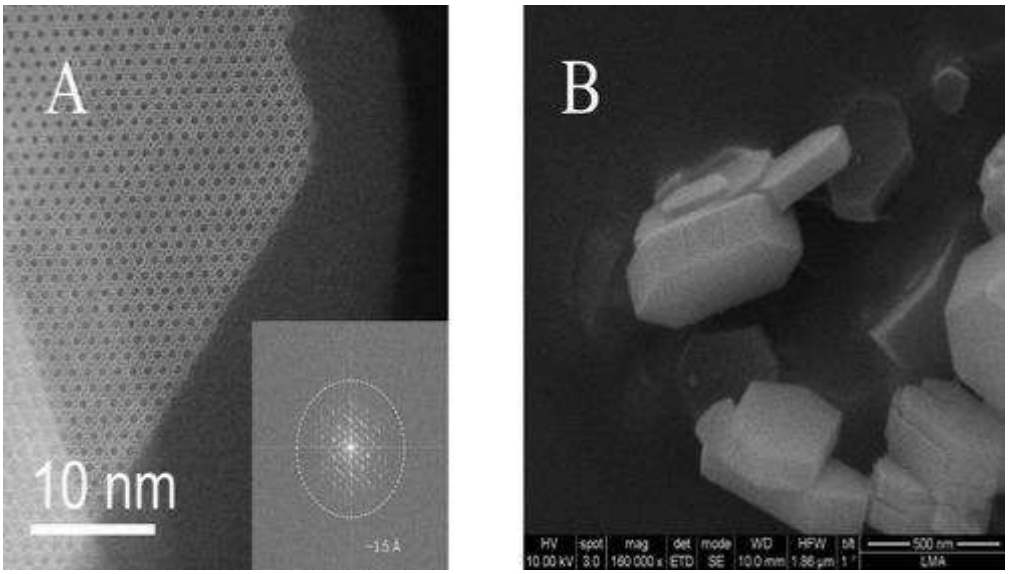

Zeolites are crystalline microporous materials primarily composed of corner-sharing tetrahedral units of SiO_4 and AlO_4, featuring a highly ordered channel structure[1]. ZSM-5 is a high-silica zeolite, **MFI** framework topology, and is one of the most widely produced and applied zeolites in industry [2]. It is extensively used in catalytic processes such as petroleum refining and fine chemical synthesis[3-4]. Mordenite (**MOR**) is one of the earliest discovered and studied zeolites and is also a major mineral component in natural zeolite deposits. **MOR** and **MFI** share certain structural similarities. **MOR** contains parallel 12-membered ring channels as well as perpendicular 8-ring channels, where the 8-membered rings indirectly connect the 12-membered channels, with channel dimensions of 6.5 × 7.0 Å. In contrast, **MFI** is composed of two intersecting 10-membered ring channel systems,

where straight and elliptical channels (5.4 × 5.6 Å) intersect with zigzag and elliptical channels (5.1 × 5.5 Å). Both frameworks are constructed from pentasil building units and contain *mor*[5^4] structural motifs .

The transformation between mordenite to ZSM-5 has been reported obtaining a successful conversion from one into the other obtaining materials with extraordinary crystallinity[5]. Building upon these findings, we investigated the structure of ZSM-5 and observed the intergrowth of ZSM-5 crystals with very high crystallinity. We also found that the phase transformation between the two structures depended on the synthesis conditions. To probe this, we employed transmission electron microscopy (TEM) and spherical aberration-corrected scanning transmission electron microscopy (Cs-corrected STEM) to examine the morphological changes of zeolites synthesized under different conditions at various growth stages, aiming to further understand the transformation mechanism.In addition, we assessed the ion-exchange capacity of the resulting materials. Finally, we developed our own reconstruction algorithm for electron ptychography and collected preliminary datasets from four different synthesis systems.

Figure 1a depicts the Cs-corrected STEM-ADF data of one of the products obtained confirming the good quality of the zeolites that can produced by this method. The shape and size of the same material was investigated by scanning electron microscopy (SEM), figure 1b.

Figure 1. (A) Cs-corrected STEM-ADF image of ZSM-5 along [010], the Fourier transform (FFT) is shown inset. (B) SEM micrograph of ZSM-5.

References:

[1] [1] J.V. Smith, Definition of a zeolite, Zeolites, 4 ,1984, 309-310.

[2] R. Bingre, B. Louis, P. Nguyen, An Overview on Zeolite Shaping Technology and Solutions to Overcome Diffusion Limitations, Catalysts, 8 (2018) 163.

[3] Q. Zhang, J. Yu, A. Corma, Applications of Zeolites to C1 Chemistry: Recent Advances, Challenges, and Opportunities, Advanced. Material, 32 (2020) 2002927.

[4] U. Olsbye, S. Svelle, M. Bjørgen, P. Beato, T.V.W. Janssens, F. Joensen, S. Bordiga, K. P. Lillerud, Conversion of Methanol to Hydrocarbons: How Zeolite Cavity and Pore Size Controls Product Selectivity, Angewandte Chemie International Edition, 51 (2012) 5810 – 5831.

[5] Y. Awoke, M. Sánchez-Sánchez, I. Arnaiz, I. Diaz, Synthesis of ZSM-5 from natural mordenite from Spain, Microporous and Mesoporous Materials, 358 (2025) 113463

Acknowledgments:

The Spanish Ministry of Science (MICIU/AEI /10.13039/501100011033 and EU NextGenerationEU/PRTR: CNS2023-144346; PID2022-136535OB-I0, to the Grant CEX2023-001286-S funded by MICIU/AEI /10.13039/501100011033), the CℏEM, School of Physical Science and Technology, ShanghaiTech University (#EM02161943), the regional government of Aragon (E13_23R). SK was hired under the Generation D initiative, promoted by Red.es, an organisation attached to the Ministry for Digital Transformation and the Civil Service, for the attraction and retention of talent through grants and training contracts, financed by the Recovery, Transformation and Resilience Plan through the European Union's Next Generation funds.

Access to State-of-the-Art Electron Microscopy Facilities through INFRACHIP Project

Carbo-Argibay, Enrique [*a], Petrovykh, Dmitri Y. [a]

[a]International Iberian Nanotechnology Laboratory, Braga, Portugal.

Limited access to large research infrastructures for materials characterization, processing/fabrication, modelling or test structures can significantly hinder progress in materials science research. To address this challenge, the INFRACHIP project (European Research Infrastructure on Semiconductor Chips) aims to establish a "European research platform for the sustainable development of next generation and future semiconductor chips" [1]. This platform offers free access to infrastructures valued at 2 billion €, resources that are not accessible elsewhere as a whole, covering all the needs to shorten the translation path from lab to the fab. By doing so, INFRACHIP lowers access barriers to academic and industrial researchers for the sustainable development of semiconductor chips. However, INFRACHIP is far more than just a platform offering free access to large research infrastructures. It also encompasses comprehensive training programmes for young researchers, such as Research Accelerator Programmes, digital or hybrid schools, hands-on training sessions and webinars. Moreover, it fosters the creation of an ecosystem of experts and collaborative network aimed at strengthening the EU capacity to develop next-generation and future semiconductor chips.

In particular, the electron microscopy instrumentation available at INL through INFRACHIP enables comprehensive structural and chemical characterization of materials or devices for applications in both physical and life sciences, including techniques such as SEM, DualBeam FIB-SEM, Cryo-TEM, Probe and Image-corrected (S)TEM, XPS, XRD and SAXS.

[1] https://infrachip.eu/

References: -

Acknowledgments:

INFRACHIP (2024-2027) has received funding from the European Union's Horizon Europe Research and Innovation Actions under GA No. 101131822

Understanding the Microstructure of High Current Carrying REBCO Superconducting Films grown via Transient Liquid Assisted Growth (TLAG)

Gupta, Kapil [*a], Saltarelli, Lavinia [b], Torres, Carla [b], Banchewski, Juri [b], Voulhoux, Mahel [b], Rasi, Silvia [b], Garcia, Diana [b], Ghiara, Emma [b], Kethamkuzhi, Aiswarya [b], Mola, Ona [b], Pach, Elzbieta [b], Solano, Eduardo [c], Mocuta, Cristian [d], Obradors, Xavier [b], Puig, Teresa [b]

[a]Catalan Institute of Nanoscience and Nanotechnology (ICN2), CSIC and BIST, Campus UAB, Bellaterra, 08193 Barcelona, Spain

[b]Institut de Ciència de Materials de Barcelona (ICMAB-CSIC), Campus UAB, Bellaterra, 08193 Barcelona, Spain

[c]NCD-SWEET Beamline, ALBA Synchrotron Light Source, 08290 Cerdanyola del Vallès, Barcelona, Spain

[d]Synchrotron SOLEIL, L'Orme des Merisiers Saint-Aubin, BP 48, 91192 Gif-sur-Yvette, France

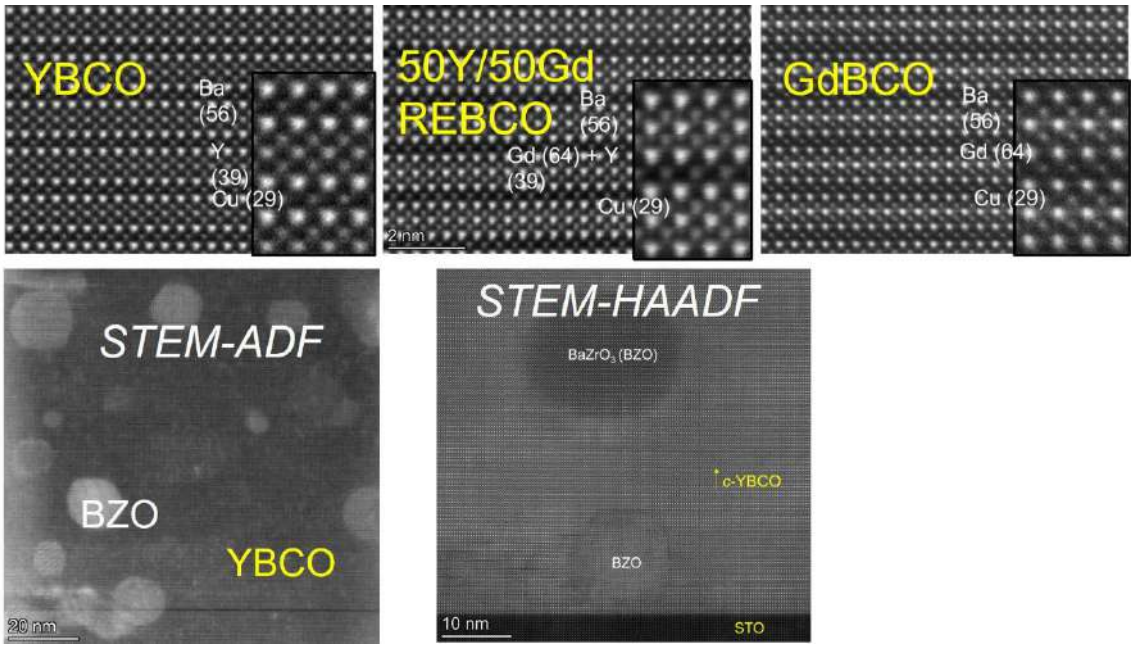

$REBa_2Cu_3O_7$ (RE= rare earth) coated conductors (REBCO CCs) are advanced, high-performance high-temperature superconductors (HTS) with the potential for integration into a range of emerging technologies, including fault current limiters, compact fusion systems, electric aviation, and high-field NMR, among others. However, a key challenge facing the community is the urgent need to lower the cost-

to-performance ratio of REBCO CC manufacturing, particularly as these conductors move toward large-scale deployment in commercial devices. For this purpose, we are developing a high-throughput scalable growth approach, called, “Transient Liquid Assisted Growth (TLAG)” [1-4], by combining chemical solution deposition methodologies with ultra-fast growth rates of over 1000 nm/s with high critical current densities (J_c) up to 3MA/cm^2 at 77K [2]. TLAG is a non-equilibrium liquid-solid growth process in which nucleation and growth are governed by kinetic factors, so microstructural study is crucial to understand the growth mechanism and determine the correlation of the kinetic process parameters with epitaxy and growth rate. Additionally, high throughput experimentation employing ink-jet printed combinatorial compositional gradients are being used for fast screening of parameters.

To this end, probe-corrected electron microscopy and spectroscopy provide an ideal tool to study the growth evolution of the thin films, the secondary phases as well as the defects and the comparative change in microstructure with atomic-resolution.

Our studies show that the microstructure of pristine REBCO can be significantly tailored using the TLAG-CSD process by optimizing various growth parameters. Additionally, flux pinning under high magnetic fields can be further improved by incorporating secondary phases, such as pre-formed nanoparticles, directly into the metal-organic inks. Consequently, we will present a detailed analysis of the atomic-scale microstructure of pristine REBCO and REBCO nanocomposites, grown under different conditions, using atomic-resolution STEM-HAADF, STEM-ADF and STEM-EELS techniques.

References:

[1] L. Soler et al, Nat. Commun., 11, 344 (2020)

[2] S. Rasi et al, Adv Sci, 9, 2203834 (2022)

[3] L. Saltarelli, K.Gupta et al, ACS Appl. Mater. Interfaces 14 48582 (2022)

[4] T. Puig et al, Nat Rev Phys 6, 132–148 (2024)

Strain and phase evolution in SrFeO3-x thin films: an HRTEM and EELS analysis of oxygen-induced structural distortions

Falcó, Ona [*a], Ruiz-Caridad, Alicia [b], Nizet, Paul [b], Chiabrera, Francesco [b], Tarancon, Albert [b], Estradé, Sònia [a], Yedra, Lluís [a], Peiró, Francesca [a]

[a]LENS-MIND, Departament d'Enginyeria Electrònica i Biomèdica, U. Barcelona (Barcelona), Spain

[b]Catalonia Institute for Energy Research (IREC) (ES)

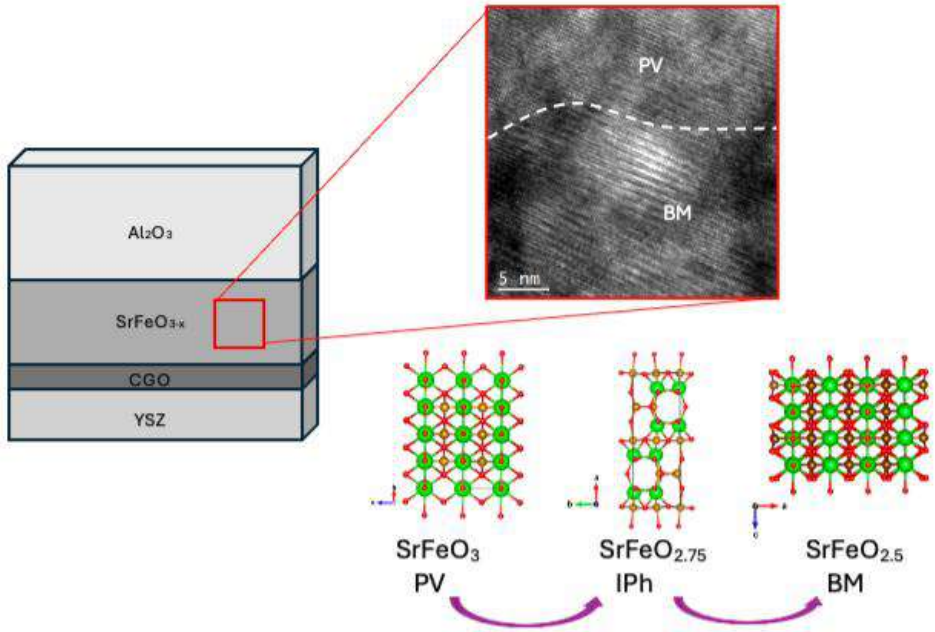

Strontium Ferrite ($SrFeO_{3-x}$) exhibits a strong structural sensitivity to oxygen concentration, transitioning between a perovskite ($SrFeO_3$) and brownmillerite ($Sr_2Fe_2O_5$) phase. These phases differ in symmetry and lattice arrangement: the fully oxidized perovskite adopts a cubic-like structure, while oxygen-deficient regions exhibit an orthorhombic brownmillerite phase. The aim of this work is to investigate the local structural distortions and oxygen stoichiometry in epitaxial $SrFeO_{3-x}$ thin films, which have undergone controlled oxidation and reduction treatments via electrochemical gating to modulate their oxygen content. High-resolution Transmission Electron Microscopy (HRTEM) and Electron Energy Loss Spectroscopy (EELS) were employed to examine the films at the nanoscale.

Pseudocubic coordinates have been used to quantify lattice parameters and assess strain by measuring in-plane and out-of- plane distances. Diffraction patterns and superstructure reflections allow us to differenciate between perovskite, brownmillerite, and intermediate regions, particularly where perovskite appears

encapsulated by brownmillerite, while EELS mapping provides insights into the spatial distribution of oxygen and iron within the sample, enabling the detection of subtle oxygen concentration variations. These local measurements provide a deeper understanding of how minor changes in oxygen content produce significant lattice deformations, offering a microscopic perspective that complements X-ray diffraction data and gives information on strain states relevant to functional properties.

References:

[1] A. Tarancón and N. Pryds, "Functional Oxide Thin Films for Advanced Energy and Information Technology," Advanced Materials Interfaces, no. 6/15, p. 1900990, 2019

[2] F. M. Chiabrera, S. Yun, Y. Li, R. T. Dahm, H. Zhang, C. K. R. Kirchert, D. V. Christensen, F. Trier, T. S. Jespersen, and N. Pryds, "Freestanding Perovskite Oxide Films: Synthesis, Challenges, and Properties," Annalen der Physik, vol. 534, no. 9, Art. 2200084, 2022

[3] F. Yan, J. Wu, S. Ning, and F. Luo, "Orienting Oxygen Vacancy Channels in Brownmillerite Strontium Ferrite Thin Films Using Strain: Implications for Facile Oxygen Ion Transport," ACS Applied Nano Materials, vol. 7, pp. 7703–7712, 2024

[4] E. Marek, W. Hu, M. Gaultois, C. P. Grey, S. A. Scott, The use of strontium ferrite in chemical looping systems, Applied Energy, vol. 223, pp. 369–382, 2018

[5] S. K. Acharya, R. V. Nallagatla, O. Togibasa, B. W. Lee, C. Liu, C. U. Jung, B. H. Park, J.-Y. Park, Y. Cho, D.-W. Kim, J. Jo, D.-H. Kwon, M. Kim, C. S. Hwang, and S. C. Chae, "Epitaxial Brownmillerite Oxide Thin Films for Reliable Switching Memory,"ACS Applied Materials & Interfaces, vol. 8, no. 12, pp. 7902–7911, 2016

[6] V. R. Nallagatla, J. Kim, K. Lee, S. C. Chae, C. S. Hwang, and C. U. Jung, "Complementary Resistive Switching and Synaptic-Like Memory Behavior in an Epitaxial SrFeO2.5 Thin Film through Oriented Oxygen- Vacancy Channels," ACS Applied Materials & Interfaces, vol. 12, no. 37, pp. 41740–41748, 2020

[7] A. Khare, J. Lee, J. Park, G. Y. Kim, S. Y. Choi, T. Katase, S. Roh, T. S. Yoo, J. Hwang, H. Ohta, J. Son, and W. S. Choi, "Directing Oxygen Vacancy Channels in SrFeO2.5 Epitaxial Thin Films,"ACS Applied Materials & Interfaces, vol. 10, no. 6, pp. 4831–4837, 2018

[8] L. Wang, Z. Yang, M. E. Bowden, and Y. Du, "Brownmillerite Phase Formation and Evolution in Epitaxial Strontium Ferrite Heterostructures", Applied Physics Letters, vol. 114, no. 23, Art. 231602, 2019

[9] M. Schmidt and S. J. Campbell, “In situ neutron diffraction study (300– 1273 K) of non-stoichiometric strontium ferrite SrFeOx,” Journal of Physics and Chemistry of Solids, vol. 63, no. 12, pp. 2085–2092, 200

[10] K. Momma and F. Izumi, “VESTA: A three-dimensional visualization system for electronic and structural analysis,”Journal of Applied Crystallography, vol. 41, no. 3, pp. 653–658, 2008

Acknowledgments:

The author wants to thank Lluís Yedra for his valuable assistance and guidance during the research process. Francesca Peiró ir also gratefully acknowledged for her support throughout this work. The author thanks the LENS group for their help in different situations. Also Alícia Ruiz and Francesco Chiabrera from the Institut de Recerca en Energia de Catalunya (IREC) are acknowledged for providing the samples used in this study. Sincere thanks are extended to the friends from the master’s program, who stood by the author through both the highs and lows of this stage.

This work is dedicated to the author’s family, with special appreciation to her father, whose steady support and belief in her academic journey have been a constant source of motivation and strength.


mfs 2025
CONFERENCE


scitoevents
SCIENCE & TECHNOLOGY ORGANIZERS